UNIVERSITEIT VAN PRETORIA
UNIVERSITY OF PRETORIA
YUNIBESITHI YA PRETORIA

Cellular effects of Coenzyme Q10 and Triton X on primary chicken embryo heart and muscle cell cultures

By

MARNIE POTGIETER

Thesis submitted in partial fulfilment of the requirement for the degree of

MASTER OF SCIENCE

in the

FACULTY OF HEALTH SCIENCES

Department of Anatomy

University of Pretoria

2007

UNIVERSITEIT VAN PRETORIA
UNIVERSITY OF PRETORIA
YUNIBESITHI YA PRETORIA

Cellular effects of Coenzyme Q10 and Triton X on primary chicken embryo heart and muscle cell cultures

By

MARNIE POTGIETER

SUPERVISOR: Prof. E Pretorius

COSUPERVISOR: Dr. MJ Bester

DEPARTMENT: Anatomy

DEGREE: MSc (Anatomy with specialization in Cell Biology)

Abstract

Coenzyme Q10 is a lipid-soluble coenzyme, synthesized in mammalian tissue to support energy production, and also act as an antioxidant. Certain medication, stress and age may deplete the body's endogenous Coenzyme Q10 store. Numerous disease conditions have been shown to benefit from Coenzyme Q10 supplementation. It is a lipid-soluble component of virtually all cell membranes, and is located in the hydrophobic domain of the phospholipid bilayer of cellular membranes. It is also the only known lipid-soluble antioxidant that animal cells can synthesize *de novo*, and for which there exist enzymatic mechanisms which can regenerate it from its oxidized product formed in the course of its antioxidant function. The aim of this study was to investigate the cellular effects of Coenzyme Q10 and Triton X-100 on primary chicken embryo heart and muscle cell cultures. Triton X-100, a well known membrane disrupter, extensively used by cell biologists for that purpose, was used to investigate whether Coenzyme Q10 might offer protection to cell membranes exposed to disruption. Due to the correlation found between the chemical structures of nonylphenol and Triton X-100, it was decided to determine whether Triton X-100 possess estrogenic properties. Using the Recombinant Yeast Screen Assay for estrogenic activity, it was found that Triton X-100 induced weak estrogenic activity.

The primary heart and skeletal muscle cell cultures were established by harvesting skeletal muscle tissue and hearts from 13 day old chicken embryos. After establishment of the cell

cultures, the concentrations of Coenzyme Q10 and Triton X-100 were tested for cytotoxicity using the MTT, NR, and CV assays, in the form of a combined colorimetric cytotoxicity assay. The MTT assay revealed an increase in cell viability in both cell cultures upon exposure to Triton X-100 and Coenzyme Q10, alone, and in combination. Triton X-100 and Coenzyme Q10, alone, and in combination, caused a decrease in lysosomal membrane integrity, as measured by the NR assay, and both substances, alone, and in combination, had no effect on cellular proteins, as measured by the CV assay.

Scanning electron microscopy (SEM) was done to determine the cellular effect of heart and skeletal muscle cell cultures on the external surface, more specifically the membranes, of cells in culture. Triton X-100 in the concentrations used in the study, caused membrane disruption, ranging from complete membrane lyses at the highest concentrations to membrane ruptures and apoptotic blebbing in lower concentrations. SEM revealed that no adverse effects were caused by Coenzyme Q10 on the membrane structure, in dissimilarity, cell differentiation and proliferation, including myoblast formation were seen in the presence of all the concentrations of Coenzyme Q10. Numerous ion channels were observed on cellular surfaces exposed to Coenzyme Q10. Upon exposure to 0.005% Triton X-100, after pre-treatment with Coenzyme Q10, SEM revealed a “membrane patch” formation on membranes disrupted by Triton X-100. Damage to cell membranes in the presence of Triton X-100, were less severe when cells were pre-treated with Coenzyme Q10. Confocal microscopy was utilized to investigate intracellular occurrences in the presence of Triton X-100 and Coenzyme Q10. Using Mito Tracker Red to stain active respiring mitochondria and DAPI to stain nuclei, confocal microscopy confirmed the observations made by SEM, that Coenzyme Q10 enhance cell proliferation and differentiation, and that the adverse effects to cells exposed to Triton X-100 are less severe after pre-treatment with Coenzyme Q10. ROS generation was detected, using dichlorodihydrofluorescein diacetate, in cultures exposed to Triton X-100, and none in the presence of Coenzyme Q10. In the presence of Triton X-100, after pre-treatment with Coenzyme Q10, ROS generation was remarkably lower.

The study provided apparent evidence that Coenzyme Q10 offer protection to cardiac and skeletal muscle cells in culture after exposure to relatively low concentrations of the membrane disrupter Triton X-100. Coenzyme Q10 also promotes the process of proliferation and differentiation in primary chicken embryonic cultures of heart and skeletal muscle cells.

Declaration

I, Marnie Potgieter, hereby declare that this research dissertation is my own work and has not been presented for any degree at another University;

Signed: …….....

Date: …….....

Department of Anatomy, School of Medicine, Faculty of Health Sciences,
University of Pretoria

South Africa

Acknowledgments

Praise be to my Father in Heaven! For allowing me this great opportunity in life, for granting me the ability to reach this milestone, and for guiding me every step of the way. I am grateful to my God for His Mercy, Love and Blessings.

Thank you to my wonderful parents for all your love and support. I am immensely grateful for all the sacrifices you've made in life to make my dreams come true. Thank you for teaching me to have faith, all your prayers and for everything I have been given undeserved. My brothers, Piet and Faan, I thank you for your unconditional love and support.

Johan, how will I ever be able to thank you enough! I am so grateful for your unconditional love and support, for always being there when I needed you most. Thank you for believing in me.

I am forever indebted to my promoter Professor Resia Pretorius, for your unconditional help and support, for always being available when I needed you, and for your guidance and motivation through this study. Thank you for granting me the invaluable opportunity to reside in my great passion for science. I am grateful for your enormous contribution to my success. I would also like to thank Dr. Megan Bester, for her contribution and help during this study.

I am also indebted to the following people for their contribution to this thesis:
Professor Riana Bornman, department Andrology, for granting me the opportunity to use the facilities in their laboratory. Dr. Natalie Aneck-Hahn for her enormous contribution to the interpretation of the results from the Recombinant Yeast Screen Assay. Catherina van Zijl, for her invaluable contribution in generating and processing the results.
Mr Alan Hall, at the Unit for Microscopy and Microanalysis, for spending so much time with me on the confocal microscope. I am infinitely grateful for your patience and kindness. Mr Chris van der Merwe for always being willing to share his remarkable knowledge with me. Mr André Botha and Nanette, for their assistance on the ZEISS ULTRA FEG.SEM.

I owe gratitude to Eureke and Jana, for sacrificing their time to help me whenever I needed it, for their kindness, advice and motivation.

"Except the Lord build the house, they labour in vain that build it: except the Lord keep the city, the watchman waketh but in vain. It is in vain for you to rise up early, to sit up late, to eat the bread of sorrows: for so He giveth his beloved sleep." (Psalm 127:1-2)

List of Abbreviations, Symbols and Chemical Formulae

%	Percentage
˙QH	Ubisemiquinone or univalently reduced state of Coenzyme Q10
°C	Degrees centigrade
β-gal	β-galactosidase
µg	Microgram
µg/µl	Microgram per microlitre
µl	Microlitres
µm	Micrometer
3D	Three dimensional
4-HB	4-hydroxy benzoic acid
8-OH-dG	8-hydroxy-deoxyguanosine
AB	Alamar Blue
abs	Absorbance
acetyl-CoA	Acetyl-coenzyme A
ADP	Adenosine 5'-diphosphate
AFM	Atomic force microscopy
AIDS	Acquired immunodeficiency syndrome
AIF	Apoptosis inducing factor
ALS	Amyotrophic lateral sclerosis
ANOVA	Analysis of variance
AOA1	Ataxia-oculomotor-aprataxia type 1
APTX	Gene that codes for aprataxin
asc˙	Ascorbyl radical
ATP	Adenosine triphosphate
Bax	BCL2-associated X protein

c fos	Protooncogene
Ca^{2+}	Calcium ion
CCCP	Carbonyl cyanide m-chloro phenylhydrazone
CDK	Cyclin-dependent kinase
CHF	Congestive heart failure
cm^2	Centimetres squared
CMC	Critical micelle concentration
c-myc	Proto-oncogene with sequence homology to viral avian myelocytomatosis viral oncogene (v-Myc)
CO_2	Carbon dioxide
CoA	Coenzyme A
COPD	Chronic obstructive pulmonary disease
Coq 1-9	The Nine Coq proteins
Coq	Coenzyme Q10 genes
CoQ	Fully oxidized ubiquinone form
CoQ/CoQ10	Coenzyme Q10
COQ1-8	Biosynthetic enzymes
COQ1-9	Q-deficient yeast mutants
CoQ9	Coenzyme Q9
$CoQH^-$	Radical semiquinone intermediate
CoQH2	Fully reduced ubiquinol form
COX	Human complex IV
CPRG	Chlorophenol red-β-d-galactopyranoside
CV	Crystal violet
Da	Dalton
DAPI	4´,6-diamidino-2-phenylindole dihydrochloride
DCF	Dichlorofluorescein
DCFH	Dichlorodihydrofluorescein

DCH_2FDA	Dichlorodihydrofluorescein diacetate
ddH_2O	Double distilled water
DMAPP	Dimethylallyl diphosphate
DMEM	Dulbecco's Modified Eagle's Medium
$DMQH_2$	5-demethoxyubiquinol
DMSO	Dimethyl sulphoxide
DNA	Deoxyribonucleic acid
DPBS	Dulbecco's Phosphate Buffered Saline
dsDNA	Double stranded DNA
e^-	Electron
E13	Embryonic day 13
E2	17β-estradiol
E6	Embryonic day 6
EC50	half maximal effective concentration
EDC	Endocrine disrupting chemical/s
EDTA	Ethylene diamine tetra acetate
ER-α	Human estrogen receptor-α
etc.	et cetera
ETFDH	Electron-transferring-flavoprotein dehydrogenases gene
$FADH_2$	Flavin adenine dinucleotide
FBS	Foetal bovine serum
$Fe^3O_2^{\cdot -}$	Perferryl radical
FRDA	Friedrich's ataxia
g	Gram
G1	A period in the cell cycle during interphase
G2	The third, final, and usually the shortest subphase during interphase within the cell cycle
GAII	Glutaric aciduria type II
GI	Gastro-intestinal

H^+	Hydrogen ion
H_2O	Water
H_2O_2	Hydrogen peroxide
HBSS	Hanks Balanced Salt Solution
HCl	Hydrochloric acid
HMG-CoA	3-hydroxy-3-methylglutaryl-CoA
hr	Hour/hours
i.e.	That is
IC50	half maximal (50%) inhibitory concentration (IC) of a substance
Inc	Incorporated
IPP	Isopentenyl-PP
KCl	Potassium chloride
kDa	Kilodalton
KH_2PO_4	Potassium dihydrogen phosphate
$L^{\cdot}$	Carbon-centered radical
LH	Polyunsaturated fatty acid
$LOO^{\cdot}$	Lipid peroxyl radicals
LOOH	Lipid hydroperoxide
M	Mitosis
M	Molar
mg	Milligram
mg/ml	Milligrams per millilitre
Mg^{2+}	Magnesium ion
ml	Millilitre
mm	Millimetres
mM	Millimolar
MRFs	Myogenic regulatory factors
MTT	1-(4,5-Dimethylthiazol-2-yl)–3,5 diphenylformazan

mV	Millivolt
Myf5	Myogenic factor 5
MyoD	Myogenic factor D
Na^{2+}	Sodium ion
Na_2HPO_4	Disodium hydrogen phosphate
NaCl	Sodium chloride
NADH	Nicotinamide adenine dinucleotide
NADPH	Nicotinamide adenine dinucleotide phosphate (reduced)
$NaHCO_3$	Sodium hydrogen carbonate
NF_KB	nuclear factor-kappa B
ng/L	Nanogram per liter
nm	Nanometre
NOX	NADH oxidase
NP	Nonylphenol
NPE	Nonylphenol ethoxylate/s
NR	Neutral red
N-SMase	Neutral sphingomyelinase
O_2^-	Superoxide
OH^-	Hydroxyl ion
OsO_4	Osmium tetraoxide
OXPHOS	Oxidative phosphorylation
Pax7	Transcription factor
PBS	Phosphate Buffered Saline Solution
PDSS1	Prenyldiphosphate synthase, subunit 1
PDSS2	Decaprenyl diphosphate synthase, subunit 2
PHB	Polyprenyl-4-hydroxybenzoate
P_i	Phosphate
PI	Propidium iodide

-PP	Diphosphate
PSF	Penicillin, streptomycin, fungizone
PTP	Permeability transition pore
p-Value	Probability value
Q 1 – 5	Five different concentrations of Coenzyme Q10, used in the study
Q	The fully oxidized state of Coenzyme Q10 or ubiqunone
RCBA	Recombinant Yeast Screen Assay
RIE	Relative induction efficiency
RNA	Ribonucleic acid
ROS	Reactive oxygen species
RSV-BH	Rous sarcoma virus (high titre strain)
RSV-BH-Ta	Mutant form of the Rous sarcoma virus
RuO_4	Ruthenium oxide
SAM	S-adenosylmethionine
SD	Standard deviation
SDH	Succinate dehydrogenase
SDS-PAGE	Sodium dodecyl sulfate polyacrylamide gel electrophoresis
SEM	Scanning Electron Microscopy
SMP	Submitochondrial particles
TEM	Transmission Electron Microscopy
TX 1 – 5	Five different concentrations of Triton X-100, used in the study
ug/ml	Microgram per millilitre
VitE-$O^{\cdot}$	α-tocopheroxyl radical
VLDL	Very low density lipoproteins

Table of Contents

List of Figures

Chapter 1: Introduction

"Be the change you want to see in this world . . ."

Mahathma Gandhi, humanitarian

First identified in 1940, Coenzyme Q10 (CoQ10) discovery was not a simple accident, but the result of a long train of investigation into the mechanism of, and compounds involved in biological energy conversion (Horowitz, 2003 and Crane, 2007). It is a lipid-soluble component of virtually all cell membranes, and is located in the hydrophobic domain of the phospholipid bilayer of cellular membranes (Quinzii *et al*., 2007a and Sohal *et al*., 2007). Coenzymes are cofactors upon which the comparatively large and complex enzymes absolutely depend for their function (Langsjoen, 1994). Coenzyme Q10 is the only endogenously synthesized lipid with a redox function in mammals and exhibits a broad tissue as well as intracellular distribution (Dallner *et al*., 2000). It is also the only known lipid-soluble antioxidant that animal cells can synthesize *de novo*, and for which there exist enzymatic mechanisms which can regenerate it from its oxidized product formed in the course of its antioxidant function (Ernster *et al*., 1995). In the human CoQ10 is biosynthesized from tyrosine through a cascade of eight aromatic precursors, via the mevalonate pathway (Folkers, 1996). Cells generally rely on *de novo* synthesis for their supply of Coenzyme Q, and its levels are subjected to regulation by physiological factors that are related to the oxidative activity of the organism (Tran *et al*., 2007 and Ernster *et al*., 1995). Current knowledge about the biosynthetic pathway of CoQ10 is mostly derived from characterization of accumulating intermediates in Q-deficient mutant strains of *Saccharomyces cerevisiae*, and so far nine complementation groups of Q-deficient yeast mutants have been identified (*COQ1 – COQ9*) (Tran *et al*., 2007).

Coenzyme Q is composed of a tyrosine-derived quinone ring, linked to a polyisoprenoid side chain, consisting of 9 or 10 subunits in higher invertebrates and mammals (Ernster *et al*., 1995). The benzoquinone ring can assume three alternate redox states: the fully oxidized or ubiqunone (Q); the univalently reduced ($1e^- + 1H^+$) ubisemiquinone ($^{\cdot}QH$), a free radical; and the fully reduced ($2e^- + 2H^+$) ubiquinol (Sohal *et al*., 2007). The polyisoprenyl chain apparently facilitates the stability of the molecule within the hydrophobic lipid bilayer. The length of the chain seems to affect the mobility,

intermolecular interaction with membrane proteins, and autoxidizability (Sohal *et al*., 2007). There are a number of indications that CoQ10 is not always functioning by its direct presence at the site of action, but also using receptor expression modifications, signal transduction mechanisms and action through its metabolites (Turunen *et al*., 2004). The physiological roles of CoQ10 in biological systems are most well characterized in the inner mitochondrial membrane, where three of its main functions are: a) carrier of electrons from respiratory complexes I and II to complex III, b) generation of superoxide anion radical by autoxidation of ubisemiquinone and c) anti-oxidant quenching of free radicals (Sohal *et al*., 2007). Coenzyme Q10 is present in all cells and membranes and in addition to be a member of the mitochondrial respiratory chain it has several other functions of great importance in cellular metabolism (Turunen *et al*., 2004). Even greater significance was apparent when it was shown that reduced CoQ10 could restore antioxidant function to oxidized tocopherol. This is important because endomembranes have enzymes that can reduce CoQ10, but none for reduction of oxidized tocopherol directly (Crane, 2007).

The CoQ10 levels in the body increase from birth up to the age of 20 – 30 years, followed by a successive decrease to the initial birth level at around the age of 80 years. The final content of CoQ10 in human cells is a consequence of both synthesis rate and catabolism (Dallner *et al*., 2000 and Fernández-Ayala *et al*., 2005). The CoQ10 content is also altered in a number of diseases of which the decrease in cardiomyopathies and degenerative muscle diseases are the most studied (Turunen *et al*., 2004). Coenzyme Q10 is commonly used for treatment of cardiomyopathy and there is substantial evidence that heart function is improved upon administration of the lipid (Langsjoen *et al*., 1999). Coenzyme Q10 has been suggested to be involved in neurodegenerative diseases such as Huntington's disease, Parkinson's disease, amyotrophic lateral sclerosis (ALS), and Friedrich's ataxia (FRDA), where these disorders responded to oral CoQ10 supplementation (Turunen *et al*., 2004; Quinzii *et al*., 2007 and Quinzii *et al*., 2007b). Coenzyme Q10 has been seen to enhance the immune function in patients with AIDS (Mutter, 2003). Geromel *et al*., 2002, found that 200mg of CoQ10 per day, taken for 12 weeks, improved glycemic control and blood pressure in patients with type 2 diabetes. A deficiency of CoQ10 has been found in gingival biopsy tissue from patients with advanced periodontal disease (Horowitz, 2003). Dramatic improvement with topically applied CoQ10 was found in patients who could no longer eat solid food because of the severity of their gum disorder (Murray, 2000). In its role as an

antioxidant, CoQ10 acts to prevent damage caused by lipid oxidation in sperm cell membranes and thus, is pivotal to sperm motility (Horowitz, 2003). A study done by Gazdik *et al*., 2002, found decreased concentrations of CoQ10 in the blood of patients with autoimmune asthma. The complexity of the biosynthesis of CoQ10 suggests that defects in different biosynthetic enzymes or regulatory proteins may cause different clinical syndromes (Quinzii *et al*., 2007b).

The importance of CoQ10 in the life of living organisms is illuminated most clearly by the number of reports describing the genetic disorders in which CoQ10 synthesis is impaired. Lowered lipid content in organs causes serious metabolic disturbances, but CoQ10 supplementation reestablishes mitochondrial and other functions (Turunen *et al*., 2004). The molecular bases and pathogenic mechanisms of the various primary and secondary forms of CoQ10 deficiency remain largely unknown (Quinzii *et al*., 2007a). To date, primary CoQ10 deficiency has been genetically and biochemically proven in just a few patients with infantile multi-systemic severe diseases, where nephropathy and encephalopathy seems to be the most consistent feature. However, CoQ10 deficiency should be considered in the differential diagnosis of subacute exercise intolerance and weakness and of all genetically undefined adult-onset cases of cerebellar ataxia, as well as in patients with ataxia-oculomotor-aprataxia type 1 (AOA1), because CoQ10 supplementation seems to improve muscle weakness and other associated symptoms in some individuals (Quinzii *et al*., 2007a).

Since CoQ10 is essential to the optimal function of all cell types, it is not surprising to find a seemingly diverse number of disease states which respond favorably to CoQ10 supplementation. All metabolically active tissues are highly sensitive to a deficiency of CoQ10, and its function as a free radical scavenger only adds to the protean manifestations of CoQ10 deficiency (Lansjoen, 1994). It is therefore necessary to expand this field of research in order to increase awareness on this nonpatentable supplement, vital for normal physiological functioning and health. One aspect that appears to be sparsely researched is the effect of CoQ10 on cell membranes, which inspired the direction of this study to investigate the cellular effects of CoQ10 in the presence of Triton X-100 on primary chicken heart and skeletal muscle cell cultures. To gain a broader background regarding the numerous properties, advances, and physiological mechanisms of this coenzyme, the literature regarding these aspects will be reviewed in Chapter 2. It was incidentally, while reviewing the literature that it became

apparent that there exists a correlation between the structures of Triton X-100, chosen to produce the desired membrane disrupting effect in this study, and nonylphenol, an endocrine disruptor well known for its estrogen mimicking effect. The question arose whether Triton X-100, in addition to its properties as membrane solublizing detergent, might induce estrogenic activity. The outcome of the investigation gained insight on a substance that call for further investigation and is presented in Chapter 3.

In order to investigate the cellular effect of Triton X-100 and CoQ10 on heart and muscle cell cultures, from chick embryos, the establishment and optimization of an appropriate cell culture system was needed. The concentration range selected to represent the properties of CoQ10 and Triton X-100 in the cell culture, needed optimization, and was tested, alone, and in combination, for cytotoxicity, more specifically their effect on cell viability, lysosomal membrane integrity and cell number, in order to provide some parameter of expectation. The procedures and results that commence the outcome of this study are presented in Chapter 4. In order to address the limitations of our knowledge on the membrane protective properties of CoQ10 and to expand on the limited literature available on the membrane protective properties of CoQ10, its cellular effect alone and in the presence of the well known membrane disrupter, Triton X-100 was evaluated, by using scanning electron microscopy (SEM), which provided surface visualization of the three dimensional appearance of the extracellular cell surface, more specifically the morphology and structure of the cell membrane and alterations thereof. These results are presented in Chapter 5. In order to substantiate the findings in Chapter 5, confocal microscopy was done to provide insight on the intracellular effects brought about in the cell cultures upon exposure to CoQ10 and Triton X-100, and to correlate the intracellular information with the extracellular information obtained with SEM. The correlation is confirmed in Chapter 6.

Chapter 2: Literature Review

2.1 Introduction

"We are now in a position to witness the unfolding of the greatest medical tragedy of all time - never before in history has the medical establishment knowingly created a life-threatening nutrient deficiency in millions of otherwise healthy people."

- Peter H. Langsjoen, MD

2.1.1 History

Coenzyme Q10 was first isolated from beef heart mitochondria by doctor Frederick Crane (University of Wisconsin, USA), in 1957 (Crane *et al*., 1957). During the same year professor RA Morton from England, defined a compound obtained from vitamin A deficient rat liver to be the same as CoQ10 (Morton, 1957). He introduced the name ubiquinone, meaning “the ubiquitous quinone” (ubiquitous = found everywhere). In 1958, professor Karl Folkers and coworkers at Merck, Inc., determined the precise chemical structure of CoQ10, synthesized it, and became the first to produce it by the process of fermentation (Langsjoen, 1994). Professor Yamamura of Japan became the world’s first to treat a human disease, congestive heart failure, with coenzyme Q7, a compound related to CoQ10, in the mid-1960’s. Other practical uses then followed and in 1966, Mellors *et al*., showed that reduced Coenzyme Q6 revealed effective antioxidant properties. In 1972 the Italian, Gian Paolo Littarru and professor Karl Folkers documented a deficiency of CoQ10 in human heart disease (Littarru *et al*., 1972). By the mid-1970’s, the Japanese perfected industrial technology to produce pure CoQ10 in quantities sufficient for larger clinical trials (Langsjoen, 1994). In 1978 Peter Mitchell received the Nobel Prize for his contribution to the understanding of biological energy transfer that occurs at cellular level, through the chemiosmotic theory, which includes the vital role of CoQ10 in energy transfer systems (Langsjoen, 1994). In 1986 professor Karl Folkers received the Priestly Medal from the American Chemical Society and in 1990 the National Medal of Science from President Bush for his work with CoQ10 and other vitamins (Langsjoen, 1994). In the late 1980’s, promotion of CoQ10 supplements in capsule form began to reach health care professionals. In the 1990’s, direct marketing to

consumers became available to people who presumably might not meet their CoQ10 requirements via biosynthesis and normal dietary intake of 5 – 10 mg per day (Horowitz, 2003).

2.1.2 Background

Coenzyme Q10, also known as CoQ10, CoQ, Ubiquinone Q10, Ubidecarenone, Vitamin 10 or ubiquinone, is a naturally occurring quinone that is found in most aerobic organisms from bacteria to mammals. It is a natural human quinone, found naturally in the energy producing center of the cell, known as the mitochondria (Shinde *et al*., 2005), but it can be chemically synthesized (Collins *et al*., 1999). Coenzyme Q10 is not a drug, it is essentially a vitamin or vitamin-like, fat-soluble coenzyme found everywhere in the body. Coenzymes are cofactors upon which the comparatively large and complex enzymes absolutely depend for their function. Coenzyme Q10 is also a potent antioxidant, as is its reduced product, ubiquinol-10. It is the only known naturally occurring lipid soluble antioxidant for which the body has enzyme systems capable of regenerating the active reduced form, ubiquinol (Escolar *et al*., 2001). Antioxidants are substances that scavenge free radicals, damaging compounds in the body that alter cell membranes, tamper with DNA, and even cause cell death. Free radicals occur naturally in the body, but environmental toxins such as radiation, cigarette smoke, ultraviolet light and air pollution, can increase the number of these damaging particles (Shinde *et al*., 2005). Antioxidants such as CoQ10 can neutralize free radicals and reduce or even help prevent some of the damage they cause (Al-Hasso, 2001). Coenzyme Q10 is the coenzyme for at least three mitochondrial enzymes (complexes I, II and III) as well as enzymes in other parts of the cell. Mitochondrial enzymes of the oxidative phosphorylation pathway are essential for the production of the high-energy phosphate, adenosine triphosphate (ATP), upon which all cellular functions depend (Langsjoen, 1994). It is now believed that CoQ10 is the key nutrient for generating 95% of the total energy required by the human body (Fonorow, 2006).

The highest concentrations of CoQ10 have been measured in vital organs such as the heart and pancreas (Fonorow, 2006). Its biosynthesis from the amino acid tyrosine, is a complex, multistage process, requiring several vitamins and trace elements (Post, 2005). An age-dependent decrease in CoQ10 has been documented; peak serum levels occur at age 19 to 21 years of age, and drop by up to 65% by the age of 80 years

(Harmon, 1988). Other factors leading to CoQ10 deficiency include inadequate dietary intake, environmental stress, strenuous exercise, and selected drugs. Deficiencies has also been reported in various disease conditions, including congestive heart failure (CHF), cardiomyopathy, chronic obstructive pulmonary disease (COPD), acquired immunodeficiency syndrome (AIDS), cancer, hypertension, and periodontal disease (Fuke *et al*., 2002). When taken orally, it is slowly absorbed by the gastrointestinal tract and transported in serum within chylomicrons. Blood levels in normal individuals range from 0.6-1.0 ug/ml (Karlsson *et al*., 1993) and its plasma concentration mirrors the metabolic demand in various tissues (Escolar *et al*., 2001). Several studies have shown that exogenous supplementation of CoQ10 results in elevation of blood levels (Turunen *et al*., 1999), with two concentration peaks in serum, the first at 6.5 ±1.5 hr and the second at 24 hr. After its absorption, CoQ10 is deposited in the liver and packaged into VLDL lipoproteins that return to the circulation about 24 hr later. Coenzyme Q10 has a relatively long plasma half-life (33.19±5.32 hr) (Tomono *et al*., 1986).

2.2 Biosynthesis of CoQ10

2.2.1 The Chemical Structure and Chemical Properties

The chemical name for CoQ10 is 2,3-dimethoxy-5-methylbenzoquinone. It is the predominant human form of endogenous ubiquinone and is synthesized in the mitochondrial innermembrane (Quinzii *et al*., 2007a). Coenzyme Q10 is comprised of a ubiquinone head group (a quinone ring, capable of transferring electrons) attached to a tail of 10 five-carbon isoprenoid units, that anchor the molecule to the cytoplasmic or mitochondrial membranes (Turunen *et al*., 2004), and is structurally similar to vitamin K (Greenberg *et al*., 1990). The 10-isoprenoid side chain with 10-isoprene units and a total of 50 carbon atoms are biosynthetically derived from mevalonic acid (Folkers, 1996). In humans CoQ10 is found in relatively higher concentrations in cells with high energy requirements such as the heart, liver, muscle and pancreas (Fuke *et al*., 2002). Intracellularly, 40 – 50 % is found in the mitochondrial membrane. Peak blood levels occur 5 – 10 hours after ingestion, and the elimination half-life is 34 hours. It is preliminary excreted through the biliary tract (Collins *et al*., 1999).

CoQ10 can exist in three oxidation states (Misner, 2005):

1. Fully reduced ubiquinol form ($CoQH_2$)
2. Radical semiquinone intermediate ($CoQH^-$)
3. Fully oxidized ubiquinone form (CoQ)

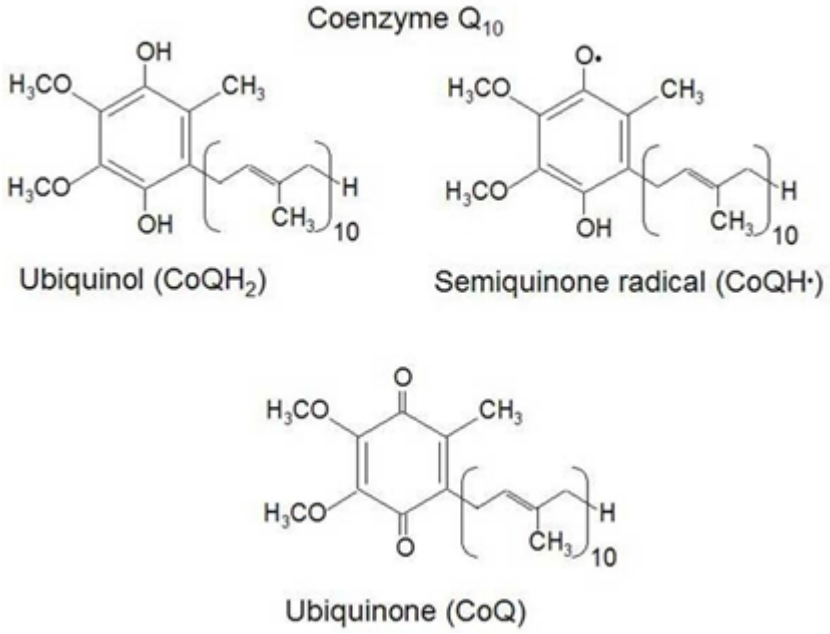

Figure 2.1: The chemical structure of CoQ10 (Shinde *et al*., 2005).

The all *trans* polyisoprene ensures an affinity for the interior of cell membranes. The two methoxy groups contribute to the specificity in enzyme action, as may the methyl group (Crane, 2001). The fully substituted quinone ring is the functional group and does not allow addition reactions with thiol groups in the cell such as thioctic acid, thioredoxin or glutathione. By reduction of the quinone to quinol, a carrier of protons and electrons is produced (Crane, 2001).

2.2.2 The Biosynthetic Pathway of CoQ10

CoQ10 can be produced by chemical synthesis, semi-chemical synthesis and microbial conversion. Biotechnological production has been done using various genera, such as *Agrobacterium*, *Rhodobacter* and *Paracoccus* (Choi *et al*., 2005). The pathway for CoQ10 is typically composed of three parts: the synthesis of a quinonoid ring, synthesis of decaprenyl diphosphate (decaprenyl diphosphate synthase produses a unique hydrophobic tail composed of ten isoprenoid units) and quinonoid ring modification (basically where the head and tail groups are combined and the reaction product are transferred to the membrane). There are differences in supplying precursors for prokaryotes and eukaryotes (Choi *et al*., 2005).

Intracellular synthesis is the major source of CoQ10, although a small proportion is acquired through diet. It has been shown that ubiquinone in animal cells occurs, in addition to the mitochondria, in the endoplasmic reticulum, the Golgi apparatus, the lysomes, the peroxisomes, and the plasma membrane (Ernster *et al*., 1995). According to evidence, ubiquinone synthesis begins in the endoplasmic reticulum and is completed in the Golgi membranes from where the quinone is transported to various other cellular locations (Ernster *et al*., 1995). It is also discharged, although to a limited extend, across the plasma membrane to the blood, where it binds serum lipoproteins (Ernster *et al*., 1995). The complexity of the biosynthesis suggests that defects in different biosynthetic enzymes or regulatory proteins may cause different clinical syndromes (Quinzii *et al*., 2007b). In order to understand the apparent effectiveness of CoQ10 in therapies, it is imperative to understand the basic questions that still exist regarding the *de novo* synthesis of CoQ10 and the mechanisms by which it is transported to and from mitochondrial sites (Clarke, 2000).

In the human, CoQ10 is biosynthesized from the amino acid, tyrosine, through a cascade of eight aromatic precursors. These precursors indispensably require eight vitamins, which are: 5,6,2,8-tetrahydrobiopterin, Vitamin B6, Vitamin C, Vitamin B2, Vitamin B12, Folic acid, Niacin and Pantothenic acid (Folkers, 1996). In 1971 Whistance *et al*., reported that the intermediates involved in the conversion of para-hydroxybenzoic acid to ubiquinones by higher animals have still to be defined, although there would appear to be evidence that they are the same as those which participate in the biosynthesis of ubiquinones by photosynthetic and some non-photosynthetic gram-

negative bacteria. In 2002 Kawamukai reported that several genes for the biosynthesis of ubiquinone in animals and plants have been reported, but that genes are basically similar to those from *Saccharomyces cerevisiae* (a yeast intensively studied for the biosynthesis of ubiquinone), and therefore it is considered that the eukaryotic type of biosynthesis is common.

Para-hydroxybenzoic acid is the first aromatic precursor from the essential amino acid, tyrosine, in the biosynthesis of CoQ10 in animals (Folkers, 1996). In yeasts, hydroxybenzoic acid is synthesized from chorismate via the shikimate pathway (Goewert, 1980). The building blocks for the synthesis of the polyisoprenyl chain are provided by dimethylallyl diphosphate and isopentenyl diphosphate (Tran *et al*., 2007). Isopentenyl diphosphate (IPP) is an important precursor in CoQ10 biosynthesis and in the biosynthesis of cholesterol, cartenoid and prenylated proteins (Choi *et al*., 2005). It is derived from acetyl-coenzyme A via the mevalonate pathway in humans, yeasts, and archaebacteria, and the non-mevalonate pathway used by eubacteria, green algae and chloroplasts of higher plants (Kuzuyama, 2002 and Eisenreich *et al*., 2004). This leads to the formation of farnesyl-PP, which after conversion to decarpenyl-PP condenses with 4-hydroxybenzoic acid to decaprenoyl-4-hydroxybenzoate, which is then converted to ubiquinone in a number of additional reaction steps (Ernster *et al*., 1995).

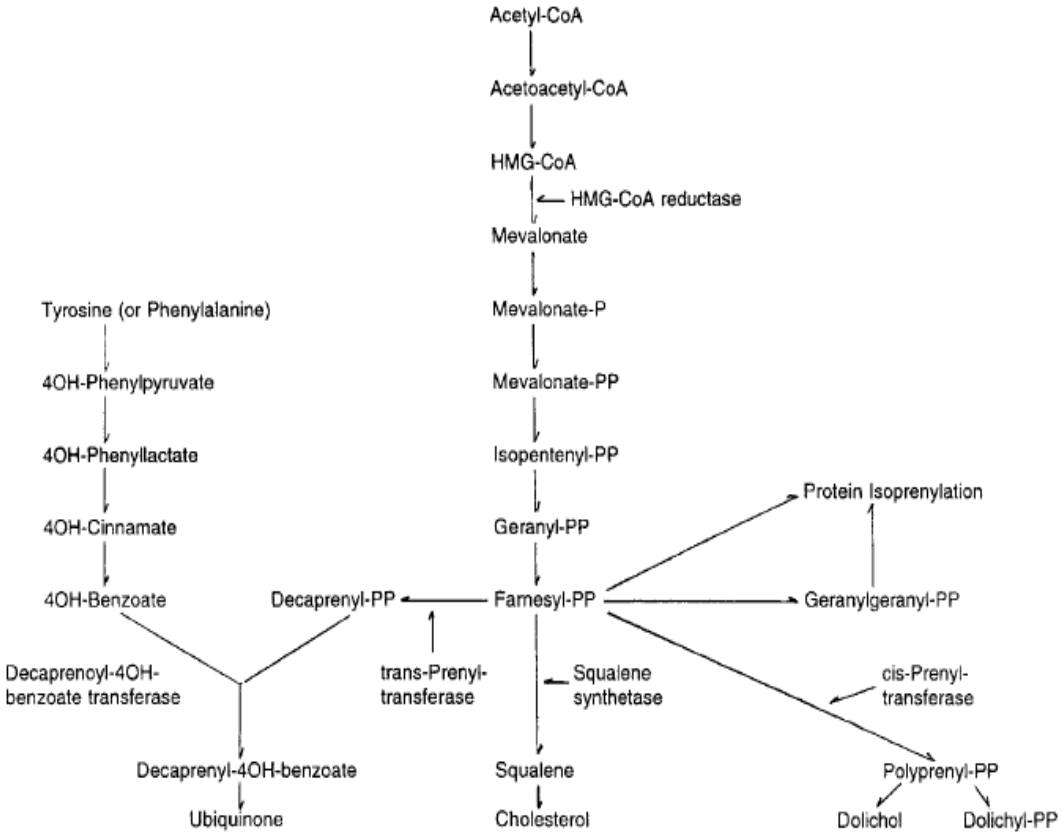

Figure 2.2: Reaction pathways of the biosynthesis of ubiquinone, cholesterol and dolichol (Ernster *et al*., 1995).

Clarke, 2000, reported evidence which suggested that the yeast *S. cerevisiae* provides an excellent prototype of a eukaryotic Q-biosynthetic pathway, and claimed that it can be used to answer fundamental questions about Q biosynthesis in higher eukaryotes. *S. cerevisiae* can synthesize Q from either chorismate or tyrosine (Meganathan, 2001). While in yeast the tyrosine is derived from chorismate *in vivo*, it has to be provided as an essential amino acid for mammals, which lack the shikimate pathway; therefore Q is not considered a vitamin (Meganathan, 2001). The methyl groups on the benzene ring are derived from S-adenosylmethionine (SAM). As stated, the isopentenyl diphosphate required for the formation of the polyprenyl side chain in eukaryotes, is derived from the mevalonate pathway. Grünler *et al*., 1994, described the mevalonate pathway as a sequence of cellular reactions that leads to farnesyl-PP, the common substrate for the synthesis of cholesterol, dolichol, dolichyl-P and ubiquinone as well as for prenylation of proteins.

2.2.2.1 The Tail

The starting precursor for the mevalonate pathway is acetyl-CoA (Meganathan, 2001). The pathway is initiated by the transfer of an acetyl group from acetyl-CoA (Begley *et al*., 1998) to the methyl carbon of a second acetyl-CoA, resulting in the formation of acetoacetyl-CoA (Eisenrieich *et al*., 2001). In the next step of the pathway, another molecule of acetyl-CoA condenses with acetoacetyl-CoA, resulting in the formation of 3-hydroxy-3-methylglutaryl-CoA (HMG-CoA) (Lange *et al*., 2000). In a two step reaction, requiring NADPH, HMG-CoA is reduced to mevalonate (Boucher *et al*., 2000). Mevalonate is then converted to mevalonate-diphosphate by two phosphorylation steps, mediated by mevalonate kinase and phosphomevalonate kinase, respectively (Cunningham *et al*., 2000). Formation of IPP takes place in the subsequent step of the pathway where mevalonate diphosphate undergoes dehydration-decarboxylation, in an ATP requiring process (Cunningham *et al*., 2000). The isomerization of IPP to dimethylallyl diphosphate (DMAPP) then takes place and is catalyzed by an IPP isomerase (Grünler *et al*., 1994 and Qureshi *et al*., 1981). In the next step, the enzyme farnesyl-PP synthetase catalyzes the sequence tail 1'-4 coupling of IPP with DMAPP and Geranyl-PP (GPP) resulting in the formation of geranyl-PP and farnesyl-PP, respectively (Meganathan, 2001). In contrast with bacteria, the mammalian transprenyltransferase prefers geranyl-PP rather than farnesyl-PP as a substrate (Teclebrhan *et al*., 1993). Only one enzyme, farnesyl-PP synthase, is responsible for the formation of farnesyl-PP from dimethylallyl-PP and isopentenyl-PP (Poulter *et al*., 1981). Whether farnesyl-PP synthase is capable of forming geranyl-PP or if there is another enzyme responsible for synthesizing this intermediate, is not known (Dallner *et al*., 2000).

2.2.2.2 The Head

Ubiquinone contains a nonisoprenoid moiety namely the benzoate ring. This benzoate ring originates from the amino acid tyrosine, which can be synthesized from phenylalanine in animals, but the aromatic ring structure is always derived from dietary sources (Dallner *et al*., 2000). After condensation of the ring with the isoprenoid side chain, several substitutions and modifications of the benzoate ring occur. The sequence of enzymatic steps includes one decarboxylation, three hydroxylations, two O-methylations and one C-methylation to obtain the final product, a fully substituted benzoate ring, contributing to the properties of ubiquinone. The steps are not completely

understood in mammals, since most studies of ubiquinone biosynthesis have been performed on bacteria and yeast. In 2000 Dallner *et al*., reported that none of the enzymes involved have been either purified or cloned from mammals. In 2007, Tran *et al*., reported that nine complementation groups of Q-deficient yeast mutants (*COQ1* through *COQ9*) have been identified and that mammalian homologues of the yeast *COQ* genes have been identified via sequence homology.

CoQ10 is the dominant species in all human tissues, while only 2 – 7% of the total ubiquinone content is CoQ9 (Aberg *et al*., 1992), which is the main species in rats, while only 10-30% of the total ubiquinone content is CoQ10 (Dallner *et al*., 2000). In bacteria transprenyltransferase, which leads to two different products in the biosynthetic pathway, is the rate-limiting enzyme. Though it has been suggested that the hydroxylation or decarboxylation step in mammalian cells may be the rate-limiting factor, it should be emphasized that mammals, in contrast with bacteria and yeast, can not synthesize aromatic rings and that the pool of ring precursors could therefore be the rate-limiting factor. However, experiments support two other possibilities (Dallner *et al*., 2000). Polyprenyl-4-hydroxybenzoate may be a dead-end product, since it is considered a side reaction product resulting from the deacylation of a CoA derivative (Trumpower *et al*., 1974). 4-hydroxybenzoyl-CoA is a much better substrate for polyprenyl-4-hydroxybenzoate transferase than the nonactivated ring, since it was found to be 6-fold more effective as a precursor than p-hydroxybenzoate alone (Trumpower *et al*., 1974). Thus the CoA-derivatized polyprenyl-4-hydroxybenzoate may be required for the subsequent reaction leading to ubiquinone (Dallner *et al*., 2000). The second possibility is that 4-hydroxybenzoate may not be used as a substrate in mammals and instead, the more complete benzoate rings from catecholamine catabolism, protocatechuic and vanillic acid, could serve as precursors (Nambudiri *et al*., 1977). The possibility was raised that PHB, similar to fatty acids, must be activated by CoA to be able to condense with polyprenyl pyrophosphates. It was suggested that the benzoquinone ring may not be the only substrate (Forsgren *et al*., 2004). Rings modified by hydroxylation and methylation, which are supposed to take place later, may also serve as substrates in the condensation reaction (Forsgren *et al*., 2004). From a metabolic point of view these possibilities are of great interest, since some of these products are generated during catecholamine catabolism. The products could then be utilized for CoQ biosynthesis (Forsgren *et al*., 2004).

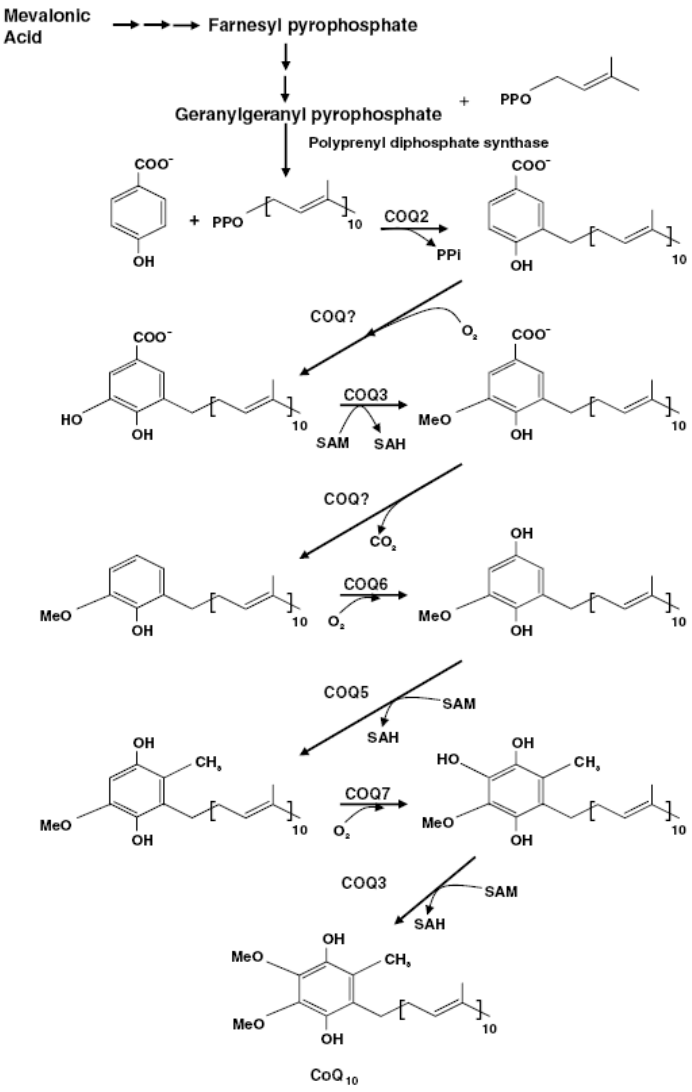

Figure 2.3: CoQ10 biosynthetic pathway with eight known biosynthetic enzymes denoted as polyprenyl diphosphosphate synthase (COQ1) and COQ2-8. Coenzyme Q10 is composed of a benzoquinone and a decaprenyl side chain. While the quinone ring is derived from amino acids tyrosine or phenylalanine, the isoprenoid side chain is produced by addition of isopentenyl pyrophosphate molecules to geranylgeranyl pyrophosphate (derived from mevalonate pathway) by decaprenyl diphosphate synthase. After para-hydroxybenzoate and decaprenyl pyrophosphate are produced, at least seven enzymes (encoded by COQ2-8) catalyze condensation, methylation, decarboxylation, and hydroxylation reactions to synthesize CoQ10 (Quinzii *et al*., 2007a).

2.3 The Genetic Link

So far nine complementation groups of Q-deficient yeast mutants (*COQ1* through *COQ9*) have been identified (Tran *et al*., 2007). Mammalian homologues of the yeast *COQ* genes have been identified via sequence homology. Human homologues of *CoQ2*, *CoQ3*, and *CoQ7* proteins were demonstrated to functionally complement the corresponding yeast null mutants, further indicating that the yeast Q-biosynthesis pathway is conserved in humans (Tran *et al*., 2007). While Coq1, Coq2, Coq3, Coq5, Coq6, and Coq7 proteins have known or proposed enzymatic functions in Q-biosynthesis, it is not clear whether other Coq proteins also possess enzymatic activities (Tran *et al*., 2007). Coq1 - Coq9 polypeptides localize to the mitochondria. *In vitro* mitochondrial import were investigated for seven of the yeast Coq polypeptides and demonstrated to be dependent on a mitochondrial membrane potential (Jonassen *et al*., 2001).

2.3.1 Function and Submitochondrial Localization of the Nine Coq Proteins (the following section refer to the study by Tran *et al*., 2007)

Coq1

Formation of the *trans*-polyprenyl diphosphate synthase tail in *S. cerevisiae* is catalyzed by the polypeptide encoded by the *COQ1* gene, which is responsible for determining the species-specific tail length of Q. The *Coq1* ortholog from the fission yeast *Schizosaccharomyces pombe* (Dps1) fails to complement the *S. cerevisiae coq1* null mutant, however, polyprenyl diphosphate synthases of fission yeast, mouse, and human, are each heterotetramers of two protein subunits, PDSS1 and PDSS2. Submitochondrial fractionation studies demonstrated that the *S. cerevisiae* Coq1 protein is peripherally associated with the inner mitochondrial membrane on the matrix side.

Coq2

The 4-HB polyprenyltransferase is a key enzyme catalyzing the attachment of the polyisoprenoid side chain to the 4-HB ring, generating the first membrane bound Q intermediate, 4-hydroxy-3-polyprenylbenzoic acid. The *S. cerevisiae* and *Homo sapiens*

gene encoding the enzyme is called *COQ2*. *In vitro* assays in isolated rat liver, demonstrated that the polyprenyl diphosphate: 4-HB activity is present mainly in the mitochondria. Polyprenyltransferases involved in Q biosynthesis generally display a lack of specificity for the chain length of the isoprenyl diphosphate substrate; however, the specificity was shown to be influenced by Mg^{2+} concentration in whole yeast extracts. Analysis of the predicted amino acid sequence of the *S. cerevisiae* Coq2 protein revealed two conserved putative substrate binding domains found in a family of polyprenyltransferases, six potential membrane spanning domains, and a typical mitochondrial targeting sequence. Coq2 protein behaves as an integral membrane protein associated to the inner mitochondrial membrane, facing the matrix side.

Coq3

Two O-methylation steps in the Q biosynthetic pathway are apparently catalyzed by the same enzyme encoded by *COQ3* gene. The amino acid sequences of the proteins encoded by these *COQ3* homologues all contain four regions that are conserved in a large family of methyltransferase enzymes utilizing S-adensymethionine (SAM or AdoMet) as the methyl donor and required a divalent cation. Like most of the other Coq polypeptides, the yeast Coq3 protein also contains a typical mitochondrial targeting sequence at the N-terminus. *In vitro* assays and subcellular localization studies showed that the Coq3 preprotein was imported and processed to the mature form in the mitochonria, in a membrane-potential-dependent manner. Submitochondrial fractionation demonstrated that it is a peripheral protein associated to the matrix side of the inner mitochondrial membrane.

Coq4

The enzymatic function of Coq4 protein, a peripheral protein associated with the inner mitochondrial membrane on the matrix side, has been a mystery. While it is appealing to speculate that Coq4 protein may serve as a hydroxylase or carboxylase in the yet-to-be-characterized step (designated Coq? In Fig 2.3), the amino acid sequence of Coq4 does not share significant homology with protein domains or motifs with known enzymatic activity. Steady-state levels of Coq3 and Coq7 proteins, which are diminished in *coq4* null mutants, are at wild-type levels in the *coq4-1* point mutation. This result together with recent work that demonstrates that the native Coq4 polypeptide co-migrates with

Coq3, Coq6, and Coq7 proteins as a high molecular mass complex indicates that the Coq4 protein has a structural role in the putative polypeptide Q biosynthetic complex.

Coq5

2-Methoxy-6-polyprenyl-1,4-benzoquinone methyltransferase catalyzes the only *C*-methylation step in the Q biosynthetic pathway, generating the 2-methoxy-5-methyl-6-polyprenyl-1,4-benzoquinone intermediate. In *S. cerevisiae*, the gene encoding this *C*-methyltransferase is designated *COQ5*. *In vitro* C-methyltransferase assays with the farnesylated analogs of the corresponding intermediates confirmed that Coq5 polypeptide is required for conversion of 2-methoxy-6-polyprenyl-1,4-benzoquinone to 2-methoxy-5-methyl-6-polyprenyl-1,4-benzoquinone in Q biosynthesis. The length of the polyisoprenoid tail does not play a crucial role in substrate recognition of Coq5 protein. Inclusion of NADH is essential for optimal enzymatic activity and is most likely required to convert the quinone to the hydroquinone, generating a nucleophile for the C-methylatransfer. Coq5 protein is peripherally associated with the inner mitochondrial membrane on the matrix side. Results suggested that Coq5 protein is essential for the stability and activity of at least two other Coq polypeptides, and provide genetic evidence for a complex of Coq polypeptides in yeast Q biosynthesis.

Coq6

COQ6 is a non-essential gene for viability, but is required for growth on non-fermentable carbon sources. The Coq6 protein is a mitochondrial protein, which is imported in a membrane-potential-dependent manner and peripherally associated with the matrix side of the inner membrane. *S. cerevisiae* Coq6 protein and its homologues in human, mouse, and *Canaerhobis. elegans*, each contains three conserved regions: an ADP-binding fingerprint, a motif with a putative dual function in FAD/NAD(P)H binding, and a consensus sequence that binds to the ribityl moiety of FAD. These conserved regions are common features of a large family of FAD-binding-aromatic hydroxylases. Consequently, Coq6 protein has been considered as a putative flavin-dependent monooxygenase responsible for adding the hydroxyl group to 4-hydroxy-3-polyprenyl benzoic acid and/or 6-methoxy-2-polyprenyl phenol, two uncharacterized hydroxylation steps in Q biosynthesis.

Coq7

Expression of *COQ7* homologues from *C. elegans*, rat, or human were shown to rescue the yeast *coq7* null mutant for growth on non-fermentable carbon resources, indicating functional conservation across species. Coq7 protein was shown to be required for the hydroxylation of 5-demethoxyubiquinol ($DMQH_2$). It was suggested that Coq7 protein is either involved in one or more mono-oxygenase steps or serves as an essential component of the putative multi-subunit enzyme complex. Biochemical function of Coq7 protein as a hydroxylase was further supported by the determination that it belongs to a family of di-iron binding oxidases containing a conserved sequence motif for the iron ligands, EXXH. It was indicated that yeast Coq7 protein functions in the hydroxylation of DMQ. Steady-state levels of the Coq3, Coq4, and Coq6 polypeptides were higher in the coq7E194K mutant than in the null mutant, suggesting that Coq7 protein and DMQ6 serve to stabilize other Coq polypeptides. Yeast Coq7 protein, like its homologues in mice, is peripherally associated to the inner membrane on the matrix side. The true nature of the Coq7 protein-membrane association awaits a structure determination for yeast Coq7p or one of its homologues.

Coq8

The *COQ8* gene was initially identified as *ABC1* for its ability to partially suppress, in multi-copy, the cytochrome b translation defect due to the cbs2-223 mutation in the *CBS2* gene, a nuclear gene encoding a translational activator of cytochrome b. Inactivation of *ABC1* resulted in respiratory defect and absence of NADH-cytochrome c reductase activity. It was subsequently shown that the respiratory complexes II, III and IV of the abc1 null mutant were thermo-sensitive, and addition of exogenous Q could partially compensate for the respiratory deficiency. These results led to a hypothesis that the *ABC1* gene product may function as a chaperone that is essential for proper conformation and activity of the bc1 and its neighboring complexes. Do *et al*., 2001 demonstrated that the *COQ8* gene required for Q biosynthesis, is the same as the *ABC1* gene and provided data indicating that Q deficiency is exclusively responsible for the pleiotropic defects of abc1/coq8 mutants. Although its biochemical function in Q biosynthesis is currently unknown, Coq8/Abc1 protein has been classified as putative protein kinase based on the identification of four kinase conserved motifs in its amino acid sequence.

Coq9

The *COQ9* gene was recently identified and characterized as a new gene that, when mutated, results in a Q-deficient phenotype, in a similar manner to other *COQ* genes. However, the function of Coq9 protein in Q biosynthesis is not yet known. Coq9 protein has no homology to proteins with known function. Based on the mobility in the SDS-PAGE, the molecular mass of Coq9 protein is about 25kDa, slightly smaller than the predicted precursor (29.9kDa), and is consistent with the removal of a putative mitochondrial targeting sequence. However, the native size of Coq9 protein estimated from its sedimentation on sucrose gradients is about three times larger, indicating that the protein is either a homo-oligomer or in a complex with other proteins, which may be Coq3 and Coq5 polypeptides, which were shown to co-sediment with the Coq9 protein. Submitochondrial localization analysis has demonstrated that Coq9 protein is a peripheral membrane protein associated with the matrix side of the mitochondrial inner membrane.

2.4 Physiological Functions of CoQ10

CoQ10 play five major physiological roles in the body (Collins *et al*., 1999):

1. It has an essential role in mitochondrial energy production through redox activity in the respiratory chain, transporting electrons between enzymes.
2. It functions as an antioxidant, inhibiting lipid peroxidation and scavenging free radicals.
3. It plays a role in extramitochondrial redox activity in the cell membrane and endomembranes.
4. It plays and important role in membrane stabilization and fluidity.
5. It has shown to prevent apoptosis by inhibiting the mitochondrial permeability transition pore (Papucci *et al*., 2003).

2.4.1 Mitochondrial Energy Production

CoQ10 is an essential part of the cellular machinery used to produce adenosine triphosphate (ATP), the energy on which the body runs. The major part of ATP production occurs in the inner mitochondrial membrane where CoQ10 is present (Crane, 2001). The unique function of CoQ10 is given by its ability to transfer electrons from the primary substrates to the oxidase system at the same time that it transfers protons to the outside of the mitochondrial membrane, resulting in a proton gradient across the membrane. As the protons return to the interior through the enzymatic machinery for making ATP, they drive the formation of ATP (Crane, 2001).

2.4.1.1 The Cellular Machinery

Energy generation in mitochondria occurs primarily through oxidative phosphorylation (OXPHOS), a process in which electrons are passed along a series of carrier molecules called the electron transport chain. The OXPHOS molecular system, which is embedded in the lipid bilayer of the mitochondrial inner membrane, consists of electron acceptors, coenzyme Q and cytochrome c, and five multisubunit protein complexes (complexes I-V) (Van den Heuvel *et al*., 2001). The electrons are generated from reduced nicotinamide adenine dinucleotide (NADH) and flavin adenine dinucleotide ($FADH_2$), which are produced by oxidation of nutrients such as glucose, and are ultimately transferred to molecular oxygen. The electron transport chain consists of four respiratory enzyme complexes arranged in a specific orientation in the mitochondrial inner membrane. The passage of electrons between these complexes releases energy that is stored in the form of a proton gradient across the membrane and is then used by ATP synthase to make ATP from adensine 5'-diphosphate (ADP) and phosphate by the fifth complex (Van den Heuvel *et al*., 2001). The ATP that is synthesized is then used for energy-requiring reactions in the matrix and is exported to the cytosol by the adenine nucleotide translocator, in exchange for cytosolic ADP.

Complex I (NADH:ubiquinone oxireductase):

The overall function of human complex I is the dehydrogenation of NADH and the transportation of electrons to coenzyme Q. This is the primary reductase where coenzyme Q is reduced by NADH (Crane, 2001). The electron transport is coupled to the translocation of protons across the mitochondrial inner membrane and creates a

proton gradient that is the proton-motive force for the production of ATP by F_1-F_0 ATP-synthetase (Van den Heuvel *et al*., 2001). During the reduction process, four protons are transported across the membrane for every coenzyme Q reduced (Crane, 2001). It has been proposed that coenzyme Q is reduced and reoxidized in the complex twice before electrons are transferred to a second loosely bound coenzyme Q, to form ubiquinol, which can travel through the lipid in the membrane to complex III, where the quinol is oxidized again, with transfer of protons across the membrane (Crane, 2001).

Complex II (succinate:ubiquinone oxidoreductase):

Human complex II catalyses the oxidation of succinate to fumarate during which electrons are transported from $FADH_2$ to the ubiquinone pool. The complex can be resolved into a soluble active succinate dehydrogenase (SDH), which is anchored to the matrix face of the inner mitochondrial membrane by two smaller subunits carrying cytochrome b558 and the ubiquinone-binding site, and a membrane-anchoring fraction (Van den Heuvel *et al*., 2001).

Complex III (decylubiquinol:cytochrome c oxidase):

Human complex III (cytochrome bc_1) catalyzes the electron transfer from ubiquinol to cytochrome c with the coupled translocation of protons across the inner mitochondrial membrane (Van den Heuvel *et al*., 2001). As in complex I, there is a cyclic oxidation-reduction-reoxidation with the oxidation and proton release step always on the outside, so that the proteins are released in the right direction (Crane, 2001). The mechanism by which electrons are transferred through the redox centers of complex III and the protons are translocated from the matrix side to the intermembrane space is called the protonmotive Q cycle (Van den Heuvel *et al*., 2001). The protonmotive Q cycle involves divergent oxidation of two molecules of ubiquinol (QH_2) and recycling of one electron from each oxidation through the bc_1 complex, while the second electron from each oxidation is passed through the Rieske iron-sulfur cluster and cytochrome c_1 *en route* to cytochrome c. Re-reduction of one molecule of ubiquinone via a stable semiquinone intermediate, is brought about by the two electrons that are recycled through the enzyme. The oxidation of two molecules of ubiquinol releases four protons to the intermembrane space, while re-reduction of ubiquionone results in the uptake of two protons from the matrix (Mitchell, 1975a; Trumpower, 1990; Hunte *et al*., 2003). The quinone cycle thus doubles the efficiency of coenzyme Q in building up the proton

charge across the membrane which allows twice as much ATP production than a simple one step oxidation of quinol (Crane, 2001). After the cycle is completed the oxidized quinone migrates through the membrane to be reduced at complex I (Crane, 2001).

Complex IV (cytochrome c oxidase):

Human complex IV (COX) is the last enzyme complex of the respiratory chain. It couples the transfer of electrons from reduced cytochrome c to oxygen, leading to a translocation of protons across the inner mitochondrial membrane. The resulting electrochemical gradient is used to drive the synthesis of ATP. The COX complex contains two copper atoms and two unique heme A iron porphyrins as redox centre, which are bound to a multisubunit protein frame that is embedded in the inner mitochondrial membrane (Van den Heuvel *et al*., 2001).

Complex V (F_0-F_1 ATP synthetase):

Human complex V catalyses the synthesis of ATP from ADP and P_i, using the energy of the proton motive force across the inner mitochondrial membrane (Van den Heuvel *et al*., 2001). The present consensus is that translocation of three protons drives the synthesis of one molecule of ATP, although it has sometimes been stated that only two protons are necessary (Brand, 1994). The F0 segment serves as a proton-conduction channel, allowing the transduction of the energy of the proton gradient and the membrane potential, through the connecting stalk subunits into the ATP-synthesizing F1 segment of the ATPase (Van den Heuvel *et al*., 2001).

The essential aspects of quinone function in energy transduction leading to ATP formation in the inner mitochondrial membranes, the plasma membrane of microbes, chromatophores, and chloroplasts, are control of the formation of hydroquinone and directed anisotropic hydroquinone movement to transfer protons across the membrane while electrons are transferred along a redox gradient (Mitchell, 1990).

2.4.2 Antioxidant Properties

Free radicals are highly reactive molecules or chemical species containing unpaired electrons that cause oxidative stress, which can be defined as an imbalance between antioxidants in favour of the oxidants, potentially leading to damage (Sies, 1997). They

are formed during normal physiological metabolism or caused by toxins in the environment. Oxidative stress can damage lipids, proteins, enzymes, carbohydrates and DNA in cells and tissue, leading to membrane damage, fragmentation or random cross linking of molecules like DNA, enzymes and structural proteins and ultimately lead to cell death induced by DNA fragmentation and lipid peroxidation (Beckman et al., 1998). The basis of our life on earth is the oxygen present in the atmosphere, but it can, under a number of conditions be a very toxic substance (Bentinger *et al*., 2007). Derivatives such as hydroxyl and superoxide radicals, hydrogen peroxide and singlet oxygen may be formed and are called reactive oxygen species (ROS). ROS appear not only in diseases but also under normal physiological conditions and interact with basic tissue components with consequences of disturbed function. Various types of antioxidant systems are available in all organisms for limitation and elimination of these unwanted species (Bentinger *et al*., 2007). The functional activity of the mitochondria greatly influences the extend of ROS formation, low levels of ADP and high mitochondrial membrane potential gives high levels of ROS, whereas high ADP levels and low membrane potential result in low production of ROS (Bentinger *et al*., 2007). Mitochondrial electron transport is accounted for two-thirds of the cellular oxygen consumption, and the observed limited leakage of electrons, 1 - 2%, is the largest contribution to the cellular O_2^- and H_2O_2 production (Papa *et al*., 1997).

Antioxidants are substances which counteract free radicals and prevent the damage caused by them (Venkat Ratnam *et al*., 2006). Antioxidants are enzymes and nonenzymatic agents that can prevent the formation of, or remove ROS (Turunen *et al*., 2004). There are four major groups of naturally occurring lipid soluble antioxidants, carotenoids, tocopherols, estrogens and coenzyme Q (Bentinger *et al*., 2007). Antioxidant enzymes include superoxide dimutase and various peroxidases such as glutathione peroxidase, catalase, thioredoxin reductase and peroxiredoxin. Nonenzymatic agents include vitamins C and E, cartenoids, glutathione, α-lipoic acid, flavinoids and the reduced form of CoQ, $CoQH_2$ that all rely on a mechanism of regeneration in the cell (Turunen *et al*., 2004). Mitochondrial $CoQH_2$ is efficiently regenerated by the respiratory chain and is normally kept in a highly reduced state (Aberg *et al*., 1992). Experiments on liposomes, mitochondria, microsomes, beef heart submitochondrial particles and lipoproteins of the blood, demonstrated that coenzyme Q in reduced form, ubiquinol, is an effective antioxidant and inhibits lipid peroxidation

(Bentinger *et al*., 2007). Bentinger *et al*., reported in 2007 that CoQ is our only endogenously synthesized lipid soluble antioxidant, and is mainly present in the activated (reduced) form. CoQ's effectiveness as lipid peroxidation inhibitor is based on its complex interaction during the process of peroxidation. The primary action is the prevention of lipid peroxyl radicals ($LOO^{\cdot}$) production during the initiation process, the first phase of the process, where an abstraction of a hydrogen atom from a methylene group of a fatty acid occurs, presupposing that it has several double bonds. $CoQH_2$ reduces the initiating perferryl radical with the formation of ubisemiquinone and H_2O_2. It is also possible that $CoQH_2$ eliminates $LOO^{\cdot}$ directly. The reduced lipid effectively regenerates vitamin E from the α-tocopheroxyl radical (Bentinger *et al*., 2007).

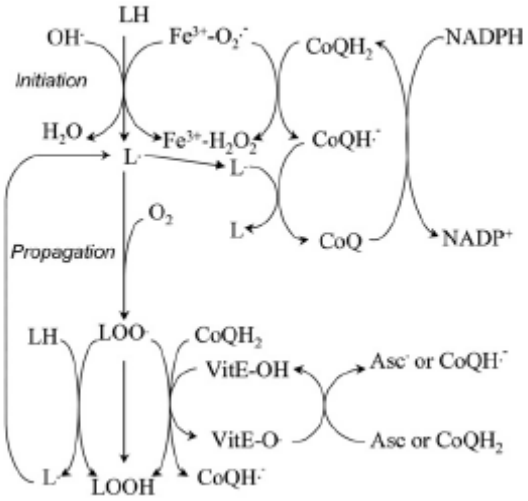

Figure 2.4: Sites of action of CoQ on lipid peroxidation. LH, polyunsaturated fatty acid; OH^{-}, hydroxyl radical; $Fe^{3}O_2^{\cdot -}$, perferryl radical; $CoQH_2$, reduced coenzyme Q; $CoQH^{\cdot -}$; ubisemiquinone; $L^{\cdot}$, carbon-centered radical; $LOO^{\cdot}$, lipid peroxyl radical; LOOH, lipid hydroperoxide; $VitE\text{-}O^{\cdot}$, α-tocopheroxyl radical; $asc^{\cdot}$, ascorbyl radical (Bentinger *et al*., 2007).

There are several mechanisms in protein oxidation and it appears that the most common is the direct oxidation of amino acid residues (Stadtman *et al*., 2000). Protein oxidation may also occur by lipid-derived free radicals and by breakdown products of phospholipid hyperperoxides. These compounds link covalently to basic amino acid residues and in the latter case also to sulfhydryl groups, causing intra- and intermolecular cross-linking (Bentinger *et al*., 2007). CoQ is effective in preventing protein oxidation by quenching the initiating perferryl radical and functioning as a chain-breaking antioxidant, thus preventing the process of propagation, the second phase in lipid peroxidation, where

$LOO^{\cdot}$ abstracts a hydrogen atom from an additional unsaturated fatty acid, leading to $L^{\cdot}$ and lipid hyperoxide (LOOH), which can be reoxidized to $LOO^{\cdot}$, which reinitiates lipid peroxidation (Bentinger *et al*., 2007). The sensitivity of proteins to oxidative stress depends on their structure, composition and localization. The close special relationship of CoQ to the neighboring membrane proteins is the main factor for its protective effect against protein oxidation (Bentinger *et al*., 2007).

CoQ also protect DNA against oxidative damage, which is of particular interest for mitochondrial DNA, since damage is not easily reparable (Bentinger *et al*., 2007). Oxidative stress may damage DNA by initiating a series of metabolic reactions in the cell leading to activation of nuclease enzymes that cleave the DNA backbone. A more common event is the interaction of H_2O_2 with metal ions bound to DNA which leads to the generation of hydroxyl radicals. DNA oxidation in isolated mitochondria takes place in the presence of ADP-Fe^{3+} and ascorbate, resulting in elevated content of 8-hydroxy-deoxyguanosine (8-OH-dG) (Ernster *et al*., 1995). Incubation in the presence of succinate and antimycin, which maximize the endogenous ubiquinol pool, eliminate the oxidative damage and decrease the increased strand breaks caused by ADP-Fe^{3+} (Bentinger *et al*., 2007). In mitochondria, ubisemiquinone radical is formed during respiration which is effectively reduced to ubiquinol by the “protonmotive Q cycle” described by Mitchell in 1975b. The large reducing capacity of the cell which is able to regenerate CoQ by reduction at all locations of the cell, is a very important property, contributing to the effectiveness of CoQ as an antioxidant (Bentinger *et al*., 2007). Supplemetation of CoQ is performed prophylactically to control oxidative events associated with oxygen radicals and therapeutically for the treatment of diseases related to impaired mitochondrial energy output (Mortensen, 1993).

2.4.3 Antiapoptotic Effect

Oxidative stress leads to mitochondrial dysfunction, which triggers the opening of the permeability transition pores (PTP), and the release of pro-apoptotic factors, causing cell death (Naderi *et al*., 2006). Physiological programmed cell death or apoptosis is essential for the maintenance of tissue homeostasis as it is responsible for the removal of damaged and infected cells. Apoptosis can be initiated through two major pathways; the extrinsic pathway (plasma membrane death receptor-dependent pathway) and the intrinsic pathway (mitochondrion-dependent pathway). Mitochondrial depolarization and

dysfunction play an important role in the intrinsic pathway, the initial steps in this pathway is represented by the opening of the PTP, followed by the collapse of inner mitochondrial membrane potential and release of pro-apoptotic factors such as cytochrome c and/or apoptosis inducing factor (AIF) (Green *et al*., 1998 and Reed, 2000). The mitochondrial permeability transition pore (PTP) is a complex, large conductance channel that plays a pivotal role in triggering apoptosis (Green *et al*., 1998). The opening of the PTP is responsible for the disruption of the mitochondrial transmembrane electrochemical gradient from -180 to 0 mV (Papucci *et al*., 2003). Ca^{2+} is the single most important factor for PTP opening *in vitro* (Walter *et al*., 2000). The inner membrane of the mitochondria has a low permeability to ions and solutes in order to permit energy conservation in the form of an electron and a pH gradient over the membrane. In order to facilitate trans-membranous transport, the inner membrane contains a number of macromolecule transporters and ion channels (Turunen *et al*., 2004). The mitochondria can undergo a generalized increase of permeability of the inner membrane under *in vitro* accumulation of Ca^{2+}. This is known as permeability transition (Turunen *et al*., 2004) and enables macromolecules with a size of approximately 1500 Da to cross the membrane, causing collapse of the protonmotive force, disruption of ionic status, loss of pyridine nucleotides, and hydrolysis of ATP (Fontaine *et al*., 1999). The PTP behaves like a voltage-dependent channel favoring a closed conformation at high membrane potentials and an open conformation at low membrane potentials. More than 40 classes of unrelated factors can modulate the PTP to open or close upon Ca^{2+} accumulation (Turunen *et al*., 2004). It is thought that the PTP serves as a fast Ca^{2+} release channel under physiological conditions (Turunen *et al*., 2004).

Walter *et al*., 2000, reported three classes of ubiquinone analogs that profoundly affect the PTP. PTP-inducers, PTP-inhibitors, and PTP-inactive quinones, which counteract the effect of the inhibitors and the inducers, were described. The structure-function correlation of the analogs has suggested that the methoxy groups are not essential for activity and that minor changes in the isoprenoid side chain can turn an inhibitor into an inducer. It was therefore concluded that the quinones modulate the PTP through a common binding site, whose occupancy would in turn modulate the PTP open-closed transitions through secondary changes of the PTP Ca^{2+} binding affinity, and that oxidation-reduction events were extremely unlikely (Walter *et al*., 2000). In a study done by Naderi *et al*., 2006, the ability of water-soluble CoQ10 to prevent apoptosis in

fibroblasts and transformed embryonic kidney cells, closely related to its ability to stabilize the mitochondrial membrane and decrease ROS generation, was shown. The results clearly indicated that mitochondrial membrane potential collapsed upon inducing oxidative stress, but if the cells were pre-treated with CoQ10 prior to oxidative stress induction, membrane potential remained intact. Their results also indicated direct inhibition of Bax activity on isolated mitochondria, suggesting that the protective effect of CoQ10 could be attributed to its ability to stabilize the mitochondrial membrane potential and blocking Bax activity (Naderi *et al*., 2006). Bax is a pro-apoptotic protein that moves from the cytoplasm to the mitochondrial membrane upon apoptotic stimulation (Naderi *et al*., 2006). Coenzyme Q10 was given to cell cultures simultaneous with cell death stimuli in a study done by Kagan *et al*., 1999. It was found that some cells were protected against cytotoxic insult by a general enhancement of mitochondrial viability and activity in the presence of CoQ10 in addition to a protection by CoQ10 of mitochondrial viability and activity after exposure to ceramide and ethanol (Kagan *et al*., 1999). They concluded that CoQ10 could interact with apoptotic machinery in the mitochondria, preventing the loss of mitochondrial potential by sequestering ROS generated in response to cell death signals and thus blocking cell death. The neuroprotective effect of CoQ10 may be due to antiapoptotic action that may vary depending on cell type and mode of cell death induction (Virmani *et al*., 2005). Alleva *et al*., 2001, pretreated Jurkat cells with $CoQ10H_2$- (the reduced form of CoQ10) and CoQ10, and then exposed the cells to α-TOS and hydrogen peroxide as well as immunological inducers of apoptosis. It was found that in $CoQ10H_2$- supplemented cells apoptosis was suppressed after exposure to α-TOS and hydrogen peroxide, but only a modest effect was exerted by these cells upon exposure to immunological agents. To clarify the mechanism by which $CoQ10H_2$- may suppress apoptosis induced by chemical and not immunological agents, the effect of CoQ10 supplementation on cellular ROS production was studied. ROS formation was suppressed in $CoQ10H_2$- but not CoQ10-enriched cells, suggesting that ROS are playing a major role in apoptosis induced by α-TOS, rather than by the immunological apoptogens, and therefore the redox function of $CoQ10H_2$- can modulate apoptosis induced by chemical stimuli. Thus, $CoQ10H_2$- may act as an antioxidant, blocking the actions of the oxidants implicated in the induction of apoptosis, which is supported by their finding that protection from apoptosis was not observed in CoQ10-enriched cells, confirming that the antioxidant potential of ubiquinol-10 is essential for its anti-apoptotic activity (Alleva *et al*., 2001). Brancato *et al*., 2000, have shown that

apoptosis of rabbit keratocytes induced by excimer lazer irradiation, a free radical-generating treatment, was prevented both *in vivo* and *in vitro* by CoQ10 (Brancato *et al*., 2000 & 2002). By using the same keratocyte cell line, Papucci *et al*., 2003, showed that CoQ10 prevent apoptosis also in response to apoptotic stimuli that do not generate free radicals. Coenzyme Q10 administration two hours prior to apoptotic stimuli prevents apoptosis not only in response to free radical-generating UVC irradiation, but also to antimycin A, C_2-ceramide and serum starvation, which do not generate free radicals, *i.e.* independently of the ability of apoptotic stimuli to trigger or not to trigger free radical generation (Papucci *et al*., 2003). The protective effect was clearly demonstrated by several evidences, including changes of cell morphology, quantification of living and apoptotic cells, and analysis of ATP cellular levels. Coenzyme Q10 significantly enhances the number of living cells, and lowers the number of cumulative apoptotic events. Coenzyme Q10 was also able to prevent massive reduction in ATP levels induced by all apoptotic stimuli, a phenomenon that is typically associated with the energy-consuming apoptosis execution and in particular with membrane potential collapse, consequent to PTP opening. The researchers suggested that the mechanism by which CoQ10 exerts its antiapoptotic activity, is associated with inhibition of PTP opening, and support their suggestion with the work of Fontaine *et al*., 1999 and Walter et al., 2000.

While in most tissues the large majority of CoQ is in reduced form, only 20% of the lipid is reduced in the brain. Since CoQ must be in the reduced form to function as an antioxidant, the large proportion of oxidized CoQ in the brain could therefore be a reflection of the high oxygen consumption in this tissue, causing an increased demand of antioxidants (Turunen *et al*., 2002). Cells require growth and survival factors that are provided by serum to maintain cell growth in culture; withdrawal of serum will induce cell growth arrest and some cells will develop the death program. Serum withdrawal causes a mild oxidative stress to cells in culture, leading to membrane damage and cell death (Ishizaki *et al*., 1995). Serum removal induces ceramide release to the cytosol by the activation of Mg^{2+} -dependent neutral sphingomyelinase (N-SMase) (Jayadev *et al*., 1995). Ceramide accumulation appears as a key component in the stress response pathway triggered by serum removal, since ceramides are able to induce cell death by activating proteases of the caspase family upon its intracellular accumulation (López-Lluch *et al*., 1999). López-Lluch *et al*., 1999, showed that the presence of CoQ10 in

serum-free cultures partially avoided the activation of apoptotic machinery through the inhibition of SMase pathway, and consequently prevented ceramide release and caspase-3 activation.

2.4.4 Extramitochondrial redox acitivity

Coenzyme Q10 is distributed among cellular membranes and it has a significant concentration at the plasma membrane. The plasma membrane contains a trans-membrane electron transport system, which is centered on CoQ10 (Gómez-Díaz *et al*., 2000). CoQ10 has access to enzymatic mechanisms able to regenerate its antioxidant reduced form, both in mitochondrial and extramitochondrial membranes (Ernster *et al*., 1995 and Kagan *et al*., 1996). CoQ10 is proposed to play a central role in antioxidant protection of the plasma membrane, either directly or through the regeneration of important exogenous antioxidants such as α-tocopherol and ascorbate (Gómez-Díaz *et a*l., 2000). CoQ10 can be considered as the central molecule in plasma membrane protection against lipid peroxidation because it is directly reduced by cytochrome b_5 reductase, and maintains both ascorbate and α-tocopherol in their reduced state (López-Lluch *et al*., 1999).

Coenyme Q10 is involved in the plasma membrane electron transport system, by which NADH in the cytoplasm transfers electrons through CoQ10 to electron acceptors such as iron or oxygen outside the cell (Crane, 2001). When this system is activated, the proton release through the H^+/Na^+ antiport is greatly increased, and when the system is inhibited by inhibitory CoQ10 analogs, the antiport is inhibited (Crane, 2001). If the H^+/Na^+ antiport is inhibited by amiloride, the transplasma membrane electron transport is accompanied by a slow release of protons equivalent to two protons released per quinol oxidized, indicating that the reduction oxidation of the CoQ10 in membranes is organized as in the lysosomes (Crane, 2001). The plasma membrane of eukaryotic cells contains an NADH oxidase (NOX) that is involved in the transfer of electrons across the membrane (Turunen *et al*., 2004). NOX is not a transmembranous protein, but is located at the external surface of the plasma membrane (DeHahn *et al*., 1997). The participation of CoQ10 in the plasma membrane electron transport was shown by the fact that the NOX activity was inhibited by the removal of CoQ10 with heptane and reconstitution of the activity by CoQ10 addition (Sun *et al*., 1992). In 1994, Villalba *et al*., 1995, showed that the participation of CoQ10 as an electron carrier is specific to trans-plasma

membrane electron transport in pig liver plasma membranes. Sun *et al*., 1992 reported additional evidence for CoQ10 function in trans-plasma membrane electron transport. Extraction of CoQ10 from the plasma membrane decreases NADH dehydrogenase, an enzyme shuttling reducing equivalents into the respiratory chain via complex I (Nohl *et al*., 2001), and NADH:oxidoreductase activity, and added CoQ10 partially restores activity. Ferricyanide reduction by transmembrane electron transport from HeLa cells is inhibited by CoQ10 analogs, which inhibit NADH dehydrogenase in plasma membranes, reduction of external oxidants by whole cells, and oxidant-induced proton release as well. The analog effects are reversed by CoQ10 (Sun *et al*., 1992). A relation between the transplasma membrane electron transport and control of the cytosolic redox state has been proposed (Crane, 2001). It is most dramatically revealed by the ability of external electron acceptors such as hexacyanoferrate to maintain Namalwa cell viability after mitochondrial energy production and substrate oxygen is lost. By maintaining cytosolic NAD, the transmembrane electron transport allows the production of ATP through glycolysis. The plasma membrane electron transport increases as cells lose their mitochondrial function (Larm *et al*., 1994).

Coenzyme Q10 can participate in several aspects of oxidation/reduction control such as signal origin and transmission in cells (Crane, 2001). The autoxidation of the semiquinone formed in various membranes during electron transport activity can be a primary basis for generation of H_2O_2 (Crane, 2001). The H_2O_2 in turn activates transcription factors such as NFκB, which protects against apoptosis, to induce gene expression (Crane, 2000 & 2001).

2.4.5 Membrane Stabilization

The membrane stabilizing property of CoQ10 has been postulated to involve the phospholipids-protein interaction that increases prostaglandin (especially prostacyclin) metabolism. It is thought that CoQ10 stabilizes myocardial calcium-dependent ion channels and prevents the depletion of metabolites essential for ATP synthesis (Greenberg *et al*., 1990). It is thought that the isoprenoid side chain may help to stabilize the lipid bilayer (Lenaz *et al*., 1999). Crane reported in 2001 that there is coenzyme Q floating in the phospholipids bilayer of the membranes. The free form may float with the all *trans* polyisoprene chain extended in the fatty acid chains of the lipid. Crane, 2001, also reported that there is evidence that in some cases the polyisoprenoid chain may be

folded into a shorter thicker structure. It is believed that the isoprenoid chain may help to stabilize the lipid bilayer (Lenaz *et al*., 1999). The quinone head group can be either oxidized (quinone), or reduced (quinol) (Crane, 2001). The quinol (hydroquinone) is more hydrophilic, so the head group can lie closer to the surface of the membrane. The change of position with oxidation and/or reduction may modify structural or enzymatic properties in the membrane. Crane, 2001, gave the redox state, which may control activity of phospholipases in the membrane, as an example. From the studies of Kagan *et al*., 1990, it appears that the membrane-stabilizing effects of ubiquinol are mainly based on recycling of α-tocopherol radicals resulting from an interference in autocatalytic lipid peroxidation. Besides α-tocopherol, ubiquinols may also react with lipid radicals; however, the rate constants of the reactions favor an interaction of lipid radicals with α-tocopherol. Irrespectively of the radical reacting with ubiquinol, the reaction product expected is the semiquinone (Nohl *et al*., 2001).

The aim of a study done by Hauβ *et al*., 2005, was the unequivocal determination of the location of CoQ10 in lipid bilayers, more precisely, the orientation and depth in the membrane profile. Neutron diffraction was employed, and data showed CoQ10 at the center of the hydrophobic core parallel to the membrane plane, and, not as might be expected, parallel to the lipid chains. This localization is of importance for its function as a redox shuttle between the respiratory complexes. Together with their results that squalane is in the bilayer center, it might be interpreted to show that all natural polyisoprene chains lie in the bilayer center. Thus, ubiquinone might also act as an inhibitor of transmembrane proton leaks (Hauβ *et al*., 2005). The distinct intramembranous localizations of lipids of the mevalonate pathway have considerable consequences on membrane properties. Polyisoprenoid chains of CoQ10, dolichol and dolichyl-P are present in the central hydrophobic region between the double layers of phospholipids fatty acids (Turunen *et al*., 2004). Turunen *et al*., 2004, suggested that they have a coiled formation and the three lipids saturate the available space. The functionally active groups, the benzoquinone ring of CoQ10 and the phosphorylated α-isoprene of dolichol-P, turn out to the outer or inner surface of the membrane depending on the functional requirement. This central localization is considered to destabilize membranes and results in an increased fluidity and permeability (Turunen *et al*., 2004). On the contrary, cholesterol is distributed between fatty acids on one side of the lipid leaflet, thereby causing stabilization with decreased fluidity and permeability. This

arrangement of isoprenoid-derived lipids has two major consequences. First, all the membranes have to be saturated with the appropriate lipid for optimal function and the level of saturation is dependent on the structural organization of the membrane type. Second, if a membrane is deficient in an isoprenoid, the consequences for membrane function, e.g. fluidity, will be deleterious (Turunen *et al*., 2004).

Results presented by Linnane *et al*., in 2002, indicate that CoQ10 functions as a major skeletal muscle gene regulator and as such, profoundly modulates cellular metabolism. Their data also suggested that CoQ10 treatment can act to influence the fibre type composition of muscle, toward the fibre type profile generally found in younger individuals (Linnane *et al*., 2002). Microarray gene expression analyses and differential gene display analyses demonstrated independently that the expression of a large number of genes is affected by CoQ10. Proteome analysis reflected the global gene response of CoQ10 supplementation on the protein expression profile of muscle tissue (Linnane *et al*., 2002). The study proposed that CoQ10 plays a key role in manipulating the redox potential poise, thereby affecting sub-cellular membrane potential changes, resulting in the differential regulation of sub-cellular membrane activities and compartments (Linnane *et al*., 2002). CoQ10 through the Q-cycle participates in the determination of mitochondrial membrane potential and in turn energy synthesis and mitochondrial substrate utilization (Linnane *et al*., 2002). CoQ10 has also been shown to be an essential co-factor of the uncoupling proteins which act to down-regulate mitochondrial membrane potential (Van Belzen *et al*., 1997). Gille *et al*., 2000, have demonstrated the occurrence of a lysosomal CoQ10 oxidoreductase system, which establishes a proton gradient across the membrane; such a system would contribute to the regulation and metabolite movement in and out of the lysosome.

2.5 CoQ10 Deficiency

Coenzyme Q10 deficiency may be caused by insufficient dietary CoQ10, impairment in CoQ10 biosynthesis, excessive utilization of CoQ10 or a combination of the three (Langsjoen, 1994). Significant lowered levels of CoQ10 have been noted in a wide variety of diseases in both animal and human studies (Langsjoen, 1994).

More than quarter a century has passed since Karl Folkers postulated that CoQ10 could have therapeutic potential for the treatment of cancer (Folkers, 1974). As CoQ10 was essential for normal cell respiration and function, any deficiency in its availability or biosynthesis could disrupt normal cellular functions, which could then lead to abnormal pattern of cell division that, in turn, might induce an oncogenic response (Folkers, 1974). The vitamins required for the biosynthesis of the four DNA bases, are also required for the biosynthesis of CoQ10 (Folkers, 1996). Mutations may be caused by the deficiencies in of one or more of these DNA bases and be considered only a dysfunction of genetics; however the initial biochemical dysfunction may actually be deficiencies of one or more of the three vitamins (vitamin B6, niacin and folic acid) required for the biosynthesis of the four DNA bases (Folkers, 1996). Although endogenous production is the body's primary source of CoQ10, it does not meet the requirements under certain pathological conditions (Bhagavan *et al*., 2005). Because of its crucial role in mitochondrial energy production, a number of systems are affected when the availability of CoQ10 becomes limiting, and tissues with high energy demands such as the heart are more readily affected (Bhagavan *et al*., 2005).

Primary CoQ10 deficiency is a clinically heterogeneous autosomal ressesive condition with a clinical spectrum that encompasses at least five major phenotypes: 1) encephalomyopathy, characterized by the triad of recurrent myoglobinuria, brain involvement and ragged red fibres; 2) severe infantile multisystemic disease; 3) cerebellar ataxia; 4) Leigh syndrome with growth retardation, ataxia and deafness; 5) isolated myopathy (Quinzii *et al*., 2007b). In most cases these disorders respond to CoQ10 supplementation.

Of the nine genes presumably involved in CoQ10 biosynthesis, and suspected of causing primary CoQ10 deficiency, three have been identified; *PDSS1*, *PDSS2* and

COQ2. There is good reason to believe that mutations in the six genes still at large may soon be found to underlie human disease (DiMauro *et al*., 2007). Mollet *et al*., 2007, reported an inbred family with CoQ10 deficiency manifesting as a multisystem disease with early-onset of deafness, encephaloneuropathy, obesity, livedo reticularis, and valvulopathy. Homozygosity mapping allowed the disease to be attributed to a homozygous missense mutation in *prenyldiphosphate synthase, subunit 1* (*PDSS1*), the enzyme that elongates the prenyl side chain of coenzyme Q. In the same study, direct sequencing of various genes involved in ubiquinone biosynthesis in an unrelated patient with fatal infantile multiorgan disease, detected a homozygous single base pair frameshift deletion in *OH-benzoate polyprenyltransferase* (*COQ2*), the gene encoding the enzyme involved in the second step of ubiquinone biosynthesis (Mollet *et al*., 2007).

López *et al*., 2006, reported the first pathogenic mutations in *PDSS2* which encodes *decaprenyl diphosphate synthase, subunit 2*, the first enzyme of the CoQ10 biosynthetic pathway, causing primary CoQ10 deficiency in an infant with fatal Leigh syndrome and nephrotic syndrome. Mutations in *PDSS2* should be considered as potential causes of CoQ10 deficiency in other patients with similar phenotypes as the patient in this study (López *et al*., 2006). Ataxia-oculomotor apraxia 1 (AOA1) is a newly identified autosomal recessive cerebellar ataxia associated with oculomotor apraxia, severe neuropathy, low levels of blood albumin, and increased levels of blood cholesterol (Le Ber *et al*., 2003). The *APTX* gene codes for aprataxin, a ubiquitously expressed protein that probably plays a role in single-strand break repair (Le Ber *et al*., 2007). A study by Le Ber *et al*., 2007, confirmed that aprataxin gene mutations are associated with decreased CoQ10 levels in muscle and that the decrease correlates with the genotype. Gempel, *et al*., 2007, described seven patients from five independent families with an isolated myopathic phenotype of CoQ10 deficiency. Coenzyme Q10 was significantly decreased in the skeletal muscles of all patients. Tandem mass spectrometry detected multiple acyl-CoA deficiency, leading to the analysis of the *electron-transferring-flavoprotein dehydrogenases* (*ETFDH*) gene, previously shown to result in another metabolic disorder, glutaric aciduria type II (GAII). All the patients in this study carried autosomal recessive mutations in *ETFDH*, suggesting that *ETFDH* deficiency leads to a secondary CoQ10 deficiency (Gempel *et al*., 2007).

CoQ10 deficiency can be also a secondary consequence of drugs, such as statins (3-hydroxy-3-methylglutaryl coenzyme A reductase inhibitors) (Quinzii *et al*., 2007). Statins have been used for the treatment of hypercholesterolemia and coronary artery disease and for the prevention of stroke. The mechanism of action by which statins elicit their effect is the inhibition of cholesterol synthesis at the level of mevalonic acid. Since the biosynthetic inhibition is not selective, statins also impair the synthesis of other compounds that share mevalonate as precursor, such as dolichol and CoQ10 (Quinzii *et al*., 2007a). For this reason, statin-related myopathy, manifesting as myalgia, muscle necrosis, and myoglobinura, has been hypothesized to be due to a partial deficiency of CoQ10 (Folkers *et al*., 1985 and Rundek *et al*., 2004).

Documented adverse effects associated with the use of CoQ10 in humans have been minor and include epigastric discomfort (0.39%), appetite suppression (0.23%), nausea (0.16%), and diarrhea (0.12%) (Greenberg *et al*., 1990).

2.6 Triton X-100

Triton X-100 is a nonionic detergent, 100% active ingredient, which is often used in biochemical applications to solubilize proteins. Triton X-100 has no antimicrobial properties and is considered a comparatively mild detergent and non-denaturing. The “X” series of Triton detergents are produced from octylphenol polymerized with ethylene oxide. The number “100” relates only indirectly to the number of ethylene oxide units in the structure. Triton X-100 has an average of 9.5 ethylene oxide units per molecule with an average molecal weight of 625, giving effective molarity of 1.7M. Any ethylene oxide polymer can form trace peroxides on exposure to oxygen. These impurities may interfere with biological reactions. For lysing cells, typically about 0.1% X-100 solution in water will be sufficient, and even up to 0.5% concentrations will usually not harm most enzymes being isolated. Many enzymes remain active in the presence of X-100; for example, a commonly used protease, Proteinase K, remains active in 1% (w/w) solutions of X-100 (Sigma Product Information Sheet).

An investigation by Deamer *et al*., 1967, has established that Triton X-100 is taken up by chloroplasts in a manner which involves a partition between the medium and chloroplast membranes, rather than by a strong, irreversible binding. This uptake causes

ultrastructural alterations consisting of a generalize swelling of all membrane structures followed by vesicle formation, at a concentration range of 50 – 200 µM, swelling initiated by Triton X-100 occurs over a period of several minutes (Deamer *et al*., 1967). Normally when Triton X-100 is added to chloroplast suspensions the chloroplast membranes become completely permeable to small ions, probably because uncharged "pores" are produced at the binding sites of Triton X-100. These pores are not necessarily true holes in the membrane, but probably represent points at which adsorbed Triton X-100 molecules have displaced normal membrane constituents (Deamer *et al*., 1967). Triton X-100 solubilizes membranes of PC12 cells and leaves behind a nucleus and an array of cytoskeletal filaments at a concentration of 0.5% (Vale *et al*., 1985), indicating the presence of proteins in the cytoskeleton that is insoluble to Triton X-100. A study done by Kőszegi *et al*., 2007, showed that Triton X-100 at alkaline pH is efficient in extracting total intracellular ATP in monolayer cell cultures. It was also shown that the detergent extract is suitable for protein determination, eliminating the need for subsequent protein-extraction steps (Kőszegi *et al*., 2007). A cross-linked form of Triton X-100, Triton WR-1339, has been shown to reduce the spread of tumour cells in laboratory animals (Picache *et al*., 2004). The outcome of a study by Picache *et al*., 2004, on the T24 bladder carcinoma cell line, provided a molecular basis for the antiproliferative effect of Triton X-100, namely its differential effects on various parts of the cell cycle machinery. Upon treatment of cells with Triton X-100, a potent antiproliferative effect resulting from the downregulation of the key cell cycle regulators, the cyclin-dependent kinases (CDK's), was seen. CDK activity was lost due to a twofold effect; the increased expression of the CDK inhibitors $p21^{Cip1}$ and $p27^{Kip1}$ in combination with the reduced expression of cyclin A, a regulatory CDK subunit, essential for CDK function (Picache *et al*., 2004). Triton X-100 seems to be a useful compound to analyze the structural and mechanistic features of complex I-associated ubiquinone oxidoreduction (Ushakova *et al*., 1999). Rapidly equilibrating Triton X-100 acts as a competitive inhibitor on Complex I and as non-competitive inhibitor on submitochondrial particles (SMP). Grivennikova *et al*., 1997, showed that rotenone binds more strongly to the active "turnover pulsed" enzyme than to its deactivated form. This appears to be also true for Triton X-100, and it is therefore expected that Triton X-100 solubilized Complex I would contain detergent molecule(s) bound at the Q-site(s), thus stabilizing the ubiquinone reactive state of the enzyme (Ushakova *et al*., 1999). The "unidirectional" preference of the inhibitory effect of Triton X-100 strengthens the proposal of the authors of different binding sites for both

pairs of the substrates (NADH/NAD^+ and ubiquinol/ubiquinone) which operates in the forward and reverse electron transfer catalyzed by the membrane-bound mammalian Complex I (Ushakova *et al*., 1999).

Biomembranes are not homogenous; they present a lateral segregation of lipids and proteins which leads to the formation of detergent resistant domains, also called “rafts”. These rafts are particularly enriched in sphingolipids and cholesterol (Kirat *et al*., 2007). Understanding the factors governing biomembranes' solubilization at the molecular level is essential in biophysics, biochemistry and cell biology. Especially in the case of rafts, examining the molecular determinants responsible for their insensitivity to Triton X-100 solubilization might clarify the mechanisms of membrane solubilization (Kirat *et al*., 2007). Kirat *et al*., 2007, reported two different Triton X-100 mediated solubilization pathways by doing real-time atomic force microscopy (AFM) study of model lipid bilayers exposed to Triton X-100 at different concentrations. It was concluded that (i) for non-resistant membranes, solubilization occurs by hole formation and the crumbling of the gel domains, and (ii) for resistant membranes, Triton X-100 erodes the bilayer patches visibly without affecting their center (Kirat *et al*., 2007).

2.7 Study Objectives

Therefore, the specific research objectives that directed this study were to:

1. Select a concentration range of Triton X-100, starting at a concentratin that will, according to the literature, cause membrane disruption and prepare a serial dilution from that.
2. Select a concentration range of CoQ10, where the recommended supplementation dosage, 100mg/day (Crane, 2001), will compare with the lowest two concentrations in the range
3. Establish and optimize methodologies used to isolate cardiac and skeletal muscle cells from chick embryos, and establish primary cultures of these chick embryonic cardiac and skeletal muscle cells.
4. Determine whether Triton X-100 and CoQ10 are cytotoxic to primary chick embryonic cardiac and skeletal muscle cell cultures by determining the effect of

Triton X-100 and CoQ10 on cell viability, lysosomal membrane integrity and cell number, using the MTT, NR and CV assays.

5. Choose two concentrations of Triton X-100, expected to cause cellular alterations, and test the cytotoxicity of the two concentrations on chick embryonic cardiac and skeletal muscle cell cultures, pre-treated with increasing concentrations of CoQ10, using the MTT, NR and CV assays.
6. Investigate the possibility that Triton X-100 might induce estrogenic activity, because of the similarity between the chemical structure of Triton X-100 and Nonylphenol, using the well established Recombinant Yeast Screen Assay (RCBA) for oestrogenic activity described by Routledge *et al*., 1996.
7. Investigate the ultrastructure of cardiac and skeletal muscle cells in primary culture, exposed to Triton X-100 and CoQ10, by SEM.
8. Determine whether CoQ10 offer any protection to cardiac and skeletal muscle cells in primary culture, ultrastructurally altered by the cell lysing properties of Triton X-100, by SEM.
9. Investigate intracellular changes in cardiac and skeletal muscle cells in primary culture, evoked by Triton X-100 and CoQ10, alone and in combination, using confocal microscopy.
10. Correlate the results obtained with SEM, with the results obtained with confocal microscopy.
11. Determine whether Triton X-100 and CoQ10, alone and in combination produce reactive oxygen species (ROS), upon exposure, in cardiac and skeletal muscle cell cultures.

Chapter 3: Investigation of Possible Estrogenic Activity of Triton X-100

3.1 Introduction

The endocrine system is a complex communication system between chemical signals and their targets responsible for regulating internal functions of the body. Any substance that alters the function of this system is termed an endocrine disruptor (Vazquez-Duhalt *et al*., 2004). An endocrine disruptor is a synthetic chemical that when absorbed into the body either mimics or blocks hormones and disrupts the body's normal functions. This disruption can happen through altering normal hormone levels, halting or stimulating the production of hormones, or changing the way hormones travel through the body, thus affecting the functions that these hormones control (Natural Resources Defense Council, 1998, http://www.nrdc.org/health/effects/qendoc.asp). Environmental chemicals that function as estrogens include, but are not limited to, chemicals that mimic the female sex hormone 17β-estradiol (Vazquez-Duhalt *et al*., 2004), and have been suggested to be associated with an increase in disease and dysfunctions in animals and humans (Klotz *et al*., 1996). The well-documented effects of environmental estrogens in animals and their potential for adverse effect in humans have led to the development of assays for identifying chemicals with estrogenic activity (Klotz *et al*., 1996). Nonylphenol ethoxylates (NPE) are surfactants used worldwide, and are transformed in the environment by microorganisms to form more toxic compounds, such as nonylphenol (NP) and short chain nonylphenol ethoxylates. These intermediates from microbial transformations, in addition to their intrinsic toxicity, seem to be able to mimic natural estrogens and disrupt the endocrine systems of higher organisms (Vazquez-Duhalt *et al*., 2004). Nonylphenol is one of the most studied estrogen mimics that appear to interact with development in several organisms (Vazquez-Duhalt *et al*., 2004). Analysis of the data compared to 17β-estradiol structure identified three structural criteria that were related to xenoestrogen activity and potency (Vazquez-Duhalt *et al*., 2004): (i) a hydrogen bonding ability of the phenolic ring mimicking the A-ring, (ii) a hydrophobic centre similar in size and shape to the B- and C-rings, and (iii) a hydrogen-bond donor mimicking the 17β-hydroxyl moiety of the D-ring, especially with an oxygen-to-oxygen

distance similar to that between the 3- and 17β-hydroxyl groups of 17β-estradiol. Moderately active compounds, such as NP, have a 4-hydroxyl substituted benzene ring with a hydrophobic moiety equivalent in size and shape to the B- and C-ring of 17β-estradiol (Vazquez-Duhalt *et al*., 2004).

a.

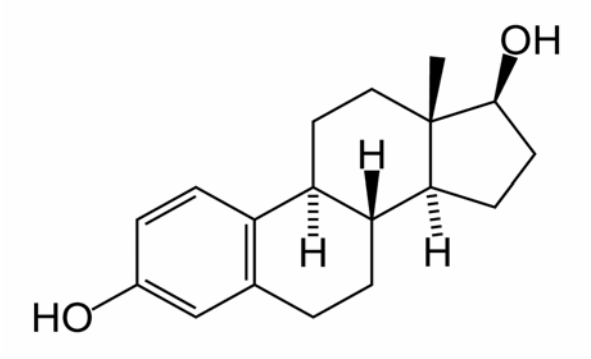

b.

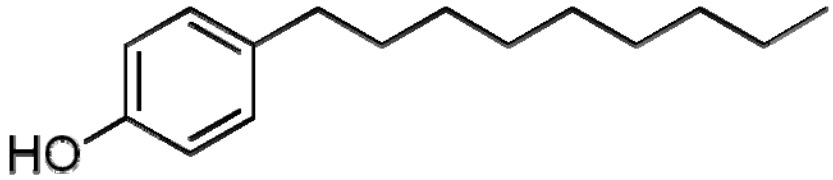

c.

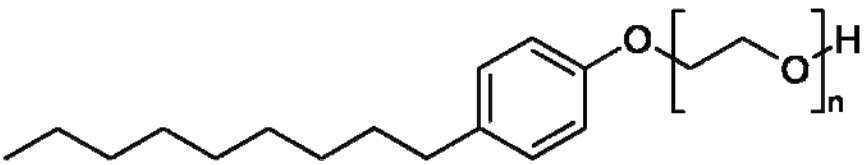

Figure 3.1: Chemical structures of **a**): 17β-estradiol, **b**): Nonylphenol and **c**): Nonylphenol Ethoxylates.

Triton X-100 is a polydisperse preparation of *p*-*t*-octylphenoxypolyethoxyethanols consisting of oxyethylene chain lengths averaging 9-10 oxyethylene units (Dennis, 1973). The hydrocarbon group is a 4-(1,1,3,3-tetramethylbutyl)-phenyl group. However, the general physical properties of this detergent are similar to those of the pure homogeneous compound having a chain length of 9 or 10 units (Becher, 1967). It is a nonionic detergent, 100% active ingredient, which is often used in biochemical applications to solubilize proteins. Triton X-100 has no antimicrobial properties. It is considered a comparatively mild detergent, non-denaturing, and is reported in numerous references as a routinely added reagent. It does absorb in the ultraviolet region of the spectrum, consequently, can interfere with protein quantitation (Sigma Product Information Sheet). Triton X-100 in aqueous solution forms micelles consisting of about 100-160 monomers corresponding to a molecular weight of about 63,000-105,000 (Dennis, 1973). Triton X-100 has a low critical micelle concentration (CMC) of 0.24 mM and can also be useful for the purification and the reconstitution of integral or lipid modified proteins in biomembranes (Kirat *et al*., 2007). Systems of nonionic polymer/surfactant possess many properties superior to those of ionic ones like higher stability, better biologic compatibility and lower toxicity, and these compounds have been widely used in material synthesis and biology simulation (Ge *et al*., 2007).

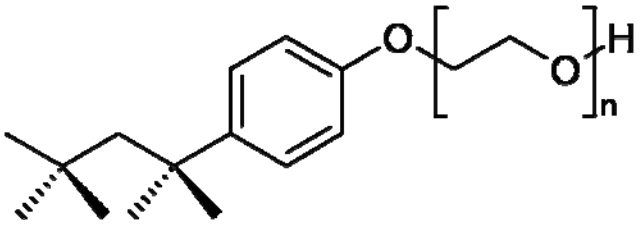

Figure 3.2: The chemical structure of Triton X-100.

a). **b).**

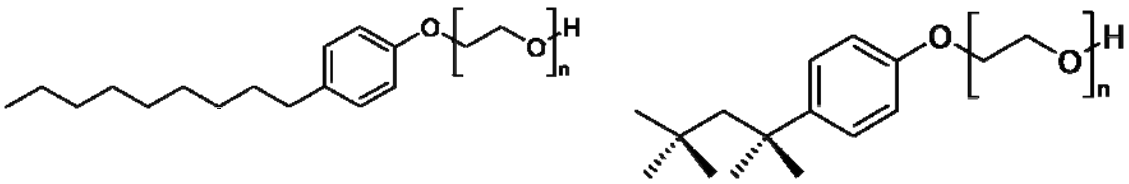

Figure 3.3: Comparing the structures of **a**): Nonylphenol Ethoxylates and **b**): Triton X-100

The clear resemblance between the chemical structures of Nonylphenol Ethoxylates and Triton X-100 (Figure 3.3) raised the question whether Triton X-100 might have estrogenic activity. In order to determine whether such properties do exist, the Recombinant Yeast Screen Assay (RCBA) for estrogenic activity was performed.

3.2 Materials and Methods

Triton X-100 (Cat. No. 9002-93-1), ethanol (Cat. No. 27,0741) and 17β-estradiol (Cat. No. E8875) were bought from Sigma-Aldrich (Pty) Ltd., Midrand, South Africa. Ninty six well, flat bottomed micro-titre plates (Cat. No. 95029780) were bought from Labsystems, Cape Town, South Africa. Chlorophenol red-β-d-galactopyranoside (CPRG) (Cat. No. 10884308001) was obtained from Roche Diagnostics, Randburg, South Africa.

The Recombinant Yeast Screen Assay (RCBA) for estrogenic activity (including details of medium components) previously described by Routledge *et al*., 1996 and Aneck-Hahn *et al*., 2005, was used. In this system, yeast cells transfected with the human estrogen receptor-α (ER-α) gene, together with expression plasmids, containing estrogen-responsive elements and the lac-Z reporter gene encoding the enzyme β-galactosidase, were incubated in a medium (minimal medium, pH 7.1) containing 17β-estradiol and the chromogenic substrate, chlorophenol red-β-d-galactopyranoside (CPRG). Active ligands, which bind to the receptor, induce β-galactosidase (β-gal) expression and these cause the CPRG (yellow) to change into a red product that can be measured by absorbance. The assay was carried out according to the standard assay procedure (Routledge *et al*., 1996) with minor adjustments (Aneck-Hahn *et al*., 2005) in a Type II laminar flow air

cabinet, to minimise aerosol formation. A 1% stock solution of Triton X-100 was prepared in ethanol and serial dilutions ranging from $1.56x10^{-11}$g/ℓ to $5.35x10^{-1}$g/ℓ were made and transferred to a 96 well micro-titre plate. Each plate also contained at least one row of blanks (assay medium and solvent ethanol) and a standard curve for 17β-estradiol ranging from 2.274µg/ℓ to 0.324pg/ℓ. After allowing the ethanol to evaporate to dryness on the assay plate, aliquots (200µℓ) of the assay medium containing the yeast and CPRG were then dispensed into each sample well. The plates were sealed and placed in a naturally ventilated incubator (Heraeus, B290) at 32°C for 3 to 4 days. After 3 days incubation the colour development of the medium was checked periodically at an absorbance (abs) of 540nm for colour change and 620nm for turbidity of the yeast culture. The absorbance was measured on a Titertek Multiskan MCC/340 (Labsystems) plate reader to obtain data with the best contrast. After incubation the control wells appeared light orange in colour, due to background expression of β-galactosidase and turbid due to the growth of the yeast. Positive wells were indicated by a deep red colour accompanied by yeast growth. Clear wells, containing no growth indicated lysis of the cells and colour varied from yellow to light orange. All experiments were performed in duplicate and repeated 6 times. The test absorbance of the samples was measured on day 4. The following equation was applied to correct for turbidity:

Corrected-value = test abs (540nm) - [test abs (650nm) - median blank abs (620nm)]

The 17 β-estradiol standard curve was fitted (sigmoïdal function, variable slope) using Graphpad Prism (version 2.01), which calculated the minimum, maximum, slope, EC50 value and 95% confidence limits. The detection limit of the yeast assay was calculated as absorbance elicited by the solvent control (blank) plus three times the standard deviation (SD).

3.3 Results and Discussion

A number of chemicals released into the environment are believed to disrupt normal endocrine function in humans and animals (Colborn *et al*., 1993 and Toppari *et al*., 1996). These endocrine disrupting chemicals (EDCs) have various endocrine and reproductive effects, believed to be due to their: (i) Mimicking effects of endogenous hormones such as estrogens and androgen, (ii) Antagonizing the effects of normal, endogenous hormone, (iii) Altering the pattern of synthesis and metabolism of natural hormones, (iv) Modifying hormone receptor levels (Soto *et al*., 1995). Chemical analysis on its own will rarely, if ever allow a confidant prediction of endocrine effects (Matthiessen *et al*., 1998). It has been shown that estrogen-mimicking chemicals are present in the aquatic environment. They are also accompanied by other substances, which can disrupt the endocrine system of aquatic fauna by alternative means (Aneck-Hahn *et al*., 2005). Bioassays and biomarkers that integrate these various endocrine disrupting processes, to achieve a more holistic picture of environmental impacts, are more cost-effective. Detection of activity can then be followed up with toxicity identification (Aneck-Hahn *et al*., 2005). One of the most widely applied *in vitro* assays uses genetically modified yeast strains that harbor an estrogen receptor expression cassette and a reporter construct (Breithofer *et al*., 1998, Arnold *et al*., 1996 and Coldham *et al*., 1997). Interaction of an estrogenic substance with the estrogen receptor causes a conformational change in the receptor, enabling the estrogen-estrogen receptor complex to bind to estrogen-responsive elements. The latter are located upstream of the *lacZ* reporter gene present on a reporter plasmid. Incubation of these recombinant yeasts with estrogenic chemicals triggers the expression of β-galactosidase (De Boever *et al*., 2001).

i.

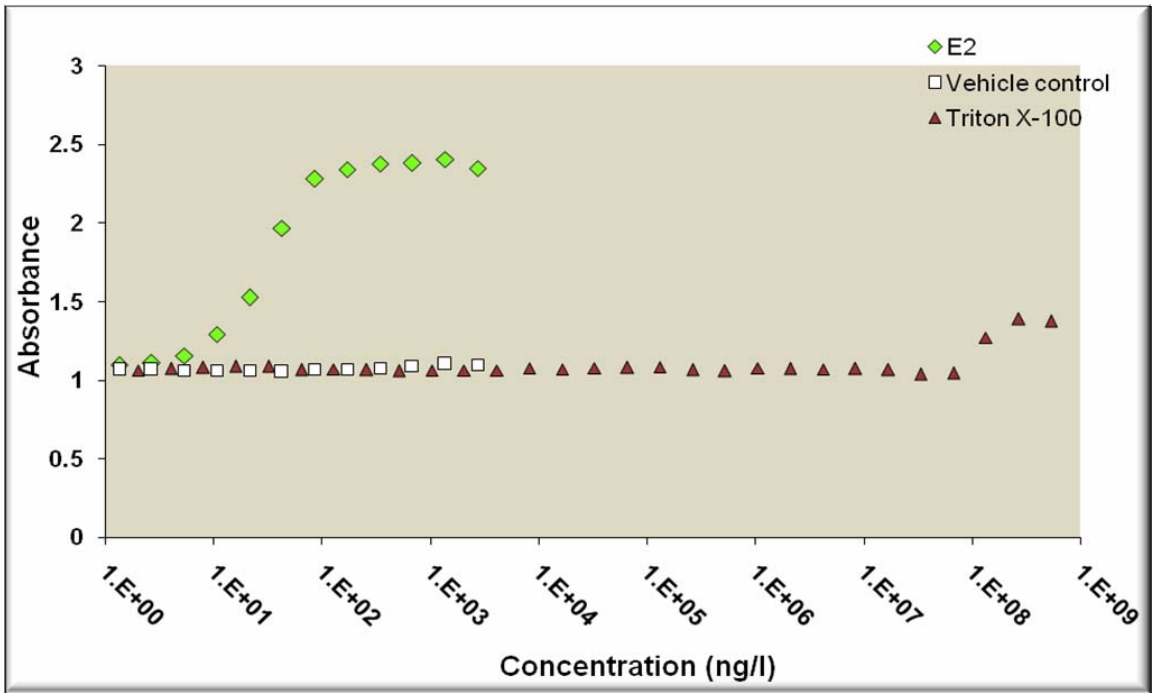

ii.

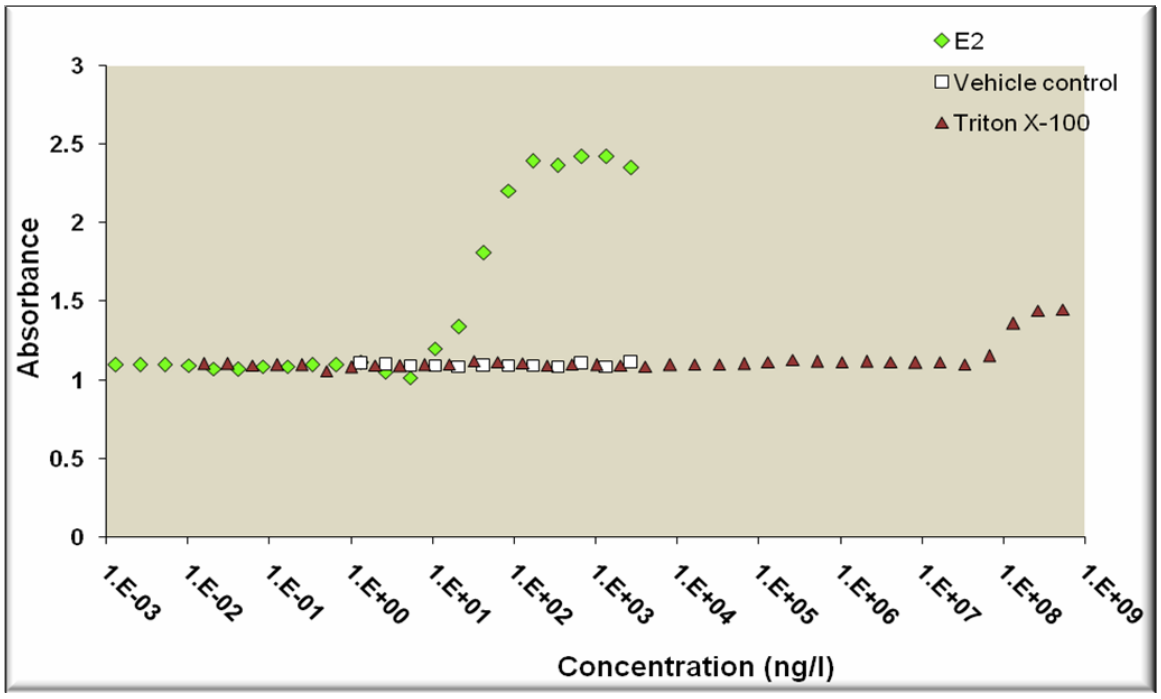

Figure 3.4 a: Log concentration of 17β-estradiol (E2) serially diluted from 2.72 x 10^{-6} g/l to 3.24 x 10^{-13} g/l and the log concentration for Triton X-100 serially diluted from 1.56x10^{-11} g/l to 5.35x10^{-1} g/l. Results for first and second repeats (**i**): sample 1 and (**ii**): sample 2 of the experiment.

i.

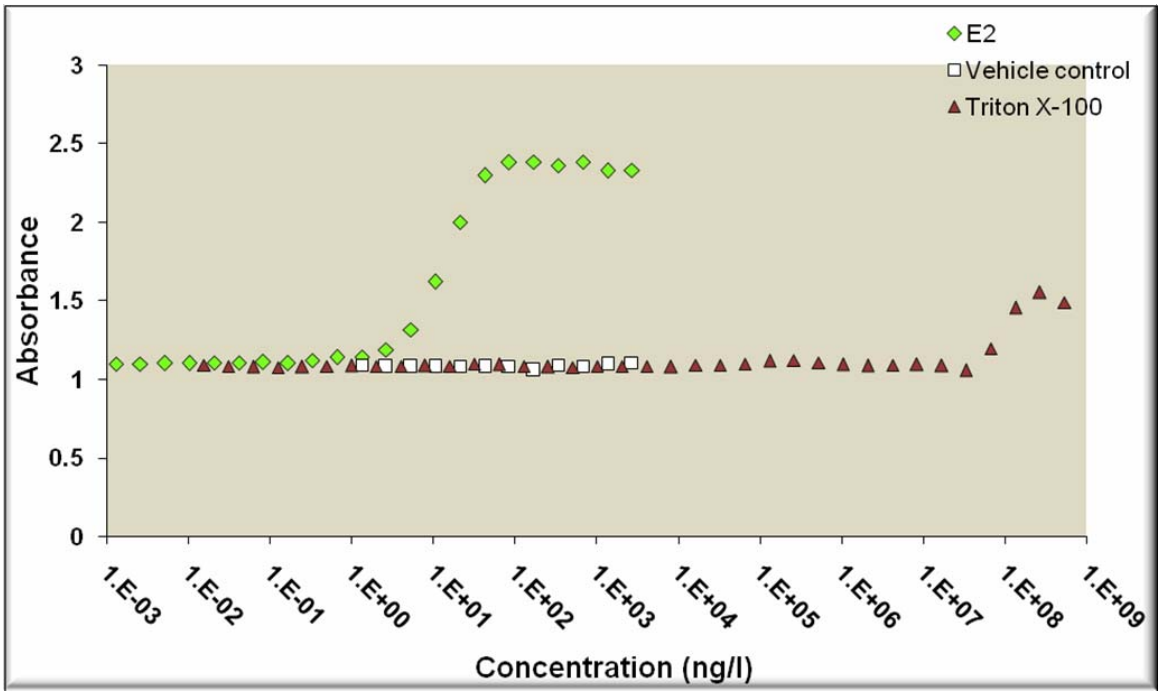

ii.

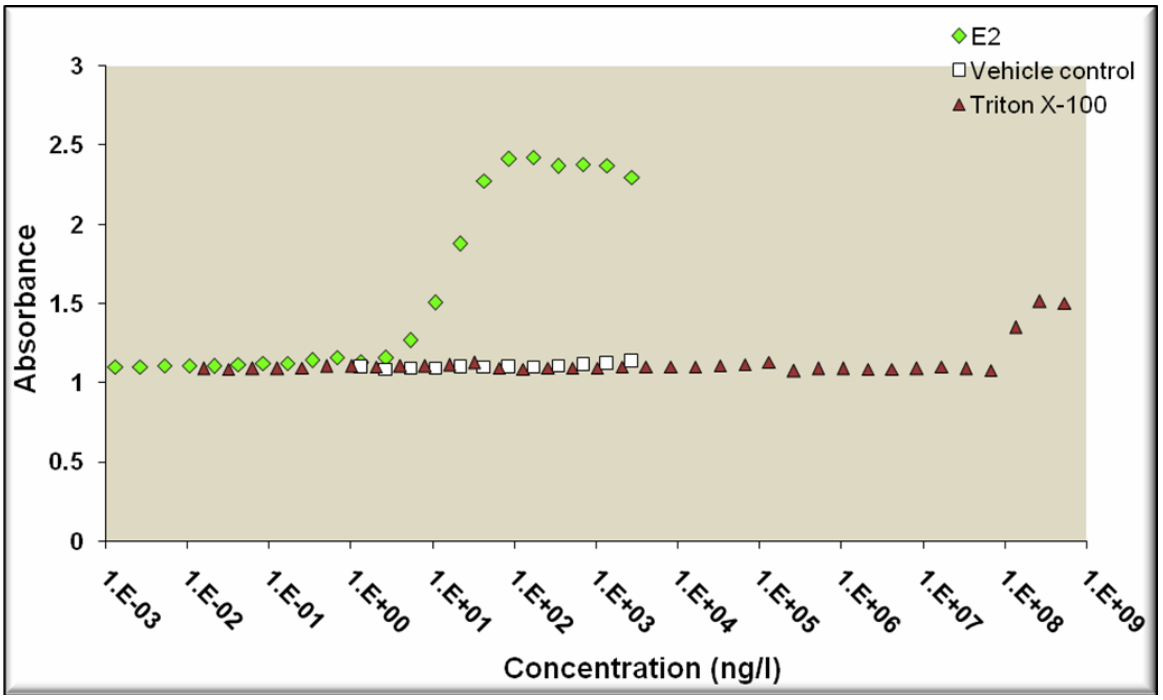

Figure 3.4 b: Log concentration of 17β-estradiol (E2) serially diluted from 2.72 x 10^{-6} g/l to 3.24 x 10^{-13} g/l and the log concentration for Triton X-100 serially diluted from 1.56x10^{-11} g/l to 5.35x10^{-1} g/l. Results for the third and fourth repeats; (**i**): sample 3 and (**ii**): sample 4 of the experiment.

i.

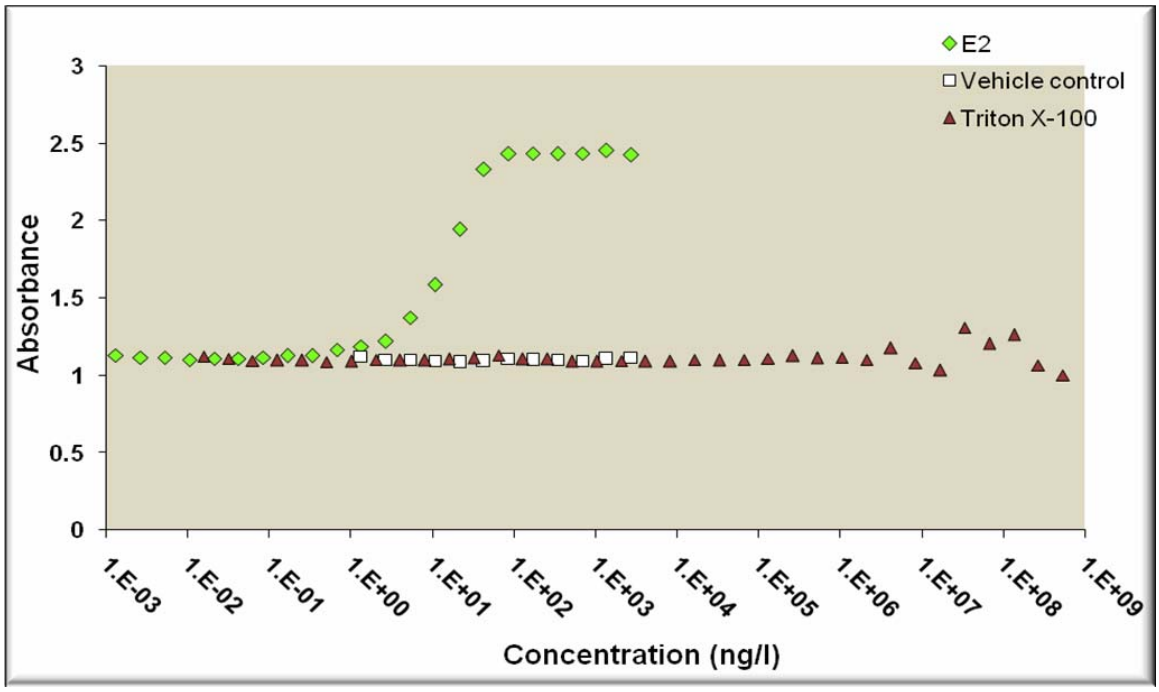

ii.

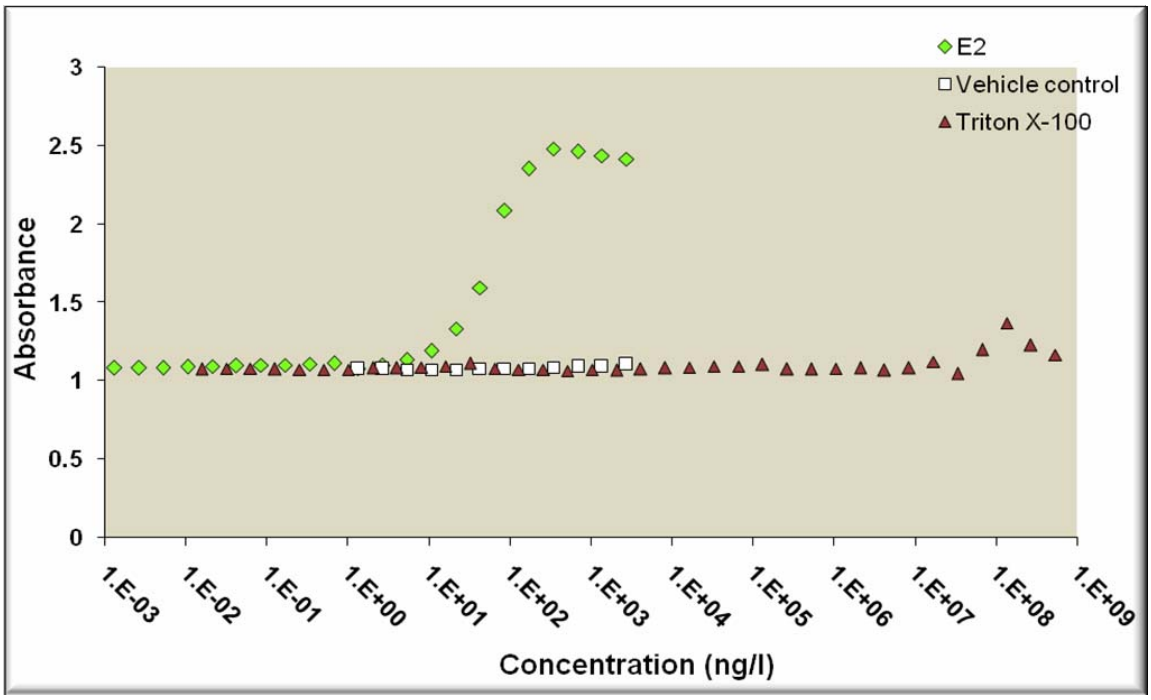

Figure 3.4 c: Log concentration of 17β-estradiol (E2) serially diluted from 2.72 x 10^{-6} g/l to 3.24 x 10^{-13} g/l and the log concentration for Triton X-100 serially diluted from 1.56x10^{-11} g/l to 5.35x10^{-1} g/l. Results for the fifth and sixth repeats; (**i**): sample 5 and (**ii**): sample 8 of the experiment.

Table 3.1: Summary of Results

Sample ID	YES result *	Type of response			Triton X-100 EC50 (ng/L)	17ß-Estradiol EC50 (ng/L)	Relative induction efficiency (RIE) %
		Toxic	Maximal	Submaximal			
1	3	x	-	x	14360	28.90	58
2	3	x	-	x	103100000	39.02	60
3	3	x	-	x	87010000	12.80	65
4	3	x	-	x	9901	16.08	64
5	3	x	-	x	2633000	14.67	53
6	2	x	-		N/Q	14.33	N/Q
7	2	x	-		N/Q	54.40	N/Q
8	3	x	-	x	64300000	52.59	55
Average					**42844544**	**29.10**	**59**
SD					**47597991**	**17.53**	**5**

Detection Limit (YES results)

* 0 Below detection limit

1 One point above detection limit

2 Two points above detection limit

3 Three or more points above detection limit (positive for estrogenic activity)

RIE = Relative induction efficiency. Max absorbance of sample/Max absorbance E2 x 100

N/Q = Not Quantifiable

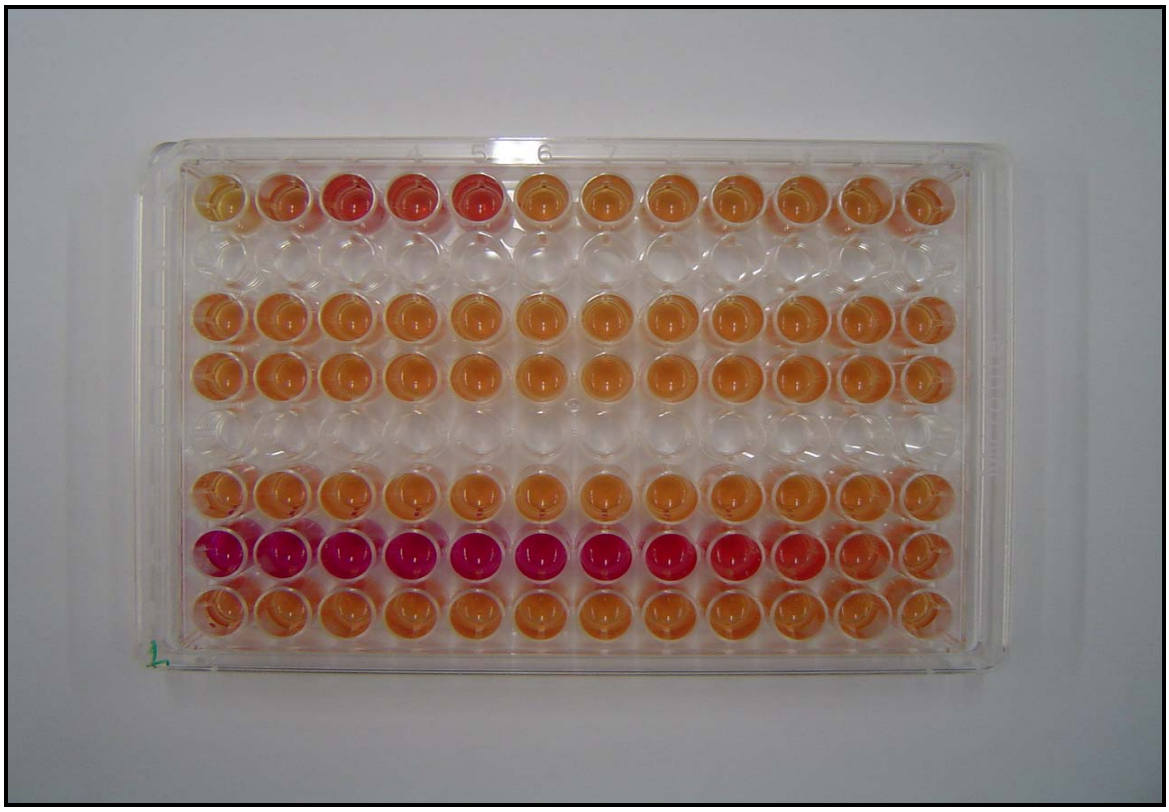

Figure 3.5: A 96-well plate used in the study photographed on day 4 of incubation. Rows 1, 3 and 4: a serial dilution of Triton X-100. Rows 2 and 5: left open, to prevent contamination due to possible creeping of the sample. Row 6: blank/control. Row 7 and 8: 17β-Estradiol. The increase in color intensity can be seen in the first (Triton X-100) row in the first 5 wells, indicating estrogenic activity and toxicity.

The recombinant yeast cells were designed and engineered for exquisite sensitivity to estrogens (McDonnell *et al*., 1991a, McDonnell *et al*., 1991b and Pham *et al*., 1991); over expression of human estrogen receptor, high amplitude frog vitellogenin estrogen response elements, and their tandem arrangement in the reporter plasmid all serve to amplify β-galactosidase production and hence sensitivity to 17β-estradiol (Klein *et al*., 1994).

A standard dose-response curve is defined by four parameters: the baseline response (bottom), the maximum response (top), the slope, and the drug concentration that provokes a response halfway between the baseline and maximum (EC50) (GraphPad Software, 1999). 17β-Estradiol produced dose response curves which occurred over the

whole of the absorbance range of the assay (full dose-response curves). A simple calculation, using EC50 values, showed that Triton X-100 is 496 times less potent than 17β-Estradiol and induced responses which were less than the maximum response obtained with 17β-Estradiol. Such curves that fail to reach the maximum response obtained with 17β-Estradiol are referred to as submaximal responses or submaximal response curves (Beresford *et al*., 2000). Parameter EC50 gives the transition center and equals the potency, which is the concentration that caused 50% efficiency (De Boever *et al*., 2001). The relative induction efficiency (RIE) is determined as the ratio of maximal β-galactoside activity induction with test compound to 17β-Estradiol x 100 (Coldham *et al*., 1997).

The detection limit of the yeast assay was calculated as absorbance elicited by the solvent control (blank) plus three times the standard deviation. When the absorbance values of the different samples of Triton X-100 were compared to the detection limit (three or more points above the detection limit is positive for estrogen activity), sample 6 and 7 had only two points above the detection limit. Sample 6 and 7 were not below the detection limit for estrogen activity and therefore, the EC50 values of Triton X-100 and the RIE were not quantifiable. The relative potency of Triton X-100 could not be determined, since Triton X-100 failed to induce β-galactosidase to 50% of the total 17β-Estradiol activity. Furthermore, Triton X-100 never provided the same induction of β-galactosidase activity as 17β-Estradiol at any concentration, as described by Coldham *et al*., 1997, and it was therefore not possible to calculate the relative potency of Triton X-100. Looking at the EC50 values of Triton X-100 (Table 3.1) it appears to be a weak estrogen despite limited repeatability. The yeast screen assay is a reliable assay to use to determine estrogenic activity. Good repeatability has been achieved when testing chemicals in this assay (Beresford *et al*., 2000). Considering that the six repeats (sample 1-5 and 8) were done in duplicate, the phenomenon of low repeatability is indistinct and obscure, and should be further investigated. Submaximal response curves in figure 3.4 c (sample 5 and 8), showed strange non-sigmoidal curves for Triton X-100. These results were strange and not interpretable, since the samples represented two repeats in duplicate, it is apparent that Triton X-100 has no repeatability. Although the relative potency of Triton X-100 was not consistent between repeats the RIE results for sample 1, 2, 3, 4, 5 and 8 were constant with a standard deviation (SD) of 5%. The maximum absorbance values of Triton X-100, ranged from 1.31 to 1.55 (control = 1.0) measured

on day 4, indicate the presence of weak estrogen activity (EEqs 0.04ng/L). One limiting factor of the recombinant yeast screen assay is that it can only measure estrogen activity if it is receptor-mediated. The weak estrogenic activity seen in sample 1 – 5 and 8 of the study must be receptor mediated. If the receptor had not been engaged there would have been no reaction. The reaction could be weak because it may function as an anti-estrogen. Alternatively Triton X-100 might possibly produce its estrogen properties by triggering other pathways in the cell contributing to endocrine disruption. Coldham *et al*., 1997, reported that competitive binding studies have shown that 2,3,7,8-tetrachlorodibenzo-p-dioxin does not bind to the estrogen receptor, but dioxins can evoke estrogenic and diverse potent antiestrogenic effects through various cellular mechanisms (Coldham *et al*., 1997, Birnbaum and Harris *et al*., 1990).

3.4 Conclusions

In conclusion, Triton X-100 showed weak estrogen activity. Upon comparison, the dose-response curves of Triton X-100 and 17β-estradiol in Figure 3.4 a and b i and ii, it was clear that Triton X-100 evoked an estrogenic response at much higher concentrations than the positive control 17β-estradiol. Similar results were obtained with Triton X-100 on the T47D-KBluc cell line (results not shown). The stable cell line, T47D-KBluc, constructed and described in a study by Wilson *et al*., 2004, resulted in the generation of a sensitive and responsive tool for the screening of chemicals for estrogenic activity. T47D human breast cancer cells, which contain both endogenous ERα and ERβ, were transfected with and ERE luciferase reporter gene construct. It provided an *in vitro* system that can be used to evaluate the ability of chemicals to modulate different assays (one for alpha and one for beta) would not be needed (Wilson *et al*., 2004). Triton X-100 showed tremendous variation in the results obtained in six duplicate repeats during the study. The results confirmed high toxicity of Triton X-100 however due to the results in YES and T47D-KBluc assay for estrogenic activity further investigations should be done on the strange and indefinable properties elicited by Triton X-100.

Chapter 4: The Toxic Effect of Triton X-100, CoQ10 Alone and in Combination on Primary Chicken Embryonic Cardiac and Skeletal Muscle Cell Cultures

4.1 Introduction

Triton X-100 is used in immunohistochemistry to make tissue permeable, to present certain antigens to antisera, and to prevent certain nonspecific interactions. This detergent is routinely dissolved in buffers at concentrations of 0.01 - 0.2% (Weruaga *et al*., 1998). Cimino *et al*., 2006, demonstrated that it is possible to successfully permeabilize mycobacteria with Triton X-100 in the concentration range 0.01% - 0.1% for intervals of 5, 10 and 15 minutes. These authors also showed that prolongation of the incubation time with Triton X-100 for more than 5 minutes generated cellular lyses (Cimino *et al*., 2006). In a study done by Fang *et al*., 1994, it was found that Triton X-100 non-enzymatically catalyzes the reduction of nitroblue diformazan (NBT) by NADPH to form formazan. Triton X-100 is also an activator of NADPH-diaphorase. Triton X-100 decreases the binding of formazan to cell membranes and dissolves the extracellular formazan. Triton X-100 also increases the permeability of cell membranes. These effects together can account for the improvement in the NADPH-diaphorase histochemical staining produced by Triton X-100 (Fang *et al*., 1994).

Coenzyme Q10 is present in the endomembranes of cells as well as in mitochondria, where it serves as a central component of the transmembrane electron transport system (Sun *et al*., 1992). The CoQ10 in endomembranes is concentrated in the Golgi apparatus and the plasma membrane (Kalin *et al*., 1987). The high concentrations of CoQ10 in these membranes raise the question of its function within the extramitochondrial membranes (Sun *et al*., 1992). Sun *et al*., 1992, listed four possible functions for CoQ10 in the extramitochondrial membranes: a) storage for transfer to mitochondria or the blood serum, b) action as a renewable antioxidant within the lipid bilayers, c) function as an electron carrier in these membranes. Plasma membranes contain oxidoreductase enzymes (Crane *et al*., 1988), including a trans-plasma

membrane electron transport system that influences the growth of cells (Crane *et al*., 1990), activates phosphorylation of membrane proteins (Harrison *et al*., 1991), and induces expression of *c-myc* and *c fos* protooncogenes (Crane *et al*., 1988 and Sun *et al*., 1992). Evidence is presented by Sun *et al*., 1992, that CoQ10 functions in transmembrane electron transport and that added CoQ10 stimulates growth of HeLa and BALB/3T3 cells in the absence of serum, by an unknown mechanism (Sun *et al*., 1992), which may indicate a possible role in cell growth (Kagan *et al*., 1999). In a study by Chopra *et al*., 1998, the relative bioavailability of typical commercially available forms of CoQ10 was compared with that of Q-Gel, a new solubilized form of CoQ10, in human subjects in two separate trials. The data from both the trials showed that Q-Gel is vastly superior to typical commercially available preparations of CoQ10, which means that much lower doses of Q-Gel will be required to rapidly reach and maintain adequate blood CoQ10 values than with any of the other currently available products (Chopra *et al*., 1998).

The heart is the first functional organ in the developing embryo (Lyons, 1996). The development of the chicken heart involves a series of cellular migrations, fusions, and tissue differentiation. The heart develops from the fusion of paired precardiac mesodermal tubes located on either side of the developing foregut. Between 25 and 30 hours of incubation, the paired heart vesicles begin to fuse at the anterior end and continue to fuse posteriorly to form one continuous tube. The heart begins to beat just after the paired heart rudiments begin to fuse, immediately before the bulbus cordis forms. Once the heart tubes have completely fused, the sinus venosus becomes the embryonic pacemaker. Eventually, when the atrium and ventricle each divide into a pair of chambers, and a typical four-chambered heart is present, the sinus venosus is incorporated into the right atrium where it gives rise to the sinoatrial node, the mature pacemaker (McCain *et al*., 1999). Contractions of cardiomyocytes can be observed in chicken embryos already after 36 hours *in ovo* (at the 9 somite stage) and after 12 further hours the entire blood flow is managed by a rhythmically contracting meshwork of myofibrils (Ehler *et al*., 1999). The limb buds are first identifiable at ~60 hours of embryonic development as small outgrowths of mesenchyme derived from both somatic and somatopleural areas adjacent to the limb, covered by body wall ectoderm (Chevallier *et al*., 1977). By 96 hours, cells of the limb mesoblast become developmentally restricted to the chondroblast, myoblast, or fibroblast lineages, and, as

development progresses, differentiated chondrocytes become evident in the core region of the limb and differentiated muscle fibers begin to form in the peripheral regions (Konieczny *et al*., 1983). All three muscle types, skeletal, cardiac and smooth muscles are composed of elongated cells specialized for contraction. Cardiac muscle cells have one nucleus but the ultrastructure is much like that of skeletal muscle cells. Skeletal muscle consists of a heterogenous population of multinucleated, striated myofibres, which are highly differentiated cells and therefore unique in structure, held together by connective tissue (Tortora *et al*., 2003).

Based on the known effects of Triton X-100, the cytotoxicity of this non-ionic detergent will be determined on primary chicken cardiac and skeletal muscle cell cultures, alone and in combination with CoQ10. The cytotoxic effects of CoQ10 on primary chicken cardiac and skeletal muscle cell cultures were determined. Cell culture is defined as growth of cells dissociated from the parent tissue by spontaneous migration or mechanical or enzymatic dispersal (Fresheny, 1994). Because of wide availability of chicken embryos and the ease of obtaining tissue from these embryos without resorting to sophisticated surgical procedures, chicken embryos are the ideal source of a variety of primary cell cultures. *In vivo* systems share the characteristic that they exclude the influence of other organs and of the circulatory and immune system, thus providing the possibility to study direct effects on a cell population (Sultan *et al*., 2001). Cell number, cell viability and lysosomal membrane integrity were determined using Crystal Violet (CV), MTT, and Neutral Red (NR) assays, respectively.

In this Chapter the following research objectives were investigated:

- Select a concentration range of Triton X-100, starting at a concentratin that will, according to the literature, cause membrane disruption and prepare a serial dilution from that.
- Select a concentration range of CoQ10, where the recommended supplementation dosage, 100mg/day (Crane, 2001), will compare with the lowest two concentrations in the range.
- Establish and optimize methodologies used to isolate cardiac and skeletal muscle cells from chick embryos, and establish primary cultures of these chick embryonic cardiac and skeletal muscle cells.

- Determine whether Triton X-100 and CoQ10 are cytotoxic to primary chick embryonic cardiac and skeletal muscle cell cultures by determining the effect of Triton X-100 and CoQ10 on cell viability, lysosomal membrane integrity and cell number, using the MTT, NR and CV assays respectively.
- Choose two concentrations of Triton X-100, expected to cause cellular alterations, and test the cytotoxicity of the two concentrations on chick embryonic cardiac and skeletal muscle cell cultures, pre-treated with increasing concentrations of CoQ10, using the MTT, NR and CV assays.

4.2 Materials

4.2.1 Primary Cell Cultures

Fertile chicken eggs used for the experiments were obtained from National Chicks (Pty) Ltd, and Eagles Pride Hatchery (Pty) Ltd, and were stored at 4˚C for a maximum of two weeks. For the embryo development the fertile eggs were placed in the Grumbach incubator for 13 days, at a temperature 37.5˚C until day of termination.

4.2.2 Triton X-100 and CoQ10

Triton X-100 (CAS number: 9002-93-1), was obtained from Sigma-Aldrich (Pty) Ltd., Midrand, South Africa. CoQ10 Q-Gel Mega, 100mg, used in this project was manufactured by the Nutraceutical Science Institute (NSI), and was obtained from *vitacost.com*. (Item number: NI 003723 or 835003003723), USA.

4.2.3 Media, Supplements, Reagents and Plasticware

Dulbecco's Modified Eagle's Medium (DMEM), Hank's Balanced salt solution (HBSS), Foetal Calf Serum (FSC), and penicillin-streptomycin-fungizone (100x) (PSF) were obtained from Highveld Biological, Lyndhurst, South Africa. Sartorius cellulose acetate membrane filters 0.22µm were from National Separations, Johannesburg, South Africa. 0.20µm Minisart-Plus filters were from Sartorius, Goettingen, Germany. Fixatives, acids and organic solvents, such as gluteraldhehyde, formaldehyde, hydrochloric acid (HCl), acetic acid, isopropanol, and formic acid were analytical grade and were purchased from Merck, Johannesburg, South Africa. Trypsin, ethylene diamine tetra acetate (EDTA),

dimethyl sulphoxide (DMSO), potassium chloride (KCl), potassium dihydrogen phosphate (KH_2PO_4), disodium hydrogen phosphate (Na_2HPO_4), sodium chloride, and sodium hydrogen carbonate ($NaHCO_3$) were from Merck, Johannesburg, South Africa.

MTT (1-(4,5-Dimethylthiazol-2-yl)–3,5 diphenylformazan), Crystal Violet (CV) powder and Neutral Red (NR) powder were form Sigma-Aldrich, Atlasville, South Africa. Water was double distilled and deionized (ddH_2O) with a Continental Water System and sterilized through a Millex 0.2µm filter. Glassware was sterilized at 140˚C in a HL-340 Series vertical Type Steam Sterilizer Autoclave.

Twenty four well plates and 96-well plates, $25cm^2$ and $75cm^2$ cell culture flasks, 5ml and 10ml pipettes, 15ml and 50ml centrifuge tubes, micro centrifuge tubes and eppendorf tubes were from NUNC™ supplied by AEC- Amersham, Johannesburg, South Africa.

4.3 Methods

4.3.1 Establishment of Chicken Cardiac and Skeletal Muscle Cell Cultures

For the establishment of primary cultures of chick cardiac and skeletal muscle cells, several parameters needed to be optimized, namely the stage of embryological development for successful establishment of primary cardiac and skeletal muscle cells. The eggs were incubated for six (E6), and thirteen (E13) days. After each incubation period, heart development and development of the leg muscle were evaluated and cells were isolated and plated as described below. The developmental phase between 4 and 9 days of incubation is characterized by rapid changes in the wings, legs, and visceral arches. From the 8^{th} to the 12^{th} day, feather-germs and eyelids provide the most useful criteria to describe and distinguish the developmental stages. The designation of stages during the last phase of incubation is difficult because practically no new structures are formed and there is mainly just growth of what already exists (Hamburger *et al*., 1951). Hamburger et al., 1951, described stage 39 (E13) of the limb development: "*Limbs:* Scales overlapping on superior surface of leg. Major pads of phalanges covered with papillae; minor pads are smooth. Length of third toe = 9.8 ± 0.3 mm". The tubular heart of chick embryos begins beating spontaneously at 36-45 hours, and its contractions are

coordinated by propagation of activity before the appearance of specialized conducting tissues. Desmosomes and intercalated discs are present at day 2. Gap junctions are not found. Myofibrils in young hearts are sparse, run in all directions, and are in various stages of formation. Sarcoplamic reticulum is present, but a transverse tubular system is absent (Sperelakis *et al*., 1972). On the 6th day of embryonic development, it was extremely difficult to obtain muscle tissue from the hind limbs, since the muscle tissue was still developing, and the limbs were very tiny. Development of the heart and leg muscle tissue were optimal on the 13th day of embryonic development (E13), since it was possible to remove the heart from the thoracic cavity without the risk of removing other tissue along with it. It was also possible to remove leg muscle tissue from the bones (cartilage), and remove the skin covering the limb from the muscle tissue without the risk of cartilage or epidermal cell contamination. Muscle tissue was of desired size and suitable for primary cell culture procedures. Embryonic day 13 was decided on to harvest tissue for culturing.

After each incubation period (13 days) eggs were removed from the incubator and sprayed with 70% ethanol. The wider side, containing the airspace was opened and the embryo was gently lifted out using a spoon spatula and placed into a sterile Petri dish, followed by immediate decapitation. Aseptic techniques were used. The leg muscle and heart were dissected from the embryo. The skin and bony structures were removed from the leg muscle, and the hearts were trimmed free of the pericardium and visible vessels. The heart and skeletal muscle tissues were then cut into small fragments in separate sterile Petri dishes, and washed thrice with Hanks Balanced Salt Solution (HBSS) (9.7g/L Hanks Balanced Salt Solution + 0.35g/L $NaHCO_3$ in 1L ddH_2O), in a 15ml test tube. The tissue was incubated in 0.025% trypsin solution (0.2g EDTA, 0.25g Trypsin in 100ml DPBS) prepared in Dulbecco's Phosphate Buffered Saline (DPBS), for 24 hours at 4˚C. A 10X DPBS stock solution was prepared by dissolving 2g/l KCl, 2g KH_2PO_4, 80g/l NaCl and Na_2HPO_4 in ddH_2O that was diluted 1:9 with ddH_2O prior to use. Thereafter, trypsin was removed, and the pellets were incubated for 20 minutes at 37.5˚C and 5% CO_2 in a NAUIRE^{TM} US Autoflow CO_2 water-jacketed incubator. After incubation Dulbecco's Modified Eagle's Medium (DMEM), containing 5% foetal bovine serum (FBS) and 2% antibiotics (PSF), (a commercially available antibiotic/fungus supplement prepared for cell culture media from Highveld Biological, Lyndhurst, South Africa who usually prepare the antibiotics at 1% each and the fungizone at 250ug/ml),

was added to inhibit digestion. The cells were then washed thrice with DMEM, by repeated resuspension and sedimentation using a Hermle Z300 centrifuge at 1250rpm for 2 minutes. The final pellet was resuspended in 4ml of DMEM containing 5% FBS and 2%PSF. Single cell suspension were prepared by mechanical trituration, accomplished by pippetting the suspension several times through a 5ml pipette, and then left for 1-2 minutes to allow any large fragments of cells to settle to the bottom of the 15ml test tube. A total cell count was performed by means of the Trypan Blue exclusion assay (0.4% Tryphan Blue solution in H_2O).

Heart cells were plated onto the surface of a 24-well plate. Skeletal muscle cells were plated onto the plastic surface of a 75cm^2 cell culture flasks to allow the attachment of fibroblasts, and then incubated for 45-60 minutes at 37.5˚C and 5% CO_2. Unattached cells were then replated onto the surface of a 24-well plate.

For each experiment, skeletal muscle cells and heart cells were plated at a cell concentration of 5 x 10^4 cells per ml in 24-well plates with a culture area of 1.9cm^2/well and were maintained at 37.5˚C and 5% CO_2 content for 72 hours to allow optimal cell development, attachment and differentiation. The medium was not changed during this period, as this causes loss of unattached cells.

4.3.2 Cellular Morphology and Cellular Structure of Primary Cultures

To examine the cardiac and skeletal muscle cell morphology and structure of the primary cultures, the primary cultures were plated onto to bottom of 24-well plates. Cells were not pre-plated to reduce fibroblast contamination. After 24hr exposure to the substances tested for cytotoxicity in this Chapter, the cells were fixed by adding 50µl of a 2% formaldehyde solution (in ddH_2O) for 30 minutes, washed with ddH_2O and left to dry overnight at room temperature. After the plates were completely dried, 300µl of Crystal Violet (CV) dye solution prepared in 200mM of formic acid, pH 3.5, was added to each well and left for 1 hour. The dye was removed and plates were washed with ddH_2O, and left to dry. Cell morphology and structure were studied by inverted light microscopy using a Zeiss Axiocam MRc5 microscope (Figure 4.2 to 4.7).

4.3.3 Preparation, Optimization and Exposure of Triton X-100 and CoQ10, Alone, and in Combination

100% Triton X-100 was obtained in liquid form and a filtered through a 0.20µm Minisart-Plus filter, before the concentrations tested were prepared. Fifty microliter of 100% Triton X-100 were dissolved in 10ml ddH_2O, a 0.5% Triton X-100 concentration in order to obtain the first concentration of five, labeled TX 1 in this study. A serial dilution of the 0.5% Triton X-100 solution was prepared and was: 0.05% (TX 2), 0.005% (TX 3), 0.0005% (TX 4), and 0.00005% (TX 5). One hundred microliter of the different Triton X-100 concentrations, TX 1 – TX 5, was added per well containing 500µl medium. Coenzyme Q10 was obtained in a 100mg gel capsule, and a stock solution was prepared using 1 x 100mg capsule dissolved in 10ml of ddH_2O, using an ultrasonic water bath. In order to obtain the five different concentrations used in the study (Q1 – Q5), 200µl, 100µl, 50µl, 20µl, 10µl, respectively were added to 5 test tubes each containing 10ml ddH_2O, making a concentration series of 0.2mg/ml, 0.1mg/ml, 0.05mg/ml, 0.02mg/ml and 0.01mg/ml. A volume of 100µl was added to each well, containing 500µl medium.

In order to study the combination effect of the substances, the cardiac and skeletal muscle cell cultures were exposed to TX 2 (0.05%) and TX 3 (0.005%), respectively, in combination with increasing concentrations of CoQ10 (Q4, Q3, Q2, Q1). After 72 hours, cells were treated with CoQ10 for two hours prior to Triton X-100 exposure.

4.3.4 The Toxic Effect of Triton X-100 and CoQ10, Alone, and in Combination

Cardiac and skeletal muscle cell cultures were established as described above. After 72 hours of maintaining the cells in culture the cells were well established and attached, and the cultures were exposed to Triton X-100 and CoQ10 alone and in combination. Following exposure to the various concentrations of the substances tested, cell number, cell viability and lysosomal membrane integrity was determined using the combined CV, MTT, and NR.

4.3.5 The Combined Colorimetric Cytotoxicity Assay

While the MTT assay is based on measurement of the mitochondrial dehydrogenase activity of cells, NR and CV stain primarily the lysosomes and the membrane of viable cells, respectively (Ishiyama *et al*., 1996). The combined NR/MTT/CV procedure was as follows. One hundred microliter of 0.15% NR prepared in ddH_2O was added to each well and then incubated for 90 minutes at 37.5˚C in a CO_2 water-jacketed incubator, then 100µl of a 0.1mg/ml 3-(4,5- Dimethylthiazol-2–yl)-2,5-diphenyltetrazolium bromide (MTT) solution was added to each well and the cell culture plates were maintained for a further 60 minutes at 37.5˚C. The medium was then carefully removed and plates were blotted dry. Cells were then fixed for 10 minutes with 200µl of a 1% acetic acid and 1% formaldehyde solution in ddH_2O. The fixative was removed and the NR was solubilized with 200µl of a 1% acetic acid and 50% ethanol solution prepared in ddH_2O. The dissolved NR was then transferred to a 96-well plate. The MTT formazan crystals were then dissolved with 200µl DMSO, by shaking the plates for 20 minutes on an electronic IKA® SCHÜTTLER MTS 2, before being transferred into a 96-well plate. Each well was washed once with DPBS and the plates were left to dry overnight. The cells attached to the bottom of the plates were stained by adding 300µl of a 0.1% (weight/volume (w/v)) CV solution prepared in 200mM of formic acid, pH 3.5, to each well, and left to stain for 60 minutes. After the plates were washed with ddH_2O and dried, the bound dye was dissolved in 10% acetic acid, prepared in ddH_2O. The solution was transferred into a 96-well plate, and the absorbance of each well was determined spectrophotometrically at 570 nm, using the EL900 plate reader. Data were processed using Microsoft Excel, and statistical analyses were performed.

4.3.6 Statistical Analysis

The CV, MTT and NR assays were analysed separately with an appropriate Analysis of Variance (ANOVA). The data was expressed as mean ± standard error of mean, and analysed for statistical significance using a one-way ANOVA for the Dunett 95% confidence interval, many samples against a control, was carried out for the Triton X-100 and CoQ10 studies, and a two-way ANOVA for the combination studies. Testing was performed at a 0.05 level of significance and pair wise comparisons were done using Tukey analysis when analyzing the effect between Triton X-100 and CoQ10. All statistical analysis was performed using the Microsoft Excel and Analyse-it program.

4.4 Results and Discussion

The study was undertaken in order to investigate the possible cytotoxic effects of Triton X-100 and CoQ10 alone, and in combination on 13 day-old chick embryo primary cardiac and skeletal muscle cell cultures' cell number, cell viability and lysosomal membrane integrity.

4.4.1 The Morphology and Structure of Cardiac and Skeletal Muscle Cells

Although many cells of multicellular organisms have limited contractile abilities, it is the capability of muscle cells, which are specialized for contraction that permits animals to move (Gartner, *et al*., 2007). These cells are therefore high energy consuming cells with a high number of mitochondria. It was decided to use muscle cells for the study, since the mechanism of action of CoQ10 are mainly located to the mitochondria. To study the cellular morphology a Crystal Violet (CV) dye solution prepared in 200mM of formic acid, pH 3.5 was added to each culture and left for 1 hour. The dye was removed and plates were washed with ddH_2O, and left to dry. Cell morphology and structure were studied by inverted light microscopy using a Zeiss Axiocam MRc5 microscope.

4.4.1.1 Skeletal Muscle Cells

During embryonic development, several hundred precursors of skeletal muscle fibers (myoblasts) line up end to end, fusing with one another to form long multinucleated cells known as myotubes, which matures into the long muscle cell with a diameter of 10 - 100 µm and a length of up to several centimeters. The newly formed myotubes manufacture cytoplasmic constitutents as well as contractile elements, called myofibrils, composed of specific arrays of myofilaments, the proteins responsible for the contractile capability of the cell (Gartner *et al*., 2007 and Kierszenbaum, 2007) Muscle cells or fibers form a long multinucleated syncytium grouped in bundles surrounded by connective tissue sheaths and extending from the site of origin to their insertion. The plasma membrane (sarcolemma) of the muscle cell is surrounded by a basal lamina and satellite cells. The sarcolemma projects long finger-like processes (transverse tubules/T tubules) into the cytoplasm (sarcoplasm) of the cell. T tubules make contact with membranous sacs or channels, the sarcoplasmic reticulum. The many nuclei of the muscle fiber are located at

the periphery of the cell, just under the sarcolemma. About 80% of the sarcoplasm is occupied by myofibrils surrounded by mitochondria (sarcosomes) (Kierszenbaum, 2007). Deep to the sarcolemma and interspersed between and among myofibrils are numerous and elongated mitochondria with many highly interdigitating cristae. The mitochondria may either parallel the longitudinal axis of the myofibril or wrap around the myofibril. Moreover, numerous mitochondria are located just deep to the sarcoplasm (Gartner *et al*., 2007). The sarcoplamic reticulum encases hundreds and sometimes even thousands of myofibrils. Myofibrils are cylindrical in shape and run in the length of the muscle fiber. Light microscopy shows that a myofibril has light and dark bands, responsible for the striated appearance of skeletal muscle. The striations are formed by the placement of protein filaments within the contractile units, called sarcomeres, which extend between two dark lines, called the Z lines (Mader, 2001). The sarcomere is the basic contractile unit of striated muscle. Sarcomere repeats are represented by myofibrils in the sarcoplasm of skeletal and cardiac muscle cells. The arrangement of thick (myosin) and thin (actin) myofilaments of the sarcomere is largely responsible for the banding pattern. Actin and myosin interact and generate contraction force. The Z disk forms a transverse sarcomeric scaffold to ensure the efficient transmission of generated force. During contraction the length of the sarcomere decreases because thick and thin filaments slide past each other (Kierszenbaum, 2007).

4.4.1.2 Cardiac Muscle Cells

Cardiac cells (cardiocytes) are branched cylinders, 85 – 100μm long, approximately 1.5 μm in diameter, with a single centrally located nucleus (Kierszenbaum, 2007). Cardiac muscle, the specialized muscle of the heart, shares features with both smooth and skeletal muscle. Like skeletal muscle fibers, cardiac muscle fibers are striated and have a sarcomere structure (Silverthorn, 2004). The organization of the contractile proteins are the same as found in skeletal muscle, however the cytomembranes exhibit some differences. Mitochondria are more abundant in cardiac muscle than in skeletal muscle and contain numerous cisternae (Kierszenbaum, 2007). Almost half the volume of the cardiac muscle cell is occupied by mitochondria, attesting to its great energy consumption (Gartner *et al*., 2007). Like single-unit smooth muscle, cardiac muscle fibers are electrically linked to each other. The cells are joined end-to-end by specialized junctional complexes called intercalated disks. Intercalated disks have a steplike arrangement, with transverse portions that run perpendicular to the long axis of the cell

and longitudinal portions running in parallel to the myofibrils (Kierszenbaum, 2007). Some cardiac muscle, like smooth muscle, exhibit pacemaker potentials. Cardiac muscle is under sympathetic and parasympathetic control, as well as hormonal control (Silverthorn, 2004).

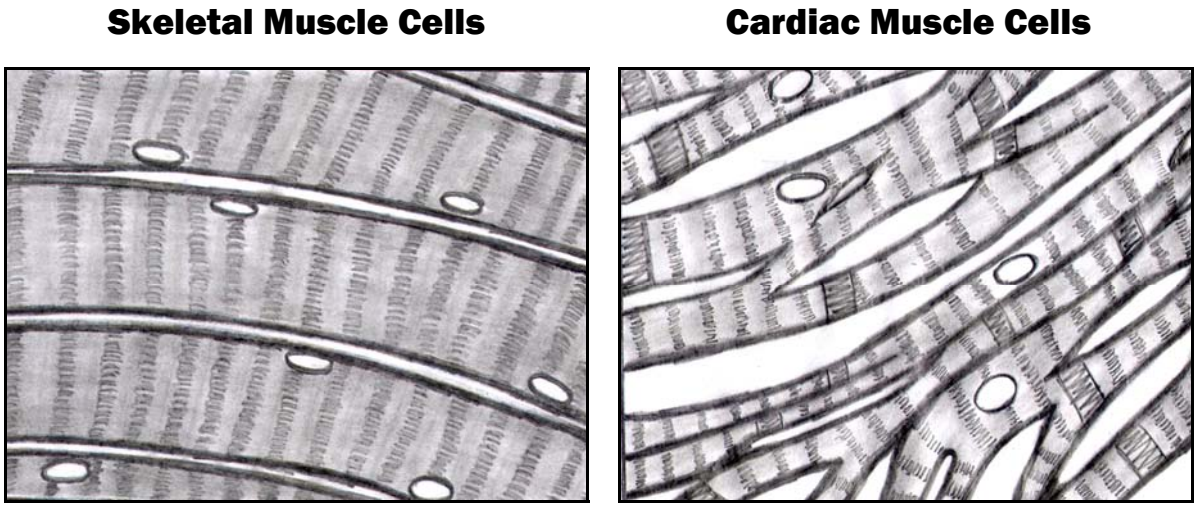

Figure 4.1: Schematic representation of skeletal and cardiac muscle.

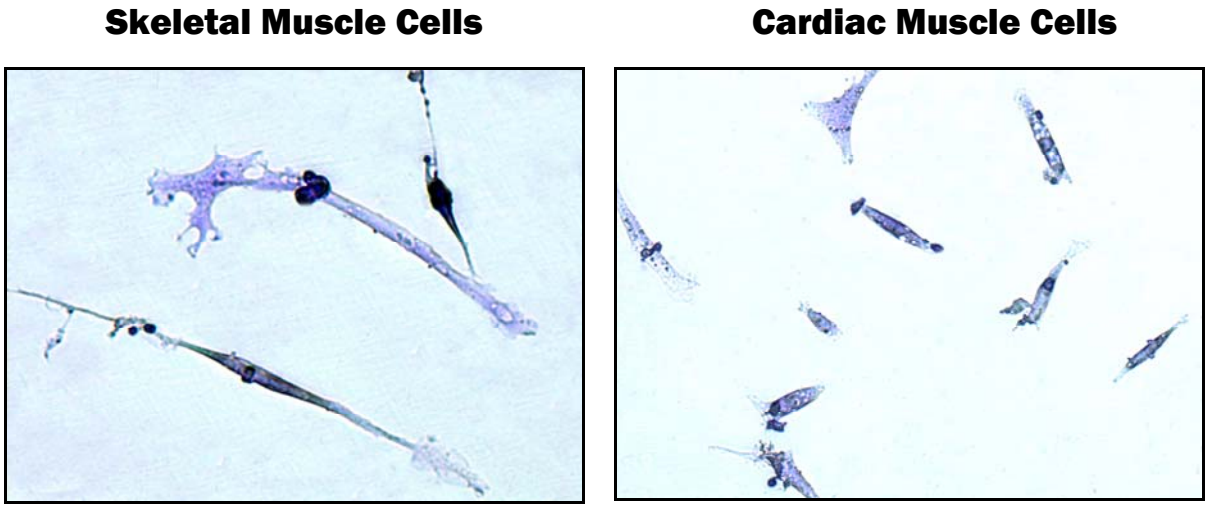

Figure 4.2: Skeletal and cardiac muscle cells of the control group at 20x long distance (LD) magnification, stained with crystal violet (CV).

Skeletal Muscle Cells

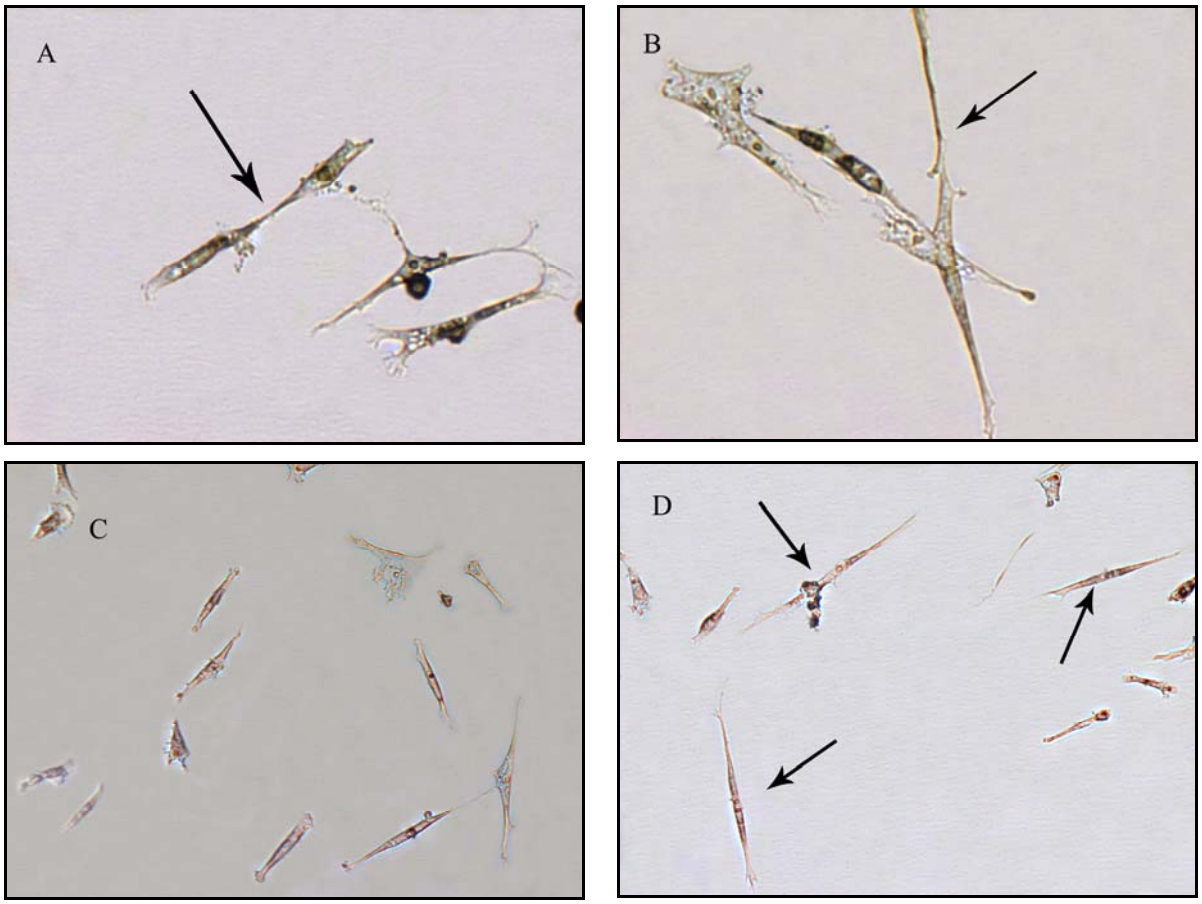

Figure 4.3: Skeletal muscle cells grown in a flask, stained with crystal violet to monitor the morphological characteristics of the cells, **A** & **B**): Skeletal muscle cells at 20x LD magnification. The black arrows indicate myoblasts that has fused to form a myotube. **C** & **D**): Skeletal muscle cells at 10x LD magnification. The black arrows indicate myotubes.

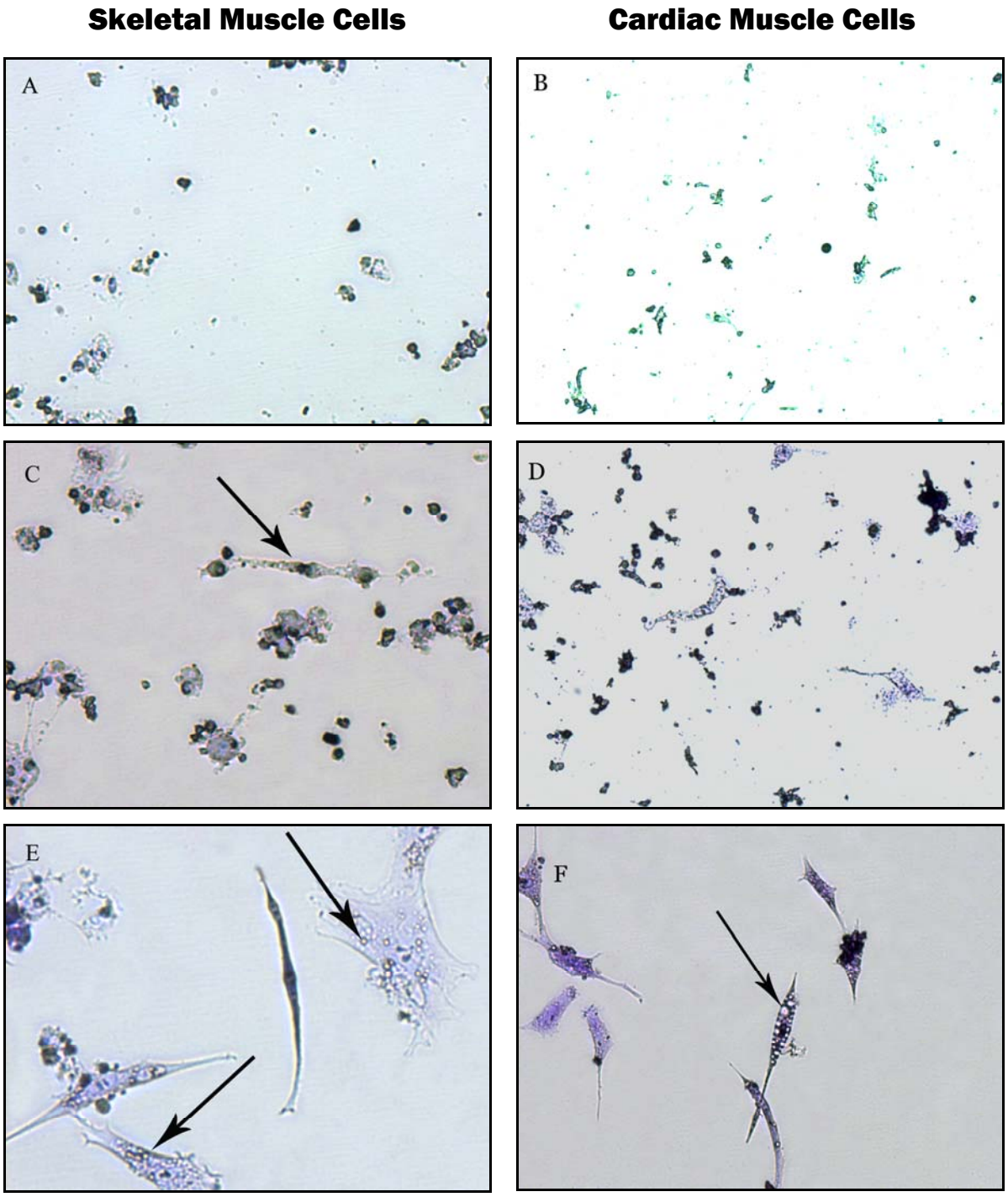

Figure 4.4 a: Skeletal and cardiac muscle cells exposed to Triton X-100. **A** & **B**): 0.5% Triton X-100, only cell fragments are present. **C** & **D**): 0.05% Triton X-100, cell fragments are present, the black arrow (**C**) indicate a skeletal muscle cell. **E** & **F**): 0.005% Triton X-100, cells seem to be intact, the presence of numerous vacuoles inside the cells was noticed (black arrows).

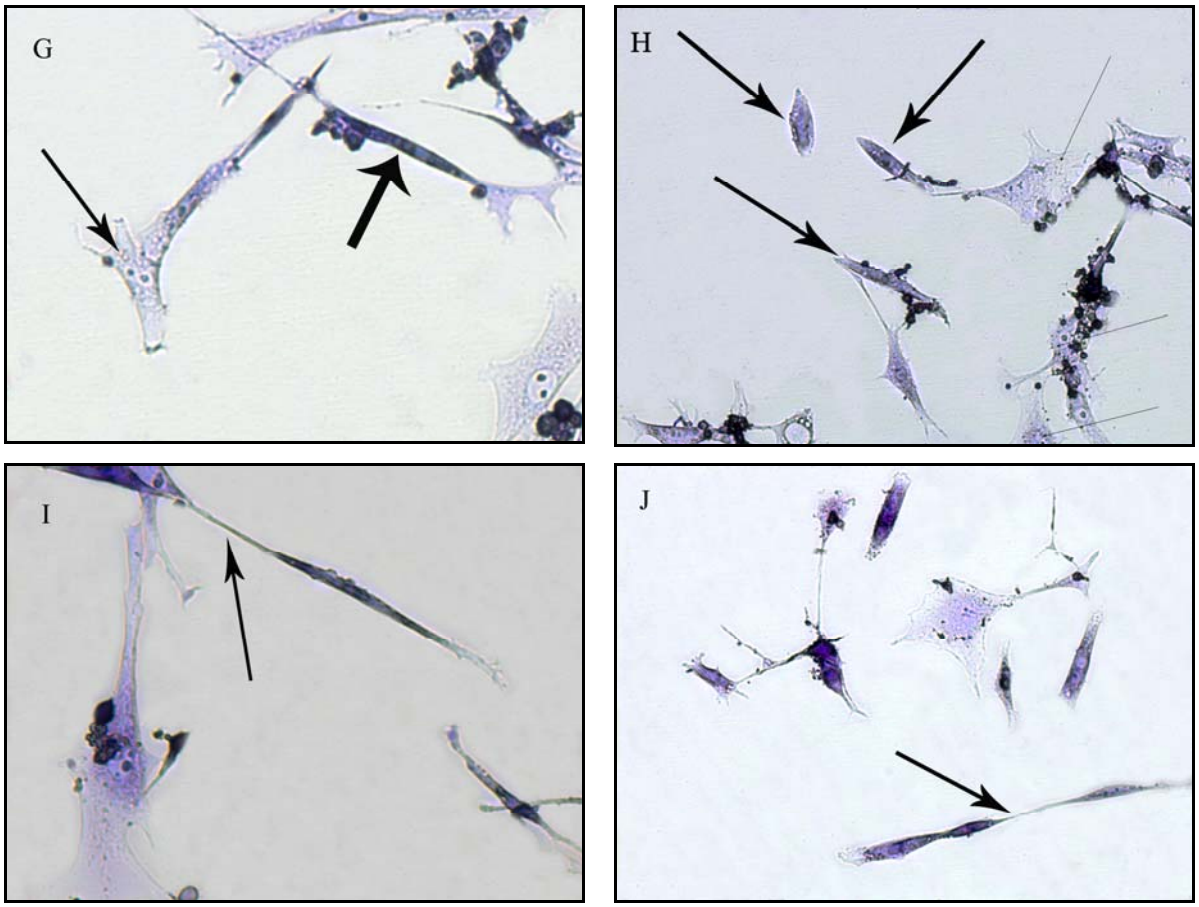

Figure 4.4 b: Skeletal and cardiac muscle cells exposed to Triton X-100. **G** & **H**): 0.0005% Triton X-100, cells appears to be structurally intact. Vacuoles present in **G** (thin black arrow). Characteristic light and dark bands of muscle cells were seen in **G** (thick black arrow). Muscle cells (thick black arrows) and fibroblasts (thin black arrows) were present in **H**. **I** & **J**): 0.00005% Triton X-100. Fusion of two myoblasts to form a myotube (indicated by black arrows). Cells are structurally intact.

Bader *et al*., 1976, found that chick embryonic cells transformed by the Bryan high titer strain of Rous sarcoma virus (RSV-BH) are heavily vacuolated. It was demonstrated that the vacuoles are cytoplasmic, bounded by membrane, and composed largely of water. Cells infected with the mutant form of the Rous sarcoma virus, RSV-BH-Ta, which induces reversible temperature-dependent transformation were used to investigate the physiological requirements for development of the vacuoles, and reversal of vacuolization. It was found that Na^+ was the only component of the cell culture medium found essential from both the development and reversal of vacuoles. Glucose depletion or dinitrophenol treatment inhibited vacuolization, suggesting a possible energy requirement in the vacuolization process. Ouabain, an inhibitor of Na^+/K^+ ATPase, enhanced vacuolization. Two sugars, glucosamine and mannosamin, prevented the disappearance of vacuoles. The observervations by Bader *et al*., 1976, suggested that cellular vacuolization may be a normal physiological response to an increase in water and Na^+.

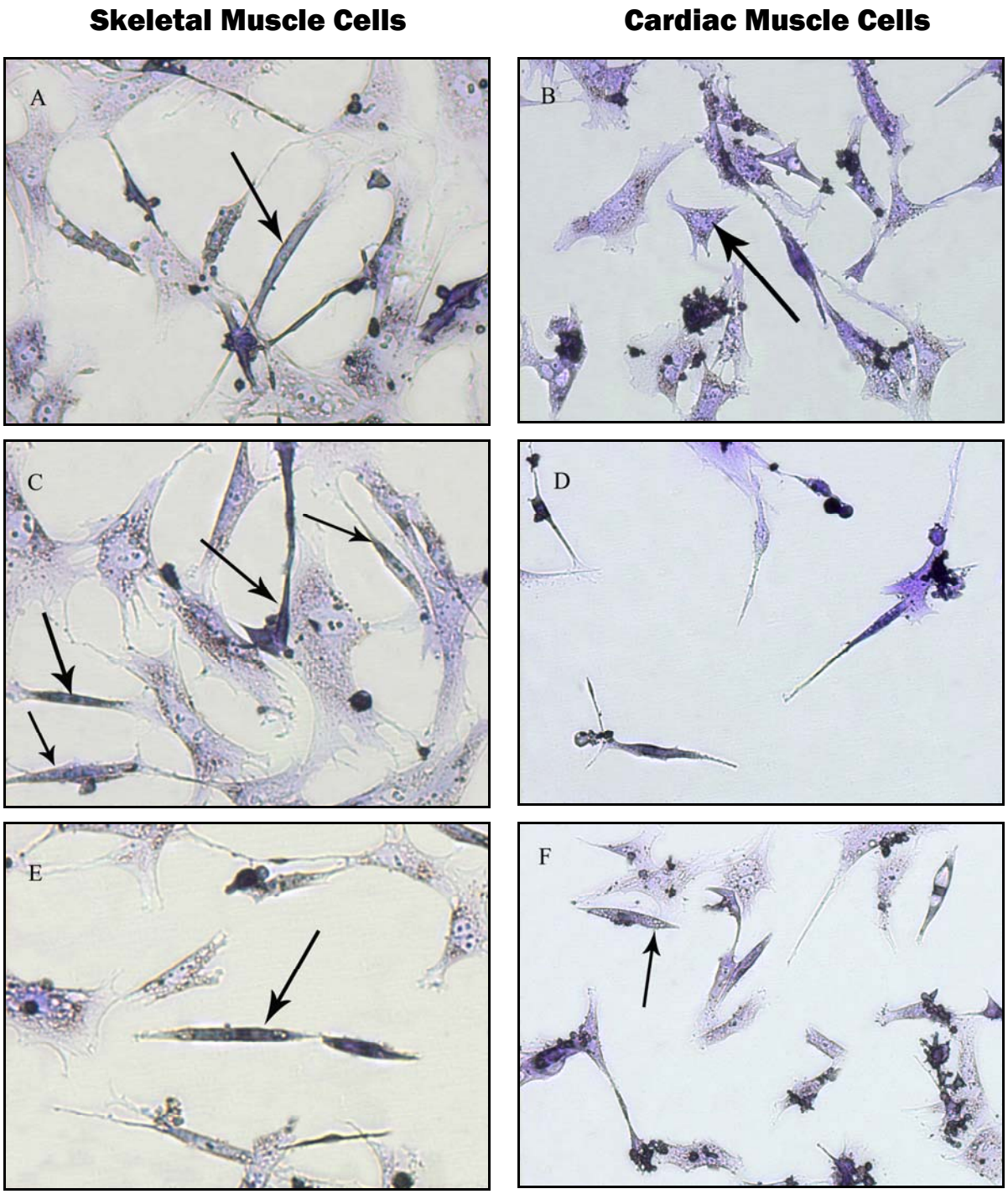

Figure 4.5 a: Skeletal and cardiac muscle cells exposed to CoQ10. **A** & **B**): 0.2mg/ml CoQ10; intact muscle cells (**A** – black arrow) were seen in both cultures. Numerous fibroblasts were present. Vacuoles were seen in some cells (**B** – Black arrow). **C** & **D**): 0.1mg/ml CoQ10; numerous intact muscle cells were seen in both cultures at this concentration, with notably more fibroblasts in the skeletal muscle cell culture. **E** & **F**): 0.05mg/ml CoQ10; Intact muscle cells in both cultures (black arrows).

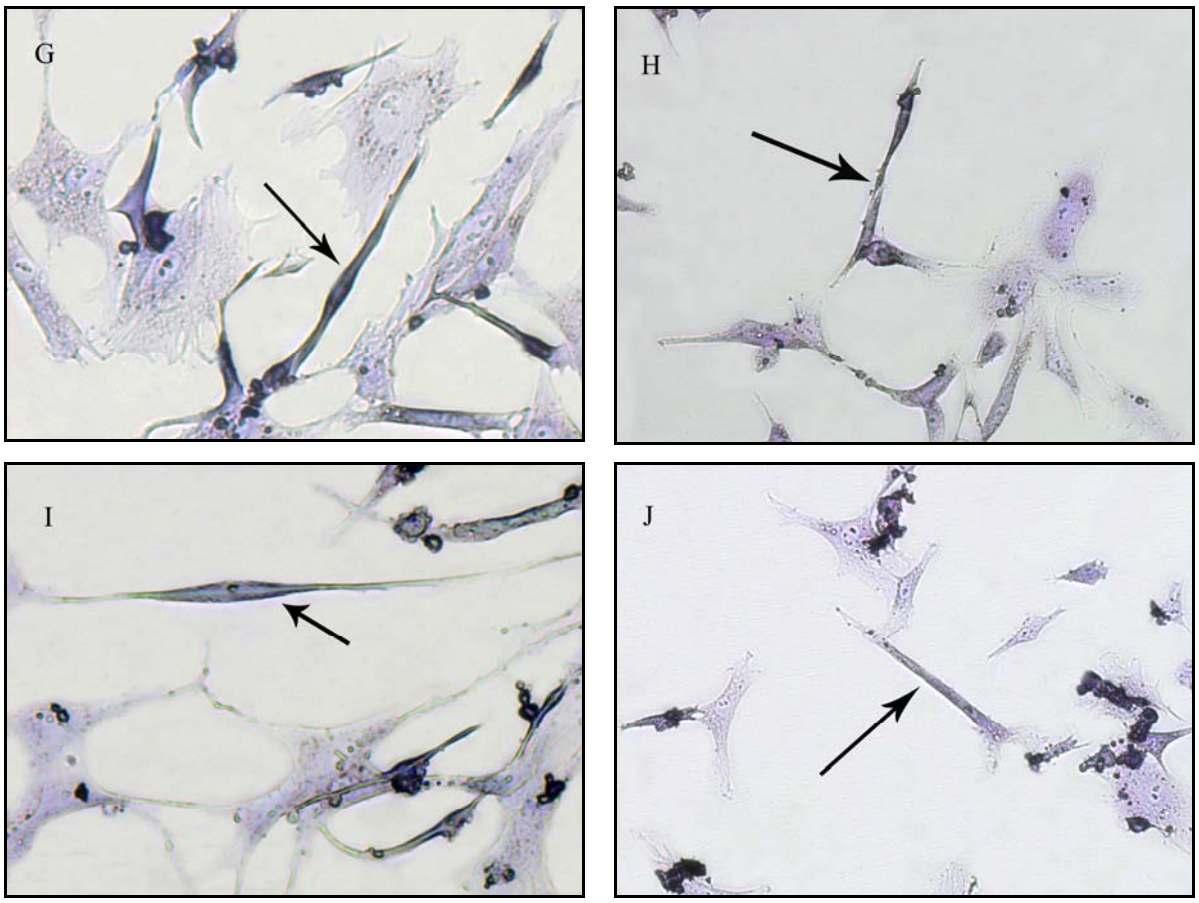

Figure 4.5 b: Skeletal and cardiac muscle cells exposed to CoQ10. **G** & **H**): 0.02mg/ml CoQ10; intact muscle cells were seen in both cultures, myoblast fusion (**H** – black arrow) and myotube formation (**G** – black arrow). **I** & **J**): 0.01mg/ml CoQ10; intact muscle cells were seen in both cultures, myotubes are indicated by the black arrows in both cultures.

Skeletal Muscle Cells

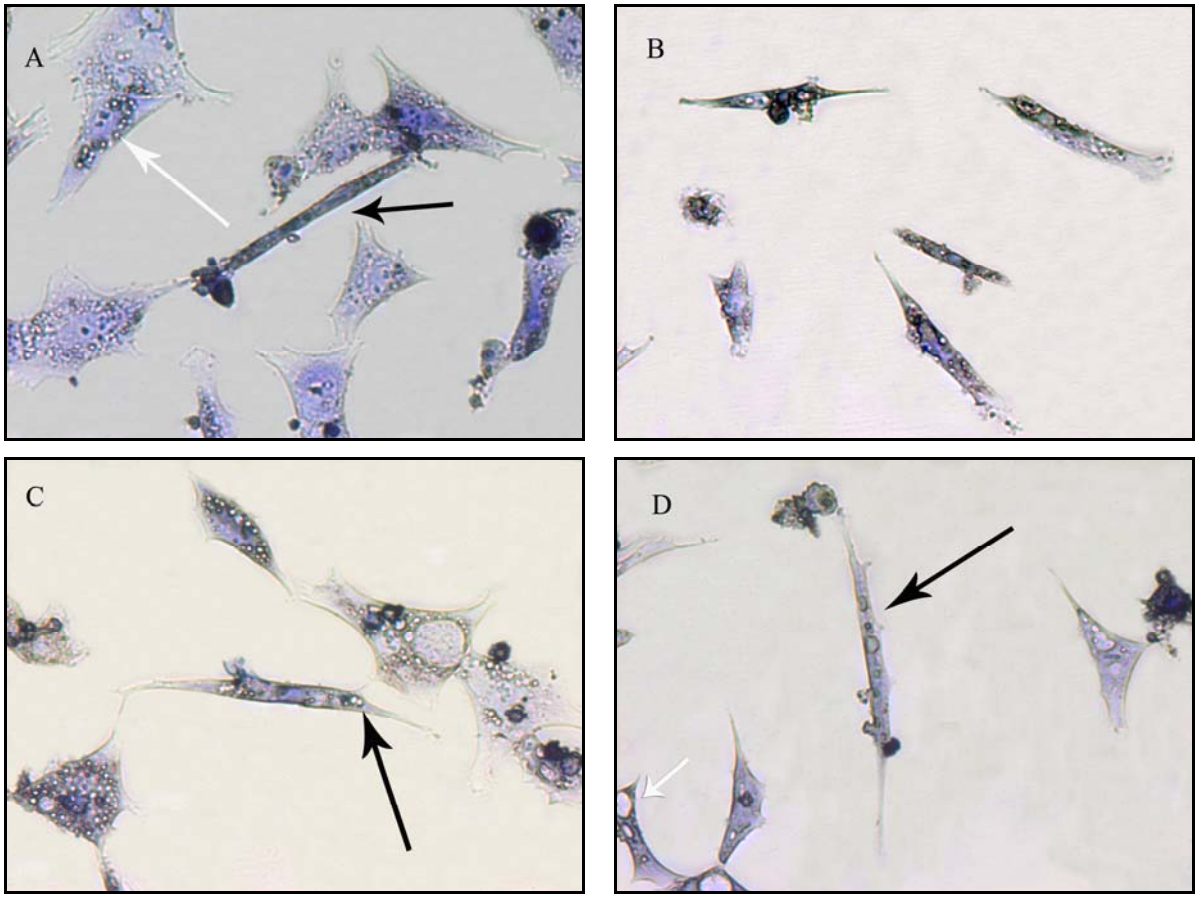

Figure 4.6: Skeletal muscle cells exposed to 0.05% Triton X-100, after two hours pre-treatment with different concentrations of CoQ10. **A**): 0.2mg/ml CoQ10; intact muscle cells were seen, myotubes were present at this concentration (black arrow), fibroblasts with numerous vacuoles were seen (white arrow). **B**): 0.1mg/ml CoQ10; muscle cells seemed less intact than the cells in **A**. **C**): 0.05mg/ml CoQ10; muscle cells presented with a disrupted with the presence of vacuoles. Fibroblasts with numerous vacuoles were present. **D**): 0.01mg/ml CoQ10; muscle cells (black arrow) showed bulging and instability of the membrane. Fibroblasts were present with vacuoles (white arrow).

Skeletal Muscle Cells

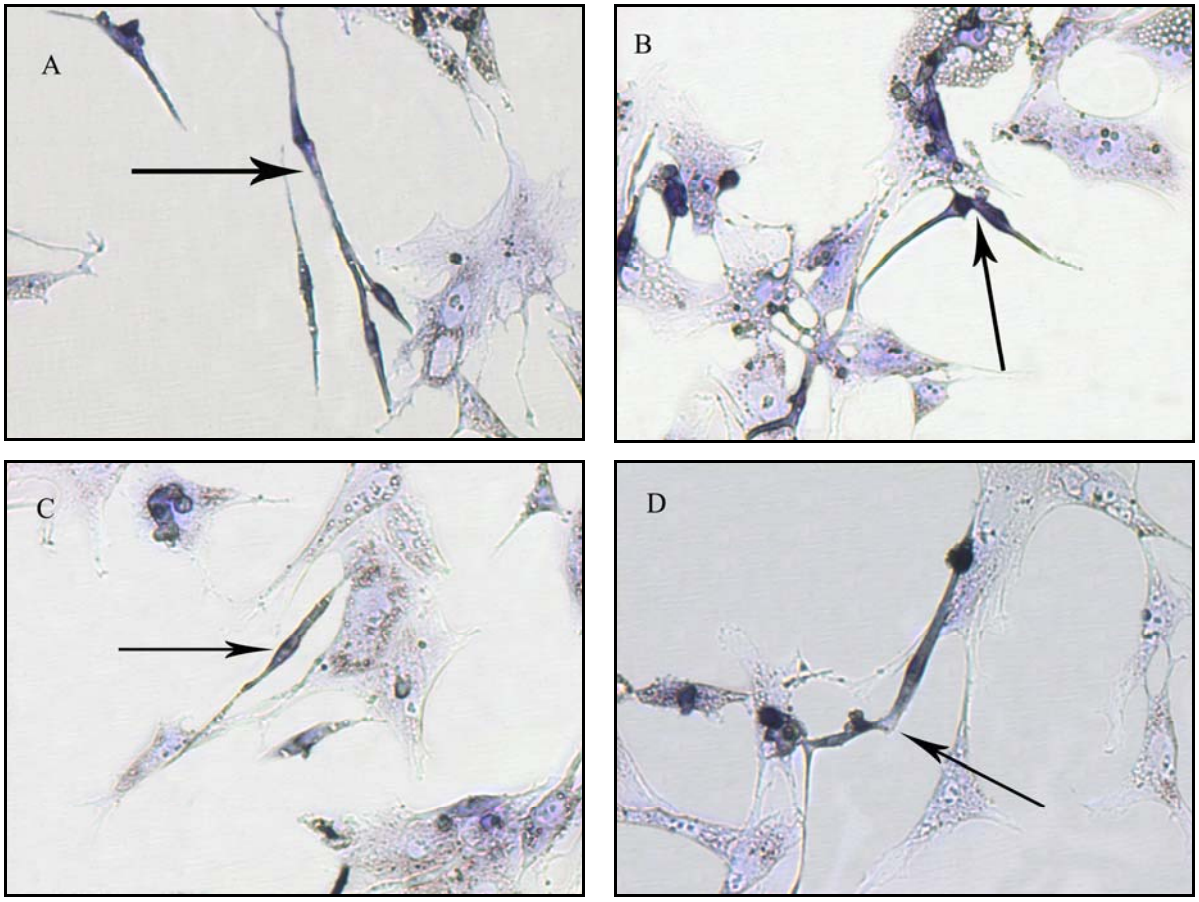

Figure 4.7: Skeletal and cardiac muscle cells exposed to 0.005% Triton X-100, after two hours pre-treatment with different concentrations of CoQ10. **A**): 0.2mg/ml CoQ10; **B**): 0.1mg/ml CoQ10; **C**): 0.05mg/ml CoQ10; **D**): 0.02mg/ml CoQ10. Myotube formation were seen in all the concentrations tested (**A** – **D** indicated by the black arrows).

4.4.2 The Effect of Triton X-100 on the Cell Number, Viability and Lysosomal Membrane Integrity of Chicken Embryo Primary Cardiac and Skeletal Muscle Cell Cultures

Considering the numerous protective effects of CoQ10 on cells, tissues, organs and systems, the question arose whether CoQ10 might have a protective effect on cells in culture, after exposure to the membrane disrupter Triton X-100. Before the effect of Triton X-100 at concentrations 0.05% and 0.005% in combination with increasing concentrations of CoQ10 (0.02mg/ml – 0.2mg/ml), on primary chicken cardiac and skeletal muscle cell cultures could be evaluated, it was necessary to determine the toxicity of each individual substance. The effect of each substance was measured using the NR, MTT, and CV assays. Since these dyes measure cell viability by different mechanisms, it was thought to be desirable to combine all these assays to obtain a better understanding of the interaction between toxicants and cells (Ishiyama *et al*., 1996). *In vitro* cytotoxicity assays with cultured cells are widely used in the sensitivity testing of chemicals because they are rapid, economical, and do not require the use of animals (Ishiyama *et al*., 1996). Ishiyama *et al*., 1995, reported that the combined assay gave similar IC_{50} values for SDS to those obtain with each independent assay, and also to the value reported in the MTT assay. At each concentration each assay was done in quadruple and triplicate experiments were done on the primary cultures.

The concentrations of Triton X-100 were decided on, after it became evident from the literature that Triton X-100 at a concentration of 0.1-0.2% are able to permeabilize biological membranes (Weruaga *et al*., 1998). Since there is no recommended daily allowance prescribed with NSI CoQ10 Q-Gel Mega, it was decided to start at a concentration of 0.2mg/ml of CoQ10 (highest concentration used in the study) and lower the concentration to 0.01mg/ml, compared to the 100mg/day required to significantly increase serum levels in humans, (Crane, 2001), 100mg/day falls between the range between the two lowest concentrations used in this study.

The cardiac and skeletal muscle cells were plated at a concentration of 5×10^4 cells per ml in 24 well plates with the culture area $1.9cm^2$/well and allowed to attach for 72 hours before being exposed to Triton X-100 and CoQ10 and a combination of Triton X-100 and CoQ10 ddH_2O was used as the carrier for both substances.

4.4.3 Assays

4.4.3.1 Neutral Red

The Neutral Red (NR) assay procedure is a cell survival/viability chemosensitivity assay, based on the ability of viable cells to incorporate and bind the supravital dye, Neutral Red. NR is a weak cationic dye that readily penetrates cell membranes by non-ionic diffusion, accumulating intracellularly in lysosomes, where it binds with anionic sites in the lysosomal matrix. Alterations of the cell surface or the sensitive lysosomal membrane leads to lysosomal fragility and other changes that gradually become irreversible, resulting in a decreased uptake and binding of NR, (Ishiyama *et al*., 1996), making it possible to distinguish between viable, damaged or dead cells. Although the MTT and NR bioassays are often used to measure toxicity and are used to distinguish viable, damaged, and dead cells, these assays test different aspects of cell function and will therefore not always provide the same information regarding toxicity (Ishiyama *et al*., 1996 and Pariete *et al*., 2002).

4.4.3.2 1-(4,5-Dimethylthiazol-2-yl)-3.5 diphenylformazan

The 1-(4,5-Dimethylthiazol-2-yl)-3.5 diphenylformazan (MTT) assay measures the number of cells and mitochondrial activity of living cells (Gerlier *et al*., 1986). Toxicity causes mitochondrial damage, leading to changes in the structure and function of the organelle, leading to leakage of internal contents including enzymes into the cytoplasm. Contraction of the mitochondrial membrane may take place with increase in ATP/ADP ratio while prolonged contraction may lead to deterioration of the inner membrane that may eventually result in rupture and deterioration of the membrane. This process normally happens before cell death that is measured with the CV assay (Roche, Bedner *et al*., 1999; Marquardt 1999). This leakage of mitochondrial enzymes may ultimately trigger both apoptosis, via the intrinsic and extrinsic pathways, and necrosis. The MTT assay is a bioassay used to determine cell viability and/or the metabolic state of the cell by demonstrating the cell's oxidative systems. The assay is based on the capacity of the mitochondrial enzyme succinate dehydrogenase to transform the tetrazolium salt of MTT into a blue coloured product, MTT formazan. The reduction of the tetrazolium salt, however, does not occur as a direct effect of the specific dehydrogenase but most cellular MTT reduction occurs outside the mitochondrial inner membrane and involves NADH and NADPH-dependent mechanisms. The conversion of MTT takes place only in living cells, and the amount of formazan produced is proportional to the number of cells

present (Bounous *et al*., 1992, Slater *et al*., 1963, Mossman, 1983, Parish *et al*., 1983, Cook *et al*., 1989, Sgouras *et al*., 1990; Munetaka *et al*., 1996, Pariete *et al*., 2002).

4.4.3.3 Crystal Violet

Crystal Violet (CV) is a triphenylmethane dye also known as gentian violet. The most commonly used application for this dye is as the primary stain in the Gram-staining procedure. Gillies *et al*., 1986, used CV to quantify the cell number in monolayer cultures as a function of the absorbance of the dye taken up by the cells. CV stains cellular protein and the nuclei of fixed cells with a direct correlation between protein staining and cell number (Kueng *et al*., 1989). Toxic effects can cause cell detachment or cell damage with the resulting leakage of protein and therefore a corresponding decrease in protein staining (Timbrell, 2000; Kanduc, *et al*., 2002; Castro-Garza, 2007).

4.4.4 The Effect of Triton X-100

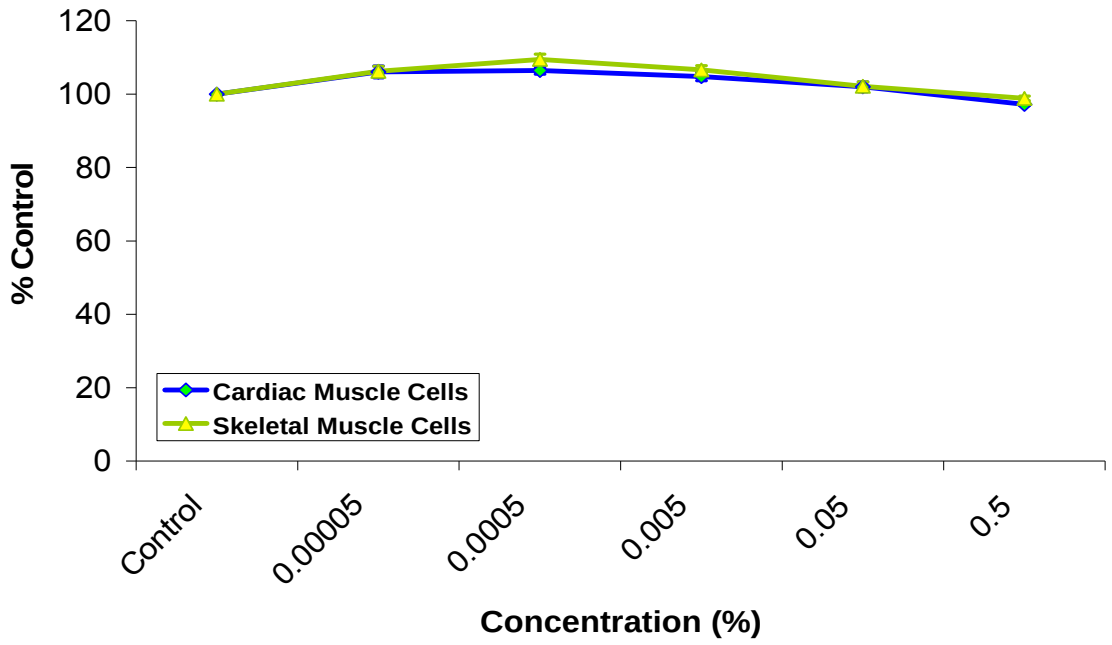

Figure 4.8 a: The effect of 0 – 0.5% of Triton X-100 on the cell viability of chick cardiac and skeletal muscle cells *in vitro,* measured using the MTT bioassay.

Using the MTT assay to determine changes in cell viability following exposure to 100µl of the five different Triton X-100 concentrations (TX 1 – TX 5), in a ddH_2O carrier dissolved in 500µl medium (Figure 4.8 **a**). Following 24 hour exposure to 0 – 0.5% of Triton X-100 an increase in cell viability was observed from 100% to 109% from control to 0.0005%. Cell viability then decreased to 97.2% in cardiac muscle cells (p= 0.0019), thus significant when compared to the increase of 9%, and 98.8% in skeletal muscle cells (p= 0.2232), thus not significant, at 0.5% Triton X-100. The increase in cell viability in both cultures was significant (cardiac muscle cells; p= 0.0022) and (skeletal muscle cells; p< 0.0001).

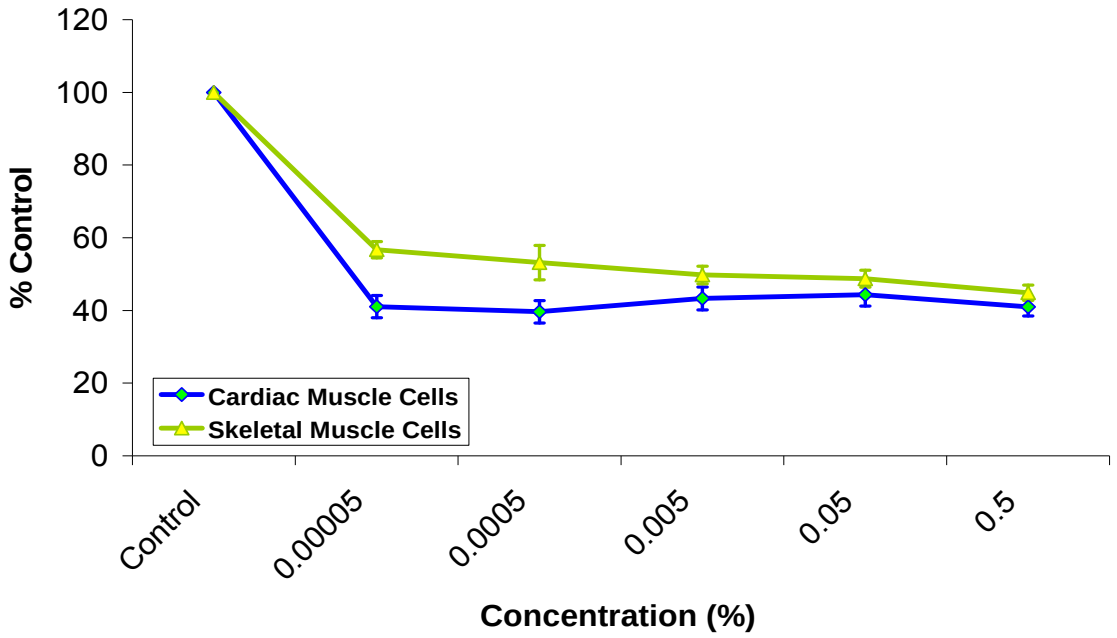

Figure 4.8 b: The effect of 0 – 0.5% of Triton X-100 on the lysosomal membrane integrity of chick cardiac and skeletal muscle cells *in vitro*, measured using the NR bioassay.

Using the NR assay to determine changes in lysosomal membrane integrity following exposure to 100µl of the five different Triton X-100 concentrations (TX 1 –TX 5), in a ddH_2O carrier dissolved in 500µl medium (Figure 4.8 **b**). Following 24 hour exposure to 0 – 0.5% of Triton X-100 a decrease in lysosomal membrane integrity was observed, both in cardiac (from 100 to 41%) and skeletal muscle cell cultures (from 100% to 57%) at 0.00005% Triton X-100. As the concentration of Triton X-100 increased, the lysosomal membrane integrity decreased significantly in both cell cultures, ($p<0.0001$), indicating that all the concentrations of Triton X-100 tested, caused alterations of the cell surface or the sensitive lysosomal membrane which lead to lysosomal fragility and other changes that gradually become irreversible, resulting in a decreased uptake and binding of NR. No significant difference in lysosomal membrane integrity was noted between the highest and lowest concentrations of Triton X-100 (cardiac muscle cell; $p=0.9900$) and (skeletal muscle cells; $p=0.3491$).

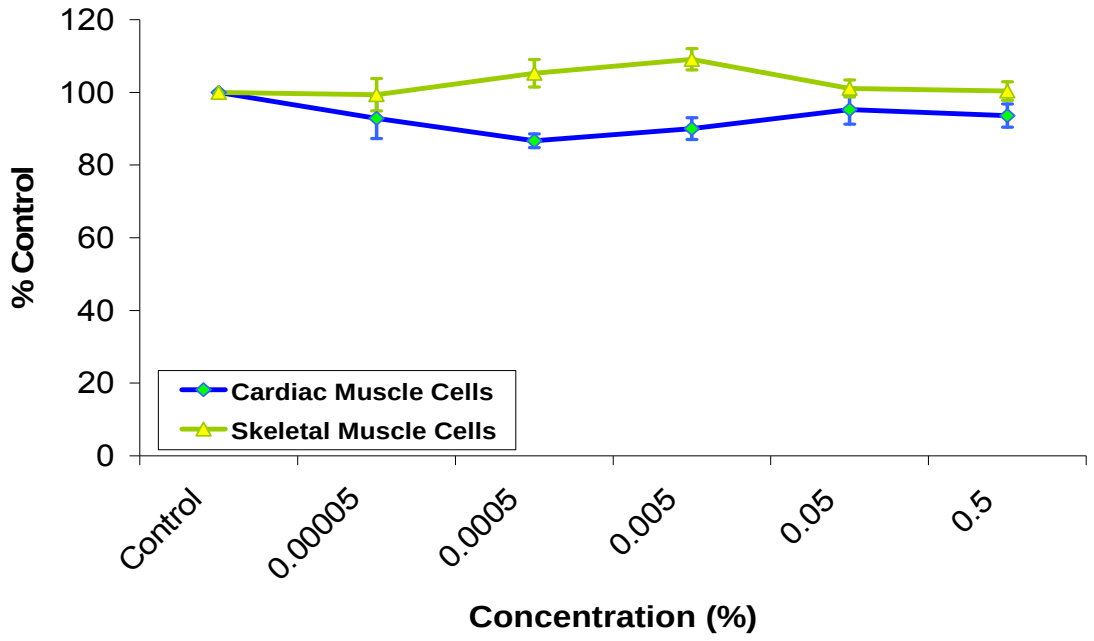

Figure 4.8 c: The effect of 0 – 0.5% of Triton X-100 on cell number of chick cardiac and skeletal muscle cells in vitro, measured using the CV bioassay.

Using the CV assay to determine changes in cell number following exposure to 100µl of the five different Triton X-100 concentrations (TX 1 –TX 5), in a ddH_2O carrier dissolved in 500µl medium (Figure 4.8 **c**). Following 24 hour exposure to 0 – 0.5% of Triton X-100, a slight but not significant decrease was seen in the cell number of cardiac muscle cells ($p=0.0189$). In contrast, the skeletal muscle cell culture revealed a slight increase in cell number at 0.0005 and 0.005% ($p=0.0071$). The increase might be an indication that the cells are trying to compensate for the toxic insult. Both cultures showed no significant difference in cell number at the highest concentration of Triton X-100 when compared to the control group, indicating that, with the exception of skeletal muscle cells at 0.005 and 0.0005%, neither of the Triton X-100 concentrations used in the study, altered the cellular proteins to such an extend that the cell number of either cultures was significantly decreased (cardiac muscle cells; $p=0.0189$) and (skeletal muscle cells; $p=0.3426$).

Dayeh *et al*., 2004, reported a loss of viability in cultures of three mammalian cell lines, two fish cell lines, and a ciliated protozoan, using three viability assays (Alamar Blue (AB), NR, and propidium iodide (PI) fluorescent dyes were used). After a 2 hour exposure to Triton X-100 (1mg/ml serially diluted) all the fluorescent dyes indicated a loss of viability in cultures. NR appeared to be the most sensitive, giving the lowest EC_{50} values and revealing no differences between the EC_{50} values for the five cell lines. The results with the animal cell lines suggested that lysosomal activity, measured as the uptake and retention of NR, is more susceptible to Triton X-100 than energy metabolism, as measured with AB, plasma membrane integrity, as measured with PI (Dayeh *et al*., 2004). Allen *et al*., 1964, incorporated Triton X-100 into reaction mixtures used for the visualization of esterases and acid phosphatases separated by electrophoresis in starch gels. The net effect was apparent enhancement of enzymatic activity with certain substrates and apparent inhibition of enzymatic activity with other substrates. It was shown by both quantitative and electrophoretic studies that Triton X-100 is an activator of certain esterases (Allen *et al*., 1964).

4.4.5 The Effect of CoQ10

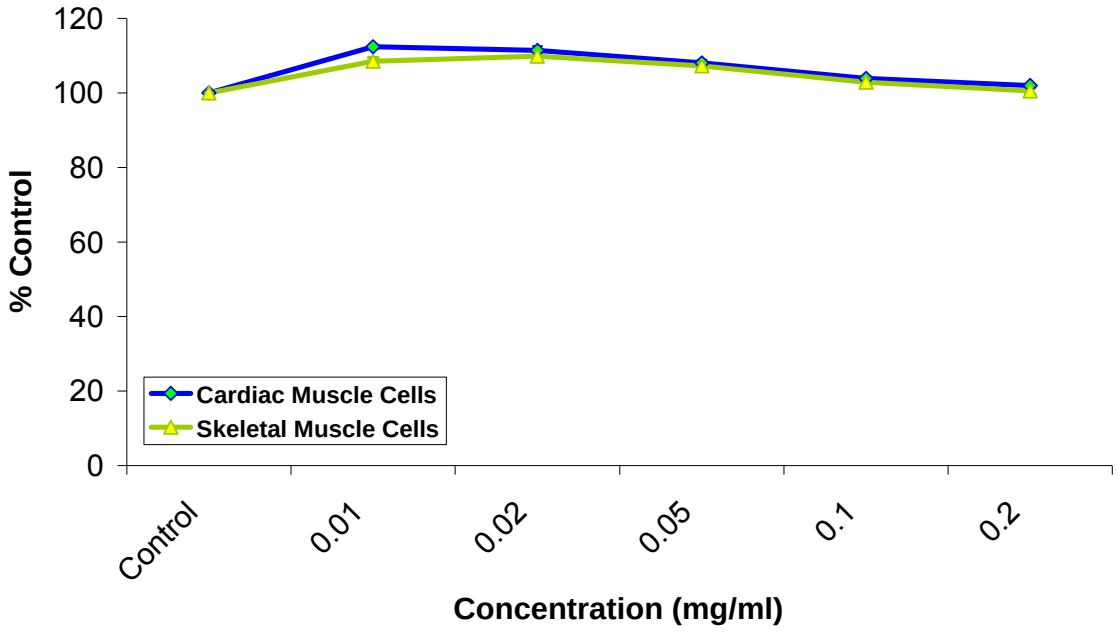

Figure 4.9 a: The effect of 0 – 0.2mg/ml of CoQ10 on the cell viability of chick cardiac and skeletal muscle cells in vitro, measured using the MTT bioassay.

Using the MTT assay to determine changes in cell viability following exposure to 100µl of the five different CoQ10 concentrations (Q1 - Q5), in a ddH_2O carrier dissolved in 500µl medium (Figure 4.9 **a**). Following 24 hour exposure to 0 – 0.2mg/ml of CoQ10, the MTT assay showed an increase in cell viability of both cardiac ($p<0.0001$) and skeletal ($p<0.0001$) muscle cells in culture. Compared to the control group, the highest concentration of CoQ10 revealed almost no increase or decrease in cell viability. The increase in cell viability (~10%) in both cultures at 0.01 and 0.02mg/ml, was significant, indicating that CoQ10 significantly enhanced mitochondrial enzyme activity, compared to the control group ($p<0.0001$).

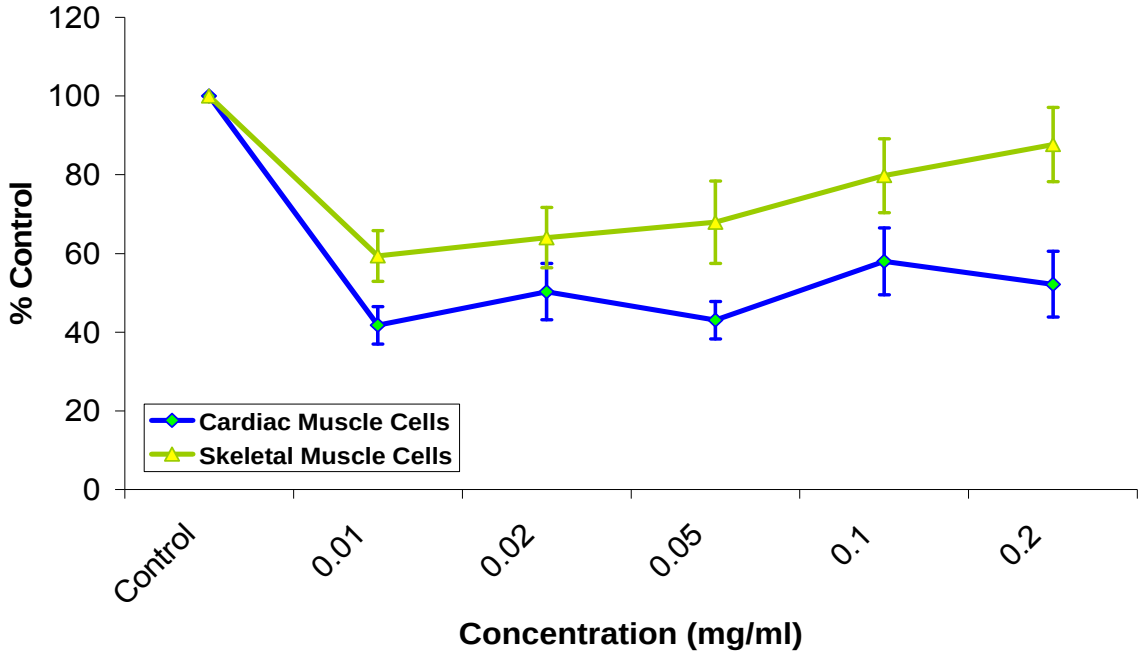

Figure 4.9 b: The effect of 0 – 0.2mg/ml of CoQ10 on the lysosomal membrane integrity of chick cardiac and skeletal muscle cells *in vitro*, measured using the NR bioassay.

Using the NR assay to determine changes in lysosomal membrane integrity following exposure to 100µl of the five different CoQ10 concentrations (Q1 - Q5), in a ddH_2O carrier dissolved in 500µl medium (Figure 4.9 **b**). Following 24 hour exposure to 0 – 0.2mg/ml CoQ10, lysosomal membrane integrity was altered significantly in both cell cultures. A decrease from 100 to 53% in skeletal muscle cells and 41% in cardiac muscle cells was seen at the lowest concentration of CoQ10. At the highest concentration, lysosomal membrane integrity in skeletal muscle cells decreased to 88% and 51% in cardiac muscle cells. This decrease in lysosomal membrane integrity in both cell cultures are significant (cardiac muscle cell; $p<0.0001$) and (skeletal muscle cells; $p=0.0011$), indicating that CoQ10 caused irreversible alterations, directly or indirectly, to the lysosomal membranes resulting in lowered NR uptake.

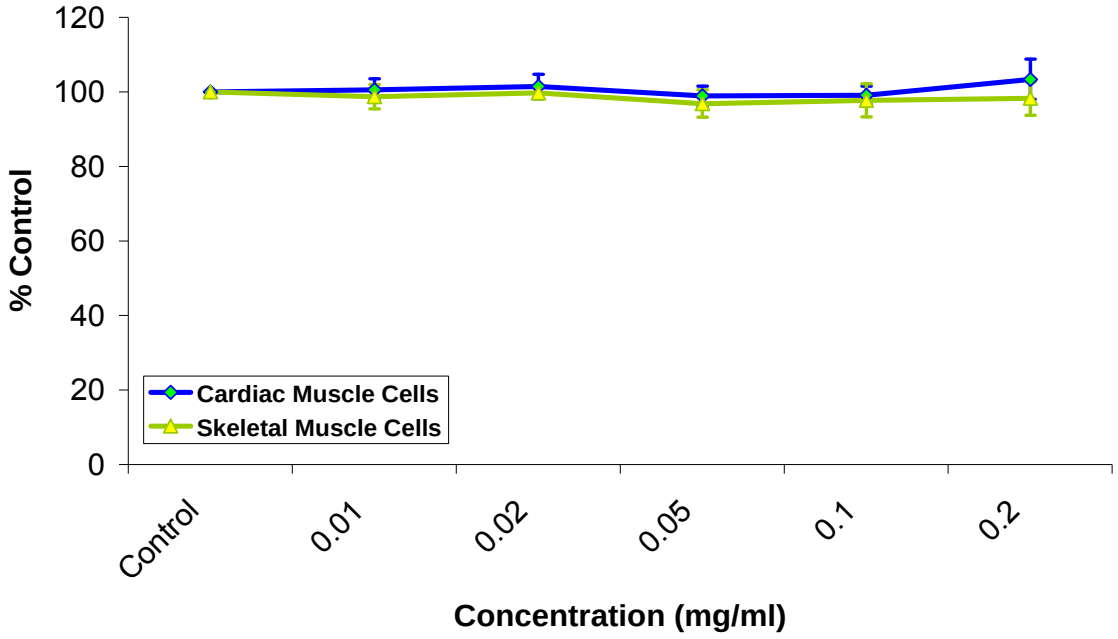

Figure 4.9 c: The effect of 0 – 0.2mg/ml of CoQ10 on cell number of chick cardiac and skeletal muscle cells in vitro, measured using the CV bioassay.

Using the CV assay to determine changes in cell number following exposure to 100µl of the five different CoQ10 concentrations (Q1 - Q5), in a ddH_2O carrier dissolved in 500µl medium (Figure 4.9 **c**). Following 24 hour exposure to 0 – 0.2mg/ml CoQ10, no significant increase or decrease was observed in cell number at any of the CoQ10 concentrations tested in the two cultures in the study (cardiac muscle cells; p=0.8392) and (skeletal muscle cells; p=0.6181). The results indicate that CoQ10 has no effect on cellular proteins, thus no difference in crystal violet colour intensity was observed when compared to the control group, following no exposure.

Alleva *et al*., 2001, linked the antioxidant capacity of redox-active compounds like CoQ10 and its analogues to their anti-apoptotic potential. The basis of the results suggested that ubiquinol-10 (the reduced form of CoQ10), but not ubiquinone-10, inhibits apoptosis induced by chemical apoptogens, which largely use the distal, mitochondrial signaling pathways, while apoptosis triggered by immunological agents, which rely on

their cognate receptors in apoptosis induction, appeared largely independent of the coenzyme Q status of the cell. The Jurkat T lymphoma cells were enriched with reduced or oxidized CoQ10, prior to apoptosis induction (Alleva *et al*., 2001). Papucci *et al*., 2003, demonstrated both *in vitro* and *in vivo* that CoQ10 prevents keratocyte apoptosis induced by laser irradiation more efficiently than other antioxidants. The administration of CoQ10 2 hours prior to apoptotic stimuli prevented apoptosis independently of the ability of apoptotic stimuli to trigger or not to trigger free radical generation. The protective effect was clearly demonstrated by several incidences, including changes of cell morphology detected by light microscopy and ultramicroscopy, quantification of living and apoptotic cells by the MTT colorimetric cytotoxicity assay, and analysis of ATP cellular levels by a bioluminescence assay. CoQ10 significantly enhanced the number of living cells evaluated by the MTT assay and lowered the number of cumulative apoptotic events scored by time-lapse videomicroscopy (Papucci *et al*., 2003). It was also able to prevent the massive reduction in ATP levels induced by all apoptotic stimuli. The suggested mechanism for its protective effect was associated with inhibition of the permeability transition pore (PTP) opening (Papucci *et al*., 2003). Kagan *et al*., 1999, tested the use of CoQ10 as a generic anti-apoptotic compound and found that its ability to protect against apoptosis varies depending on both cell type and mode of cell death induction. It was established that the protective effect offered by CoQ10 was mediated by its effect on the mitochondrial function and viability. Coenzyme Q10 at a concentration of 25-200μM was given to cell culture simultaneous with cell death stimuli and it appeared that in limited circumstances, CoQ10 can prevent apoptosis, where its effectiveness may be derived from directly stabilizing mitochondrial membrane potential or by indirectly protecting against loss in mitochondrial enzyme activity (CoQ10 at these concentrations did not have any adverse effects on cell death). Histiocytic lymphoma (U937) and mouse melanoma (B16F10) represented freely proliferative cells in the study, and were shown not to be protected by CoQ10. Differential rat adrenal pheochromocytoma (PC12) cells represented a differentiated non-proliferative phenotype, and exhibited the most consistent protection afforded by CoQ10 after exposure to cell death inducers (Kagan *et al*., 1999).

4.4.6 The Effect of Triton X-100 and CoQ10 in Combination

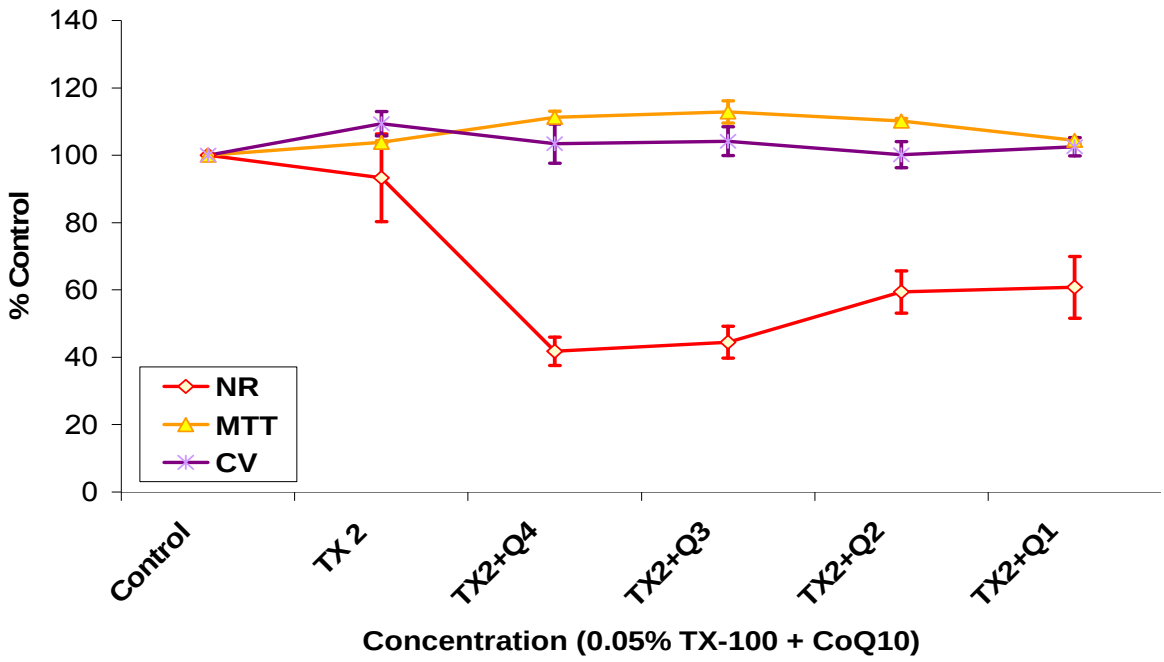

Figure 4.10 a: The effect of 0.05% Triton X-100 (TX2) in combination with increasing concentrations (0.02 – 0.2mg/ml) CoQ10 on chick cardiac muscle cells, as measured by the MTT, NR, and CV bioassays.

A slight increase was seen in cell viability of chick cardiac muscle cells upon exposure to Triton X-100 at a concentration of 0.05% in combination with increasing concentrations of CoQ10 (0.02 – 0.2mg/ml), a significant increase on cell viability (an average of 109%) (Figure 4.10 a) as indicated by the MTT assay ($p<0.0001$) was seen. No significant changes in cell number as indicated by the CV assay was measured ($p=0.3319$), indicating that no alterations to cellular proteins was caused upon exposure. The NR assay indicated a significant decrease in lysosomal membrane integrity, upon exposure of 0.05% Triton X-100 in combination with 0.02mg/ml CoQ10 ($p<0.0001$). A difference in the percentage decrease in lysosomal membrane integrity was noted as the concentration of CoQ10 increased from 0.05 to 0.2mg/ml ($p=0.0143$). The results reflect toxic insult to cardiac muscle cells caused by 0.05% Triton X-100 in combination with increasing concentrations of CoQ10, when the lysosomal membrane integrity was measured.

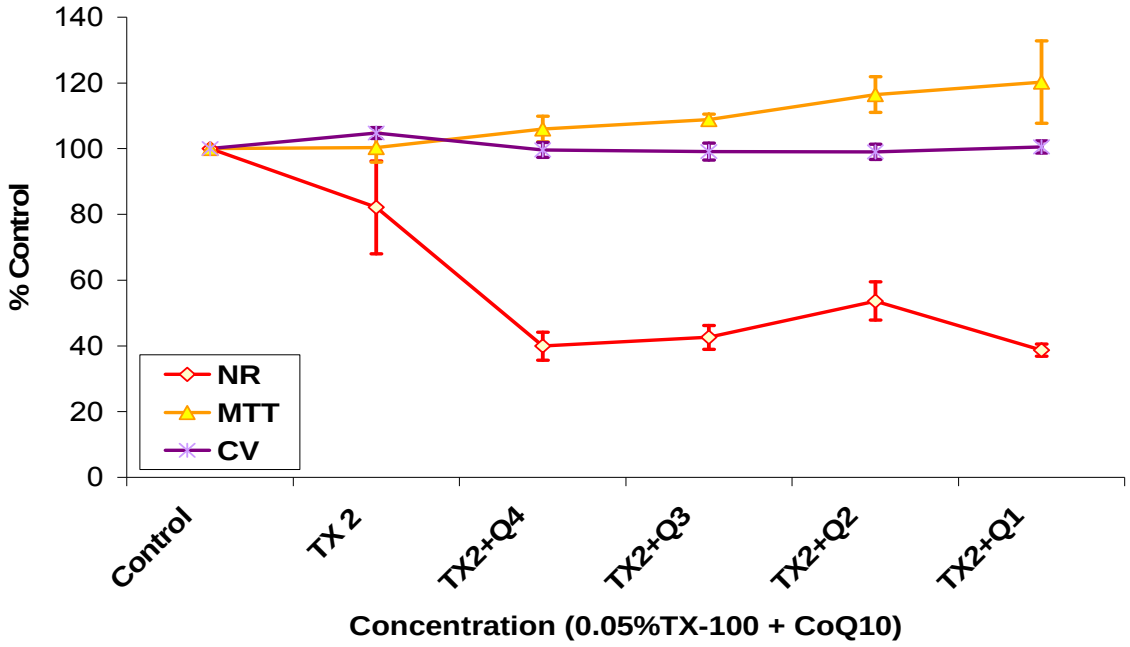

Figure 4.10 b: The effect of 0.05% Triton X-100 (TX2) in combination with increasing concentrations (0.02 – 0.2mg/ml) CoQ10 on chick skeletal muscle cells, as measured by the MTT, NR, and CV bioassays.

Cell viability in skeletal muscle cell cultures, as indicated by the MTT assay was significantly increased ($p<0.0001$), following exposure to 0.05% Triton X-100 in combination with increasing concentrations of CoQ10 (0.02 – 0.2mg/ml) (Figure 4.10 b). The cell viability increased from 106 to 120% as the concentration of CoQ10 increased from 0.02 to 0.2mg/ml, which indicate an increase in mitochondrial activity in the presence of 0.05% Triton X-100 when cells were pretreated with increasing concentrations of CoQ10. No significant changes was noted in cell number as measured by the CV assay ($p=0.7695$). In disparity to the cell viability increase, the lysosomal membrane integrity was significantly decreased following the combination exposure of Triton X-100 and CoQ10 ($p<0.0001$). No significant differences was observed between lysosomal membrane damage between the highest and lowest concentrations of CoQ10 ($p=0.7657$).

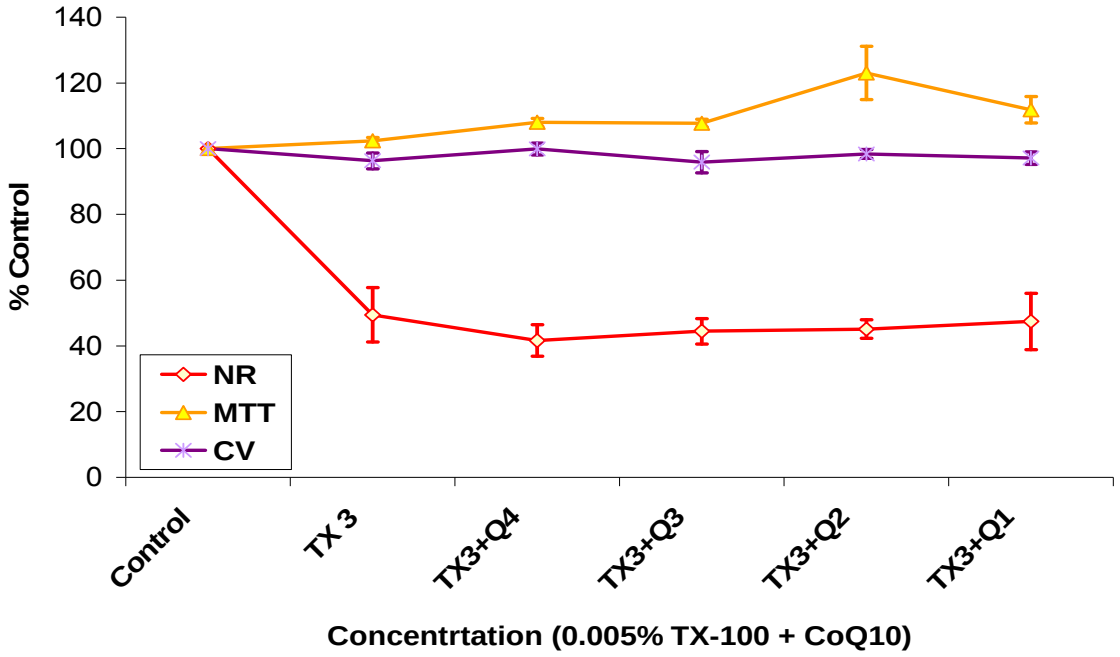

Figure 4.10 c: The effect of 0.005% Triton X-100 (TX3) in combination with increasing concentrations (0.02 – 0.2mg/ml) CoQ10 on chick cardiac muscle cells, as measured by the MTT, NR, and CV bioassays.

An increase in cell viability (an average of 112.6%) as measured by the MTT assay upon exposure of chick cardiac muscle cells to 0.005% Triton X-100 in combination with increasing concentrations of CoQ10 (0.02 – 0.2mg/ml) was seen ($p=0.0006$) (Figure 4.10 c). A definitely significant increase in cell viability was observed when cells were pretreated with 0.1mg/ml CoQ10 ($p<0.0001$), when compared to the other concentrations of CoQ10. No significant increase or decrease was seen in cell number as measured by the CV assay upon exposure to 0.005% Triton X-100, when pretreated with increasing concentrations of CoQ10, indicating no alterations caused to cellular proteins ($p=0.2505$). Contradictory to the increased cell viability, the lysosomal membrane integrity was significantly decreased from 100 to 49% ($p<0.0001$) in the presence of 0.005% Triton X-100 when pretreated with increasing concentrations of CoQ10. No significant difference was seen in the decreased lysosomal membrane integrity of different CoQ10 concentration in the presence of 0.005% Triton X-100 ($p=0.2093$).

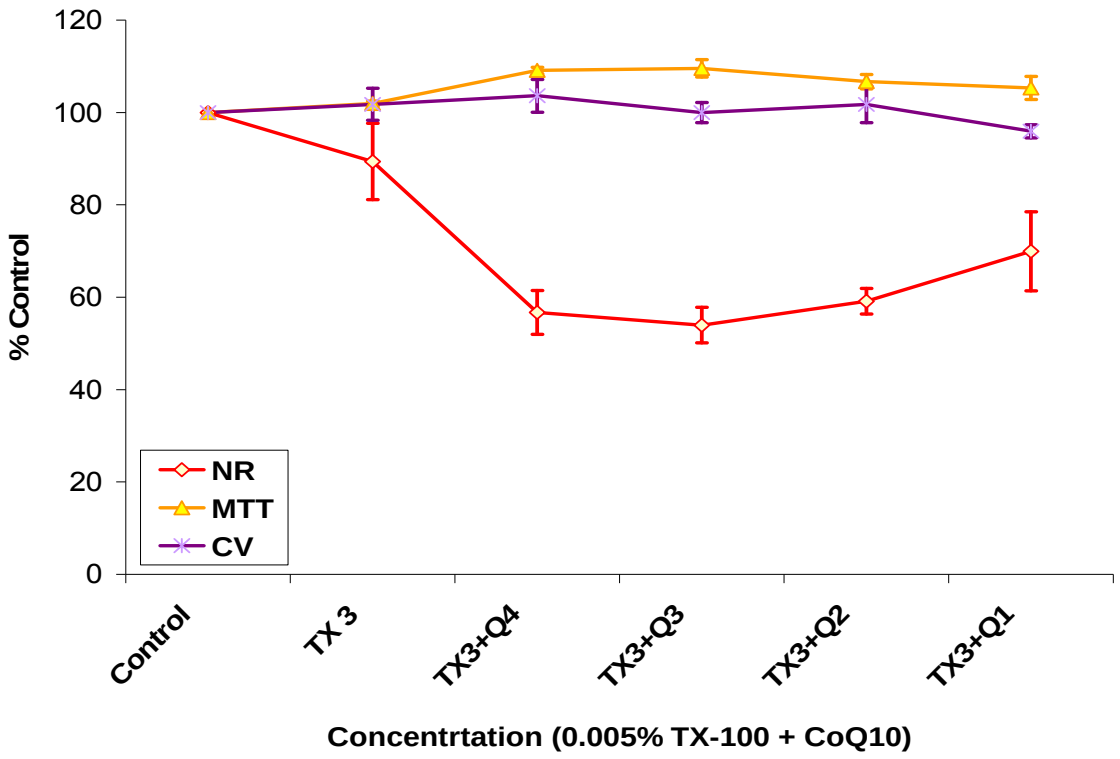

Figure 4.10 d: The effect of 0.005% Triton X-100 (TX3) in combination with increasing concentrations (0.02 – 0.2mg/ml) CoQ10 on chick skeletal muscle cells, as measured by the MTT, NR, and CV bioassays.

Cell viability, as measured by the MTT assay, of chick skeletal muscle cells, in culture increased (with an average of 107.7%) when pretreated with increasing concentration of CoQ10 in the presence of Triton X-100 at 0.005% ($p<0.0001$) (Figure 4.10 d). The CV assay measured no significant increase or decrease in cell number of the cells ($p=0.8382$), indicating no alterations to cellular proteins were caused upon the combination exposure. The lysosomal membrane activity of the skeletal muscle cells was significantly decreased upon exposure to 0.005% Triton X-100 after pretreatment with increasing concentrations of CoQ10 ($p<0.0001$). A difference in the decrease in the lysosomal membrane activity was noted between the different concentrations of CoQ10 ($p=0.0080$).

In conclusion, Triton X-100 and CoQ10, at all the concentrations tested in the study, is toxic to cardiac and skeletal muscle cells when evaluated by the NR assay. A slight increase in cell viability as measured by the MTT assay was measured in both cardiac and skeletal muscle cell cultures upon exposure to both Triton X-100 and CoQ10. Upon exposure to 0.05% and 0.005% Triton X-100, CoQ10 offered protection to the cell viability of cardiac and skeletal muscle cells in culture after pre-treatment with CoQ10, as determined by the MTT assay. No alterations in cellular proteins or cell number were measured by the CV assay. Toxicity was seen when cells were exposed to Triton X-100 and CoQ10, in combination as measured by the NR assay indicating that Triton X-100 and CoQ10, alone and in combination, have an irreversible effect on lysomal membrane integrity.

Chapter 5: The Cellular and Structural Effect of Triton X-100 and CoQ10, Alone, and in Combination as Determined by Scanning Electron Microscopy (SEM)

5.1 Introduction

Many cellular structures are so small that they can only be resolved in the electron microscope. Furthermore, it is often crucial to visualize and reconstruct the three-dimensional (3D) structure of biological tissue. Scanning electron microscopy (SEM) in which a tightly focused beam of electrons is raster-scanned over the specimen while secondary or backscattered electrons are detected, is used in biological imaging mostly as a surface visualization tool, creating a 3D appearance. The prevalent contrast mode in the SEM is the detection of so-called secondary electrons, which are low-energy electrons that are emitted when the primary electron beam strikes the sample surface, providing high-resolution imaging of fine surface morphology. The secondary-electron signal depends strongly on the orientation of the surface, leading to topographic images that characteristically resemble obliquely illuminated solid objects. The orientation of surface features influences the number of electrons that reach the secondary electron detector, which creates variations in image contrast that represents the sample's surface topography. SEM is a method for high-resolution imaging of surfaces, and the advantages over light microscopy include magnification of up to 100 000 times and much greater depth of field (Denk *et al*., 2004 and Hanke *et al*., 2006). Scanning electron microscopy is a useful method for studying the cell surface during muscle development in cell culture (Shimada, 1972).

Skeletal muscle fibers are multinucleated cells, with their numerous nuclei peripherally located just beneath the cell membrane (sarcolemma). An endomysium, whose fine reticular fibers intermingle with those of neighboring cells, surrounds each cell. Small satellite cells, which have only a single nucleus and act as regenerative cells, are located in shallow depressions on the muscle cell's surface, sharing the muscle fiber's external lamina. Much of the skeletal muscle cell is composed of longitudinal arrays of cylindrical myofibrils, each 1 to 2μm in diameter. A myofibril consists of thick

myofilaments (15nm in diameter and 1.5μm long), composed of myosin II, and thin filaments (7nm in diameter and 1.0μm long), composed primarily of actin. These extend the entire length of the cell and are aligned precisely with their neighbours. This strictly ordered parallel arrangement of the myofibrils is responsible for the cross-striations of light and dark banding that are characteristic of skeletal muscle viewed in longitudinal section. The dark bands are known as A bands (anisotropic with polarized light) and the light bands as I bands (isotropic with polarized light). The center of each A band is occupied by a pale area, the H band which is bisected by a thin M line. Each I band is bisected by a thin dark line, the Z disc. The region of the myofibril between two successive Z discs, known as a sarcomere, is 2.5μm in length and considered the contractile unit of skeletal muscle fibers. Myofibrils are held in register with one another by the intermediate filaments desmin and vimentin, which secure the periphery of the Z discs of neighbouring myofibrils to each other. These bundles of myofibrils are attached to the cytoplasmic aspect of the sarcolemma by various proteins including dystrophin, a protein that binds to actin (Gartner *et al*., 2007). Traditionally, the Z disc has been viewed as a passive constituent of the sarcomere, which is important only for the cross-linking of thin filaments and transmission of force generated by the myofilaments. During the last decade, remarkable progress has been made in deciphering the functional role of the Z disc in striated muscle. Starting from a mainly structural perception of the Z disc, the recent discovery of a progressively increasing number of “Z disc proteins” as well as novel protein-protein interactions implicated the Z disc as a nodal point in striated muscle signalling. The pivotal position of the Z disc is further underscored by the fact that cardiomyopathies and muscle dystrophies have been linked to mutations in numerous genes encoding for proteins of the Z-disc and closely adjacent structures of the myocyte (Frank *et al*., 2006).

The fine structure of the sarcolemma is similar to that of other cell membranes, but a distinguishing feature is that it is continued within the skeletal muscle fiber as numerous long, tubular invaginations that intertwine among the myofibrils, known as T tubules (transverse tubules). T tubules extend deep into the interior of the fiber and facilitate the conduction of waves of depolarization along the sarcolemma. Associated with this system of T tubules, is the sarcoplamic reticulum, which stores intracellular calcium and is maintained in close register with the A and I bands as well as with the T tubules. The sarcoplasmic reticulum forms a meshwork around each myofibril and displays dilated

terminal cisternae at each A-I junction. Two of these cisternae are always in close apposition to a T tubule, forming a triad in which a T tubule is flanked by two terminal cisternae. This arrangement permits a wave of depolarization to spread, almost instantaneously, from the sarcolemma throughout the cell, reaching the terminal cisternae, which have voltage-gated calcium release channels in their membrane. The sarcoplasmic reticulum regulates muscle contraction through the controlled sequestering and release of calcium ions within the sarcoplasm. The wave of depolarization transmitted by the T tubules triggers calcium ion release, which causes opening of the calcium release channels of the terminal cisternae, resulting in release of calcium ions into the cytosol in the vicinity of the myofibrils (Gartner *et al*., 2007).

Cardiac muscle differs from smooth and skeletal muscles in that it possesses an inherent rhythmicity as well as the ability to contract spontaneously. Although the resting volume of individual cardiac muscle cells varies, on average they are 15μm in diameter and 80μm in length. Each cell possesses a single, large, oval, centrally placed nucleus; although two nuclei are occasionally present (Gartner *et al*., 2007). The bandings of cardiac muscle are identical with those of skeletal muscle, including alternating I and A bands. Each sarcomere possesses the same substructure as its skeletal muscle counterpart; therefore, the mode and mechanism of contraction are virtually identical. The sarcoplasmic reticulum of cardiac muscle does not form terminal cisternae and is not nearly as extensive as in skeletal muscle; instead, small terminals of sarcoplasmic reticulum approximate the T tubules. These structures do not normally form a triad, as in skeletal muscle, but rather the association is usually limited to two partners, resulting in a dyad. Unlike skeletal muscle, where the triads are located at the A-I interfaces, the dyads in cardiac muscle are located in the vicinity of the Z disc. The T tubules of cardiac muscle cells are almost two and a half times the diameter of those in skeletal muscle and are lined by an external lamina. The highly specialized end-to-end junctions formed by cardiac cells are referred to as intercalated discs. The cell membranes involved in these junctions approximate each other, so that in most areas they are separated by a space of less than 15 to 20 nm. Intercalated discs have transverse portions, where fasciae adherents and desmosomes abound, as well as lateral portions rich in gap junctions. On the cytoplasmic side of intercalated discs, thin myofilaments attach to the fasciae adherens, which are analogous to Z discs. Gap junctions which function in

permitting rapid flow of information from one cell to the next, also form in regions where cells lying side by side come in close contact with each other (Gartner *et al*., 2007).

Triton X-100 is one of the most commonly used non-ionic detergents for solubilizing membrane proteins during isolation of membrane-protein complexes (Roche). Non ionic surfactants, such as Triton X-100, have been used extensively in a wide variety of biological systems for both preparative and functional studies of membrane proteins. The interaction of such micelle-forming amphiphiles with biological membranes is a highly complex process, which involves the initial insertion of individual surfactant molecules into the lipid bilayer, followed by the formation of mixed lipid-detergent micelles and even large lipoprotein bilayer discs stabilized by a pseudo-micellar annulus of detergent (Dunahay *et al*., 1984). The process culminates in the incorporation of all of the membrane components into detergent micelles (Murphy *et al*., 1985).

CoQ10 is present in the endomembranes of cells as well as in mitochondria, where it serves as a central component of the transmembrane electron transport system (Sun *et al*., 1992). Antioxidants such as CoQ10 can neutralize free radicals and reduce or even help prevent some of the damage that is caused (Al-Hasso, 2001). Coenzyme Q10 is effective in preventing protein oxidation by quenching the initiating perferryl radical and functioning as a chain-breaking antioxidant, thus preventing the process of propagation, the second phase in lipid peroxidation, where $LOO^{\cdot}$ abstracts a hydrogen atom from an additional unsaturated fatty acid, leading to $L^{\cdot}$ and lipid hyperoxide (LOOH), which can be reoxidized to $LOO^{\cdot}$, which reinitiates lipid peroxidation (Bentinger *et al*., 2007). Coenzyme Q10 is proposed to play a central role in antioxidant protection of the plasma membrane, either directly or through the regeneration of important exogenous antioxidants such as α-tocopherol and ascorbate (Gómez-Díaz *et a*l., 2000). Coenzyme Q10 can be considered as the central molecule in plasma membrane protection against lipid peroxidation because it is directly reduced by cytochrome b_5 reductase, and maintains both ascorbate and α-tocopherol in their reduced state (López-Lluch *et al*., 1999).

In order to investigate whether CoQ10 will elicit a protective effect, as described in the literature, (Papucci *et al*., 2003 and Kagan *et al*., 1999) on cells exposed to different concentrations of Triton X-100, scanning electron microscopy was used to determine

structural and morphological alterations to cell membranes exposed to increasing concentrations of Triton X-100, CoQ10 and a combination of the two substances.

In this Chapter the following research objectives were investigated:

- Investigate the ultrastructure of cardiac and skeletal muscle cells in primary culture, exposed to Triton X-100 and CoQ10, SEM.
- Determine whether CoQ10 offer any protection to cardiac and skeletal muscle cells in primary culture, ultrastructurally altered by the cell lysing properties of Triton X-100, by SEM.

5.2 Materials and Methods

Poly-L-lysine was from Sigma-Aldrich (Pty) Ltd., Midrand, South Africa. The 22mm x 22mm Menzel Glazer coverslips were from Agar Scientific, Cambridge, England.
The primary chick embryonic cardiac and skeletal muscle cell cultures were prepared as for cytotoxicity testing in Chapter 4. To examine the cardiac and skeletal muscle cell morphology and structure of the primary cultures, the primary cultures were plated at a concentration of $5x10^4$cells/ml onto the surface of Menzel Glazer glass coverslips coated with Poly-L-lysine (1ml Poly-L-lysine in 9ml sterile ddH_2O) positioned on the bottom of 24-well plates. After 72 hours of incubation the cell cultures were exposed to Triton X-100 and CoQ10, alone and in combination, for 24 hours. To determine the effect of CoQ10 on cells exposed to Triton X-100, cell cultures were pre-treated with the different concentrations of CoQ10, 0.02 – 0.2mg/ml, 2 hours prior to exposure to Triton X-100, and maintained for the rest of the 24 hours at 37°C and 5% CO_2. Samples were then prepared for detailed morphological investigation using SEM. After 86 hours in culture the medium was removed and the monolayer was washed with a phosphate buffered saline solution (PBS). The monolayer of each well was fixed with 2.5% gluteraldehyde in a 0.075M phosphate buffer pH7.4. After 90 minutes the fixative was removed and each well was washed 3 times (15 minutes each) with 0.075M phosphate buffer. Postfixation was then done for 60 minutes in a 1% osmium tetraoxide (OsO_4) solution. After postfixation each well was washed 3 times, (15 minutes each) with 0.075M phosphate buffer to remove any remaining osmium tetraoxide. Once the washing step was complete, a dehydration step took place in which each well went through serial

dehydration with ethanol, 30%, 50%, 70%, 90% and three times 100%, each dehydration step took place for 15 minutes. The coverslips were then removed from the 24-well plates and dried, by means of a CO_2 critical point drying procedure; samples were mounted and examined with a ZEISS ULTRA 55 FEG.SEM. According to Boyde *et al*., 1979, during critical point drying a sample can loose up to 20% of its volume, which is probably the reason why fine cracks and broken muscle cell tips were seen in the results of this study (Boyde *et al*., 1979). Before the samples were visualized it had to be made conductive, using ruthenium oxide (RuO_4) vapour. Depositions of the RuO_4 crystals were seen on the results and were identified by Van der Merwe (1999), as ruthenium artefacts.

5.3 Results and Discussion

The effect of Triton X-100 and CoQ10, alone, and in combination, on the cellular structure and morphology of cardiac and skeletal muscle cells, and more specifically the membranes of the cells, was determined by visualization of the high-resolution surface images produced by SEM.

5.3.1 Control Group

Skeletal and cardiac muscle cells in the control group were not exposed to either of the two substances being tested. The cell morphology, structure and membrane integrity reflect that of normal intact cells. During muscle cell differentiation many changes take place in the surface properties of the cells (Masuko *et al*., 1983). Masuko *et al*., 1983, determined that in the late G_2 phase of the cell cycle, cells have bulged in anticipation of rounding for mitosis, and many microvilli (Figure 5.1b and 5.2b, indicated by the thin white arrows), some blebs, and long slender filopodia (Figure 5.1a and 5.2 a, at bipolar ends of cells) appeared on the surfaces (Masuko *et al*., 1983). During G_1 and S, the cells are spindle-shaped with a relatively smooth surface. During the M phase cells are generally spherical and their surface is covered with numerous microvilli and some blebs (Masuko *et al*, 1983).

a)

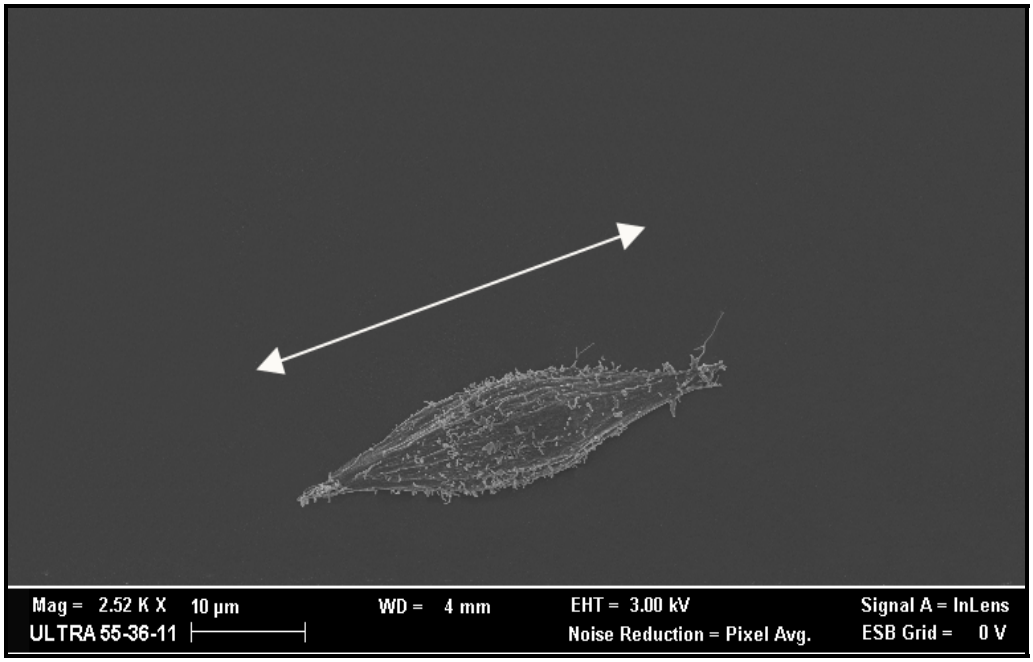

b)

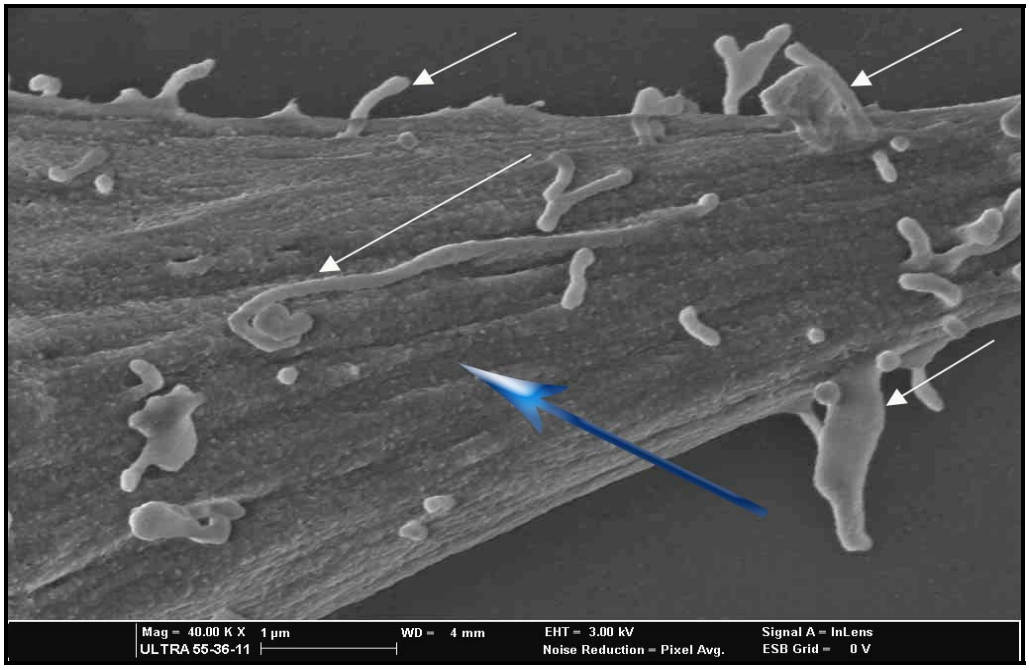

Figure 5.1: Skeletal muscle cells from the control group, at high and low magnification. Intact membranes were observed (blue arrow). **a**): Low magnification; bipolar cytoplasmic extensions become slender with filopodia extending into the substrate. **b**): High magnifications of (**a**); presence of microvilli on the membrane surface (**b** - thin white arrows).

a)

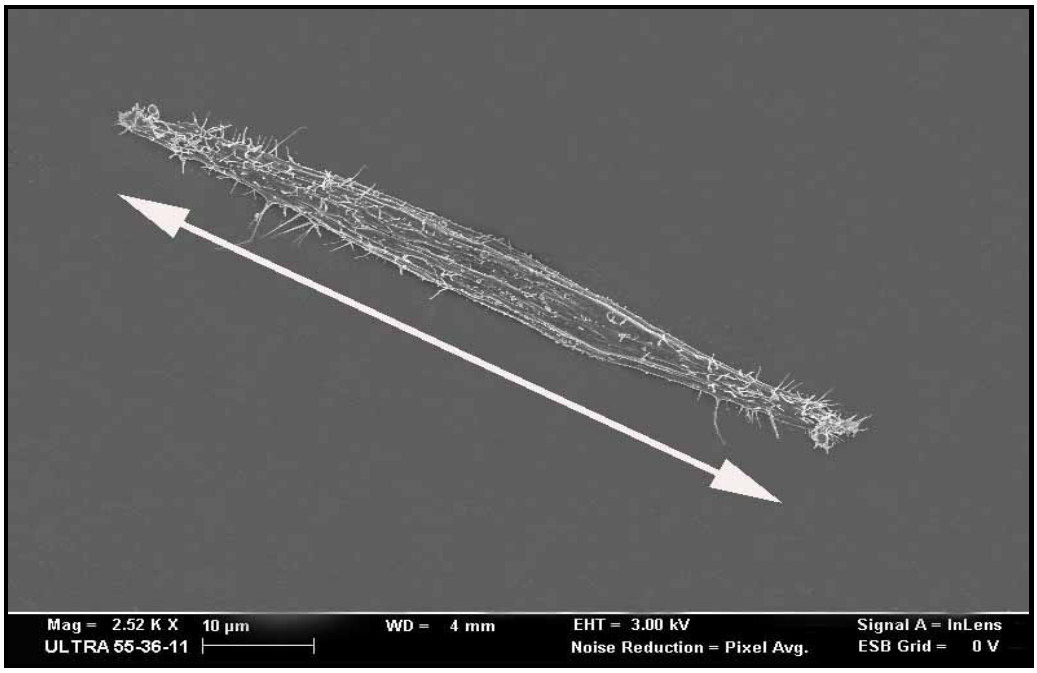

b)

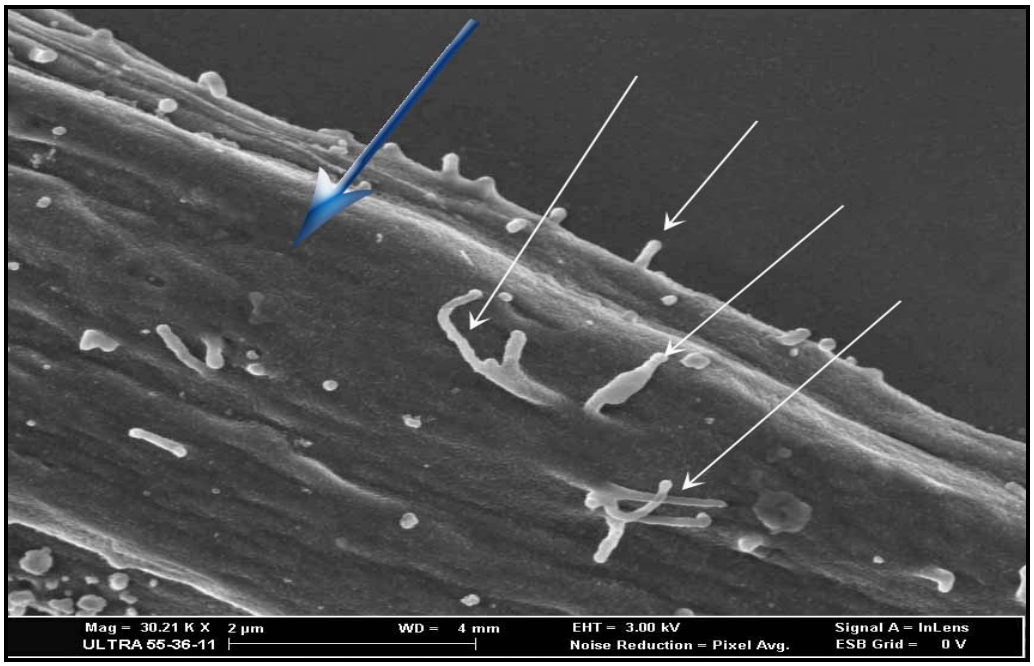

Figure 5.2: Cardiac muscle cells from the control group, at high and low magnification. Intact membranes were observed (blue arrow). **a**): Low magnification; bipolar cytoplasmic extensions become slender with filopodia extending into the substrate. **b**): High magnifications of (**a**); presence of microvilli on the membrane surface (**b** - thin white arrows).

5.3.2 Cells exposed to Triton X-100

a)

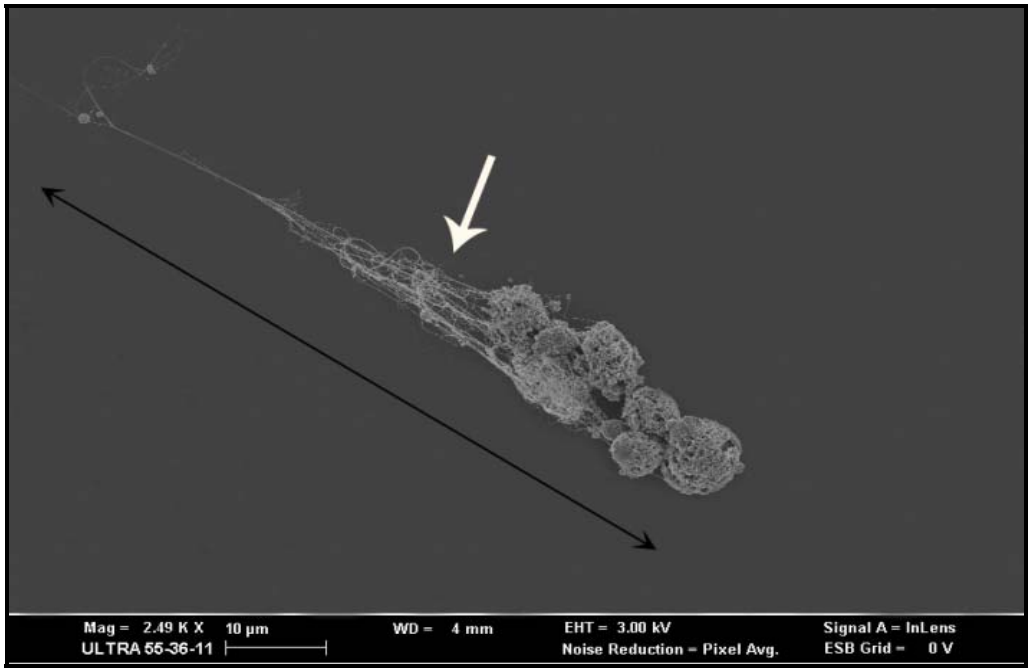

b)

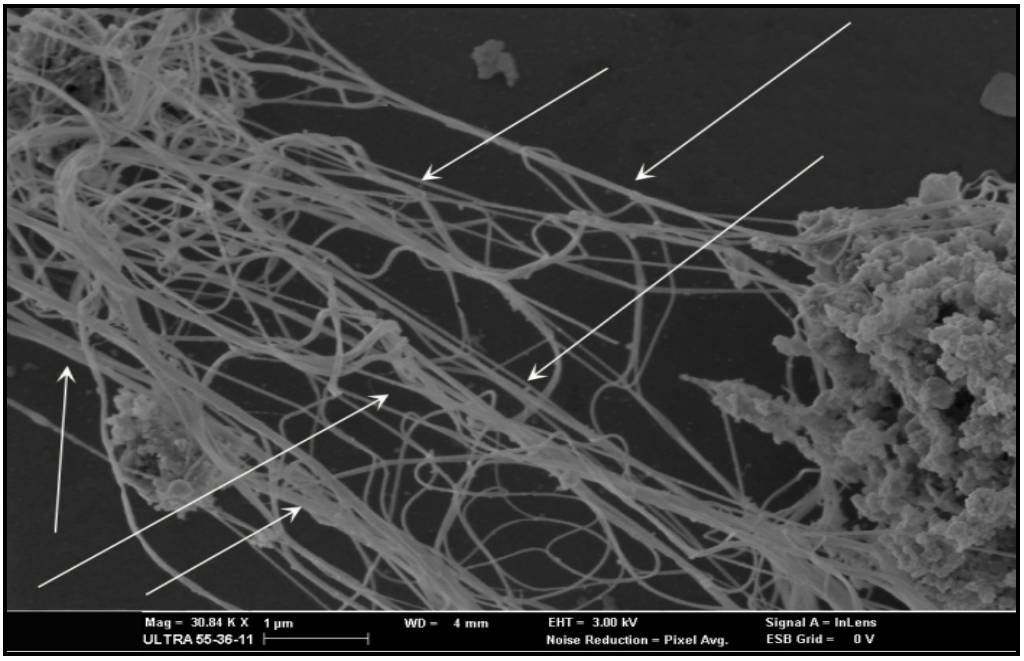

Figure 5.3: Skeletal muscle cells exposed to 0.5% Triton X-100. Complete membrane lyses were seen in these cells. **a**): Low magnification; the thick white arrow indicate the cytoskeleton insoluble to Triton X-100. **b**): Components of the cytoskeleton, thin white arrows indicate microfilaments, intermediate filaments and microtubules.

a)

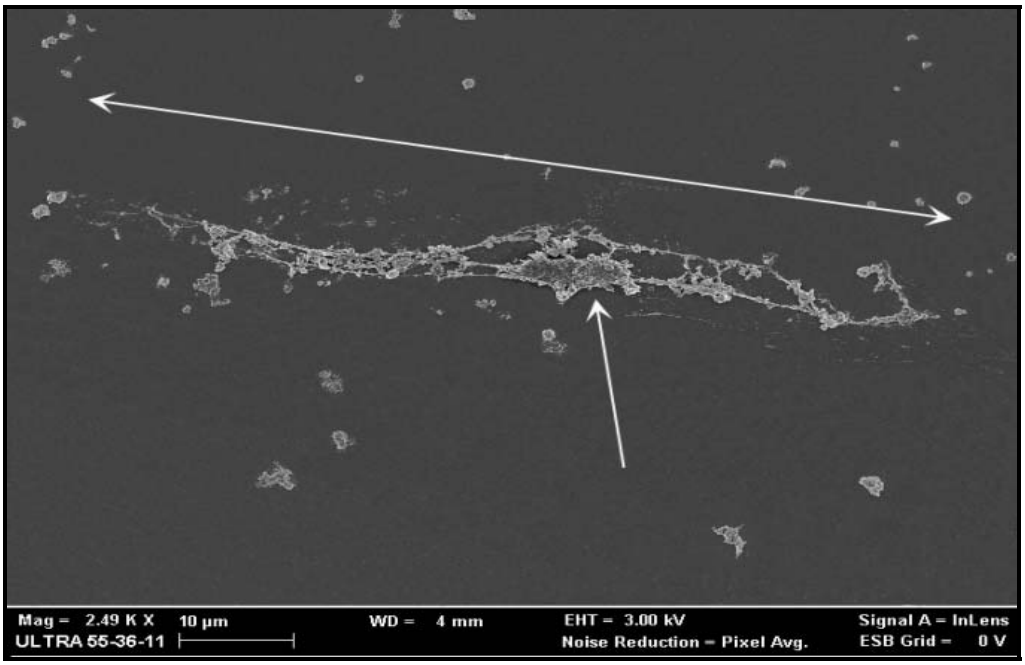

b)

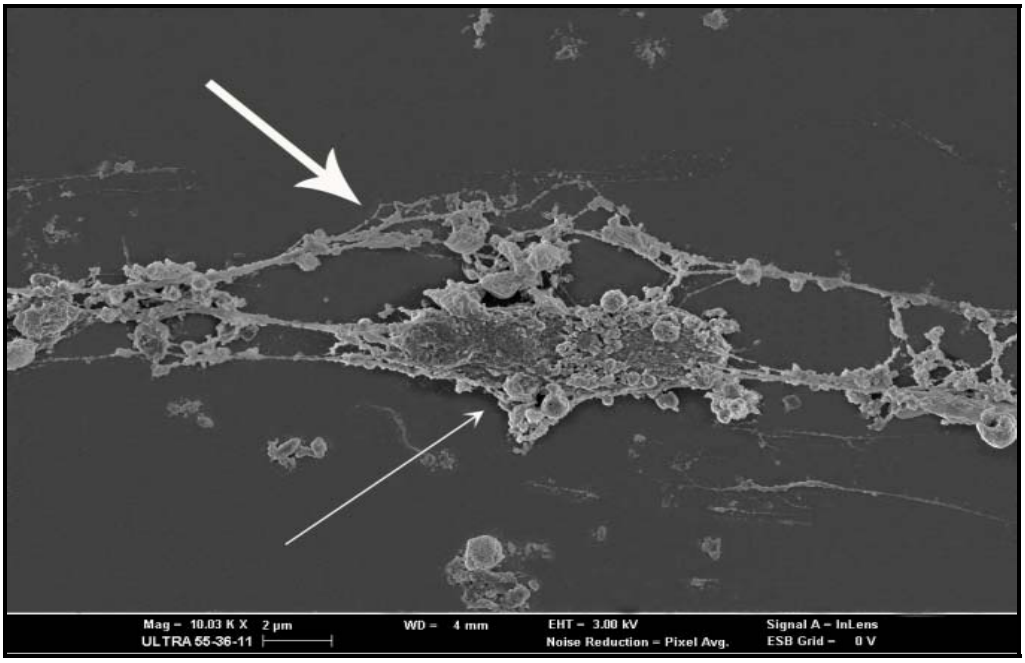

Figure 5.4: Cardiac muscle cells exposed to 0.5% Triton X-100. **a** & **b**): Low and high magnification showing a part of the cytoskeleton (thick arrow in **b**) and the nuclear remnant (thin arrow in **b**), insoluble to Triton X-100 are left.

Wallace *et al*., 1979, demonstrated that, with suitable specimen preparation, it is feasible to resolve and identify the various classes of filamentous structures within a cell or cytoskeleton by SEM, and thus obtain direct three-dimensional information regarding their organization *in situ*. Evidence was presented that cytoskeletal structures (actin filaments, intermediate filaments, and microtubules) in chick embryonic skeletal and cardiac muscle cells can be resolved by SEM after osmium impregnation of biological material, using thiocarbohydrazide as a ligand, followed by critical-point drying (Wallace *et al*., 1979). These different classes of filaments or tubules could be identified both as purified protein polymers and as structured organelles within cryofractured or detergent-extracted cells (Wallace *et al*., 1979). As a prelude to their SEM study of cytoskeletal elements within cryofractured or detergent-extracted cells, it was decided to examine samples of purified F-actin, intermediate filaments (10 nm), and microtubules by negative staining and SEM. When F-actin was deposited on coverslips, processed by the osmium-TCH procedure, and examined at instrumental magnifications of 20 000 – 50 000 by SEM, the filaments exhibited a diameter of 14 - 16 nm, which is approximately twice the width of actin filaments examined by negative stain TEM. The filaments tended to be straight or gently curved, unbranched, and often appear beaded. Polymerized microtubules were also resolved by SEM after the osmium-TCH procedure. The diameter of these structures measured 32 - 37 nm as compared to a diameter of 25 - 28 nm after uranyl acetate negative staining. By SEM, the microtubules exhibited an electron-transparent core, presumably the result of beam penetration through the upper layer of protofilaments. Some microtubules appear rough surfaced but no obvious periodicity had been detected. Intermediate filaments had a complex, branched appearance in which considerable variability of filament diameters were evident. Presumably, this variability reflects extensive side-to-side aggregation of individual filaments. In areas where single filaments were resolved, their diameters measured 10 - 12 nm by negative-stain TEM and 18 - 22 nm by SEM (Wallace *et al*., 1979). In the interior of vertebrate cells, there are dense, heterogeneous and highly interconnected networks; these include the well known structural filaments (microfilaments, intermediate filaments, and microtubules) and the extensive system of highly cross-linked microtrabeculae (Fulton *et al*., 1981). An important aspect of cell structure seen after extraction with Triton X-100 is the surface lamina, an external protein sheet derived from the plasma membrane, which retains the overall morphology and many details of the intact cell. The surface lamina retains most plasma membrane proteins and surface-

specific structures such as binding sites for virusses and lectins (Ben-Ze'ev *et al*., 1979). Fulton *et al*., 1981, suggested that this extracted structure, bound by the protein sheet or lamina formed by the plasma membrane proteins, be designated the "skeletal framework" to distinguish it from the more narrowly defined cytoskeleton.

Severe cellular destruction was seen in both cell cultures upon exposure to the highest concentration of Triton X-100 (0.5%) tested in this study (Figure 5.3 and 5.4). Yu *et al*., 1973 showed that Triton X-100 extraction of cells or membranes solubilizes the bilayer and most integral membrane proteins, leaving only the spectrin matrix and associated proteins in an insoluble, and thus, readily form. The work of Mesher *et al*., 1981, showed that a Triton-insoluble matrix of proteins was associated with the inner face of plasma membranes from murine turmor cells and lymphocytes. The location and properties of the matrix suggested that it might form a membrane skeleton continuous over the inner plasma membrane face of these cells, and consistent with this suggestion, Apgar *et al*., 1985, found that extraction of intact cells (P815 tumour cells) under the same conditions (1% Triton X-100) resulted in structures with a continuous layer of detergent-insoluble protein at the cell periphery. Confined within this peripheral layer was a nuclear remnant (Figure 5.4 b, thin white arrow), the cytoplasmic space was largely empty and clearly lacked filamentous cytoskeletal elements (as seen in Figure 5.3 of this study) (Apgar *et al*., 1985). Low magnification SEM of cardiac and skeletal muscle cells in the present study showed cytoskeletons and cell remnants (Figure 5.3 a & b). Higher magnification showed the complete lyses of membranes (Figure 5.4 a & b), and total loss of cellular integrity, cell cytoskeletons were left without any organelles visible, except for the nucleus, as seen in the cardiac muscle cell in Figure 5.4 b (thin white arrow). Triton X-100 solubilizes membranes of PC12 cells and leaves behind a nucleus and an array of cytoskeletal filaments (as seen in this study in Figure 5.2 b, indicated by thin white arrows) at a concentration of 0.5% (Vale *et al*., 1985). This might be an indication of the presence of proteins in the cytoskeleton that is insoluble to Triton X 100. Biomembranes are not homogenous, they present a lateral segregation of lipids and proteins which leads to the formation of detergent resistant domains, also called "rafts" (Kirat *et al*., 2007), The plasma membrane of cells are composed of the lipid bilayer, integral membrane proteins, and peripheral proteins associated with, but not embedded in, the bilayer (Singer *et al*., 1972 and Bretscher *et al*., 1975). In the erythrocyte membrane, a set of peripheral proteins including spectrin, actin, band 4.1, and ankyrin interact to form

a membrane skeleton associated with the cytoplasmic face of the membrane. This skeleton is a rigid layer that provides mechanical stability to the membrane, plays a role in determining morphology of the cell and appears to influence cell surface protein mobility and lipid distribution in the bilayer (Apgar *et al*., 1985). Fulton *et al*., 1981, showed by direct measurements that most of the surface membrane proteins of prefusion myoblasts and postfusion myotubes remain with the cytoskeletal framework while three-quarters of total cellular proteins are removed (Fulton *et al*., 1981). After mild detergent extraction (0.5% Triton X-100), Prives *et al*., 1982, detected the association of surface acetylcholine receptors with the cytoskeletal framework in cultured muscle cells. The authors found that this procedure distinguished between two subpopulations of this integral membrane protein. The experimental results indicated the following: that i) aggregated acetylcholine receptors were tightly bound to the myotube skeletal framework; ii) a portion of the diffusely distributed acetylcholine receptors were not tightly bound and were extracted with detergent; and iii) the proportion of the tightly bound acetylcholine receptors increased with muscle cell development (Prives *et al*., 1982). Masuko *et al*., 1983, showed with fluorescence microscopy in combination with SEM, that acetylcholine receptor accumulation sites, were associated with smooth surfaced areas of the myotube. The finding was consistent with earlier observations by TEM and freeze-fracture techniques (Masuko *et al*., 1983). Fambrough *et al*., 1978, reported that newly synthesized acetylcholine receptors appeared in the Golgi apparatus and that they may be placed in the membranes of vesicles and subsequently transported to the cell surface by a pathway similar to that taken by secretory proteins. Since areas of acetylcholine receptor clusters in cultured cells represent sites of the most rapid addition of new receptor molecules, rather than of accretion of receptors from surrounding areas of membrane, the smooth surfaced areas corresponding to fluorescent speckles of acetylcholine receptors seem to be areas of insertion of new membranes containing receptor molecules into the sarcolemma.

Many cell types have been shown to contain 3 morphological filament systems: microtubules, intermediate filaments and microfilaments (Goldman *et al*., 1973 and Ishikawa *et al*., 1969). Microfilaments bind heavy meromyosin with the same specificity and morphology as do the thin filaments of muscle and purified filamentous actin (Ishikawa *et al*., 1969 and Huxley, 1963). Microfilaments were therefore considered to be largely composed of actin (Trotter *et al*., 1978). Trotter et al., 1978, used 2% Triton X-

100 to solubilize the membranes of 3T3 cells and extracted the bulk of the cytoplasm, leaving a residue composed of the nucleus and an elaborate system of fibres. Scanning electron microscopy was used to study the distribution of intracytoplasmic fibres. The results of the study argued that the 3-dimensional fibrous network seen in the scanning electron microscope, performs a support function in the cytoplasm, and also plays an important role in cell-substratum adhesion (Trotter *et al*., 1978). The microfilament systems preserved by this method were composed of stereo-chemically intact actin filaments, as shown by their ability to specifically bind heavy meromyosin in characteristic fashion. Intermediate filaments were also retained in the detergent residue, while most microtubules were extracted (Trotter *et al*., 1978).

a)

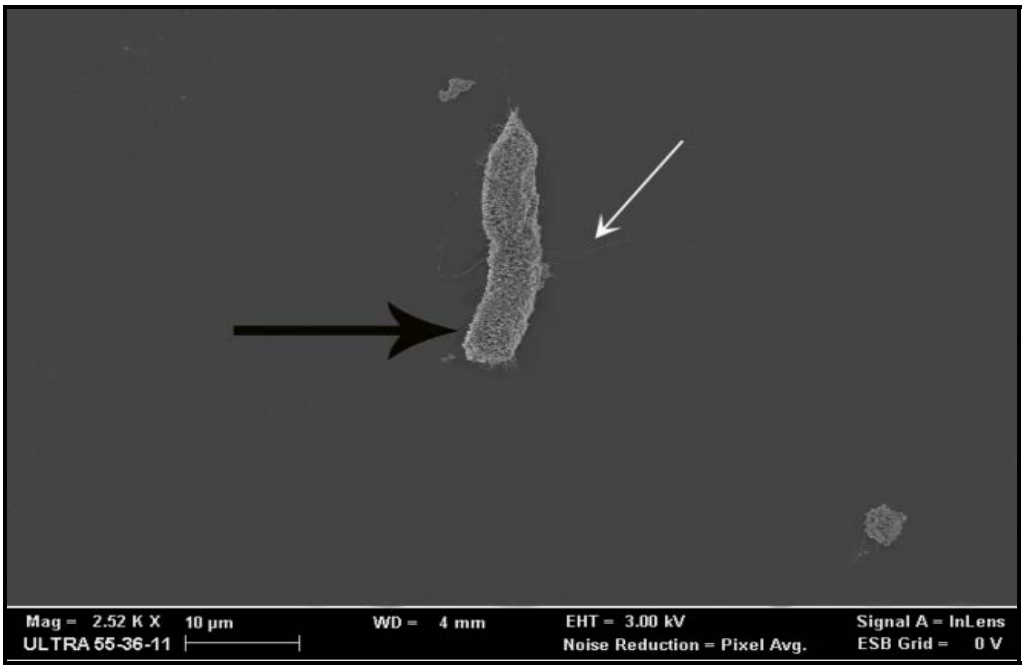

b)

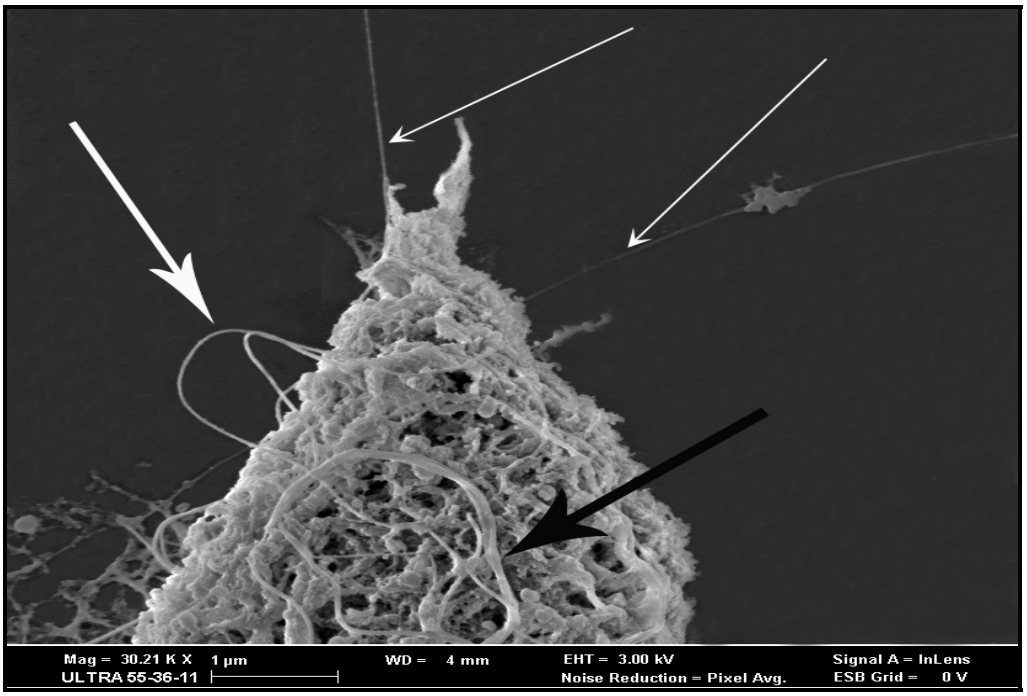

Figure 5.5: Skeletal muscle cells exposed to 0.05% Triton X-100. Low magnification (**a**): showed cell debris and a cell of which the membrane was completely lysed (thick black arrow), with thin filaments extending from the tip of the cell (thin white arrow). **b**): Higher magnification enables visualization of exposed cytoskeletal components. Thin white arrows indicate f-actin filaments, the thick white arrow indicates intermediate filaments, surrounded by vesicular bodies (beaded appearance); the thick black arrow indicates a microtubule (Wallace *et al*., 1979).

a)

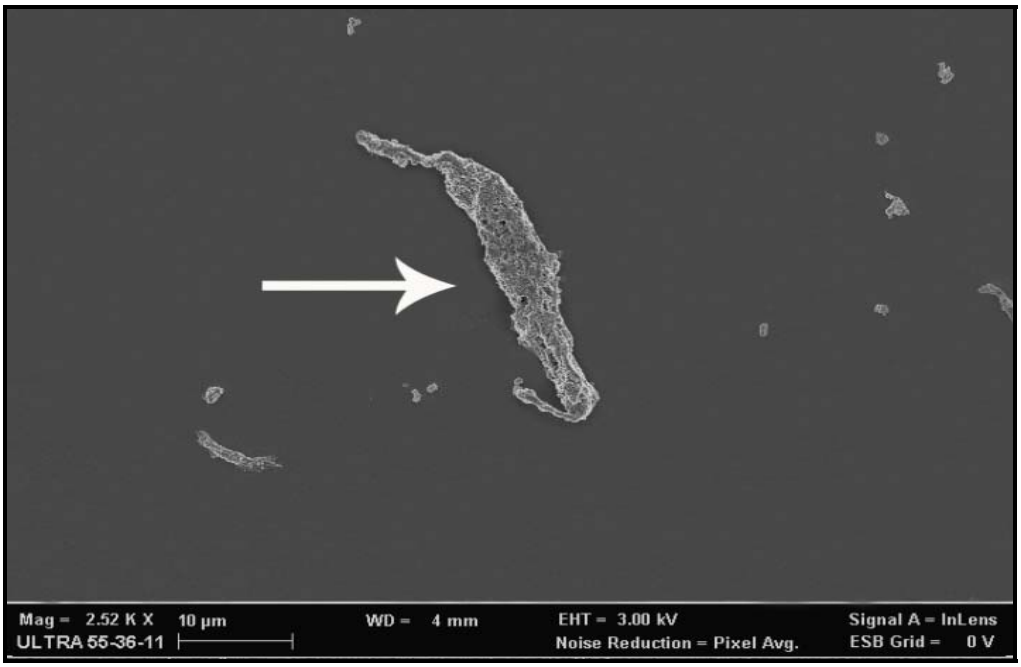

b)

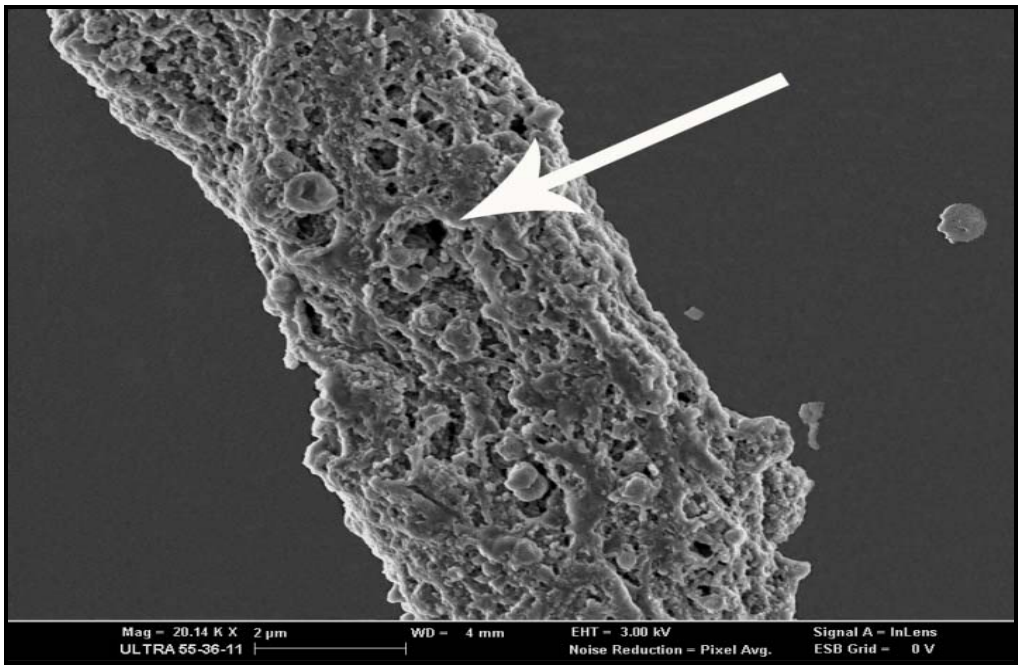

Figure 5.6: Cardiac muscle cells exposed to 0.05% Triton X-100. **a**): At low magnification part of a cell with completely lysed membrane (thick white arrow) and cell debris lying in the vicinity. **b**): At higher magnification, the cell membrane was clearly absent. The thick white arrow indicates what Fulton *et al*., 1981, described as a lacuna. Lacunae in the surface lamina correspond to regions deficient in lectin binding protein, presumably lipid-rich domains in the plasma membrane. The surface proteins form a sheet or lamina that covers the internal skeletal framework remaining after detergent extraction (Ben'Zev *et al*., 1979).

a)

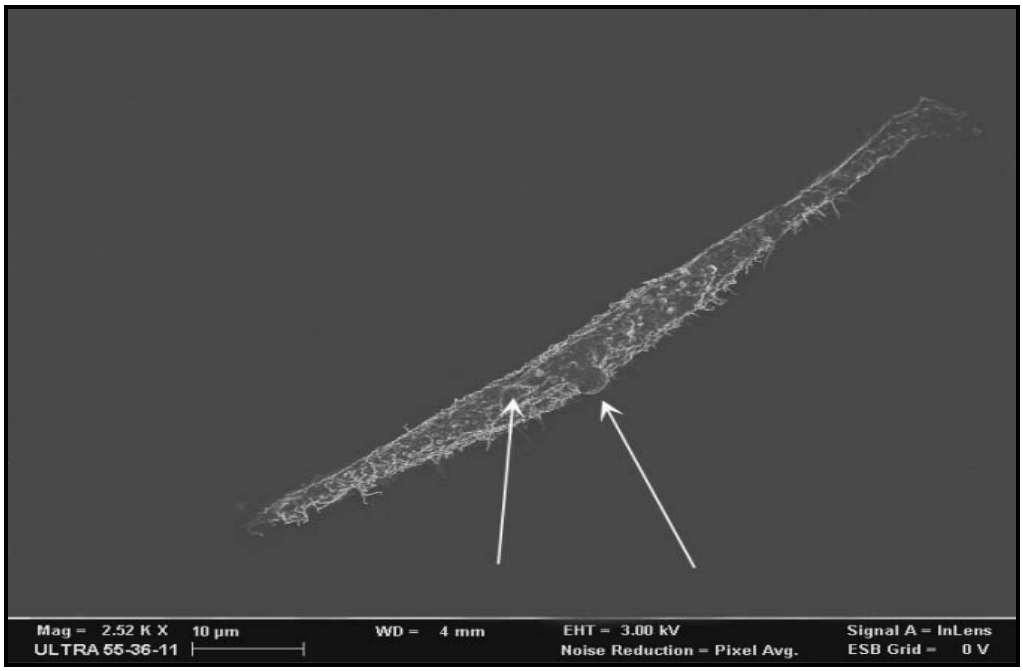

b)

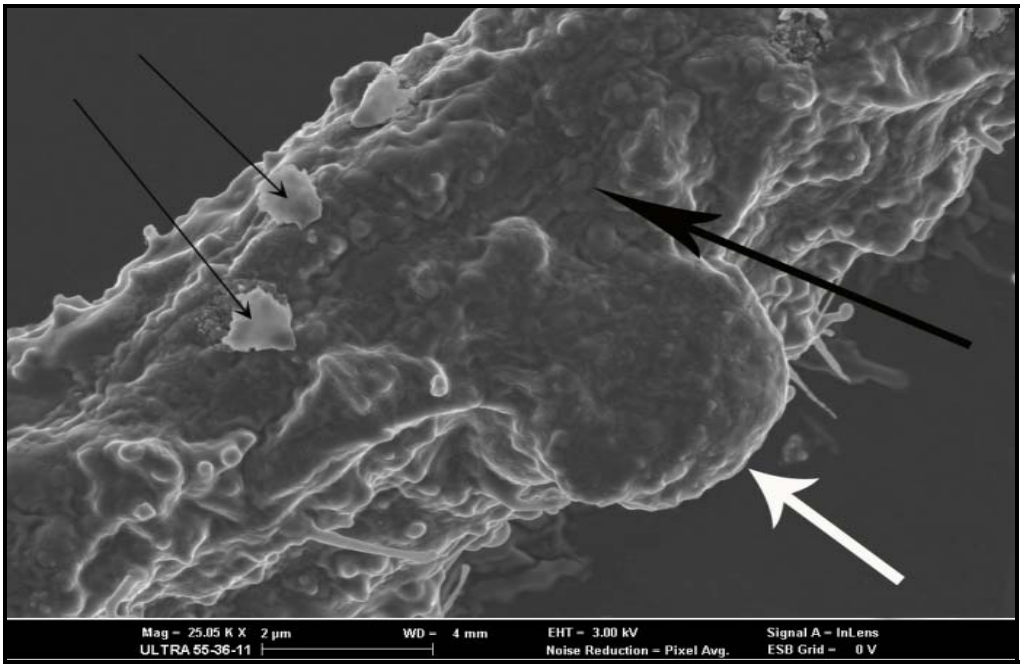

Figure 5.7: Skeletal muscle cells exposed to 0.005% Triton X-100. **a**): At low magnification blebbing was observed on the membrane (thin white arrows). **b**): At higher magnification, it was seen that the membrane was shrunken (thick black arrow). The apoptotic bleb (thick white arrow). Contractile force generated by actin-myosin cytoskeletal structures is thought to drive the formation of membrane blebs and apoptotic bodies (Coleman *et al*., 2001). Ruthenium artefacts (thin black arrows).

a)

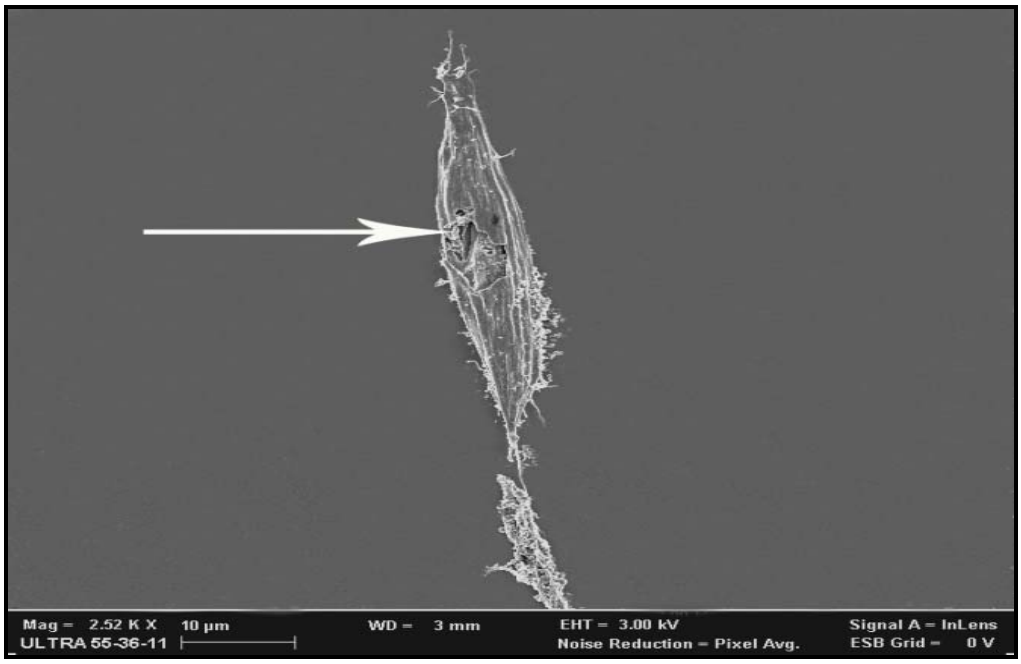

b)

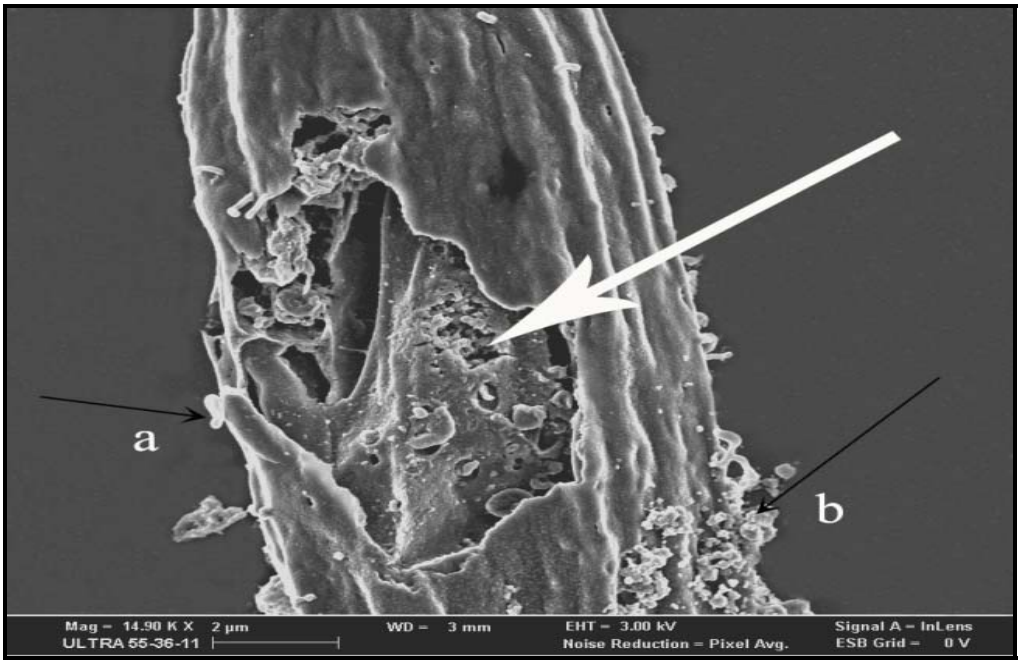

Figure 5.8: Cardiac muscle cells exposed 0.005% to Triton X-100. **a**): Low magnification showed disruption of the membrane (thick white arrow). **b**): At higher magnification it was seen that the membrane collapsed almost in the center of the cell. The surface lamina (thick white arrow) was partly intact, with severe disruptions visible. The thin black arrows show (**a**) a rhutenium artefact; (**b**) protein precipitation, possibly derived from the 5% foetal bovine serum in the culture medium.

The evolutionary conserved execution phase of apoptosis is characterized by events that occur during the final stages of death, including cell contraction, dynamic membrane blebbing and DNA fragmentation (Coleman *et al*., 2001). The distinct morphological transformation is one of the earliest described and most obvious aspects of apoptosis. Contractile force generated by actin-myosin cytoskeletal structures is thought to drive the formation of membrane blebs (as seen in Figure 5.7) and apoptotic bodies (Coleman *et al*., 2001).

It seems likely that the lacunae in the surface lamina relate to the requirements for cell fusion (Fulton *et al*., 1981). Myotube formation requires juxtaposing fusion-competent cell surfaces. The lacunae seen in the postproliferative myoblast in the study by Fulton *et al*., 1981, may reflect an early stage of this process. The act of melding together two surfaces must require unusual membrane properties, perhaps met by the lipid-rich patches characteristic of this stage of muscle development (Fulton *et al*., 1981). Transient lipid-rich patches, relatively free of protein may explain the observation that myoblast lipid fluidity change with fusion (Prives *et al*., 1977). Fulton *et al*., 1981, indicated with fluorescence depolarization measurements a large increase in lipid fluidity just before fusion followed by a decline to normal values after fusion (Fulton *et al*., 1981). Studies by Herman *et al*., 1978, and Kalderon *et al*., 1979, suggested that the lacunae seen in the surface lamina resulted from the protein-free, highly fluid lipid; thus the change in plasma lamina organization may account for the transient increase in lipid fluidity (Fulton *et al*., 1981, Herman *et al*., 1978 and Kalderon *et al*., 1979). The disruption of the membrane surface in Figure 5.8 might be explained by this phenomenon, considering that the concentration of Triton X-100 (0.005%) might be too low to dissolve the membrane proteins, but high enough to disrupt the membrane in protein-free, lipid-rich regions.

a)

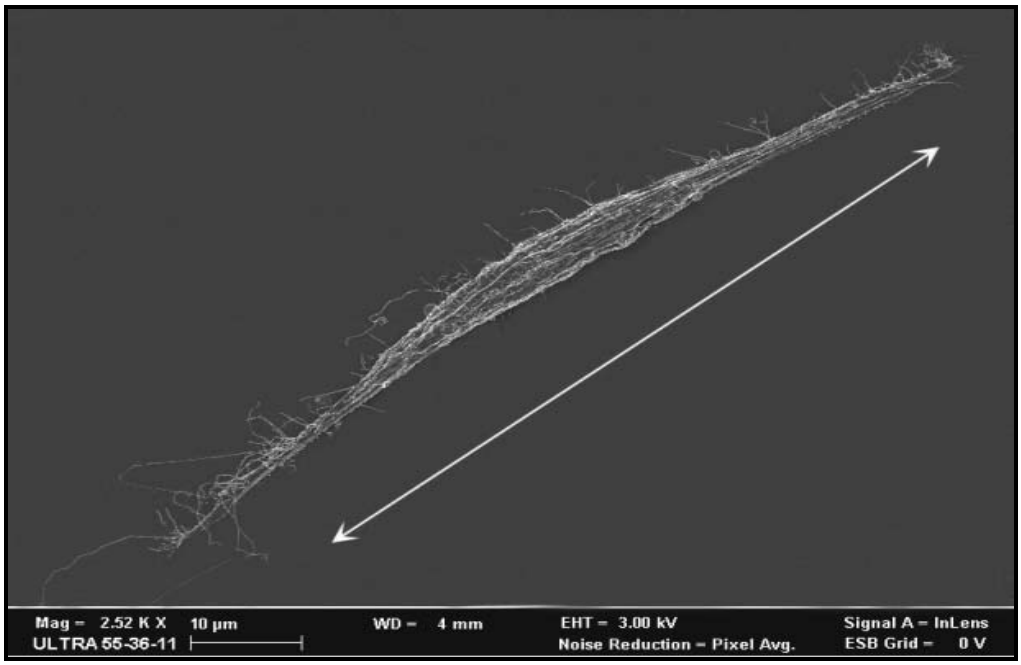

b)

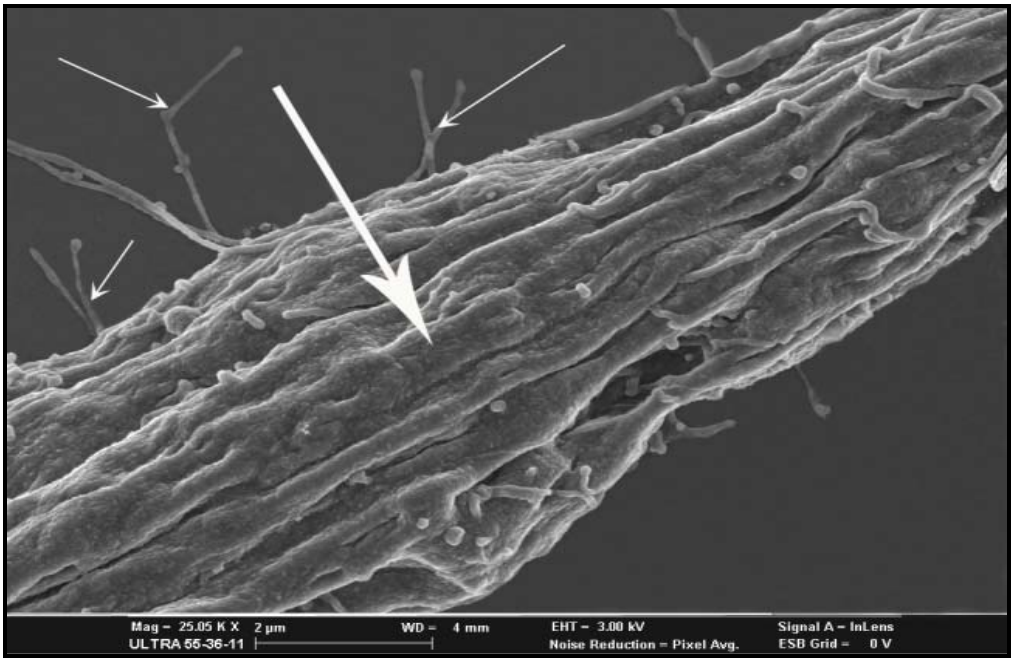

Figure 5.9: Skeletal muscle cells exposed to 0.0005% Triton X-100. **a**): Low magnification shows an intact cell (myoblast) with microprocesses/filopodia extending from the bipolar ends. **b**): At higher magnification it was clear that the membrane was shrunken (thick white arrow) and instable. Microvilli (thin white arrows) extended from the membrane, which might be a possible indication of the cell's state in the cell cycle (Late G_2, Masuko *et al*., 1983). Although no myotubes or fusion of myoblasts were observed at this concentration, the myoblast (**a**) might be in proliferating state.

a)

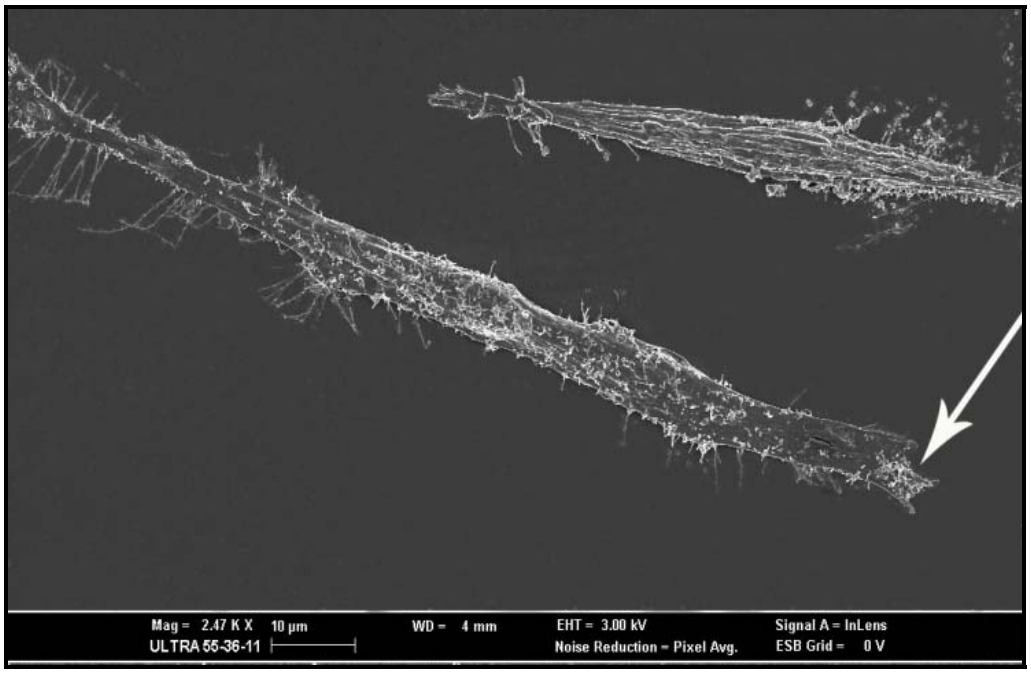

b)

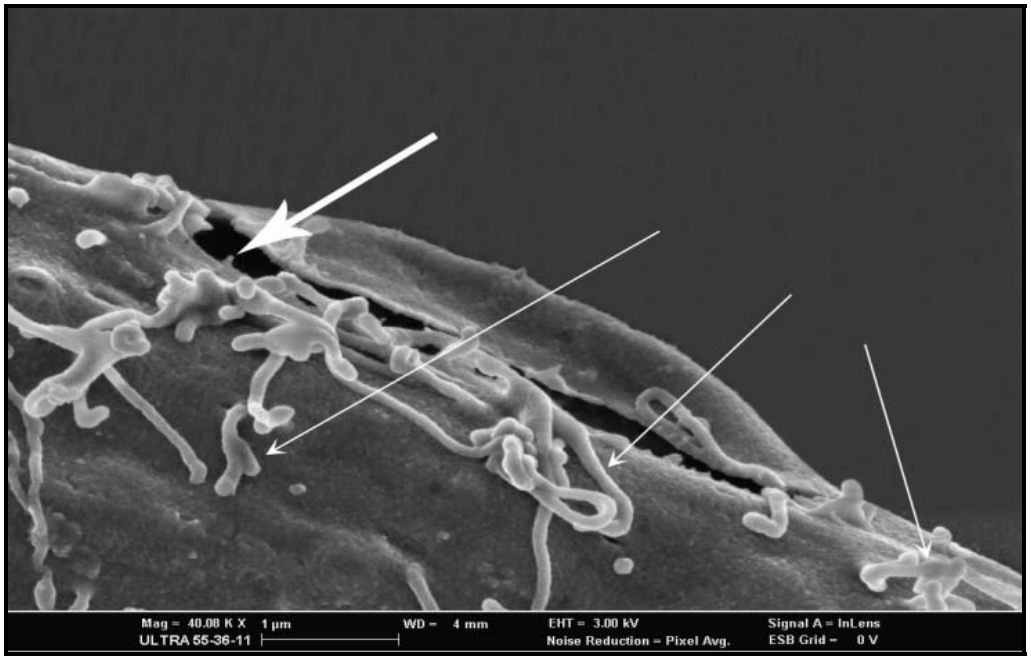

Figure 5.10: Cardiac muscle cells exposed to 0.0005% Triton X-100. **a**): Low magnification shows two intact cells (myoblasts) with bipolar ends with extending microprocesses/filopodia possibly in proliferating state. The thick white arrow indicates the very characteristic end of a cardiac cell. **b**): higher magnification showed a smooth membrane surface, possibly unstable (thick white arrow indicate a tear in the membrane), thin white arrows indicate microvilli confirming the state of proliferation.

a)

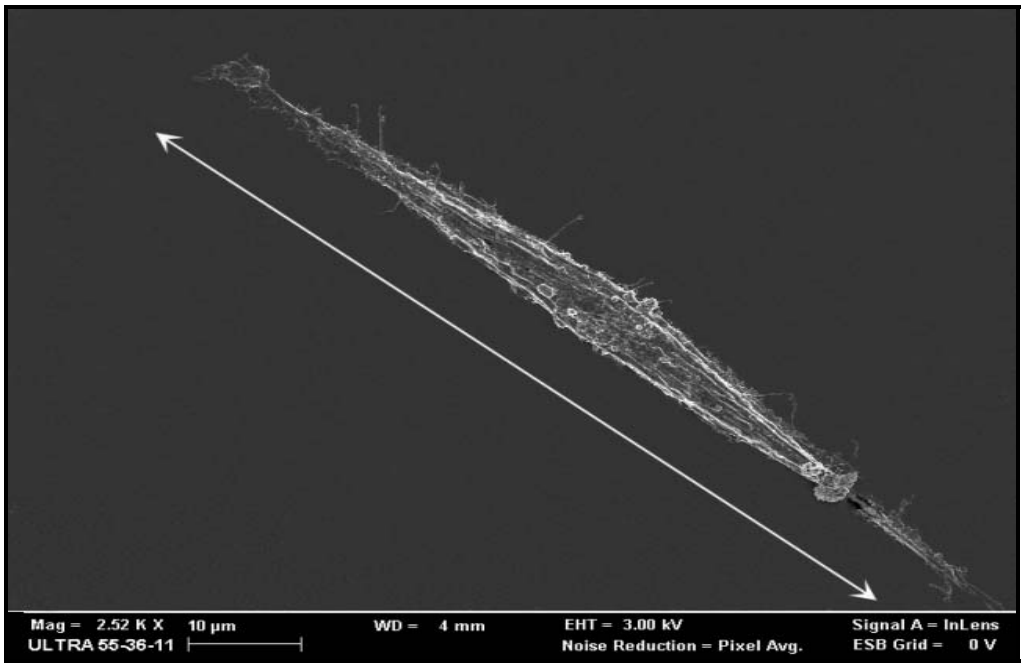

b)

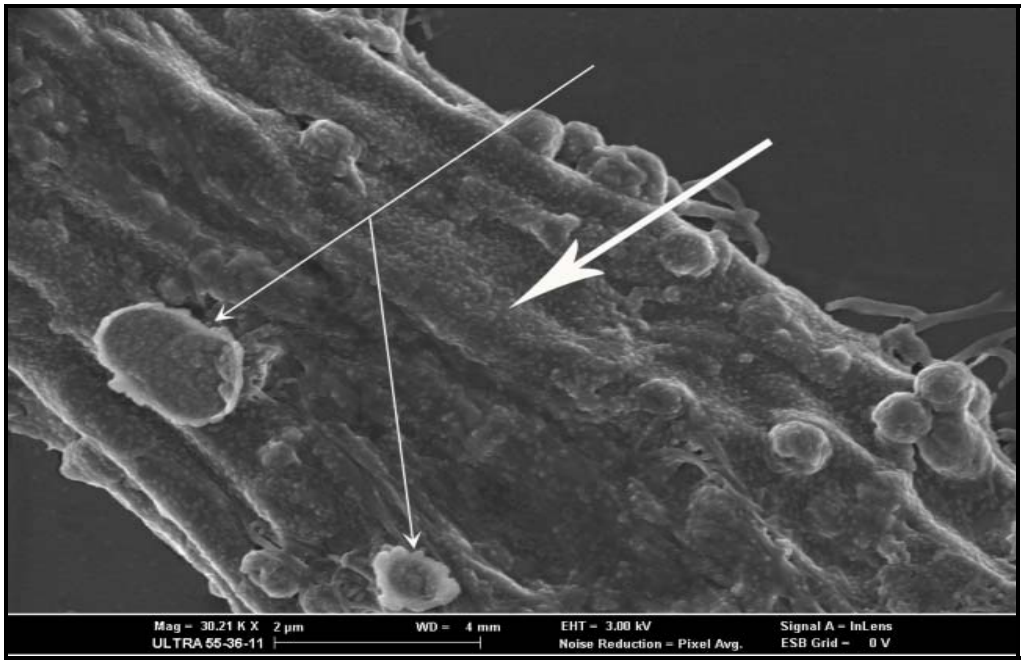

Figure 5.11: Skeletal muscle cells exposed to 0.00005% Triton X-100. **a**): Low magnification shows bipolar ends with extending microprocesses. **b**): Higher magnification shows that the membrane is not smooth, it almost appear to have a rough surface (thick white arrow). Thin white arrows indicate ruthenium artefacts.

a)

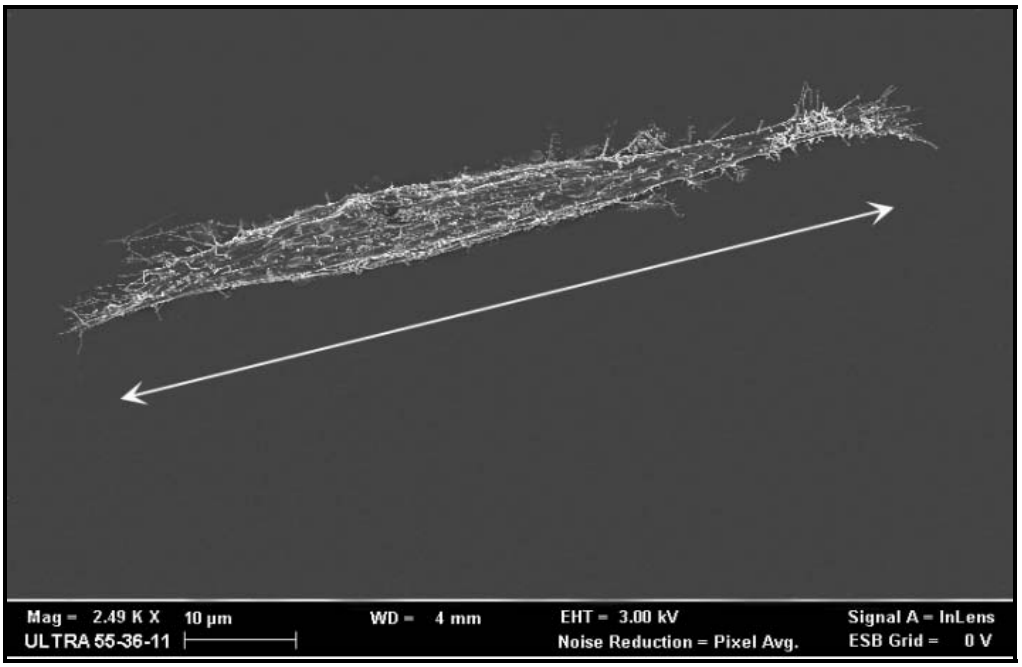

b)

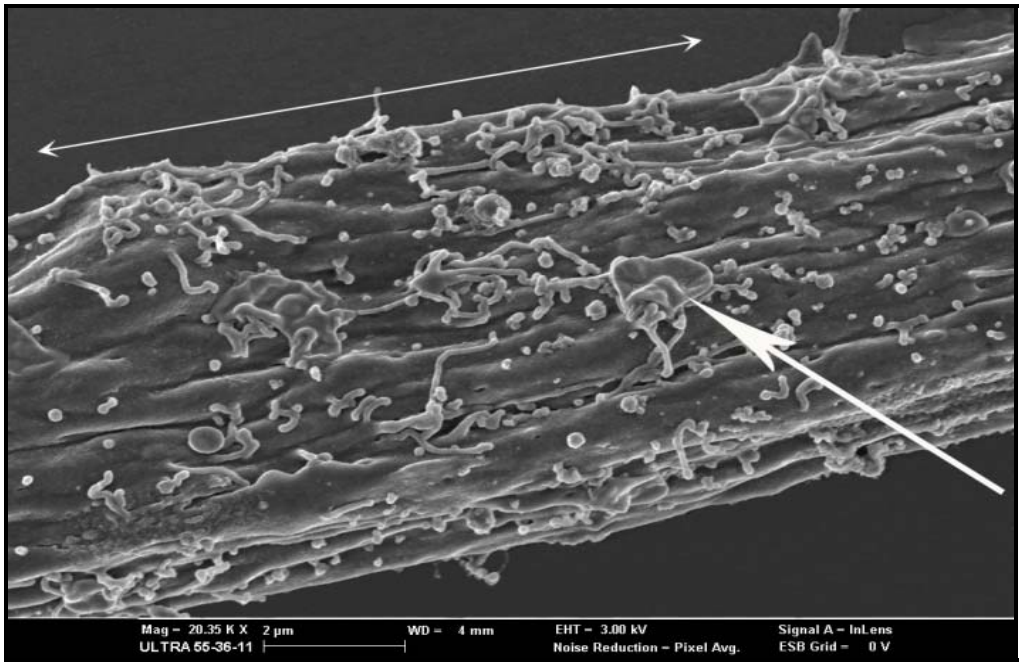

Figure 5.12: Cardiac muscle cells exposed to 0.00005% Triton X-100. **a**): Low magnification shows a bipolar intact cell with extending microprocesses. **b**): On higher magnification the membrane show shrinkage with numerous microvilli, possibly the cell is in proliferating state. Thick white arrow point to an artefact lying on the membrane surface.

5.3.3 Cells Exposed to CoQ10

a)

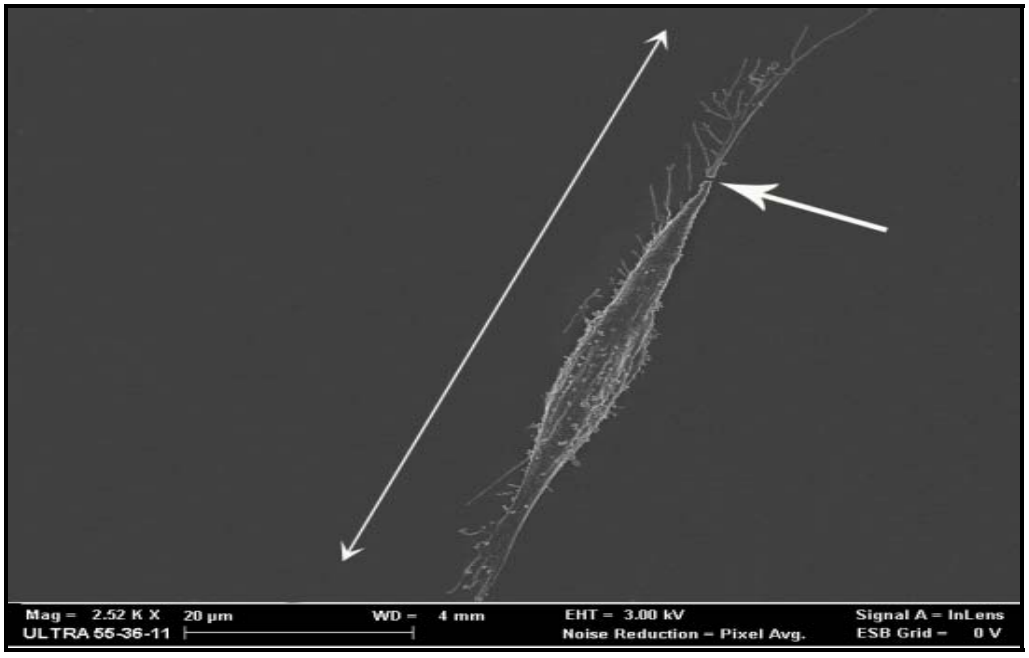

b)

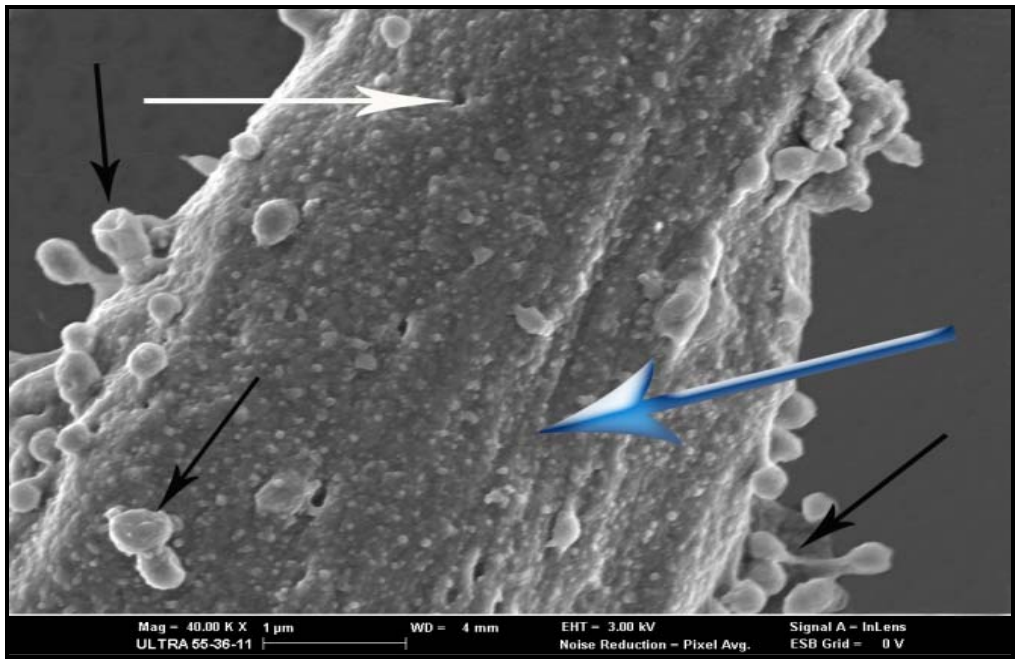

Figure 5.13: Skeletal muscle cells exposed to 0.2mg/ml CoQ10. **a**): Low magnification shows an intact spindle-shaped cell with bipolar ends and microprocesses (thick white arrow indicate breakage of the upper tip of the cell, which might be due to critical point drying. **b**): Higher magnification shows an intact membrane (blue arrow), the surface seems rough with numerous mcirovilli (thin black arrows) and small spherical protrusions starting to protrude from the membrane. The thick white arrow indicates an ion channel in the membrane.

a)

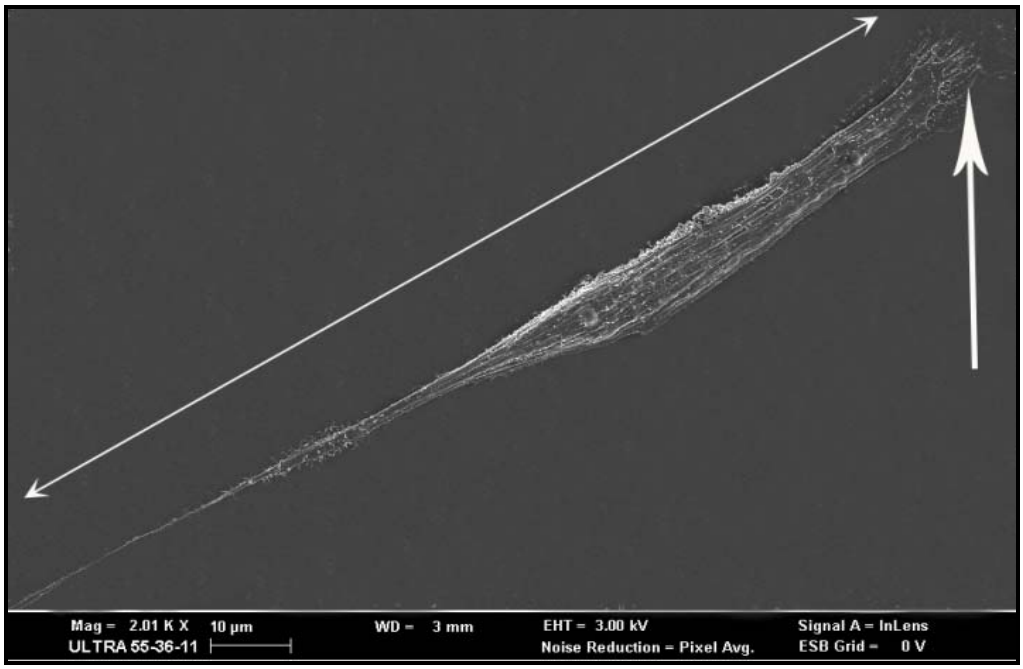

b)

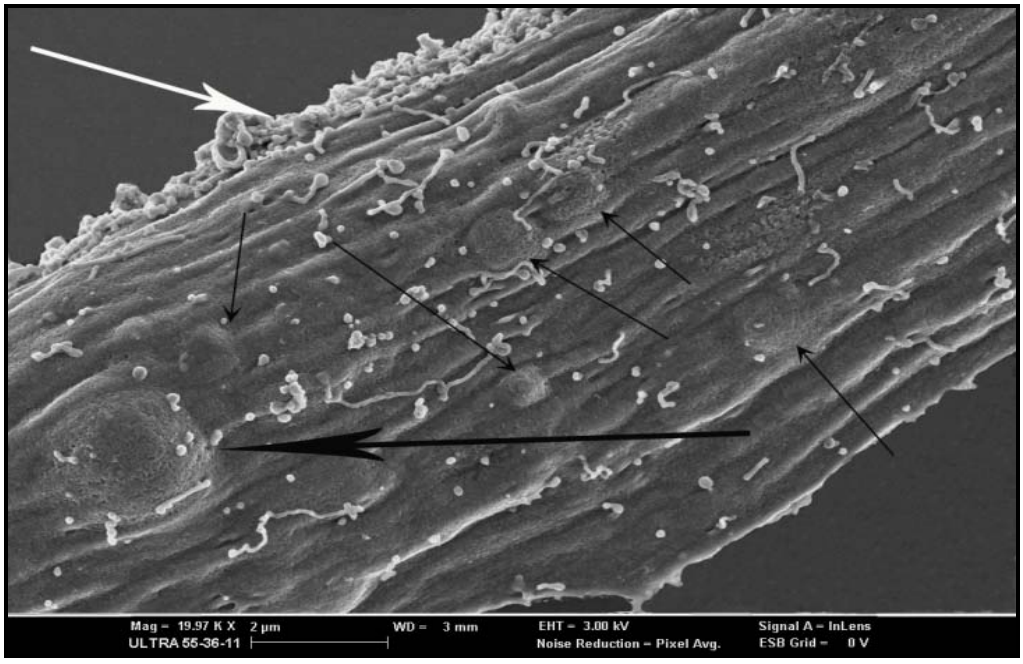

Figure 5.14: Cardiac muscle cells exposed to 0.2mg/ml CoQ10. **a**): Low magnification possibly shows a myoblast entering fusion. Broad flat upper end with numerous extending microprocesses, numerous microvilli, small spherical protrusions (**b**: thick white arrow), and a bulging appearance (**b**: thick and thin black arrows), indicating that the cell are possibly in the M phase of the cell cycle. **b**): The membrane is largely intact with a few slightly rough patches.

a)

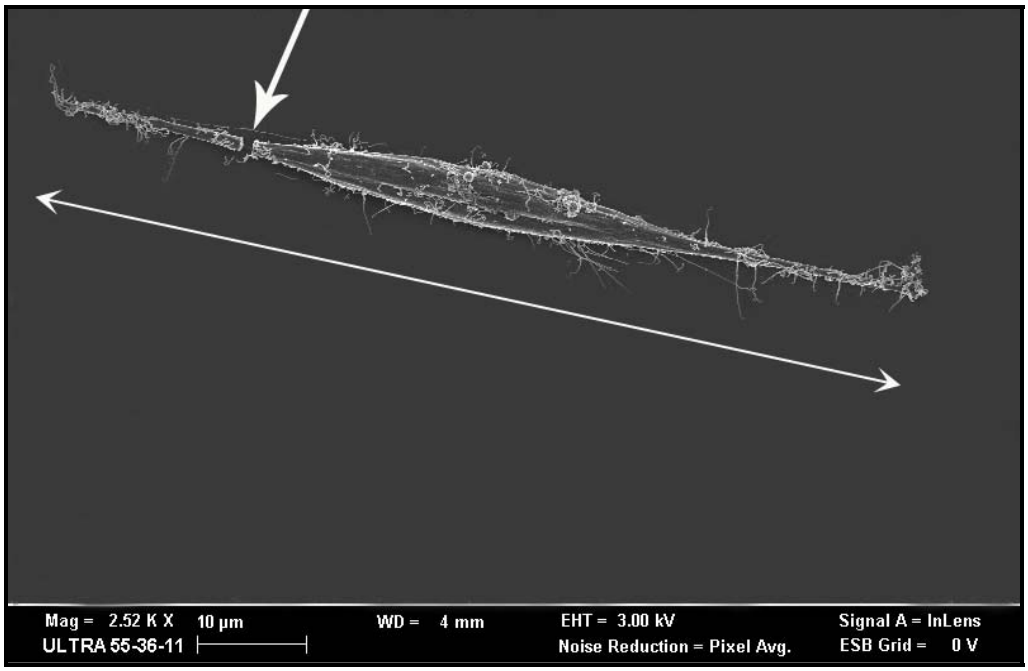

b)

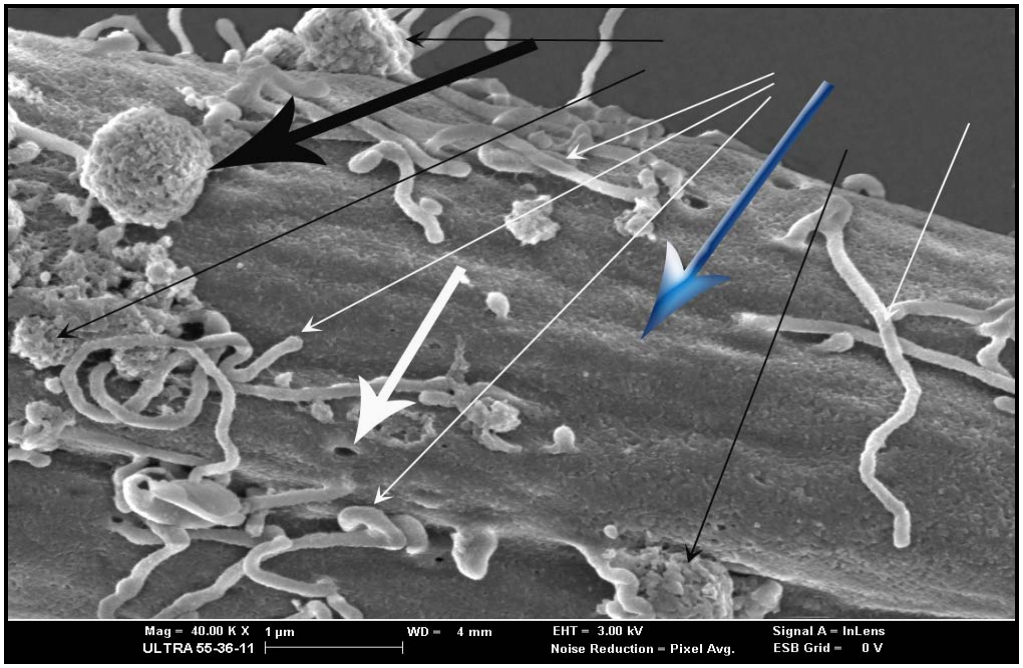

Figure 5.15: Skeletal muscle cells exposed to 0.1mg/ml CoQ10. **a**): Low magnification shows an intact skeletal muscle cell with extending microprocesses. Breakage of the tip is probably due to critical point drying procedure (thick white arrow). **b**): High magnification shows and intact membrane (blue arrow), microvilli (thin white arrows). Ion channels are visible (thick white arrow). Protein precipitation occurred due to proteins present in culture medium (black arrows).

a)

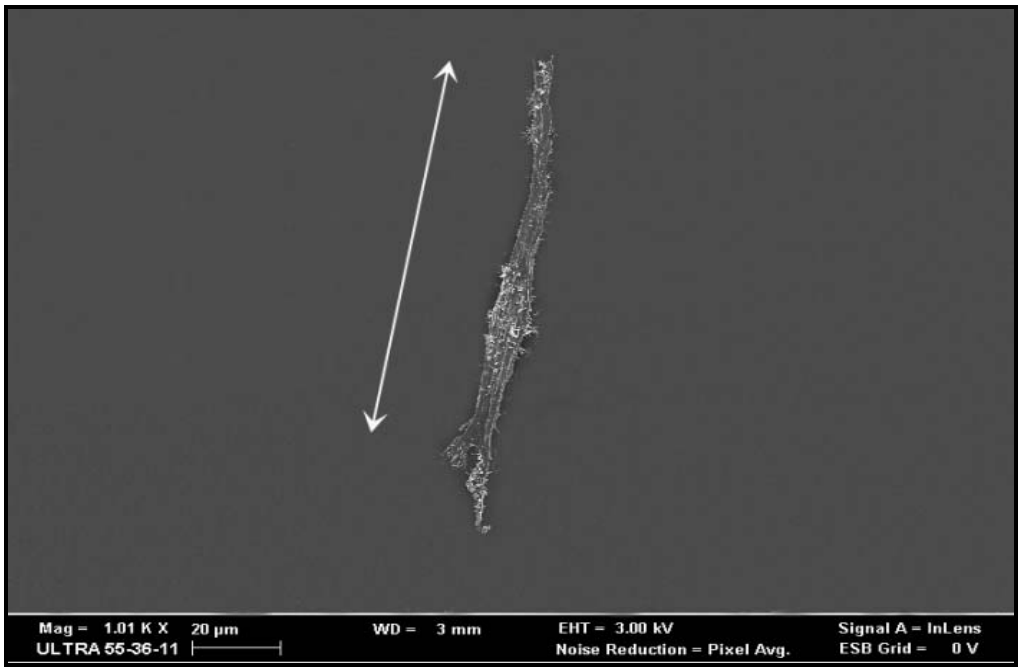

b)

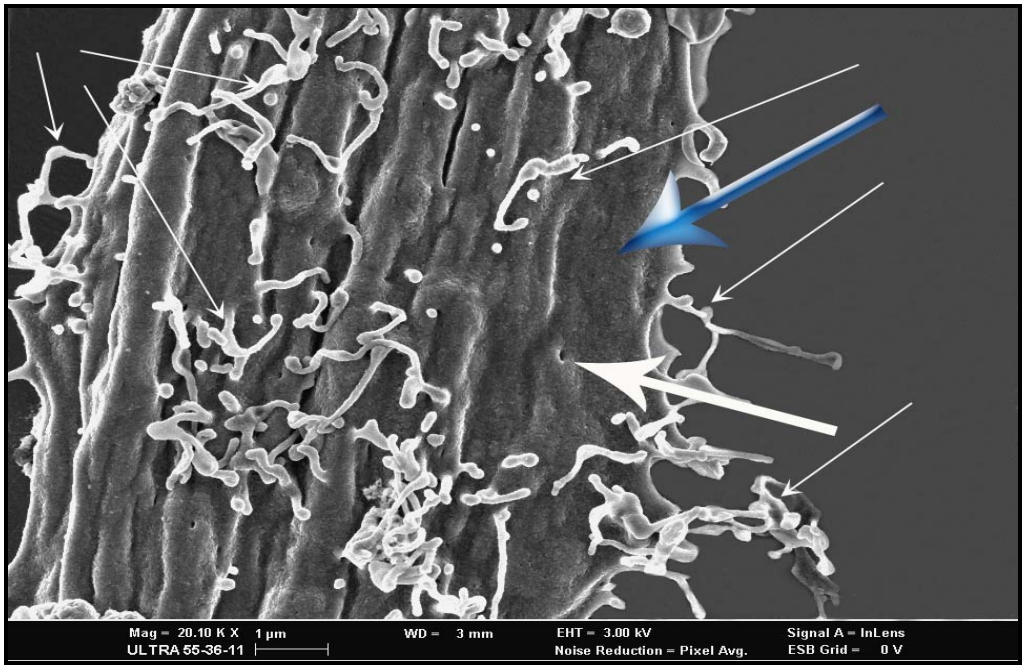

Figure 5.16: Cardiac muscle cells exposed to 0.1mg/ml CoQ10. **b**): High magnification shows numerous microvilli (thin white arrows), although the membrane presented with a slight shrunken appearance, it was intact (blue arrow). Ion channels are visible (thick white arrow).

a)

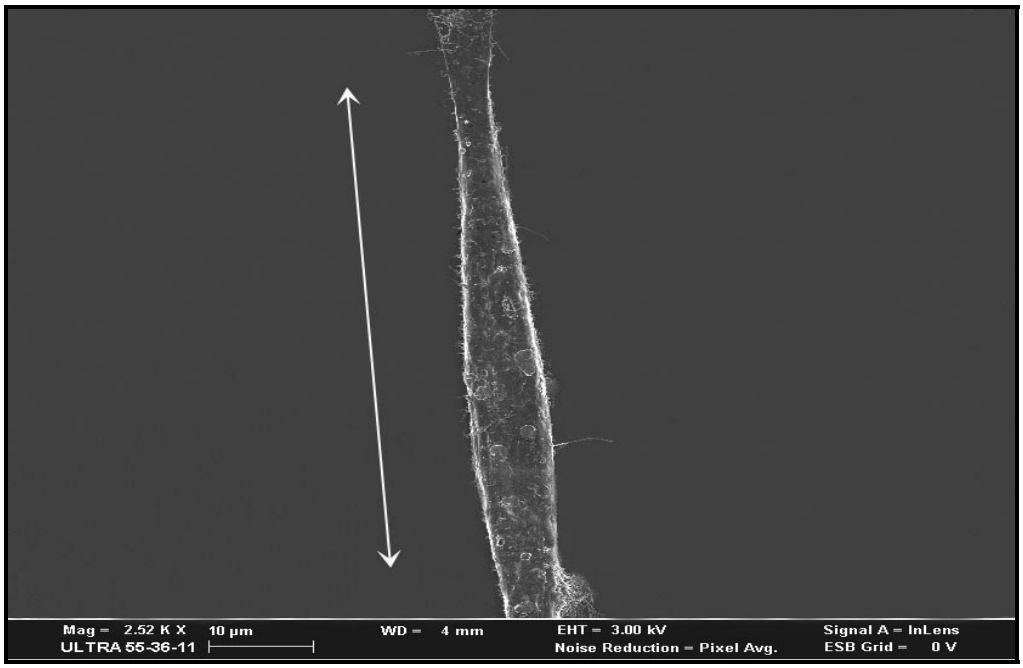

b)

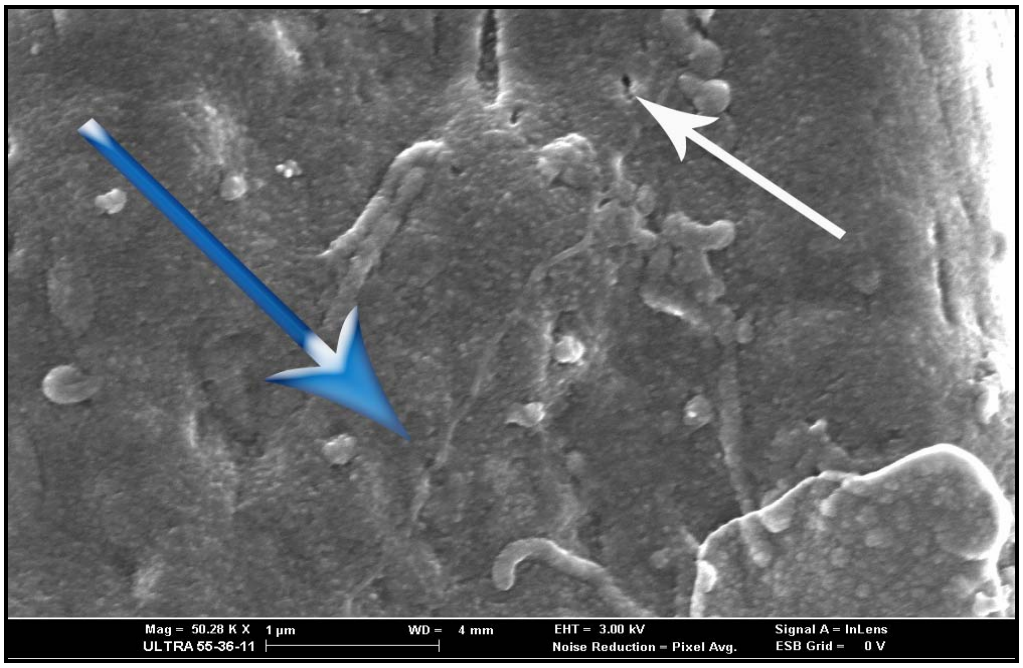

Figure 5.17: Skeletal muscle cells exposed to 0.05mg/ml CoQ10. **a**): Low magnification shows a cell which is possibly postproliferative (myotube), when considering the size. The relatively smooth cell surface seen at higher magnification (**b**), is characteristic of cells capable of undergoing fusion, probably in the G_1 phase of the cell cycle (Masuko *et al*., 1983). The membrane was perfectly intact (blue arrow). Ion channels are visible (white arrow).

a)

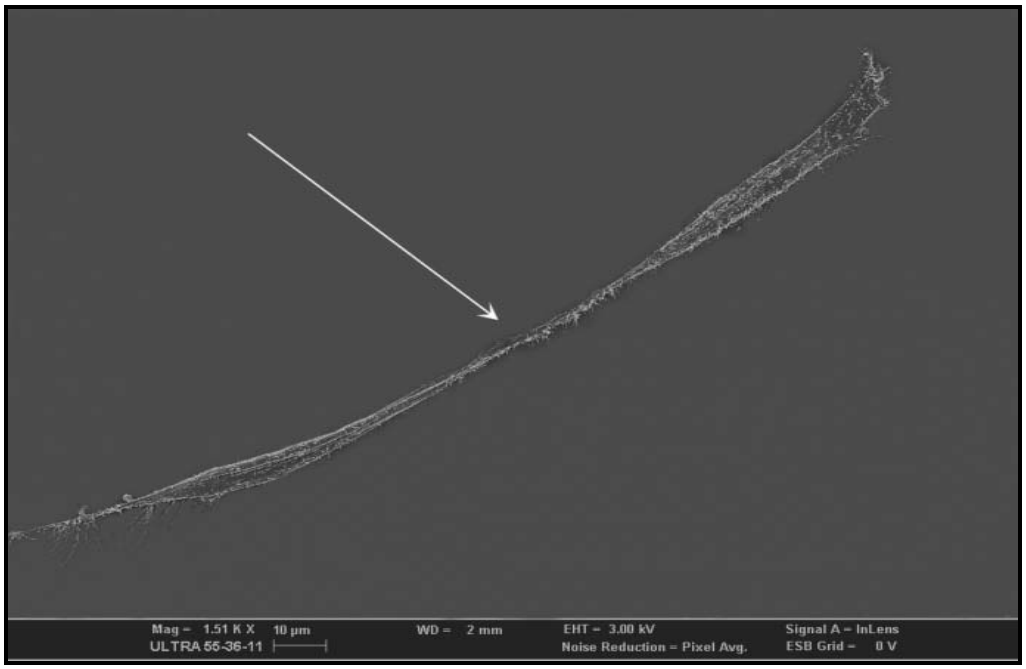

b)

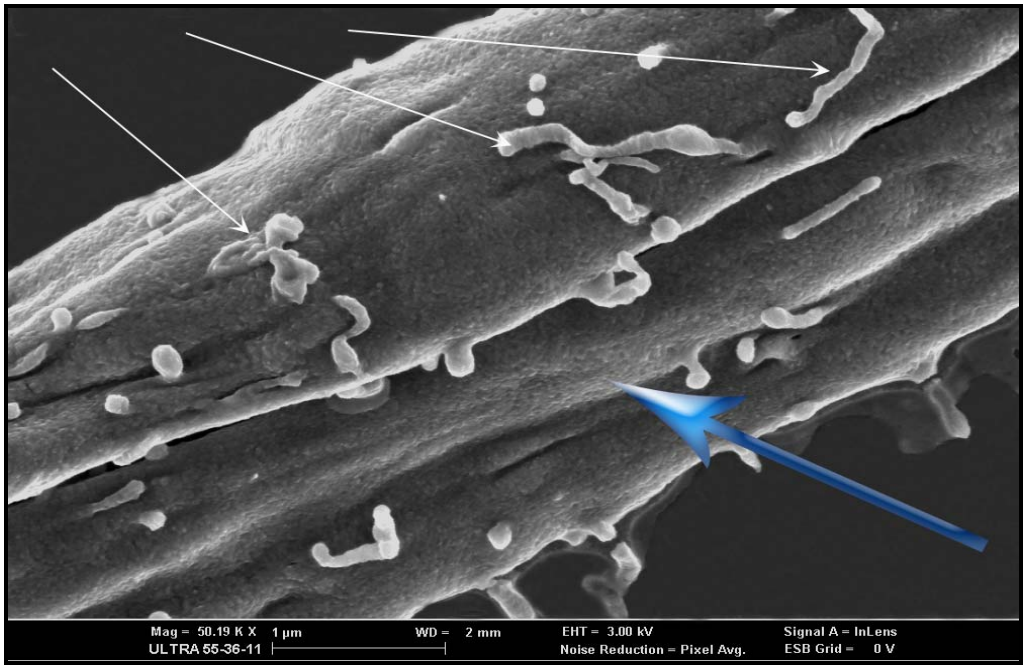

Figure 5.18: Cardiac muscle cells exposed to 0.05mg/ml CoQ10. **a**): Low magnification shows two myoblasts after fusion, forming a myotube. **b**): High magnification shows a smooth, intact membrane (blue arrow), microvilli and small spherical protrusions are present (thin white arrows), characteristic of the surface structure of newly formed myotubes.

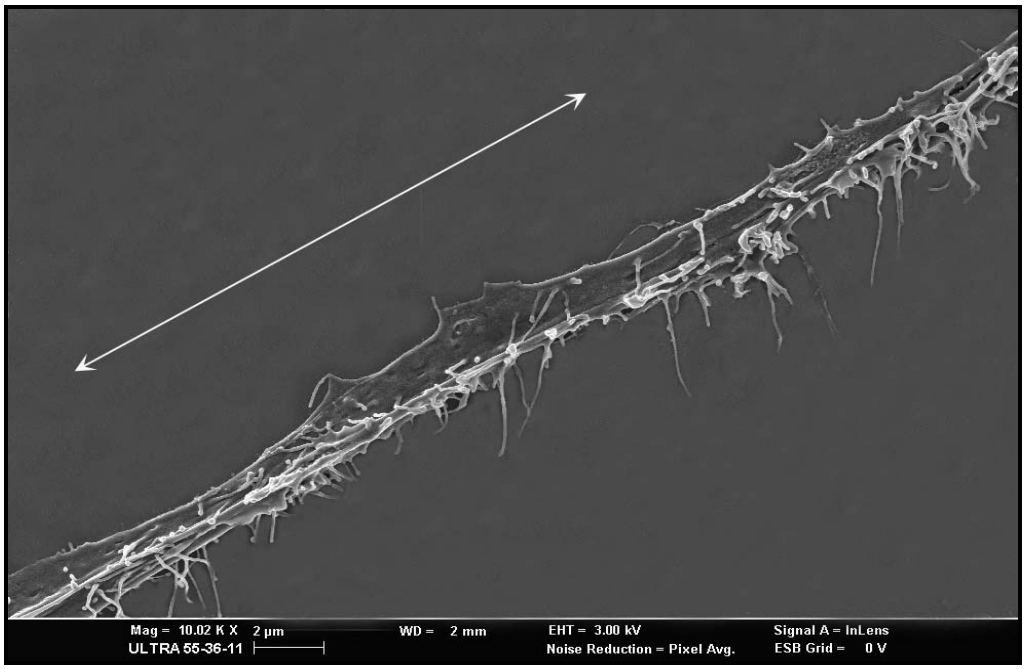

Figure 5.19: The arrow showed the area where the two myoblasts in Figure 5.17 **a**, has fused to form a myotube. The establishment of this connection generate considerable tension indicating that possibly these cells are drawn together (Singer *et al*., 1984).

The formation of muscle fibres by myoblasts fusing is a striking example of the skeletal framework (described by Fulton *et al*., 1981) reorganizing during development (Fulton *et al*., 1981). During differentiation, the structural aspect of the cell becomes reorganized from a diffuse network of filaments in pre-myoblast cell into linear, axially orientated filament bundles characteristic of myoblasts fusing together (Pudney *et al*.,1980). Myoblasts fuse to form multinucleated myotubes which then synthesize and organize the banded actomyosin contractile apparatus. Cells develop under optimum *in vitro* conditions to mature, twitching muscle fibers. Both the internal networks and surface lamina in the myoblast undergo profound, concurrent, yet distinct changes in preparation for and after fusion (Fulton *et al*., 1981). To form the multinucleated myotube, plasma membranes of fusion–competent myoblasts must meld; at this time, large openings, or lacunae, in the surface lamina appear. The work of Huang *et al*., 1978, indicated that prior to the formation of the myotube, long actin-rich processes, “microprocesses”, were extended from myoblasts, sometimes over a distance of 200µm. These long cytoplasmic microprocesses (0.1µm in diameter) exhibit splayed ends resulting from the unravelling

of the microfilament, reminiscent of the “growth cone” of axons (Yamada *et al*., 1971), and is a characteristic of cultured differentiating chick muscle cells (Singer *et al*., 1984). When these processes contacted each other, they fuse prior to the union of the respective cell bodies; then undergo a complex realignment which seemingly reorientates both microprocesses into a single filament bundle, resulting in generation of considerable tension indicating that these cells are actively drawn together (Singer *et al*., 1984). The junction formed between two myoblasts (Figure 5.17 & 5.18) at fusion then disappears and the internal structural networks reorganize to form a continuous structure oriented along the muscle fibre axis (Fulton *et al*., 1981). Myoblasts that are still proliferating also form an almost continuous surface lamina. These proliferating myoblasts are typically short, bipolar cells with ruffled or knobbed tips (Figure 5.13 & 5.15). When cells prepare to fuse, they have a sparse skeletal structure, lightly cross-linked and nearly empty, with a few major filamentous cables that terminate the cell periphery. The morphology and surface lamina of postproliferative myoblasts show marked specialization, as they take on a new morphology as they prepare to fuse and form multinucleated myotubes, becoming elongated and more spindle-like. One or both tips have a complex ruffled and knobbed configuration; the other end may be pointed. The remainder of the plasma membrane appears relatively smooth (Fulton *et al*,. 1981).

Fulton *et al*., 1981, investigated myoblasts from 12 day chick embryo breast muscle. Upon detergent extraction, many large opening or lacunae were seen in the surface lamina of the postproliferative myoblast. The extremities of the postproliferative myoblast framework have largely collapsed and the surface lamina in these regions has a very discontinuous, reticulate appearance. An extracted tip showed the typical fibrillar substructure underlying the lacunae, prominent fibrous structures were seen where the surface lamina was absent. The lacunae in the surface lamina of the postproliferative myoblasts were very likely related to the formation of cell-to-cell junctions during fusion and were found principally in regions where junction formation was expected. The lacunae in postproliferative myoblasts disappear quickly after fusion and the lamina becomes almost entirely continuous. Because the surface lamina is formed by plasma membrane proteins, these lacunae indicated that myoblasts organize plasma membrane proteins in an exceptional and characteristic way. Fulton *et al*., 1981, showed that these lacunae were not formed by extensive loss of surface protein, and suggested that the

lacunae in the surface lamina corresponded to regions deficient in lectin binding protein that are presumably lipid-rich domains in the plasma membrane.

Changes in surface morphology were observed in newly formed chick myotubes by Masuko *et al*., 1983. The surface over the nucleus is smooth whereas the surface in perinuclear regions has become broad flat excrescences, microvilli, and small spherical protrusions. These surface features become less prominent as the myotubes mature, and spherical protrusions and microvilli are widely distributed on the cell surface of striated myotubes (Masuko *et al*., 1983). Myoblasts arrested at fusion in the study by Masuko *et al*., 1983, had a relatively smooth surface resembling that of cells in the G_1 phase of the cell cycle. Since myogenic cell fusion occurs during the G_1 phase of the cell cycle (Okazaki *et al*., 1966 and O'Neill *et al*., 1972), this relatively smooth surface may be characteristic of cells capable of undergoing fusion that have not yet entered the fusion process (Masuko et *al*,. 1983). Huang *et al*., 1978 found that calcium-deficient medium (160μM) inhibits fusion of chick myoblasts from chick embryonic breast muscle cells. Subsequent to the addition of the medium, they found that the deficiency in calcium augments the proportion of long processes in the culture and inhibits the pulling together of the cells, thus making it difficult to draw conclusions on the state of fusion.

Ion channels are proteins, forming transmembrane pores in biological cell membranes. Opening and closing of the pores regulate the ion currents through the membrane, and consequently vital bodily functions from hormonal homeostasis to cognition (Elinder *et al*., 2007). The ubiquitous presence of ion channels among cells of unicellular and multicellular organisms suggests their importance in maintaining cellular integrity (Laniado *et al*., 1997). Ion channels are classified broadly by the principal ion they carry (Sodium, Potassium, Calcium, Chloride) and the mechanisms by which they are opened and closed. Changes in membrane voltage or concentrations of intracellular ions and molecules such as calcium and ATP can also open ion channels (Laniado *et al*., 1997). Stimuli activating channels are multifarious; channels are opened chemically by ligands such as neurotransmitters, calcium ions, and cAMP; mechanically by stretching the membrane; or electrically by changing the transmembrane voltage. The detailed molecular mechanisms of these opening processes are poorly understood (Elinder *et al*., 2007).

The membrane stabilizing property of CoQ10 has been postulated to involve the phospholipid-protein interaction that increases prostaglandin (especially prostacyclin) metabolism. It is thought that CoQ10 stabilizes myocardial calcium-dependent ion channels and prevents the depletion of metabolites essential for ATP synthesis (Shinde *et al*., 2005). It has also been shown to help preserve myocardial sodium-potassium adenosine triphosphatase activity and stabilize myocardial calcium-dependent ion channels (Terao *et al*., 2006). The results of a study by Okamoto *et al*., 1995, suggested that one of the causal mechanisms of muscular injury is an increase in calcium concentration, due to the excess entry of extracellular calcium, and that CoQ10 can protect skeletal muscle cells against such undesirable biochemical changes (Okamoto *et al*., 1995). Crane, 2001, reported the participation of the quinine in oxidation of thiol groups on growth factor receptors or membrane ion channels, and gave the example of ryanodine receptors, controlled by calcium release which may also be related to oxygen sensing (Crane, 2001). Crane, 2001, also indicated the role of Coenzyme Q in proton movement, indicated at the plasma membrane. In this situation Coenzyme Q is involved in activation of Na^+/H^+ exchange across the membrane carried out by the Na^+/H^+ antiport. The energy for this process is based on a high concentration of Na^+ outside the cell which exchanges for protons in the cell. The Na^+ is then pumped out of the cell by the Na^+/K^+ ATPase which obtain energy from ATP. During this ATP action excess Na^+ is released so the cell develops an inside negative membrane potential which is important for many cellular functions and transport action (Crane, 2001).

a)

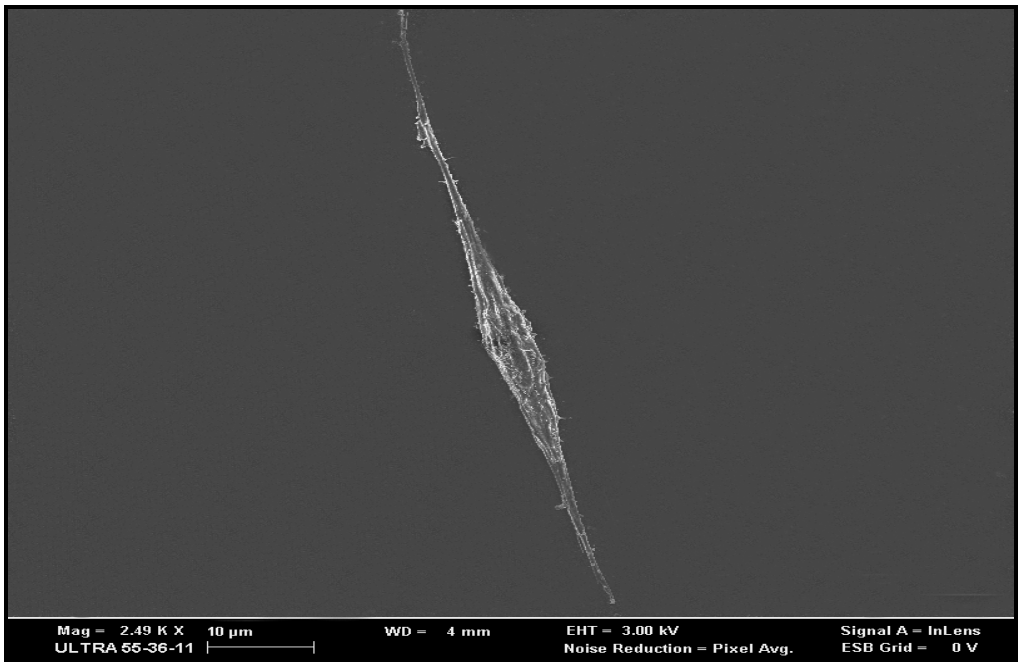

b)

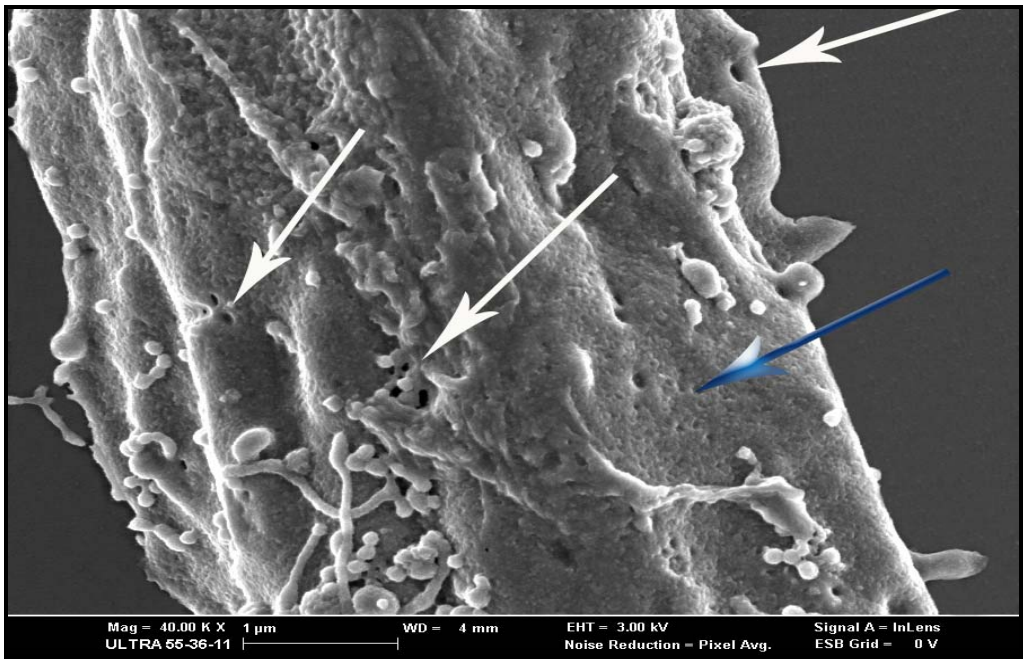

Figure 5.20: Skeletal muscle cells exposed to 0.02mg/ml CoQ10. **a**): An intact spindle-shaped cell with extending bipolar ends. **b**): The membrane surface is relatively smooth and intact (blue arrow), with rough patches. Numerous ion channels can be seen (thick white arrows).

a)

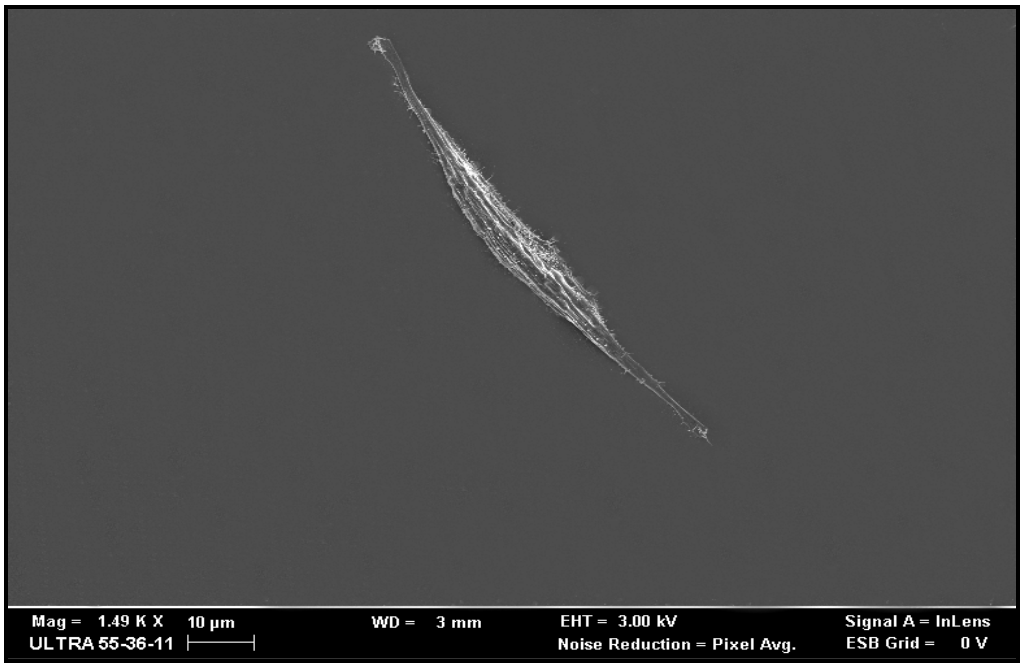

b)

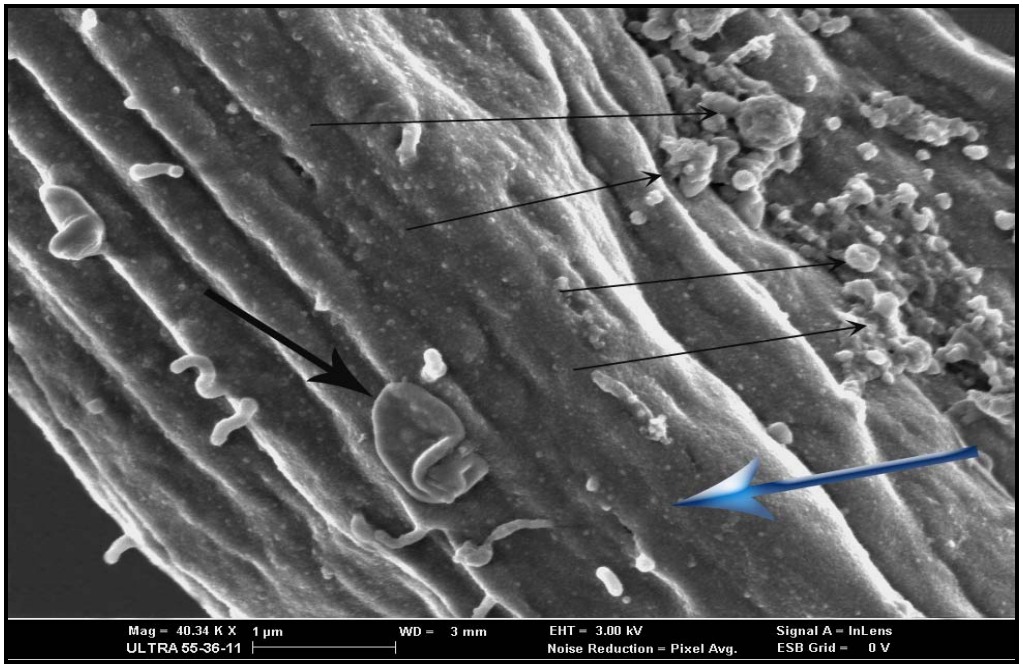

Figure 5.21: Cardiac muscle cells exposed to 0.02mg/ml CoQ10. **a**): A perfectly intact cardiac muscle cell at low magnification. **b**): The membrane is intact and smooth (blue arrow). Protein precipitations (thin black arrows) and artefacts (thick black arrow) are present.

a)

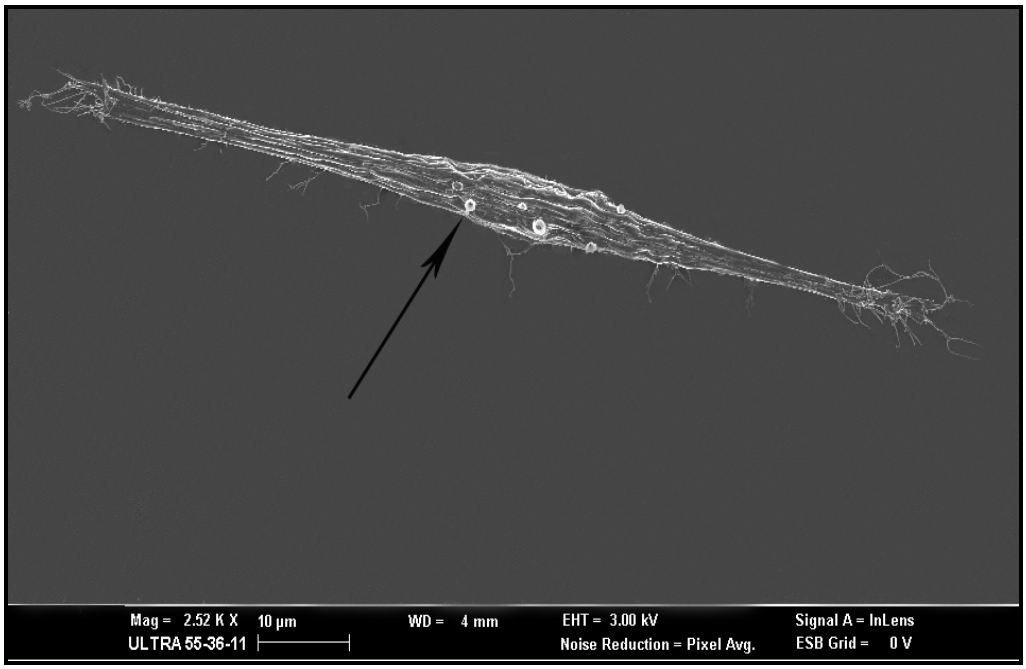

b)

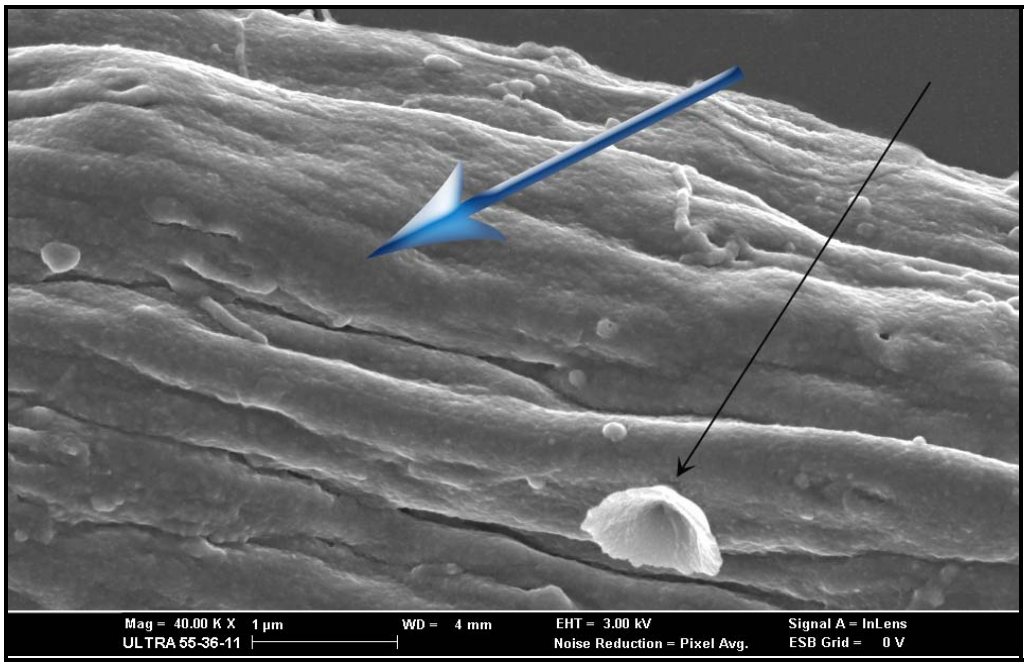

Figure 5.22: Skeletal muscle cells exposed to 0.01mg/ml CoQ10. **a**): Intact skeletal muscle cell with bipolar ends. **b**): The membrane surface appear smooth and intact (blue arrow). Ruthenium artefact is present (thin black arrow).

a)

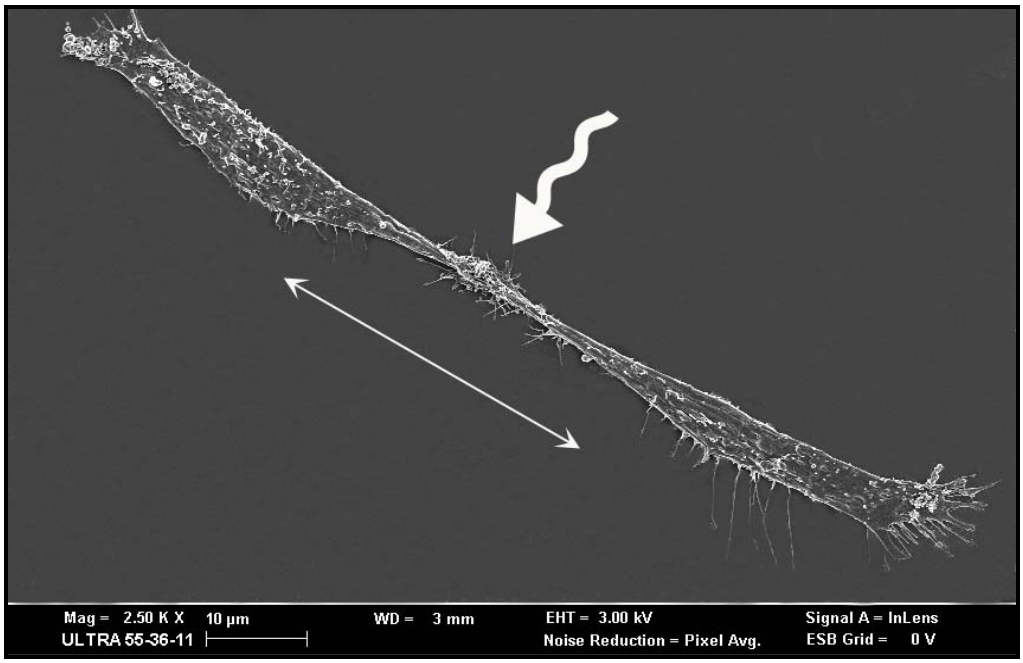

b)

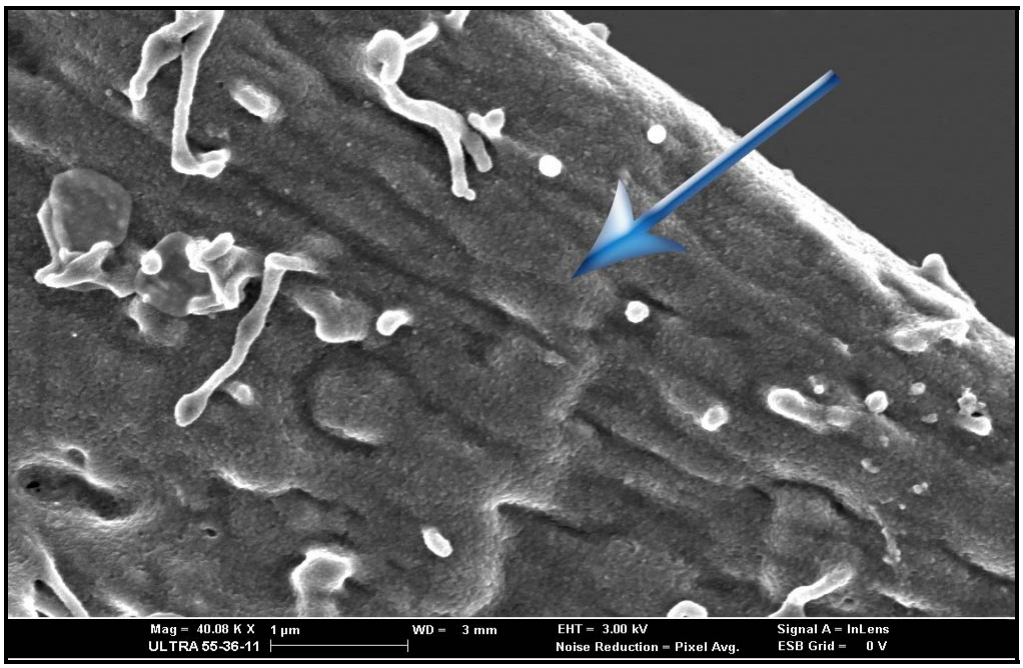

Figure 5.23: Cardiac muscle cells exposed to 0.01mg/ml CoQ10. **a**): Two fusing myoblasts. **b**): A smooth intact membrane surface (blue arrow).

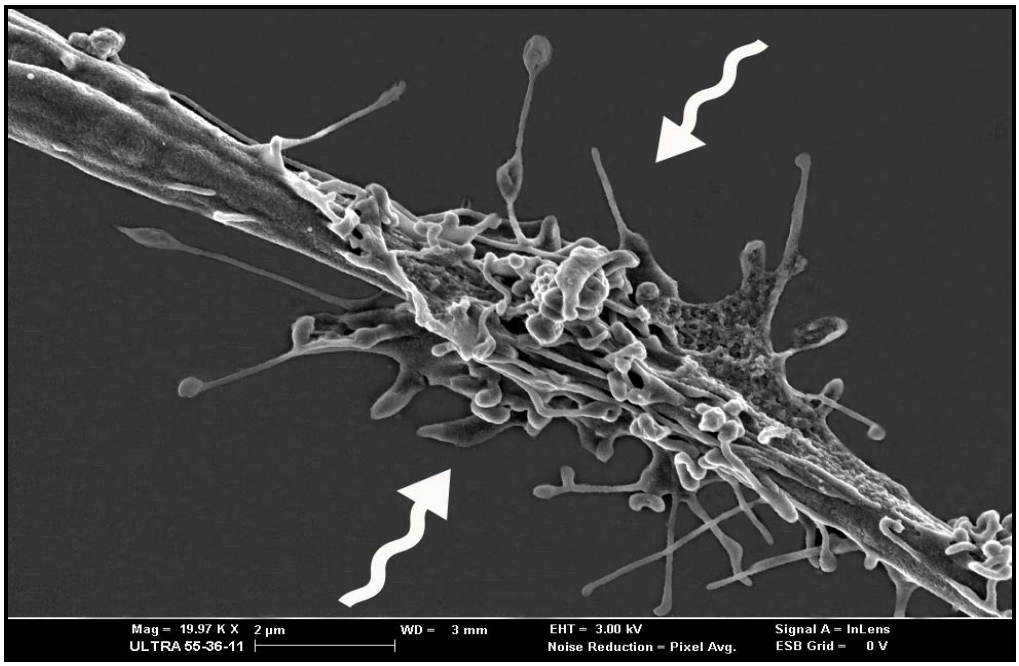

Figure 5.24: The connection between the two myoblasts in Figure 5.22 **a**. The interaction of these microprocesses with each other, or with cell bodies, establishes a connection between the cells resulting in the union of their respective filamentous systems. Presumably the microconnection between two cells develops into a cytoplasmic bridge which facilitates the integration of the filament network of both cells into a syncytium (Singer *et al*., 1984).

5.3.4 Cells Exposed to Triton X-100 after Pre-treatment with CoQ10

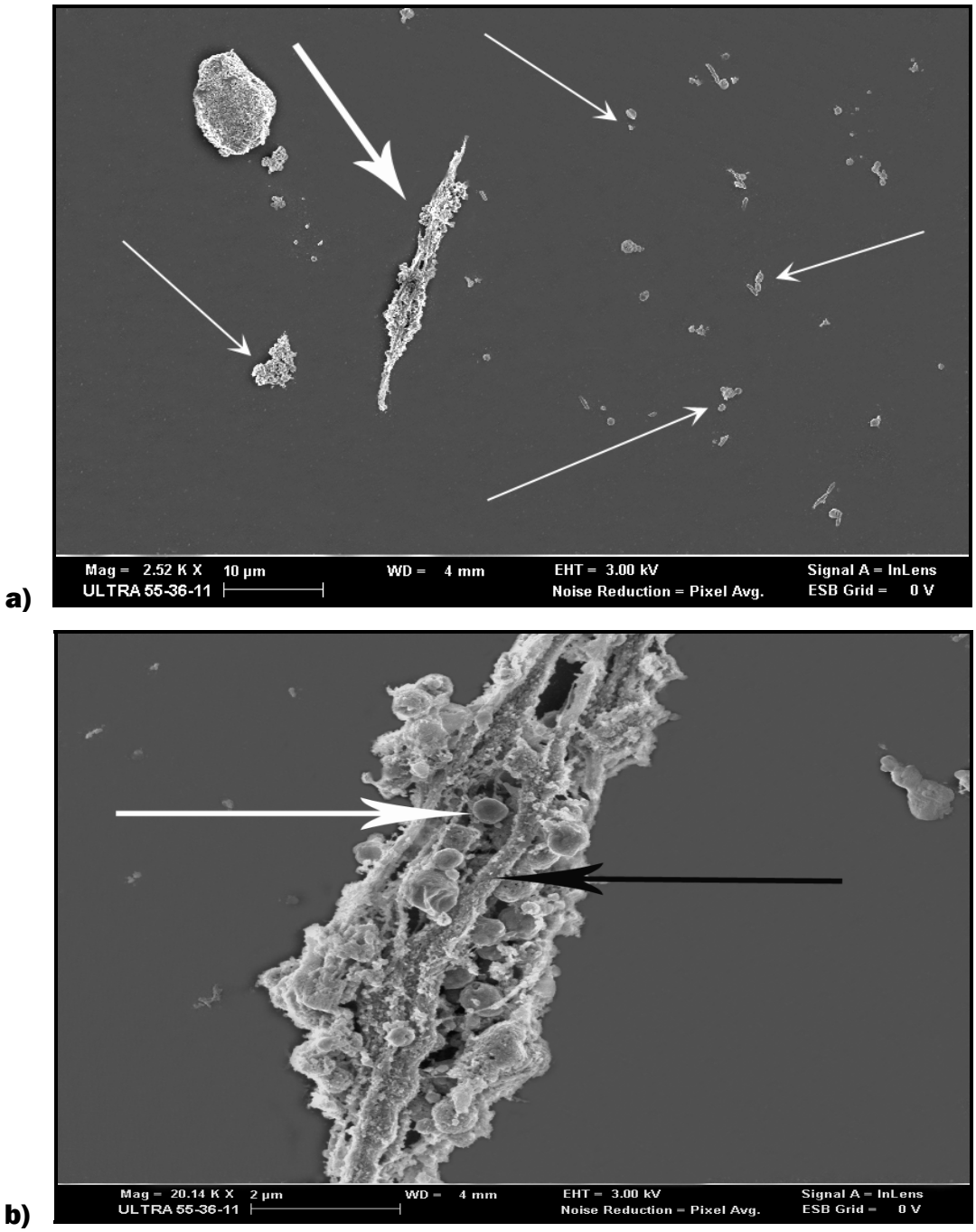

Figure 5.25: Cardiac muscle cells exposed to 0.05% Triton X-100 two hours after treatment with 0.2mg/ml CoQ10. Complete membrane lyses were seen. **a**): Part of a cell (thick white arrow) and cell debris (thin white arrows). **b**): Cytoskeleton exposed (arrows indicate the circular and cable protein structures which are insoluble to Triton X-100).

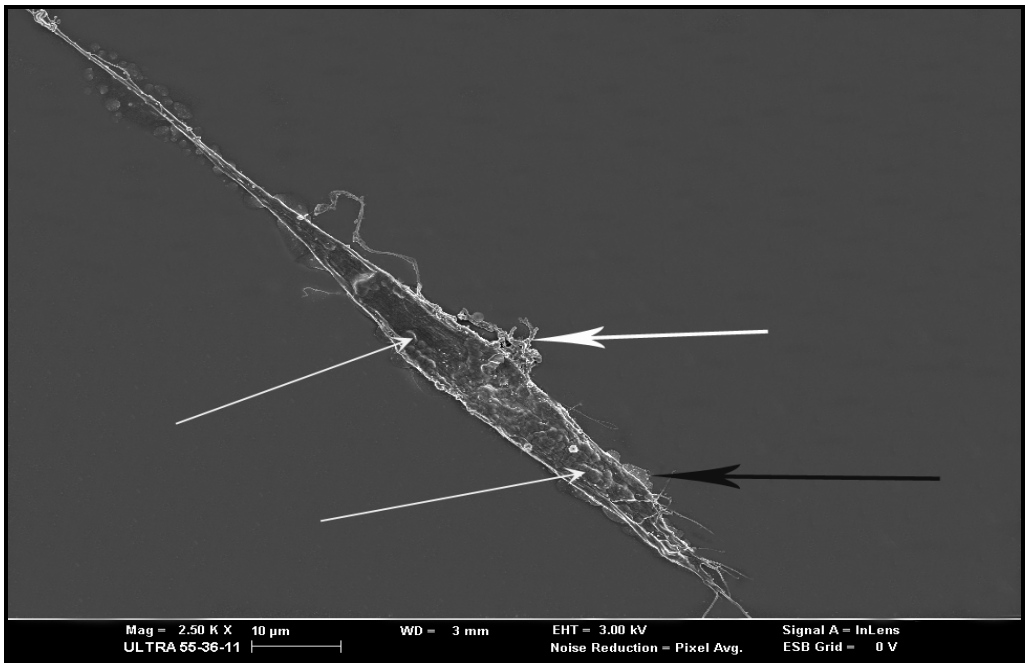

a)

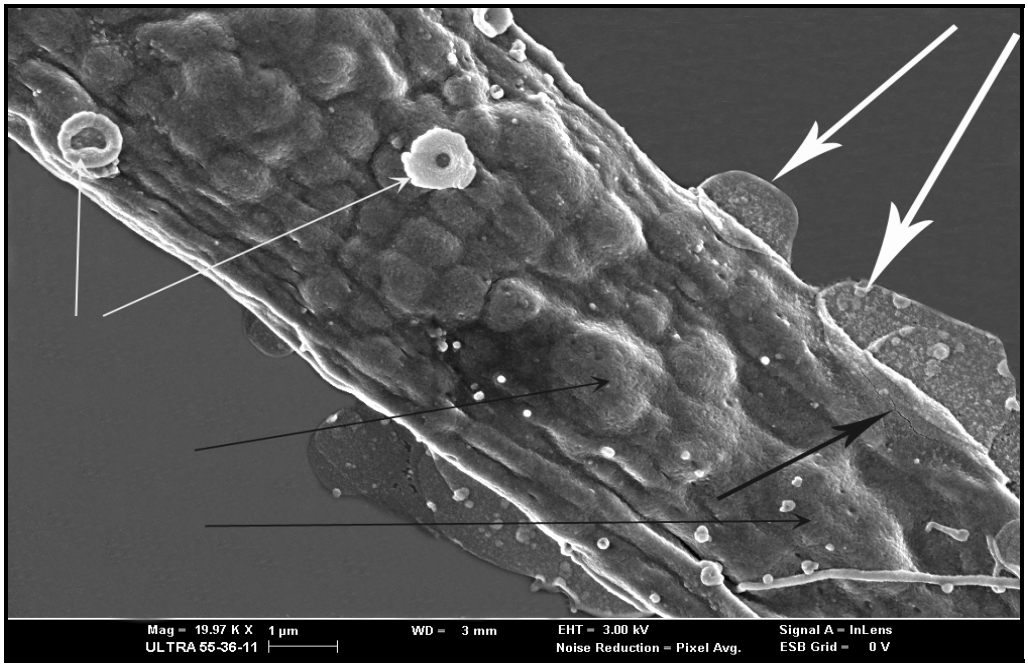

b)

Figure 5.26: Skeletal muscle cells exposed to 0.05% Triton X-100 two hours after treatment with 0.2mg/ml CoQ10. **a**): Low magnification shows membrane blebbing (thin white arrows), leakage of cytoplasmic constituents (thick white arrow & thick black arrow). **b**): Higher magnification clearly shows membrane blebs (thin black arrows) due to apoptotic changes in the cell, cytoplasmic constituents leaking through a possible rupture in the membrane (thick black & white arrows). Ruthenium artefacts (thin white arrows).

a)

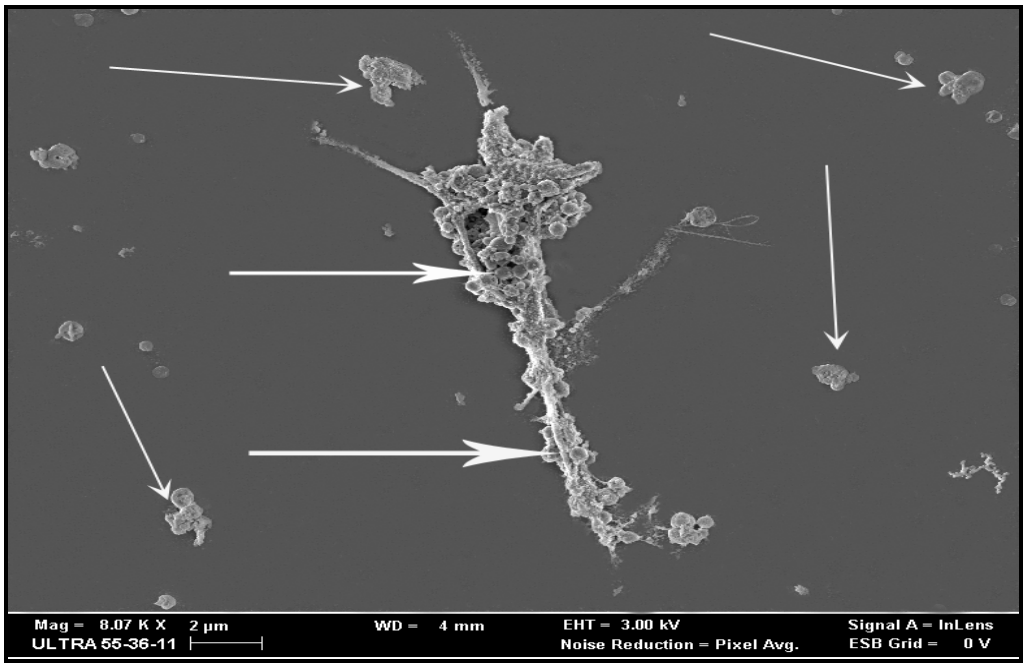

b)

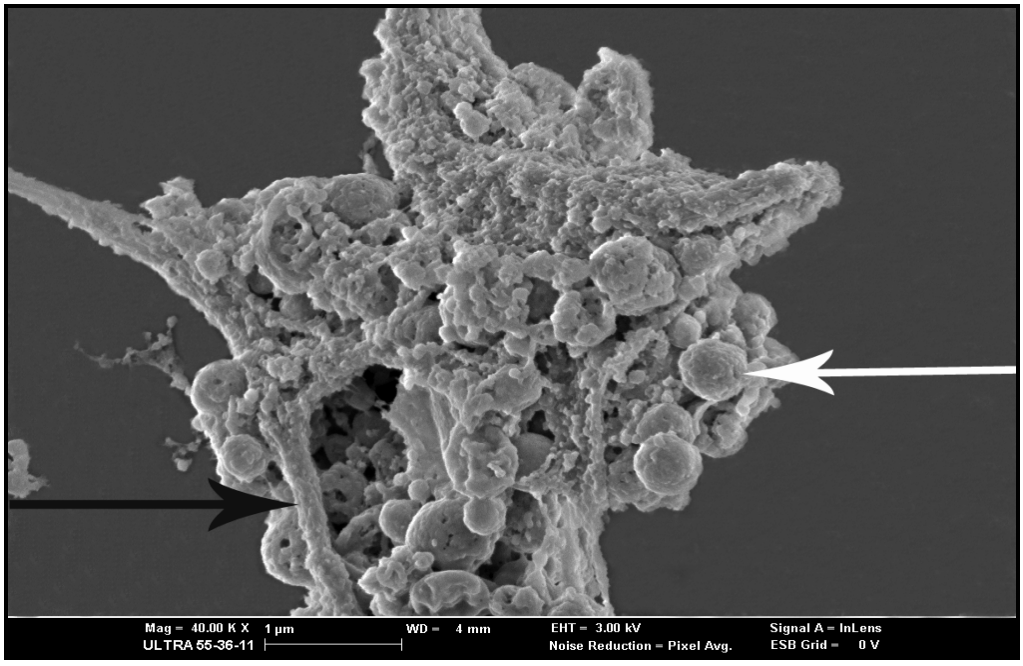

Figure 5.27: Cardiac muscle cells exposed to 0.05% Triton X-100 after pre-treatment with 0.1mg/ml CoQ10. **a**): Low magnifications shows a part of a cell (thick white arrow) and cellular debris (thin white arrows) lying around. **b**): The cell membrane is completely lysed. Insoluble proteins of the cytoskeleton (filament bundles or cables as described by Fulton *et al*., 1981 and acetylcholine receptor protein clusters as described by Connoly, 1984) are exposed (indicated by thick black and white arrows).

a)

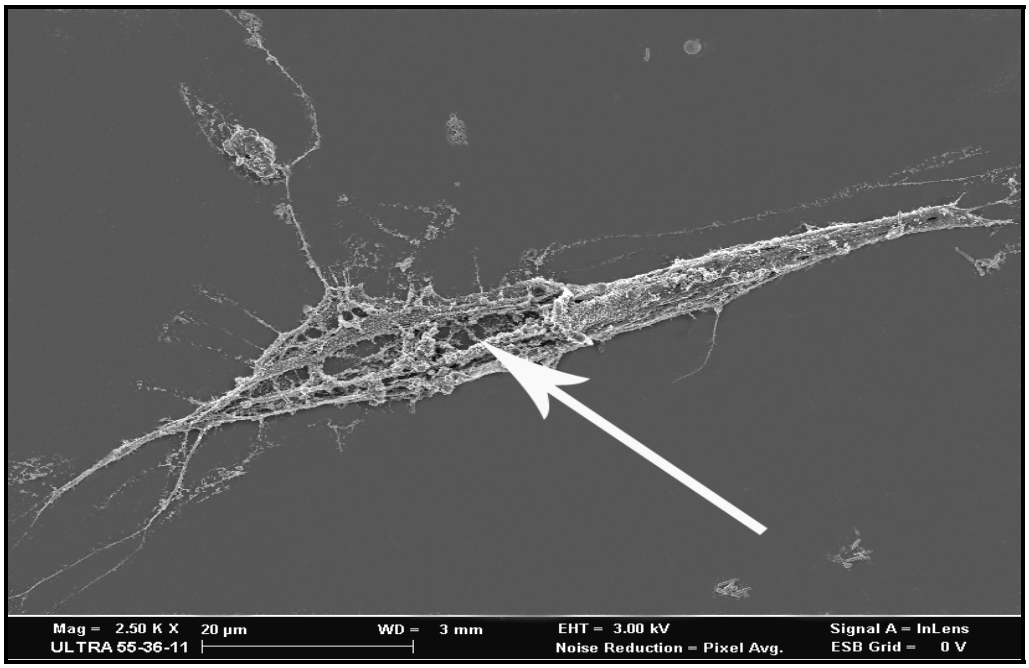

b)

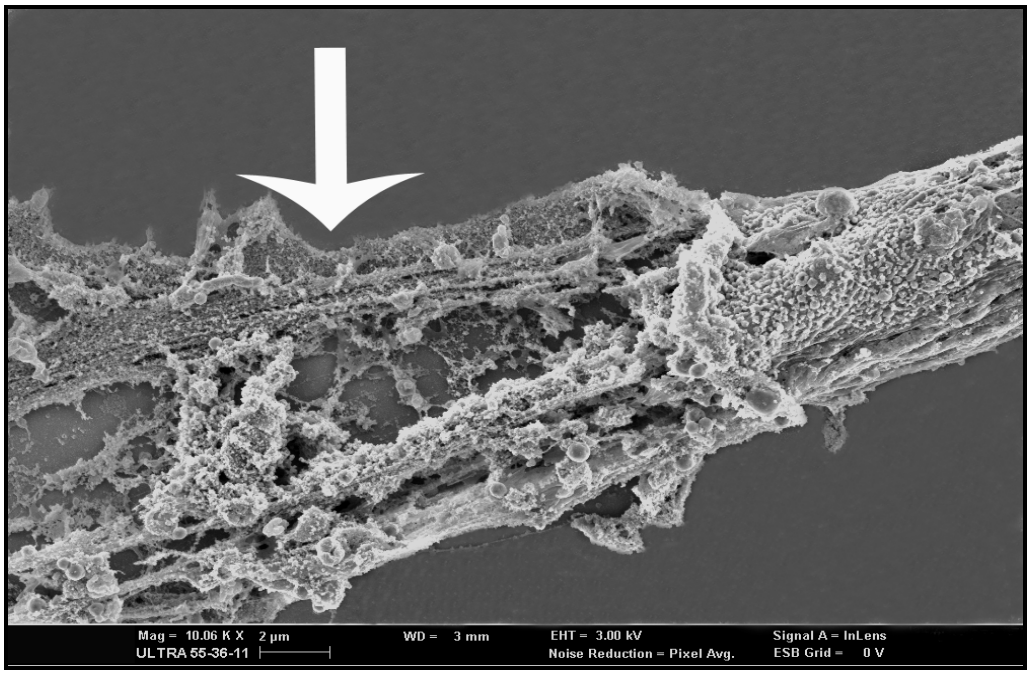

Figure 5.28: Skeletal muscle cells exposed to 0.05% Triton X-100, after being pre-treated with 0.05mg/ml CoQ10. **a**): A cell with bipolar ends and extending microprocesses. Half of the cell is still surrounded by the surface lamina, but the membrane is lysed. **b**): Major filament bundles or cables extending from deep within the cytoplasmic structure to the outer cell periphery traversing large, nearly empty regions (Fulton *et al*., 1981).

a)

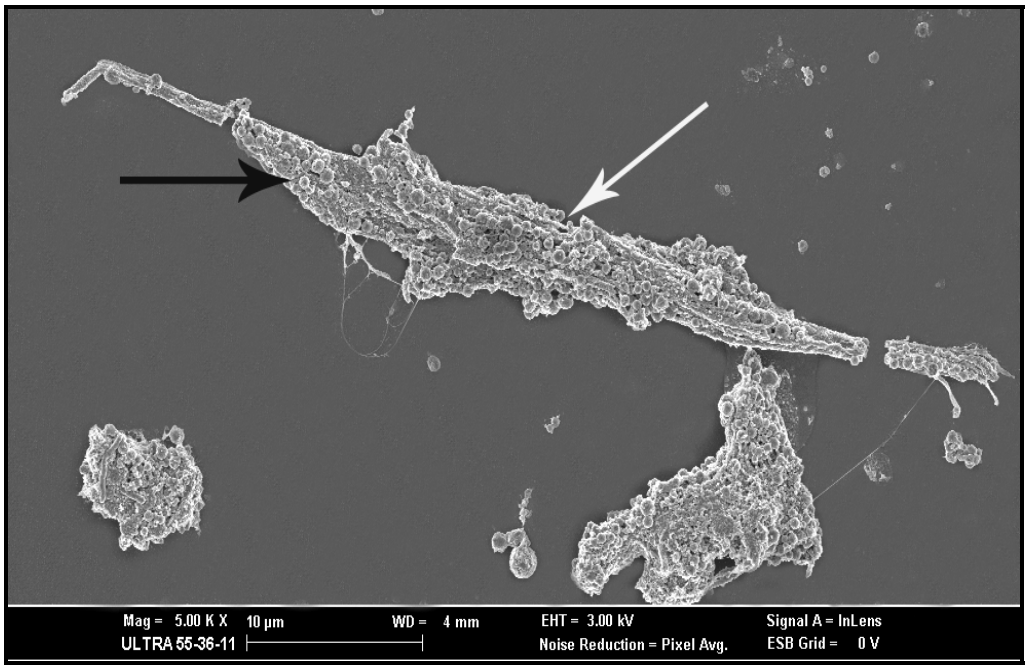

b)

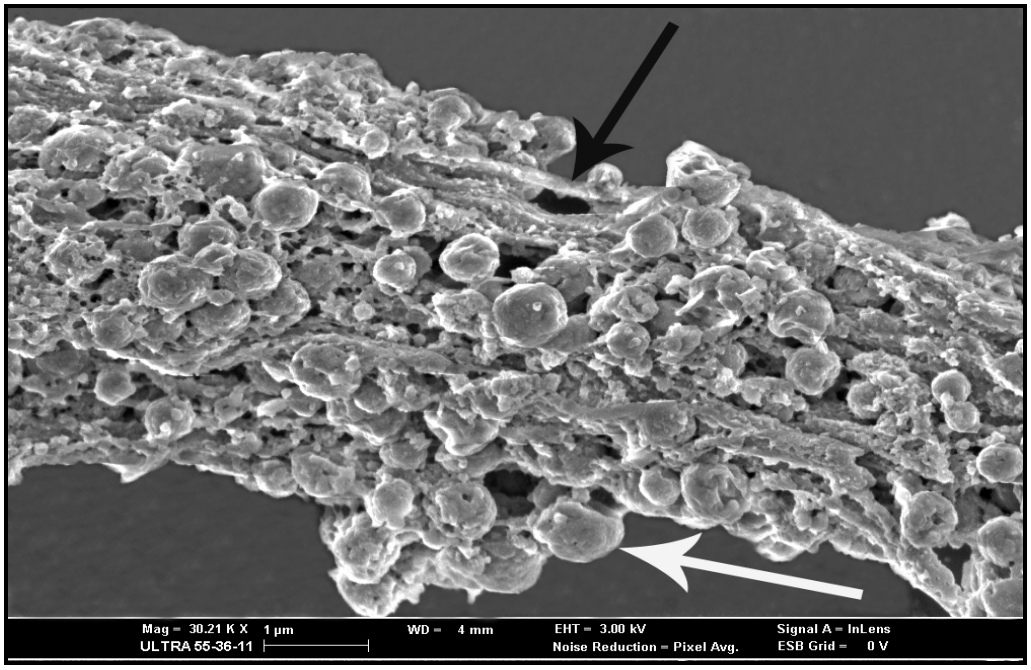

Figure 5.29: Cardiac muscle cells exposed to 0.05% Triton X-100, after being pre-treated with 0.05mg/ml CoQ10. **a**): Complete membrane lyses were seen with cell debris lying around. **b**): The filament bundles or cables (thick black arrow) described by Fulton *et al*., 1981. The circular structure indicated by the white arrow is protein constituents of the cytoskeleton, possibly acetylcholine receptor clusters described by Connoly, 1984, insoluble to Triton X-100.

Notable structures in the postproliferative myoblast are the major filament bundles or cables extending from deep within the cytoplasmic structure to the outer cell periphery (Fulton *et al*., 1981). These cables (Figure 5.27 & 5.29 **b**, black arrow), traversing large, nearly empty regions (Figure 5.28 **b**), are characteristic of and always found in postproliferative myoblasts (Fulton *et al*., 1981). In myoblasts preparing to fuse, both the surface lamina and the internal networks show highly specific spatial rearrangement; in addition, the internal networks become more extractible. After fusion, both the internal networks and the surface lamina rapidly reorganize in a stable arrangement as the muscle cell begins to construct the extensive contractile apparatus, thus a critical stage in muscle development is accompanied by rapid, extensive, and transient reorganization of skeletal framework and its surface lamina (Fulton *et al*., 1981).

Before innervations of the muscle cell (both *in vivo* and *in vitro*) acetylcholine receptors are widely distributed over the surface of the myotube, but once the nerve cell contacts the myotube, there is a reorganization of the acytylcholine receptors and the clusters under the nerve process innervating that muscle cell (Connoly, 1984). Tank *et al*., 1982, found that when blebs are induced in L6 myotubes, the acetylcholine receptors in these blebbed regions are free to diffuse in the plane of the membrane, whereas receptors in intact cell membranes are much more constrained, with some fractions virtually nondiffusible. They proposed that bleb formation mechanically broke connections anchoring these receptors to the cytoskeleton (Tank *et al*., 1982). Prives *et al*., 1980 and 1982, found that the majority of acetylcholine receptors were retained on the insoluble cytoskeleton after detergent extraction of cells. Stya *et al*., 1983, found a correlation between the average mobility of acetylcholine receptors in the plane of the membrane and their extractability by Triton X-100. Both of these studies concluded that clustered receptors were attached to the cytoskeleton. The results of the study by Connoly, 1984, supported the hypothesis of the attachment of acetylcholine receptors to a submembranous cytoskeleton. They further proposed that receptor clusters are stabilized by actin-containing filaments within the cytoplasm, because existing clusters could not be destabilized with Colcemid, therefore, cluster stability is not dependent on microtubules, but the movement of receptors in the plane of the membrane (Connoly, 1984).

a)

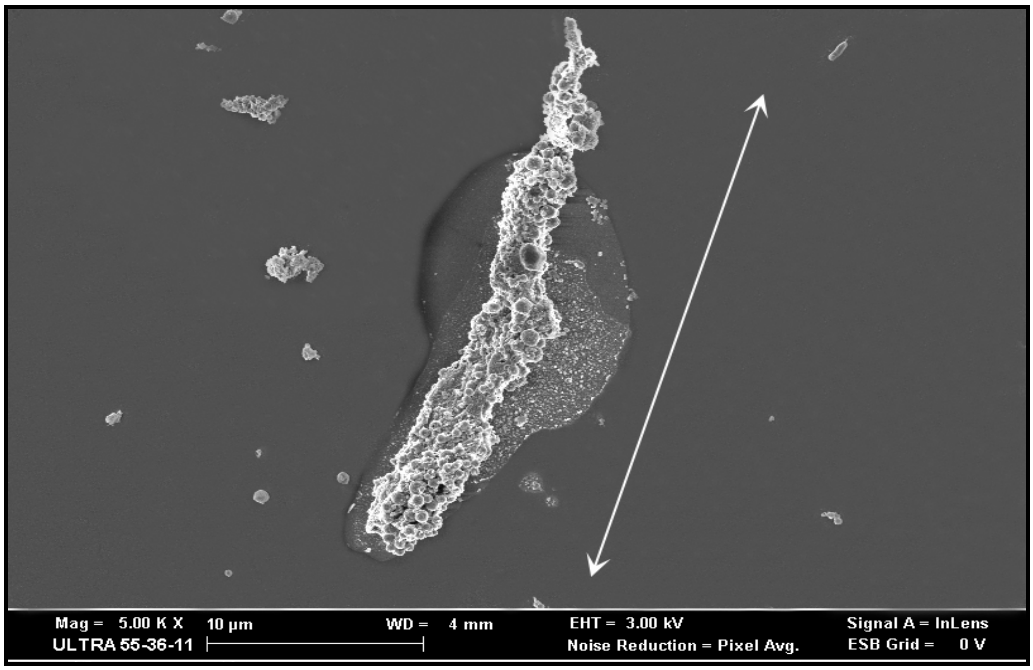

b)

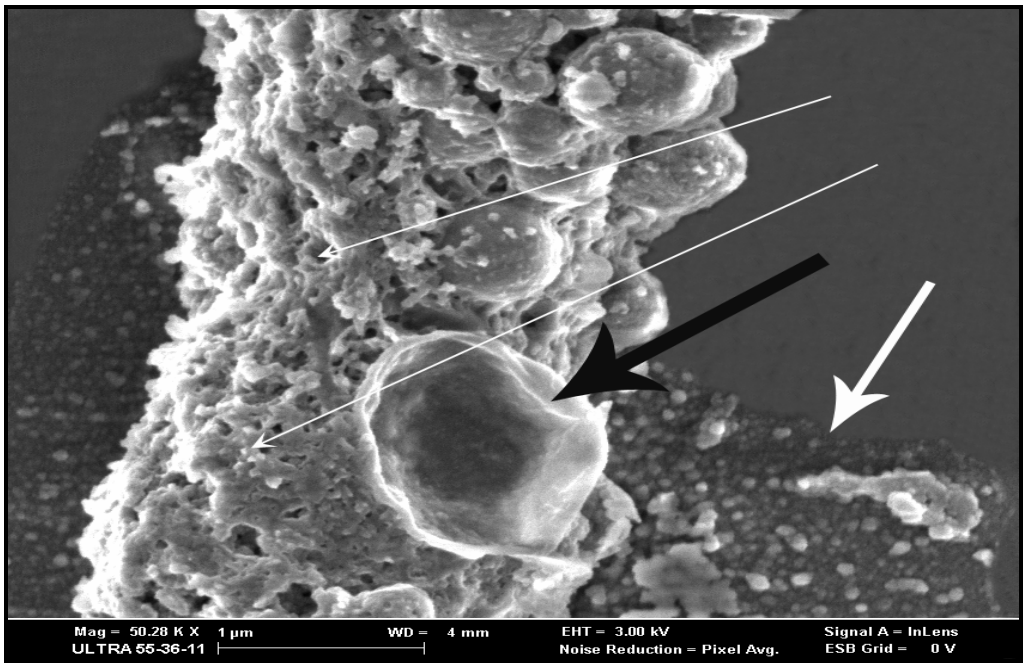

Figure 5.30: Cardiac muscle cells exposed to 0.05% Triton X-100 after 0.02mg/ml CoQ10 pre-treatment. **a**): Part of a cell with lysed membrane can be seen. Cell debris lying in the vicinity. **b**): Components (possibly a remnant of an apoptotic body or a protein cluster) of the cytoskeleton are visible (thick black arrow). Leakage of cytoplasm indicated by thick white arrow. The plasma lamina is disrupted but still present (thin white arrows).

a)

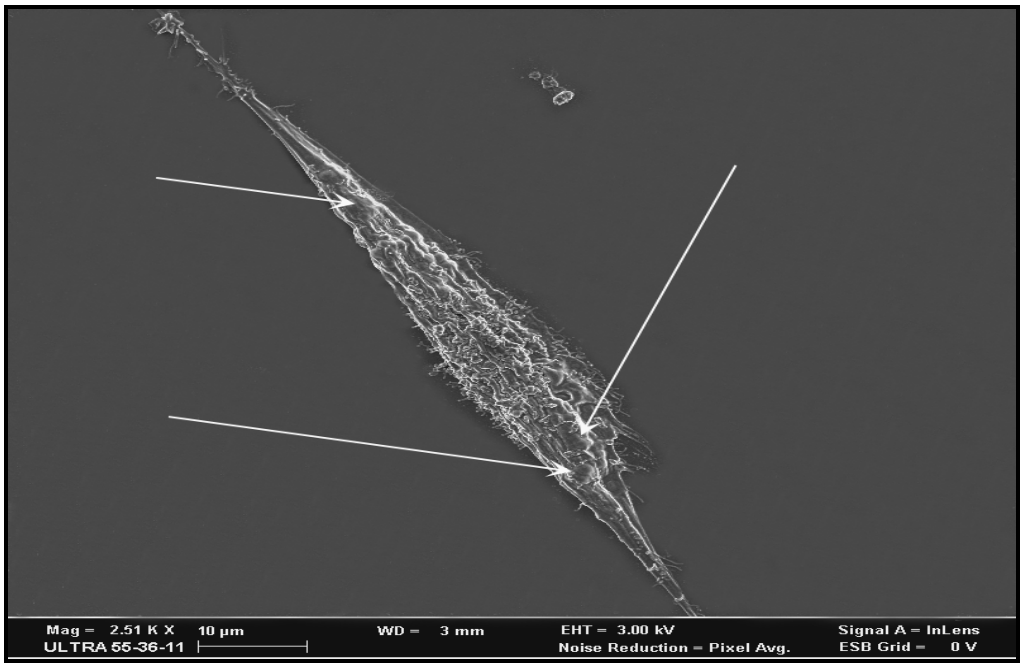

b)

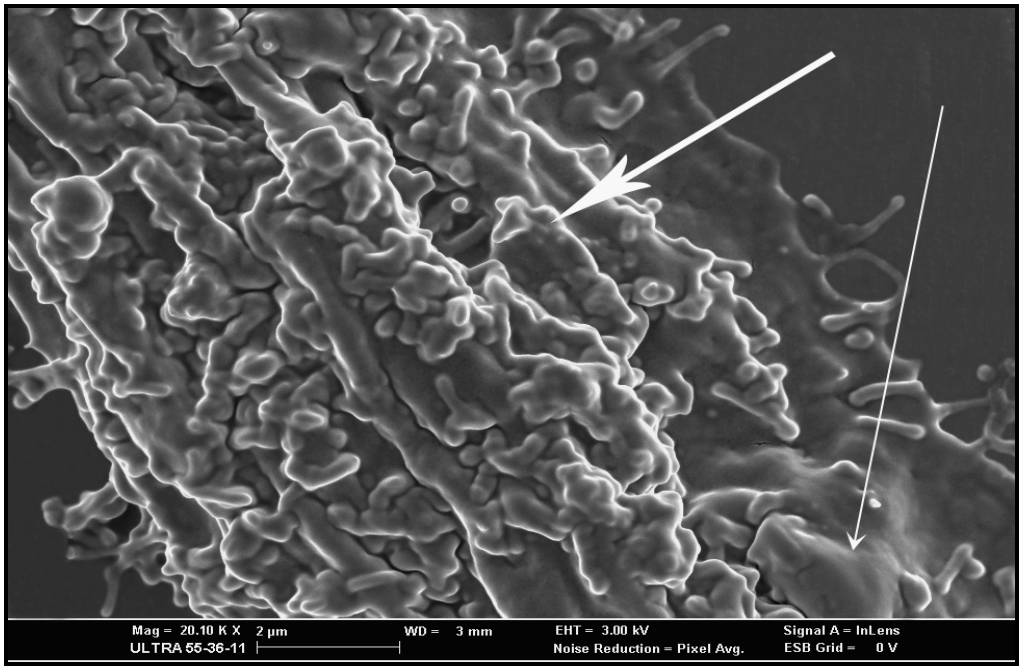

Figure 5.31: Skeletal muscle cells exposed to 0.005% Triton X-100 after pre-treatment with 0.2mg/ml CoQ10. **a**): Membrane blebs were seen at low magnification (thin white arrows). **b**): Higher magnification shows a shrunken membrane (thick white arrow) and membrane blebbing (thin white arrow), characteristic of a cell in which the process of apoptosis is present.

a)

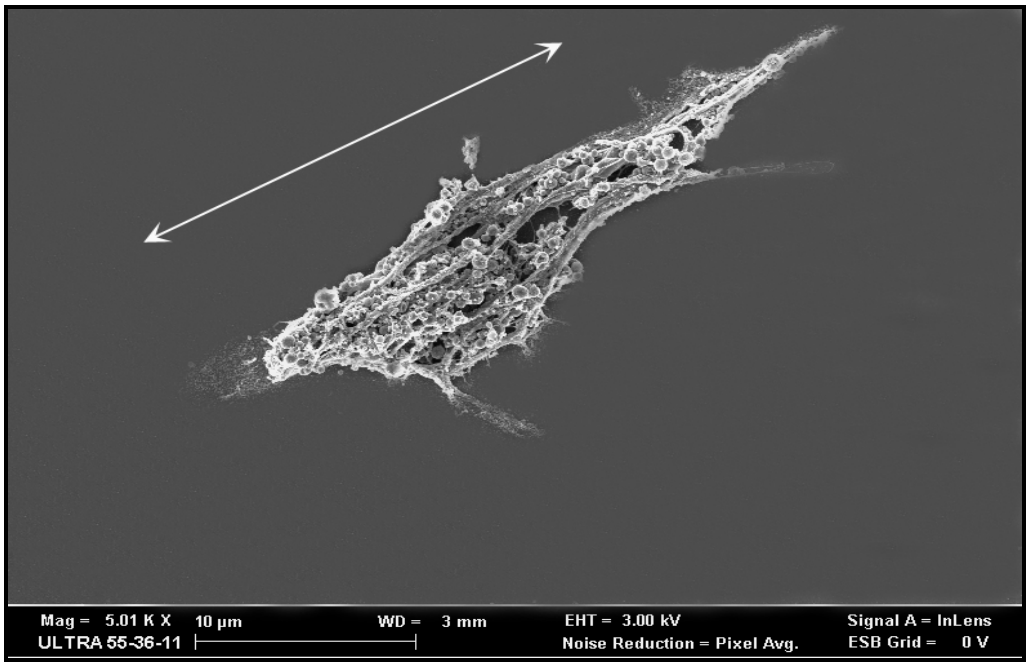

b)

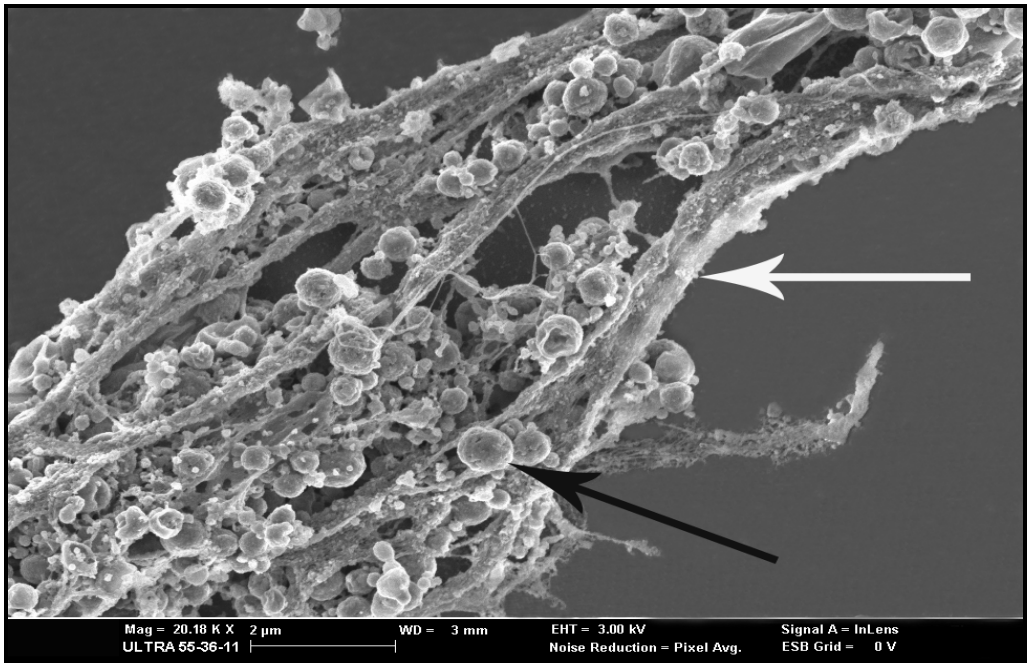

Figure 5.32: Cardiac muscle cells exposed to 0.005% Triton X-100 after pre-treatment with 0.2mg/ml CoQ10. **a**): Complete membrane lyses were seen at low magnification. **b**): Filament bundles and clusters (thick black and white arrows) traversing empty spaces can be seen at high magnification.

a)

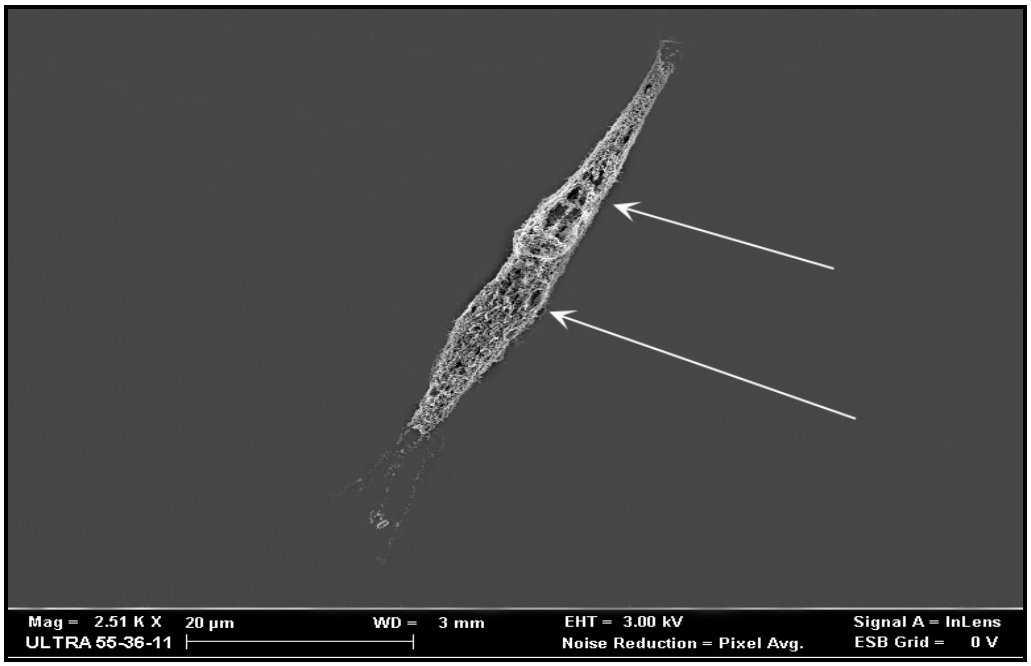

b)

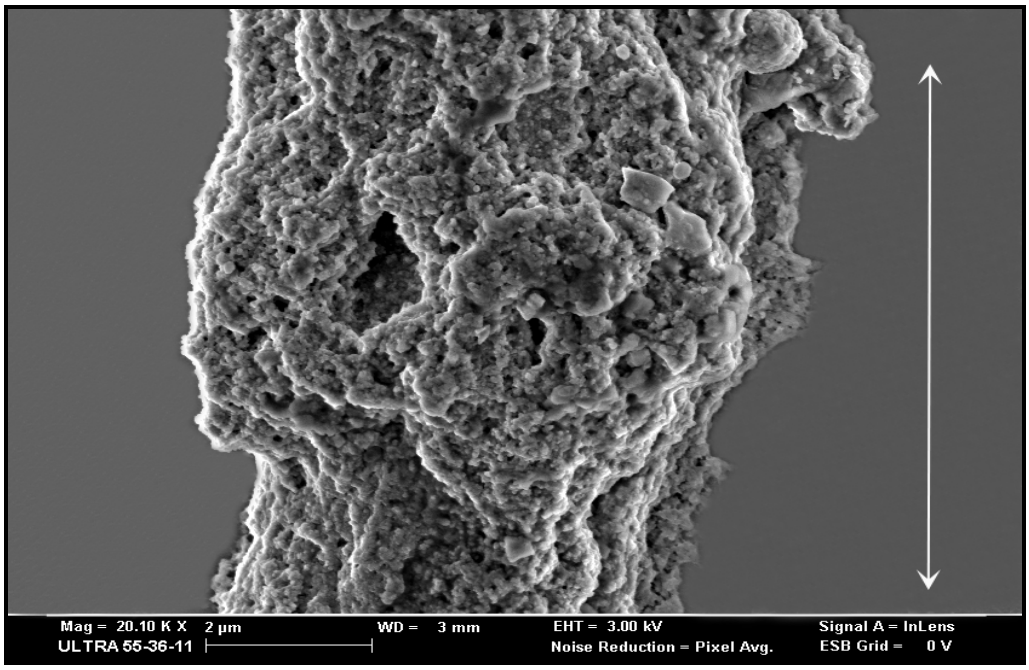

Figure 5.33: Skeletal muscle cells exposed to 0.005% Triton X-100 after pre-treatment with 0.1mg/ml CoQ10. Membrane lyses were seen. Plasma lamina were present but largely disrupted. **a**): Empty spaces (thin white arrows).

a)

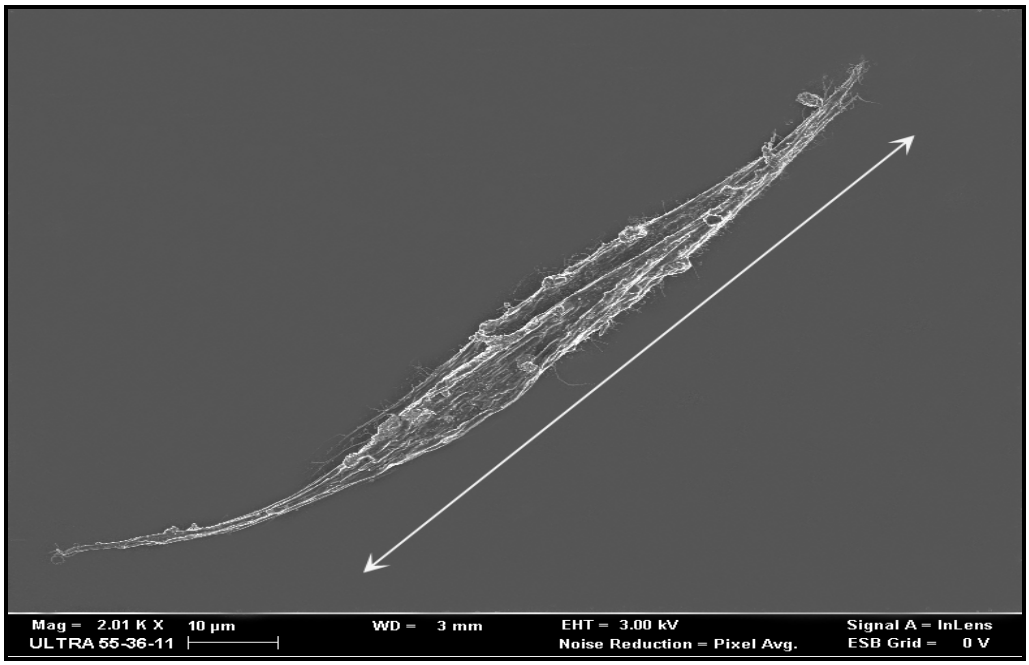

b)

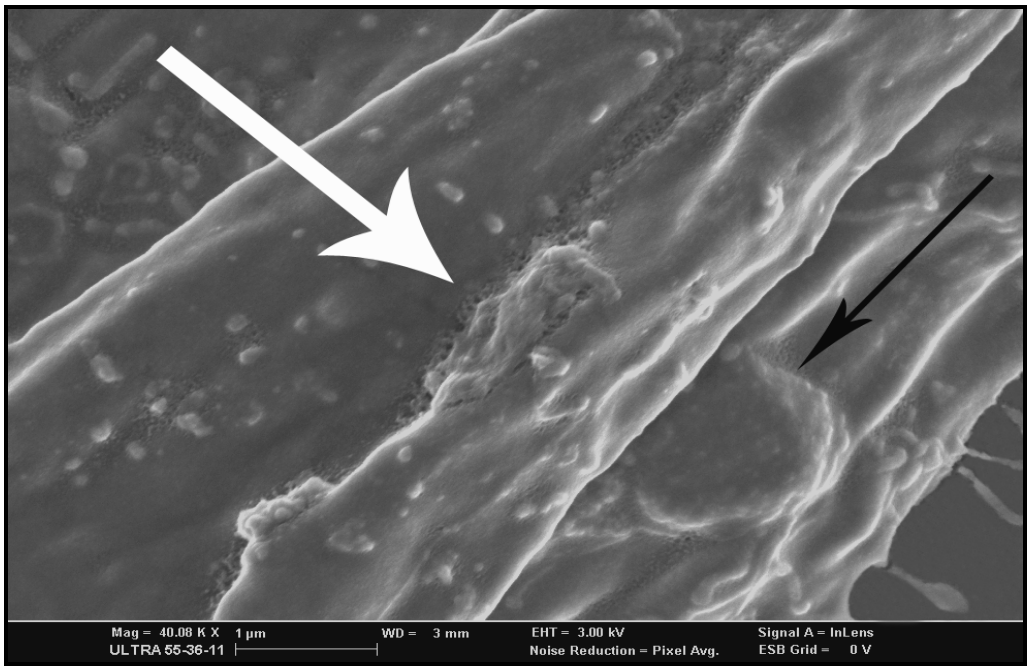

Figure 5.34: Cardiac muscle cells exposed to 0.005% Triton X-100 after pre-treatment with 0.1mg/ml CoQ10. **a**): Bipolar ends extending from the spindle-shaped cell. Cell seems largely intact. **b**): High magnification shows an intact membrane with bulging (black arrow), and a rare appearance of a "***membrane patch"*** on a part of the membrane that present more rough and slightly damaged (thick white arrow).

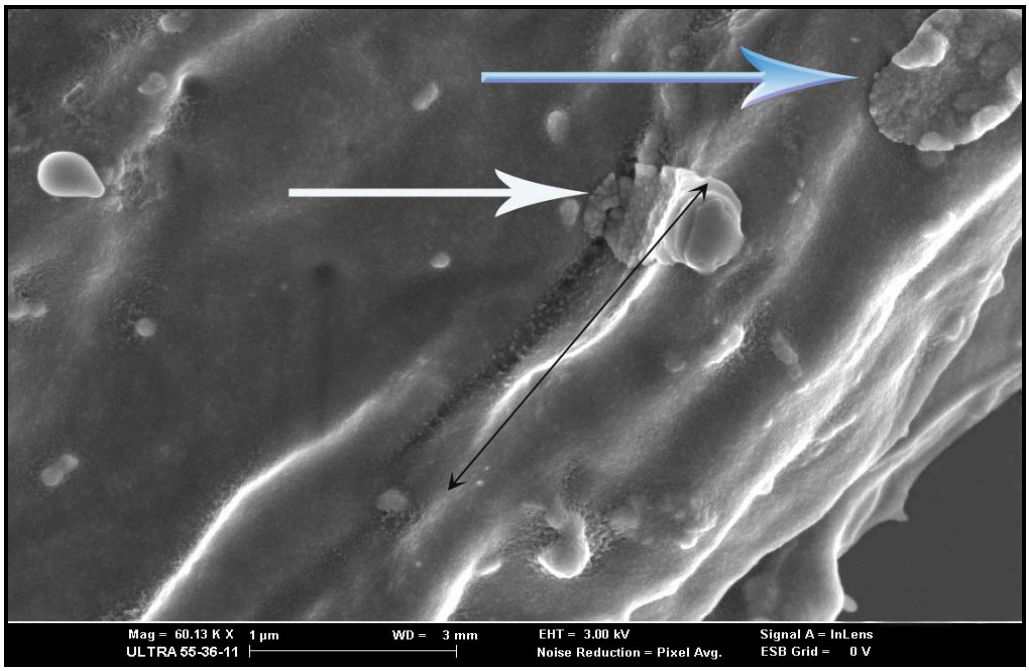

Figure 5.35: Higher magnification of Figure 5.34 **a**. The thin black arrow shows a part in the membrane that looks like a tear, on part of the tear is a patch (thick white arrow). The blue arrow indicates a patch-like formation on the surface of the cell membrane which appears to have the same structural composition as the membrane itself.

Disruption of the plasma membrane is a common event in various normal animal cells, and membrane-repair machinery is essential to prevent disruption-induced cell death. In skeletal muscle, membrane disruptions are most often observed under physiological conditions, because muscle fibres contract repeatedly and are often susceptible to varying degrees of mechanical stress. The fragility of the sarcolemma makes it unable to withstand the mechanical stress, and a defective membrane-repair easily results in necrosis of the muscle fibres (Hayashi, 2003). Membrane rupture leads to exposure of hydrophobic phospholipids to the aqueous environment, an energetically unfavourable state (Lammerding *et al*., 2007). The entropic forces that draw the membrane ends together are insufficient to reseal membrane lesions larger than 1µm in nucleated cells under physiological conditions (McNeil *et al*., 2003). Membrane tension, driven by interaction of phospholipids with the underlying cytoskeleton, slows or completely blocks self sealing (Lammerding *et al*., 2007). Instead, cells utilize an active membrane-repair process based on active trafficking of endomembrane vesicles to the damage site and subsequent fusion with the plasma membrane by exocytosis. Many of the molecular details of this process remain unclear. It appears that membrane repair involves both a

reduction in membrane tension - possibly by local depolymerization of the cortical cytoskeleton - and patch formation. In the latter process, homotypic fusion of membrane vesicles creates a patch at the rupture site that then fuses with the plasma membrane in a Ca^{2+}-dependent process (Lammerding *et al*., 2007). Depending on the cell type, the vesicular membrane compartments participating in the repair may include cortical granules, yolk granules, endocytic components, lysosomes, and enlargosomes (McNeil *et al*., 2003 and 2005). The active membrane fusion process requires several membrane proteins, including SNARE proteins, a family of transmembrane proteins essential in most intracellular membrane fusion processes, and synaptotagmins, transmembrane proteins containing two highly conserved Ca^{2+}-binding domains that are thought to serve as Ca^{2+} sensors (Giraudo *et al*., 2006). Most recently, ferlins have been identified as a conserved protein family that participate in membrane repair. The ferlin family consists of four different genes that encode dysferlin, myoferlin, otoferlin, and Fer1L4; dysferlin-null cells show accumulation of membrane vesicles near the damaged membrane (McNeil *et al*., 2003 and 2005).

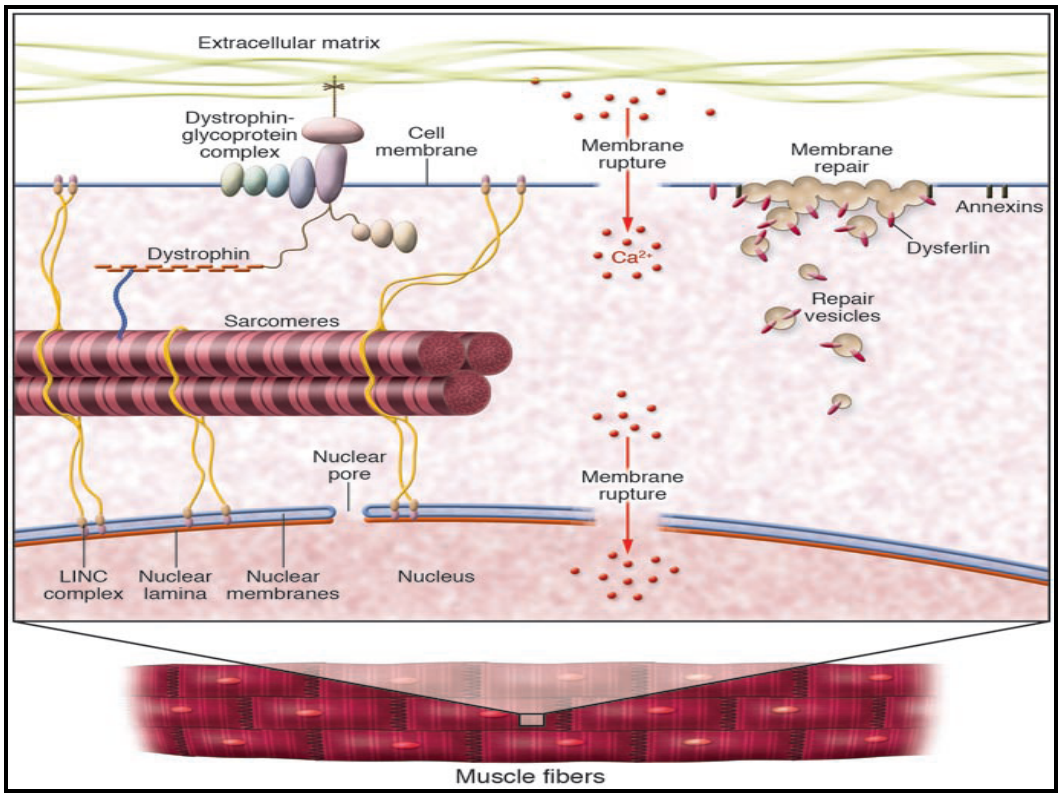

Figure 5.36: Schematic representation of the membrane repair machinery in a muscle cell as presented by Lammerding *et al*., 2007.

a)

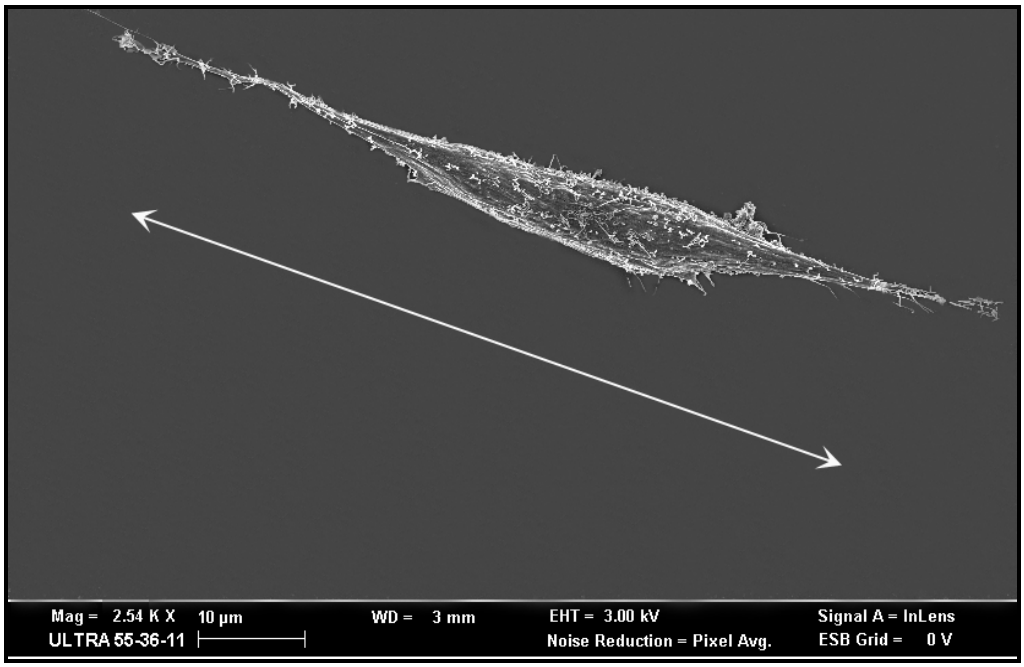

b)

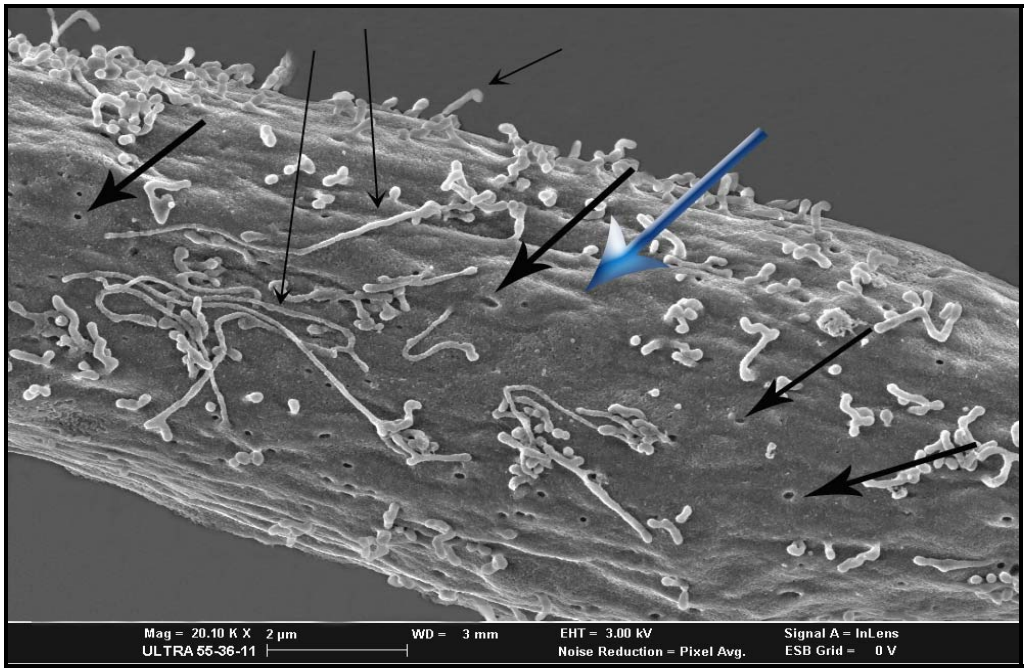

Figure 5.37: Skeletal muscle cells exposed to 0.005% Triton X-100, after pre-treatment with 0.05mg/ml CoQ10. **a**): A perfectly intact bipolar cell. **b**): Higher magnification shows and intact membrane (blue arrow) with numerous microvilli an spherical protrusions (thin black arrows), and numerous ion channels on the surface of the cell.

a)

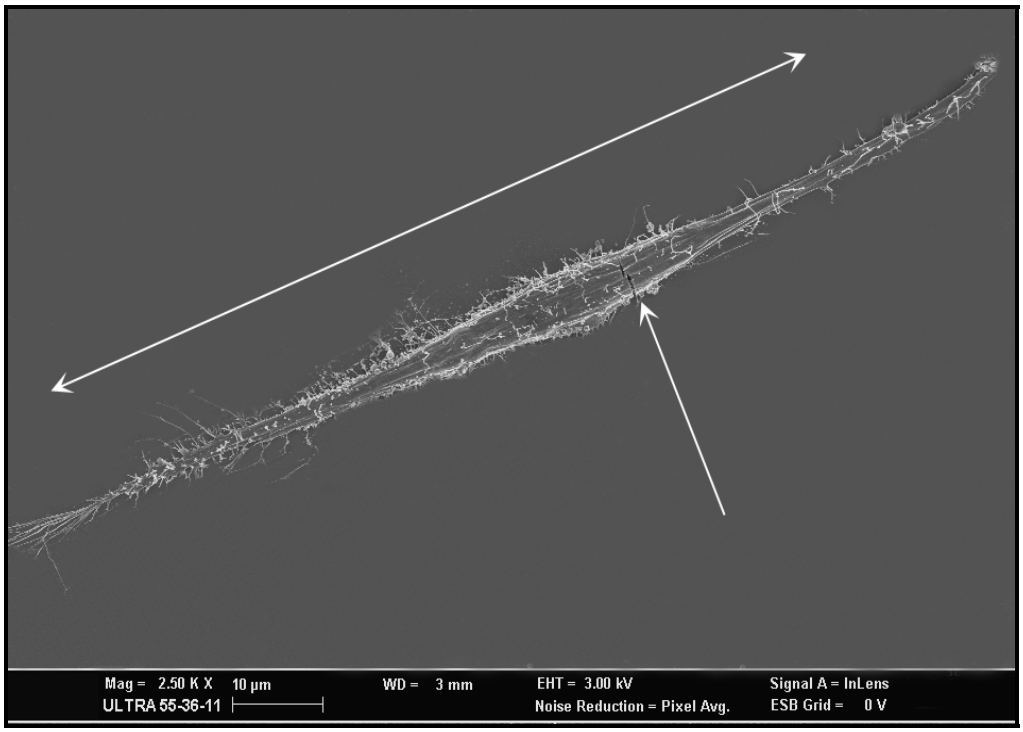

b)

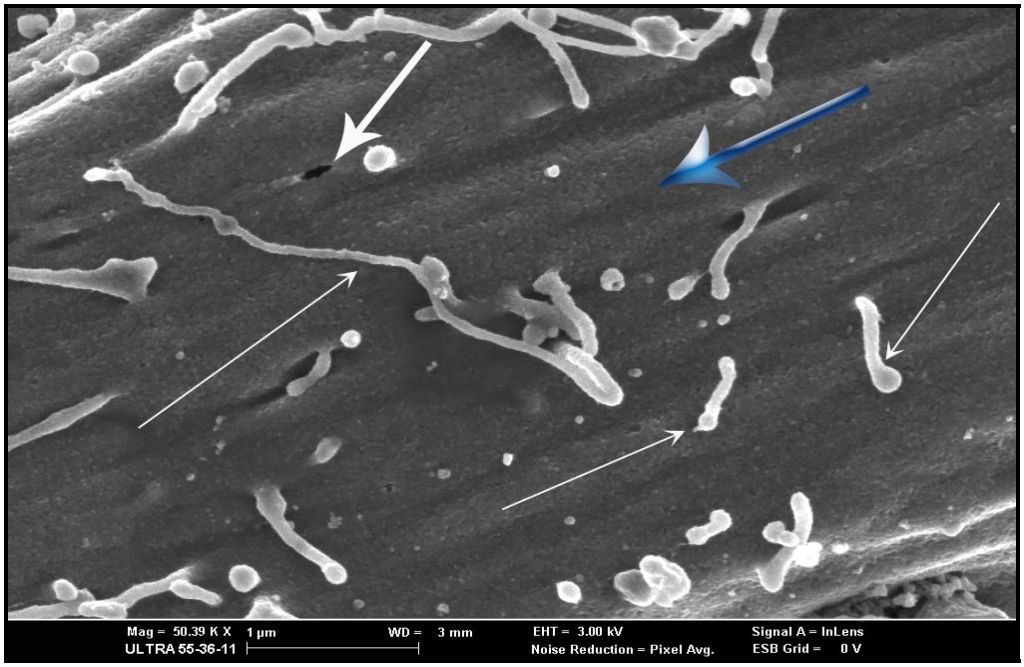

Figure 5.38: Cardiac muscle cells exposed to 0.005% Triton X-100, after pre-treatment with 0.05mg/ml CoQ10. **a**): An intact bipolar cell (double-headed arrow). Breakage of the upper tip was probably caused by critical point drying (thin white arrow). **b**): A perfectly intact membrane surface (blue arrow) with microvilli and small spherical protrusions (thin white arrows), and ion channels (thick white arrow).

a)

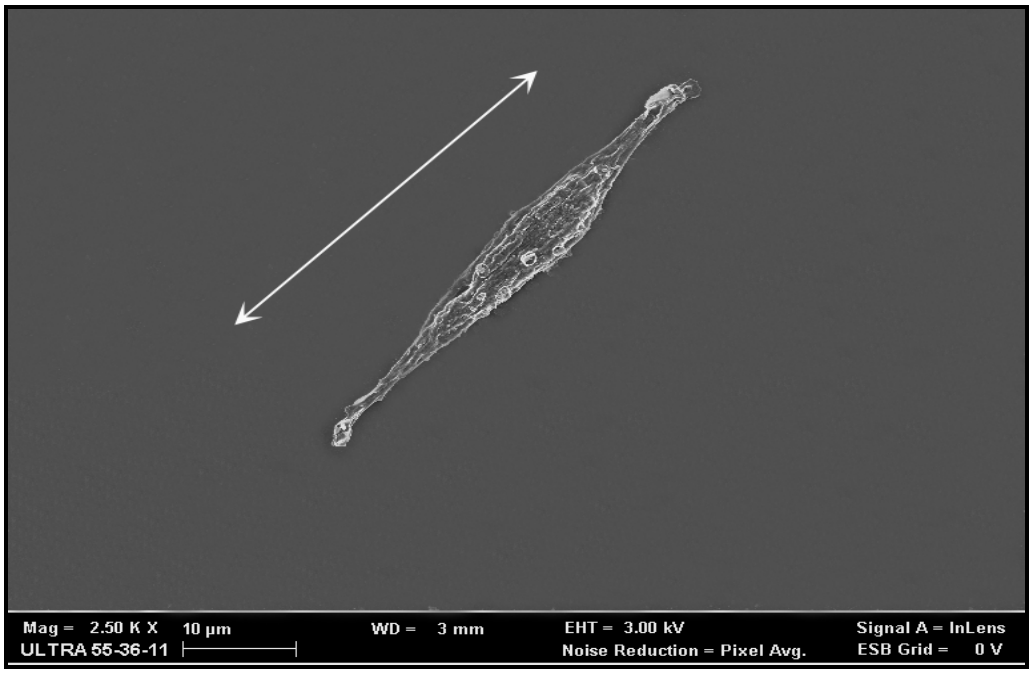

b)

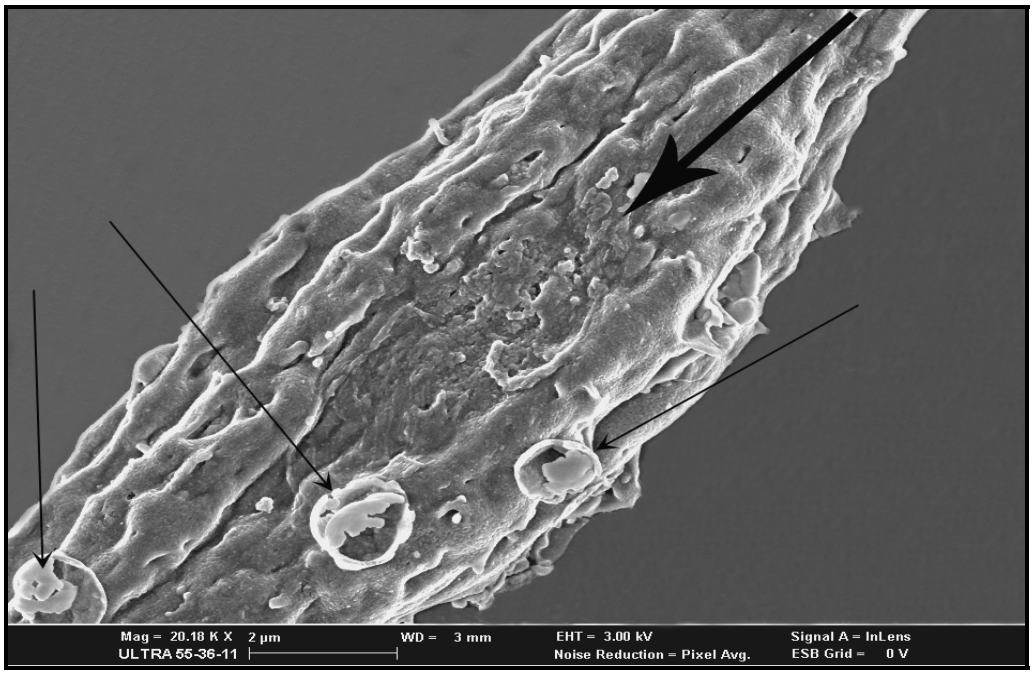

Figure 5.39: Skeletal muscle cells exposed to 0.005% Triton X-100 after pre-treatment with 0.02mg/ml CoQ10. **a**): An intact skeletal muscle cell. **b**): Cell membrane has a rough patch (thick black arrow), but seems largely intact. Presence of ruthenium artefacts were noted (thin black arrows).

a)

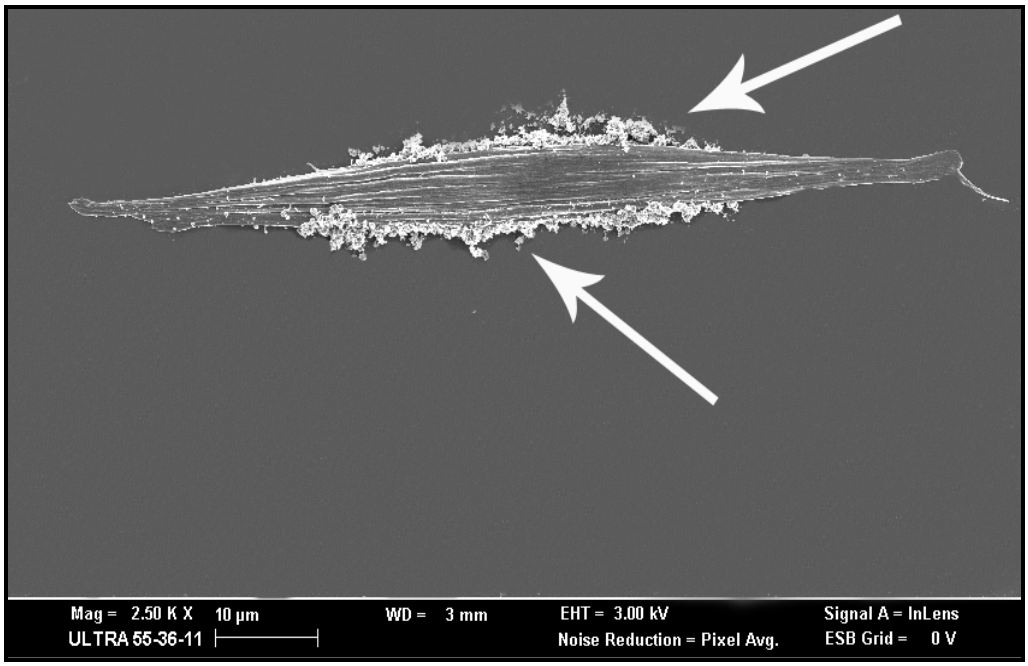

b)

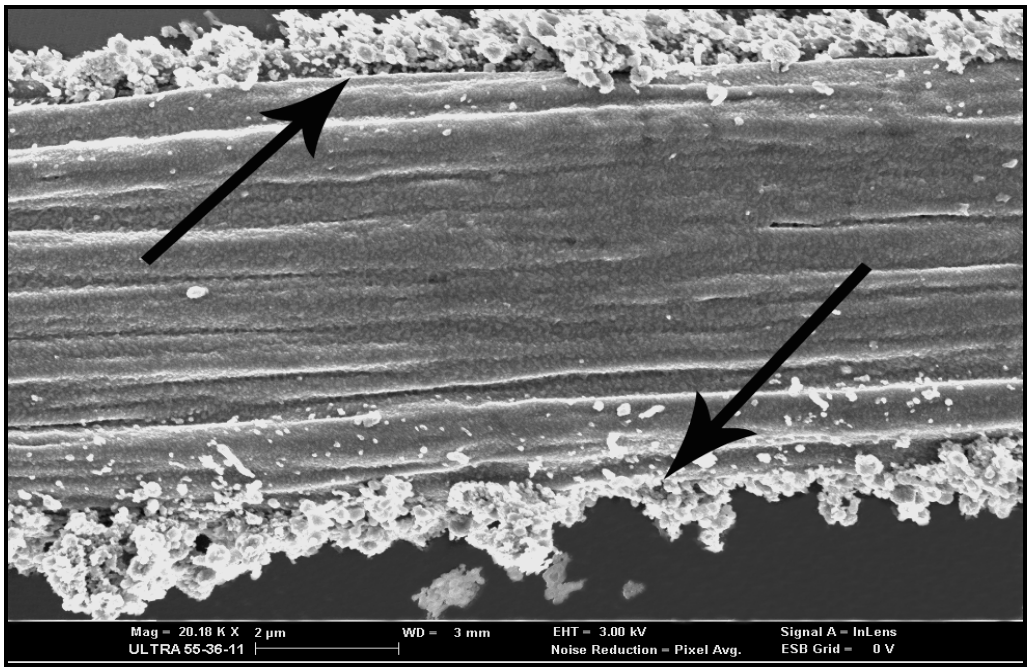

Figure 5.40: Cardiac muscle cells exposed to 0.005% Triton X-100 after pre-treatment with 0.02mg/ml CoQ10. **a**): Low magnification shows an intact cell, the white arrows indicate a presipitation on the membrane surface. **b**): Higher magnification shows an intact membrane surface. The precipitation (thick black arrows) might be derived from the protein components in the culture medium (5% foetal bovine serum).

5.4 Conclusion

To study the cellular and morphological effect of Triton X-100 and CoQ10, alone and in combination on primary chick embryonic cardiac and skeletal muscle cell cultures, scanning electron microscopy provide a powerful tool for high-resolution imaging of surfaces.

Triton X-100 has been used extensively in a wide variety of biological systems for both preparative and functional studies of membrane proteins and membrane permeabilization. In the present study we observed the solubilisation properties of Triton X-100 on membranes of primary cardiac and skeletal muscle cells in cultures. Investigation of Triton X-100 concentrations ranging from 0.5% to 0.00005% resulted in complete membrane solubilization (Figure 5.3 and 5.4) to slight shrinkage of the muscle cell membranes (Figure 5.9 and 5.11) with an indication of apoptotic process progression (Figure 5.7 and 5.8). Triton X-100 is a useful tool for investigating cytoskeletal composition and properties, as indicated by the highest two concentrations (0.5 and 0.05%) used in the study, which enabled the visualization of cytoskeletal components and variation in the cytoskeletal composition as the cell progress through the different phases of the cell cycle. Triton X-100 at 0.5% solubilizes the bilayer and most integral membrane proteins, leaving only the spectrin matrix and associated proteins in an insoluble form. Confined within this peripheral layer was a nuclear remnant. The cytoplasmic space was largely empty surrounded by a filamentous network (Figure 5.3 and 5.4). As the concentration decreased, the intensity of structural and morphological alterations was reduced. At none of the concentrations of Triton X-100 tested in the study, after 24 hours of exposure, did cells in culture show any reparative actions. No remarkable differences between the cardiac and skeletal muscle cell alterations were observed. Coenzyme Q10 (CoQ10), known to have antioxidant and membrane stabilizing properties, is the only endogenously produced lipid with a redox function in mammals. Coenzyme Q10 is necessary for adenosine triphosphate (ATP) production. Its role as a mobile electron carrier in the mitochondrial electron-transfer process of respiration and coupled phosphorylation is well established. Coenzyme Q10 has been demonstrated to scavenge free radicals produced by lipid peroxidation and prevent mitochondrial deformity during episodes of ischemia, and it may have some ability to maintain the integrity of myocardial calcium ion channels during ischemic insults. Coenzyme Q10 appears capable of stabilizing cellular membranes and

preventing depletion of metabolites required for ATP resynthesis (Greenberg *et al*., 1990 and Dallner *et al*., 2000). No cellular or morphological damage to cells were observed in the presence of the different concentrations of CoQ10 (0.2mg/ml – 0.02mg/ml) tested in the study. Cell membranes appeared smooth, intact, and most of the cells seem to be in the process of fusion or postproliferative, which might indicate that CoQ10 might enhance the proliferation process in muscle cells. Fusion of myoblasts into myotubes were seen at 0.05 and 0.01mg/ml CoQ10 (Figure 5.17 & 5.18, and Figure 5.22 &5.23), and not in any cultures exposed to Triton X-100 or in the control group, indicating that CoQ10 enhances the process of proliferation and syncytium formation in cardiac and skeletal muscle cells in culture. Membrane surfaces were remarkably smooth and intact, confirming the membrane stabilizing properties of CoQ10 discussed by Greenberg *et al*., 1990 and Dallner *et al*., 2000, with the presence of microvilli and small spherical protrusions, characterizing certain phases of the cell cycle. In all cells exposed to CoQ10, very distinct pores were visible (e.g. Figure 5.12), in some instances they appeared in larger quantities. These pores, designated “ion channels” according to the literature, are clearly activated or their function is enhanced in the presence of CoQ10 to such an extend that they appear in larger numbers in an “open” state on the surface of the cell membranes. Ion channels were present at all the concentrations of CoQ10 being tested confirming the ability of CoQ10 to maintain the integrity of myocardial calcium ion channels as described by Greenberg *et al*., 1990, Dallner *et al*., 2000, Shinde *et al*., 2005 and Terao *et al*., 2006). To determine whether CoQ10 might elicit some form of protection when cardiac and skeletal muscle cells were exposed to Triton X-100, the cultures were pre-treated with the different concentrations of CoQ10 (0.01 – 0.2mg/ml) 2 hours prior to Triton X-100 exposure at 0.05 and 0.005%. Triton X-100 at a concentration of 0.05% induced cellular and morphological alterations in the presence of CoQ10, the same as seen in the Triton X-100 group in the absence of CoQ10. We can conclude that the concentrations of CoQ10 (0.01 – 0.2mg/ml) used to pre-treat cells exposed to 0.05% Triton X-100, did not offer any protection to cells in culture. Cells exposed to 0.005% Triton X-100 after pre-treatment with CoQ10, showed membrane shrinkage (Figure 5.31) in skeletal muscle cells and membrane lyses of cardiac muscle cells (Figure 5.32) at 0.2mg/ml CoQ10. At a concentration of 0.1mg/ml CoQ10, membrane lyses were seen but the surface lamina was still present in skeletal muscle cells (Figure 5.33), while cardiac muscle cells seemed largely intact (Figure 5.34 a) at high magnification (Figure 5.34 b and 5.35). An intact membrane with bulging and a rare

appearance of a "*membrane patch"* on a part of the membrane that present more rough and slightly damaged, were seen. At a concentration of 0.05mg/ml CoQ10, skeletal and cardiac muscle cells exposed to 0.005% Triton X-100 seemed perfectly intact, with smooth membrane surfaces and the presence of ion channels. At 0.01mg/ml CoQ10 in the presence of 0.005% Triton X-100, the membrane surface of skeletal muscle cells appeared slightly shrunken, while cardiac muscle cells were intact and presented with a smooth membrane surface. The results of the study lead to the conclusion that when the concentration of Triton X-100 is too high (0.05% or higher), CoQ10 is not able to offer any protection to skeletal and muscle cells in culture. In the presence of 0.005% Triton X-100 cardiac and skeletal muscle cells showed membrane disruption and apoptotic body formation (Figure 5.7 & 5.8). When the cells were pre-treated with CoQ10 before exposure to this concentration of Triton X-100, the highest and second highest concentrations of CoQ10, showed to disrupt cell integrity, while at 0.1mg/ml in cardiac muscle cells and 0.05mg/ml CoQ10 in both cell cultures, the CoQ10 offered protection in the form of repairing cell membrane rupture by means of a "*membrane patch*" formation on the surface of the membrane where the integrity of the membrane was altered. This phenomenon was not seen in any of the other groups including the control group of the study.

Chapter 6: Investigating the Cellular Effects of Triton X-100 and CoQ10, using Confocal Microscopy

6. 1 Introduction

Seeing a cell is an essential aspect of cell biology. To the small world of the cell, confocal microscopy is a major advance upon normal light microscopy since it allows one to visualize not only deep into cells and tissues, but to also create images in three dimensions (Hibbs, 2000). A confocal microscope creates sharp images of a specimen that would otherwise appear blurred when viewed with a conventional microscope (Semwogerere *et al*., 2005). The confocal microscope incorporates the ideas of point-by-point illumination of the specimens and rejection of out-of-focus light. One drawback with imaging a point onto the specimen is that there are fewer emitted photons to collect at any given instant (Semwogerere *et al*., 2005). Thus, to avoid building a noisy image each point must be illuminated for a long time to collect enough light to make an accurate measurement (Minsky, 1988). The solution is to use a laser light source. The ability of the microscope to create sharp optical sections makes it possible to build 3D renditions of the specimen. Data gathered from a series of optical sections imaged at short and regular intervals along the optical axis are used to create the 3D reconstructions.

Fluorescent probes were first used to reveal cell morphology and biochemistry in static conditions in the same manner as classical electron microscopy studies are used to assess cell ultrastructure (Bkaily *et al*., 1997). In recent years, numerous fluorescent probes have been developed which selectively label macromolecules or interact with specific sites within the cell. The advantage of these site selective probes is that they can be used to investigate structure and activity inside living cells with minimal disruption of cellular function (Lemasters *et al*., 1993). The advent of confocal microscopy has not only made it possible to determine biological structure in three dimensions, but more importantly, has enabled investigators to correlate dynamic processes or events in relation to specific subcellular structures through dual and/or multiple labelling (Bkaily *et al*., 1997). Among the most important aspects of fluorescence confocal microscopy is the choice of fluorescent probe (fluorophore). It is typically influenced by several factors

(Semwogerere *et al*., 2005). The fluorophore should tag the correct part of the specimen. It must be sensitive enough for the given excitation wavelength. For living specimens it should not significantly alter the dynamics of the organism; and an extra consideration is the effect of the specimen on the fluorophore – its chemical environment can affect the position of the peaks of the excitation and emission spectra (Sheppard *et al*., 1997). A major problem with fluorophores is that they fade irreversible when exposed to excitation light. Although the process is not completely understood, it is believed in some instances to occur when fluorophore molecules react with oxygen and/or oxygen radicals and become non-fluorescent (Becker , 1996 and Chen *et al*., 1995). The reaction can take place after a fluorophore molecule transitions from the singlet excited state to the triplet excited state. Although the fraction of fluorophores that transitions to the triplet state is small, its lifetime is typically much longer than that of the singlet state. This can lead to significant triplet state fluorophore population and thus to significant photobleaching (Semwogerere *et al*., 2005).

Biological laser scanning confocal microscopy relies heavily on fluorescence as an imaging mode, primarily due to the high degree of sensitivity afforded by the technique coupled with the ability to specifically target structural components and dynamic processes in chemically fixed as well as living cells and tissues. Many fluorescent probes are constructed around synthetic aromatic organic chemicals designed to bind with a biological macromolecule (for example, a protein or nucleic acid) or to localize within a specific structural region, such as the cytoskeleton, mitochondria, Golgi apparatus, endoplasmic reticulum, and nucleus. Other probes are employed to monitor dynamic processes and localized environmental variables, including concentrations of inorganic metallic ions, pH, reactive oxygen species, and membrane potential. Fluorescent dyes are also useful in monitoring cellular integrity (live versus dead and apoptosis), endocytosis, exocytosis, membrane fluidity, protein trafficking, signal transduction, and enzymatic activity. In addition, fluorescent probes have been widely applied to genetic mapping and chromosome analysis in the field of molecular genetics (Dunn *et al*., 2006).

In this study the cellular effect of Triton X-100 and CoQ10, alone, and in combination on cardiac and skeletal muscle cells were investigated with confocal microscopy. The following fluorescent probes were used in the study:

(i) Mito Tracker Red 580, a cationic dye that is selectively pumped into healthy respiring mitochondria in response to its negative membrane potential.

(ii) 4'6-diamino-2-phenylindole diydrochloride (DAPI), a dye that stains nuclei specifically with little or no cytoplasmic labelling.

(iii) diclorodihydrofluorescein diacetate (DCH_2FDA) is a fluorescent probe that detects the formation of ROS, specifically the ROS, H_2O_2 (only skeletal muscle cells were used).

In this Chapter the following research objectives were investigated:

- Investigate intracellular changes in cardiac and skeletal muscle cells in primary culture, evoked by Triton X-100 and CoQ10, alone and in combination, using Confocal Microscopy.
- Correlate the results obtained with SEM, with the results obtained with Confocal Microscopy.
- Determine whether Triton X-100 and CoQ10, alone and in combination produce reactive oxygen species (ROS), upon exposure, in cardiac and skeletal muscle cell cultures.

6.2 Materials and Methods

The primary chick embryonic cardiac and skeletal muscle cell cultures were prepared as for cytotoxicity testing in Chapter 4. To examine the cardiac and skeletal muscle cell morphology and structure of the primary cultures, the primary cultures at a concentration of at $5x10^4$cells/ml were plated onto the surface of Menzel Glazer glass coverslips coated with Poly-L-lysine (1ml Poly-L-lysine in 9ml sterile ddH_2O) positioned on the bottom of 6-well plates. After 72 hours of incubation the cell cultures were exposed to Triton X-100 (0.00005 – 0.5%) and CoQ10 (0.01 – 0.2mg/ml), alone and in combination, for 24 hours. To determine the effect of CoQ10 on cells exposed to Triton X-100, cell cultures were pre-treated with the different concentrations of CoQ10, 0.02 – 0.2mg/ml, two hours prior to exposure to Triton X-100 (0.005 – 0.05%). The cultures were maintained for the rest of the 24 hours at 37°C and 5% CO_2 before Mito Tracker® Red 580 (Invitrogen Molecular Probes™, Cat #: M22425), to identify cells with healthy respiring mitochondria and DAPI (Invitrogen Molecular Probes™, Cat #: D1306) to investigate possible alterations to the nuclei, were added to the cells. A stock solution of

1mM Mito Tracker was prepared in DMSO. DAPI was prepared at a concentration of 5mg/ml in ddH_2O and further diluted to a stock solution of 300nM. After the incubation period 1µl of Mito Tracker was added to the medium in each well and left in the dark for 25 minutes, 300µl of DAPI was then added to the medium and left in the dark for a further 5 minutes. The medium was removed from each well, and the attached cardiac and skeletal muscle cells were washed with DPBS. A 10x DPBS stock solution was used. Coverslips were removed from the 6-well plates and mounted onto microscope slides. The area between the coverslip and the microscope slide was wetted with DPBS and the edges were sealed. Cardiac and skeletal muscle cells were examined using a Zeiss LSM 510 META confocal microscope (Carl Zeiss Werke, Göttingen, Germany), with fluorescence excitation wavelengths 543 and 358nm for Mito Tracker and DAPI, respectively and emission wavelengths of 644 and 461nm for Mito Tracker and DAPI, respectively. Both Mito Tracker and DAPI were evaluated simultaneously, in order to produce a sharp contrast between nuclei labelling and active respiring mitochondria. Result images are presented in the form of an overlap of the two signals obtained at different excitation and emission wavelengths.

To determine the presence of ROS, skeletal muscle cells were kept unexposed in the incubator at 37ºC and 5% CO_2 for 86 hours. The skeletal muscle cells were only exposed to CoQ10, two hours before the fluorescent dye DCH_2FDA (Sigma-Aldrich, Johannesburg, South Africa) was added to indicate ROS formation. The cells were exposed to Triton X-100 10-15 minutes before DCH_2FDA was added and for cells exposed to Triton X-100 and CoQ10 in combination, the cells were exposed to CoQ10 two hours before Triton X-100 was added, and then exposed to the substances in combination for 15 more minutes, before DCH_2FDA was added to indicate ROS formation. Cells were exposed to the same concentrations as mentioned for Mitotracker Red and DAPI fluorescence. A 5µg/ml stock solution of DCH_2FDA was prepared in ddH_2O. After the exposure time, the medium from each well was removed and the attached skeletal muscle cells were washed with DPBS. A volume of 800µl DPBS was added to each well, together with 40µl of the stock solution of DCH_2FDA. After 7 minutes in the dark, the solution was removed and coverslips were mounted onto microscope slides (as described for Mito Tracker and DAPI), and evaluated with a Zeiss LSM 510 META confocal microscope to locate areas where ROS generation had occurred.

6.3 Results and Discussion

Confocal microscopy imaging studies in single cells and tissue sections confirm the importance of this non-invasive technique in the study of cell structure and function as well as the modulation of working living cells by various constituents of cell membranes, organelles and cytosol (Bkaily *et al*., 1997). Confocal laser scanning microscopy uses optical sections and digitized images to achieve a similar goal over tens of micrometers. These images were collected and can be processed for stereo viewing or presented in a collected form that provides extreme depth of focus (Borman *et al*., 1994).

6.3.1 Mito Tracker Red 580

In the mitochondrial respiratory pathway, an electrochemical gradient is generated by the active extrusion of protons from the mitochondrial matrix to the intermembrane space via complexes of the electron transport chain. This gradient is generated as reduced pyridine nucleotides are oxidized, protons are pumped, and electrons are passed down the chain. ATP is generated as Complex V (F_OF_1, ATP synthase) couples phosphorylation of ADP with NADH/$FADH_2$ oxidation, a process known as oxidative phosphorylation (OXPHOS). This inner mitochondrial membrane potential attracts some dyes to actively respiring mitochondria. Although conventional fluorescent stains for mitochondria, such as rhodamine 123 and tetramethylrosamine, are readily sequestered by functioning mitochondria, they are subsequently washed out of the cells once the mitochondrion's membrane potential is lost. This characteristic limits their use in experiments in which cells must be treated with aldehyde-based fixatives or other agents that affect the energetic state of the mitochondria. To overcome this limitation, Molecular Probes has developed the MitoTracker Orange and MitoTracker Red probes - dyes that accumulate in mitochondria in a membrane-potential–dependent manner and remain during subsequent processing steps for immunocytochemistry, *in situ* hybridization, or electron microscopy. In addition, MitoTracker Orange and MitoTracker Red reagents eliminate some of the difficulties of working with pathogenic cells because, once the mitochondria are stained, the cells can be treated with fixatives before the sample is analyzed (Invitrogen™). MitoTracker Red 580 dye is useful for staining mitochondria in fixed or live cells (staining is not membrane-potential sensitive), but the staining pattern is not retained following fixation and permeabilization (invitrogen™). Mito Tracker Red is a cationic dye that is selectively pumped into healthy respiring mitochondria in response

to its negative membrane potential. Once pumped into the mitochondria, the dye is covalently bound to proteins through its chloromethyl moiety and thus is retained after fixation of cells. Treatment of cells with an uncoupler of mitochondria such as carbonyl cyanide m-chloro phenylhydrazone (CCCP), resulted in a marked decrease in Mitotracker red fluorescence intensity that is indicative of a loss of membrane potential (Bova *et al*., 2005).

6.3.2 DAPI

4´,6-diamidino-2-phenylindole dihydrochloride (DAPI), is a popular nuclear and chromosome counterstain, DAPI emits blue fluorescence upon binding to AT regions of DNA. DAPI stains nuclei specifically with little or no cytoplasmic labelling. Although the dye is cell impermeable, higher concentrations will enter a live cell (InvitrogenTM). The blue-fluorescent DAPI nucleic acid stain preferentially stains dsDNA; it appears to associate with AT clusters in the minor groove. Binding of DAPI to dsDNA produces a ~20-fold fluorescence enhancement, apparently due to the displacement of water molecules from both DAPI and the minor groove. DAPI also binds RNA, however in a different binding mode one thought to involve AU-selective intercalation (Invitrogen^{TM}). DAPI is due to its colour a very convenient stain for nuclei labelling during counterstaining experiments. In this study DAPI clearly differentiate the nucleus of muscle cells from the rest of the cell, making it possible to observe possible cell fusion.

6.3.3 Dichlorodihydrofluorescein diacetate (DCH_2FDA)

Dichlorodihydrofluorescein diacetate (DCH_2FDA) is a fluorescent probe that detects the formation of ROS, specifically the ROS, H_2O_2. This probe can easily enter the cell, where it is also cleaved by non-specific esterase into diclorodihydrofluorescein (DCFH). DCFH is oxidised by H_2O_2 to form diclorofluorescein (DCF), which is fluorescent and the cell exhibits a green fluorescence (Hipler *et al*., 2002). DCH_2FDA is a nonpolar, nonfluorescent probe that easily crosses the cell membrane due to two esterified acetate functional groups (Chini *et al*., 1997). On entering the cell, the diacetate group is cleaved enzymatically by esterases to form polar, dichlordihydrofluorescein that accumulates intracellularly (Scivittaro *et al*., 2000; Kim *et al*., 2000). In the presence of the ROS, H_2O_2, dichlordihydrofluorescein is oxidized to the highly fluorescent 2'7'-dichlorofluoresein. Consequently the fluorescent signal produced by 2'7'-

dichlorofluoresein is an index of oxidative stress in the biological system (Grishko *et al*., 2001).

No significant difference was seen between cardiac and skeletal muscle cells in the different groups on which the combined colorimetric cytotoxicity assays were performed. Neither did cardiac and skeletal muscle cells showed a drastic difference when cell structure was evaluated upon exposure to Triton X-100 and CoQ10, alone and in combination, using SEM. No difference was observed between the fluorescence produced by cardiac and skeletal muscle cells in each group when evaluated using confocal microscopy. Results of the different concentrations tested in this experiment are therefore shown irrespective of the cell culture/muscle cell type.

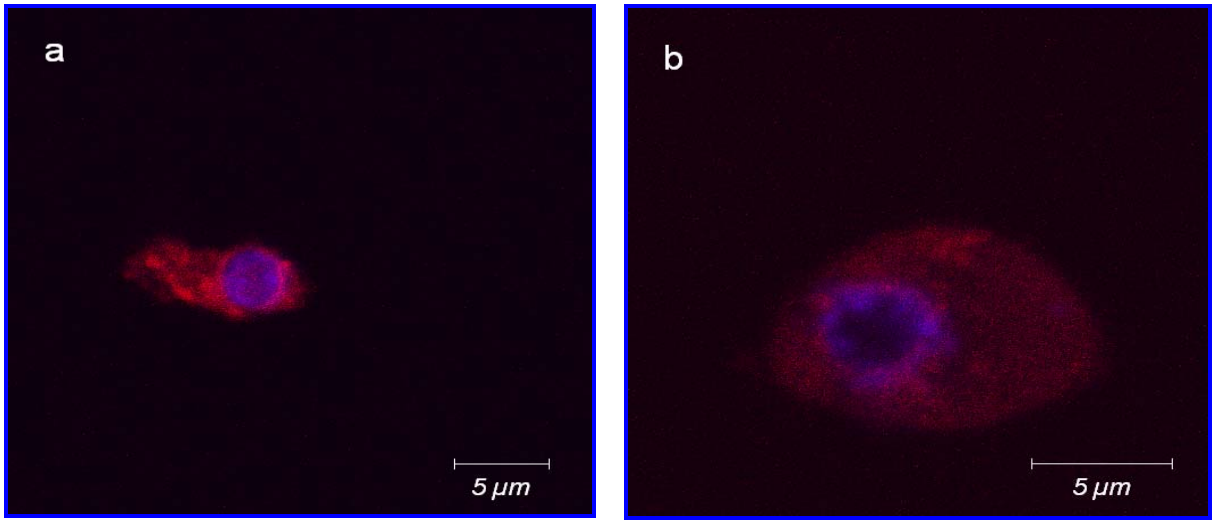

Figure 6.1: Muscle cells in the control group (**a** & **b**) stained with Mito Tracker Red and DAPI. A major problem with fluorophores (fluorescent probes) is that they fade irreversible (**b**) when exposed to excitation light (Semwogerere *et al*., 2005).

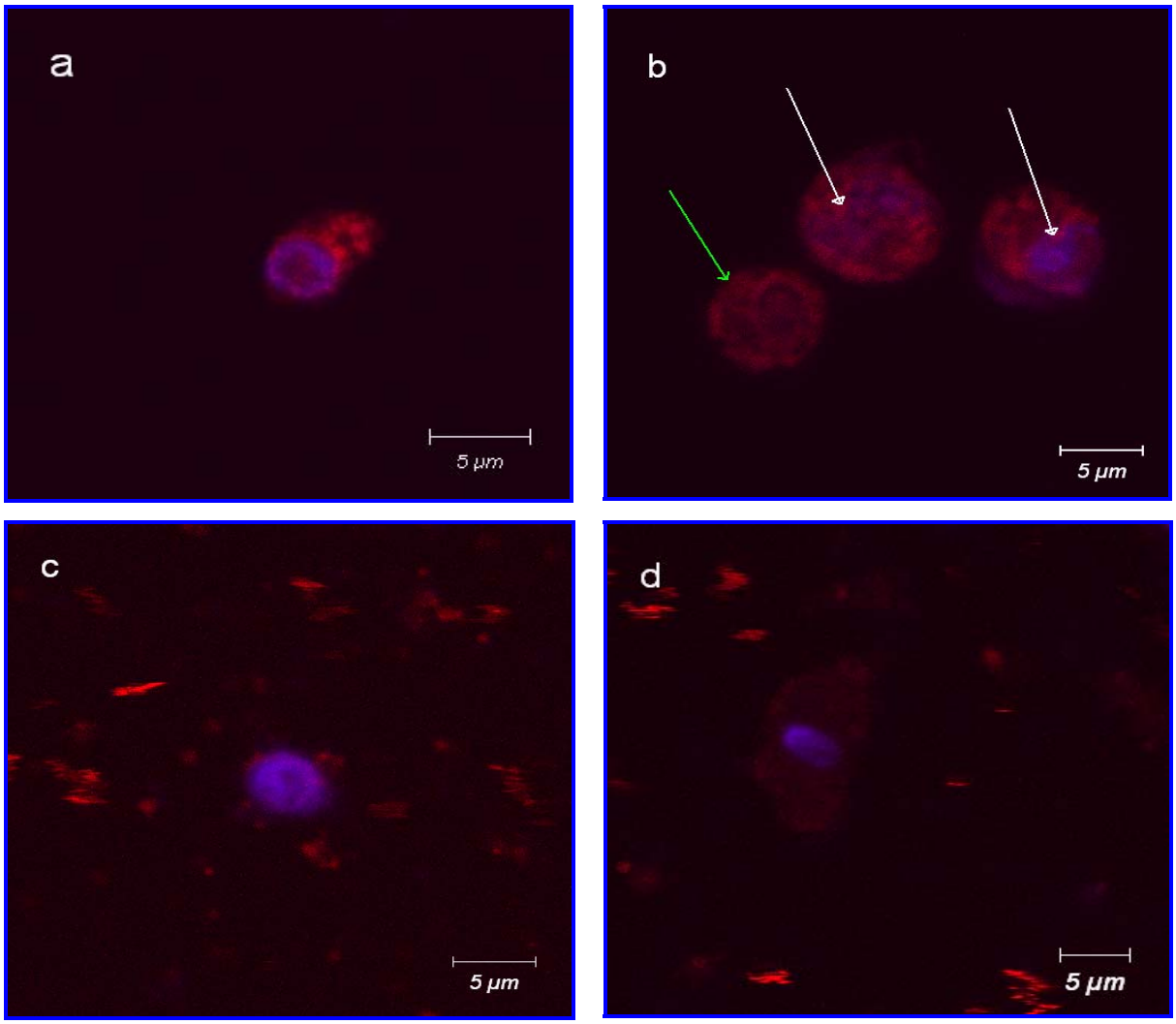

Figure 6.2 A: Muscle cells in the Triton X-100 group, stained with Mito Tracker Red and DAPI. **a**): 0.5% Triton X-100, little mitochondrial staining were seen, as the red signal produced by Mito Tracker Red was very weak. DAPI produced a weak blue signal, but the position indicates that the nucleus was not disrupted. **b**): Three muscle cells in the same culture as (**a**), the white arrows point to the distribution of the blue signal throughout the cell. The green arrow points to a cell where no blue signal was produced. **c**): 0.05% Triton X-100. **d**): 0.005% Triton X-100. In both (**c**) and (**d**) a relatively strong blue fluorescence was obtained, in disparity to the weak, almost absent Mito Tracker Red signal. Photos (**c**) and (**d**) point to the possibility that the nucleus was still intact, when mitochondrion were destroyed during the process of possible cell death caused by 0.05% and 0.005% Triton X-100.

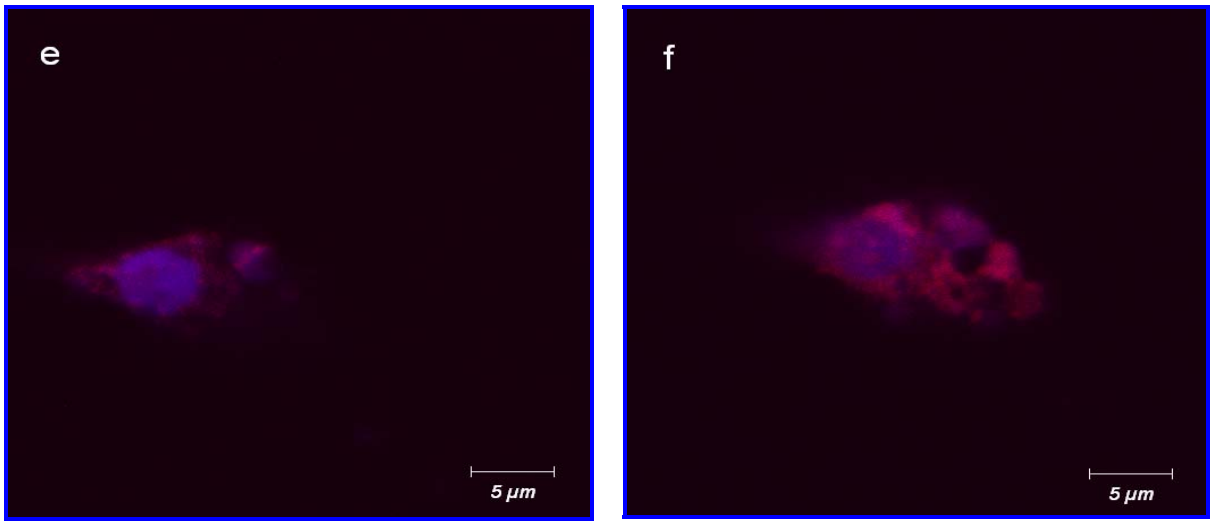

Figure 6.2 B: Muscle cells in the Triton X-100 group at the second lowest and lowest concentrations tested in the study. **e**): 0.0005% Triton X-100, a clear blue signal was observed indicating the position of the nucleus, which seems to be intact. A weak blue fluorescence can be seen outside the circular blue signal assumed to represent the nucleus. This phenomenon indicates that nucleic acid/nuclear material was also dispersed outside the boundaries of the nucleus. This was also observed in the muscle cell in (**f**), the dispersed blue signal was slightly stronger and the circular blue signal to the left of the cell was less pronounced than in (**e**).

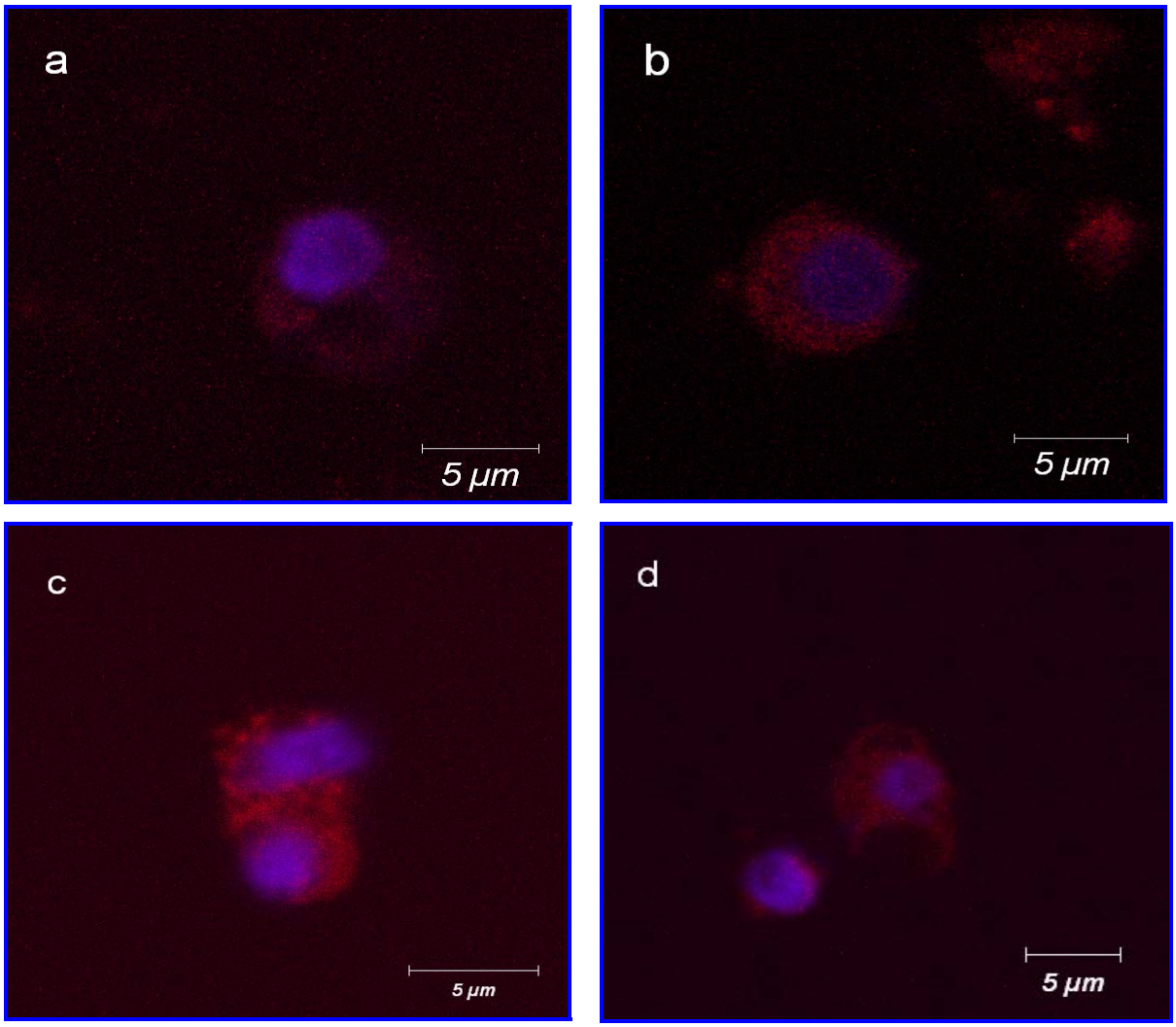

Figure 6.3 A: Muscle cells in the CoQ10 group stained with Mito Tracker Red and DAPI. **a**): 0.2mg/ml CoQ10. **b**): 0.1mg/ml CoQ10. In both the highest and second highest concentrations (**a** & **b**) of CoQ10 used in the study a definite circular blue signal was produced by DAPI, although the signal was very weak, it confirmed an intact nucleus. A very weak red signal was produced by Mito Tracker Red in both (**a**) and (**b**). Since Mito Tracker red is selectively pumped into healthy respiring mitochondria in response to its negative membrane potential, it might be possible that the membrane potential was altered, but since the blue signal produced by DAPI was also very weak, and not dependent on the membrane potential it can be safely assumed that the dye faded due to photobleaching, since "anti-fade" was not used in the study. **c** & **d**): 0.05mg/ml CoQ10. In both the photos shown, two very distinct blue signals in circular form, assumed to represent the nucleus was seen. This probably represents the process of fusion between two myoblasts to form a myotube, the mechanism whereby muscle cells form a syncitium in the process of muscle formation.

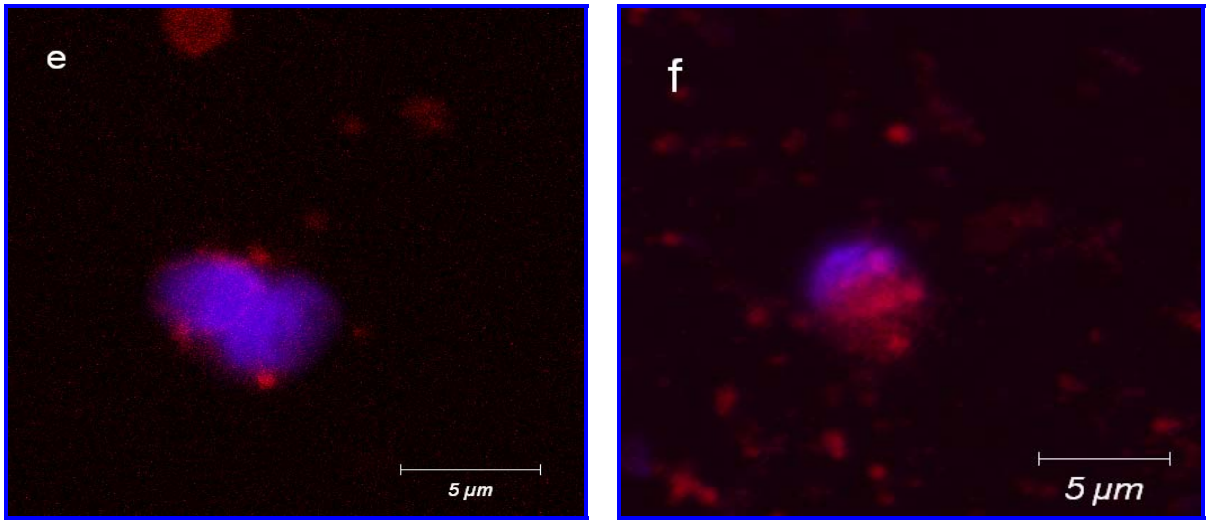

Figure 6.3 B: Muscle cells in the CoQ10 group at the two lowest concentrations of CoQ10 used in the study. **e**): 0.02mg/ml CoQ10. Two very distinct blue signal in circular form, very close to each other. Little, but intense red fluorescence was produced. It is possible that this cell is in the process to undergo proliferation, since there are two distinct nuclei. The little red fluorescence may point to the fact that cells in this phase minimize cytoplasmic contents in order to go through the proliferation process, thereafter the cytoplasmic contents and organelles are restored in order to maintain normal cellular metabolism. **f**): A clear blue fluorescence produced by DAPI at 0.01mg/ml. The nucleus appears to be intact. A bright red fluorescence was produced by Mito Tracker Red, indicating the healthy respiring mitochondria in the cells in both (**e**) and (**f**).

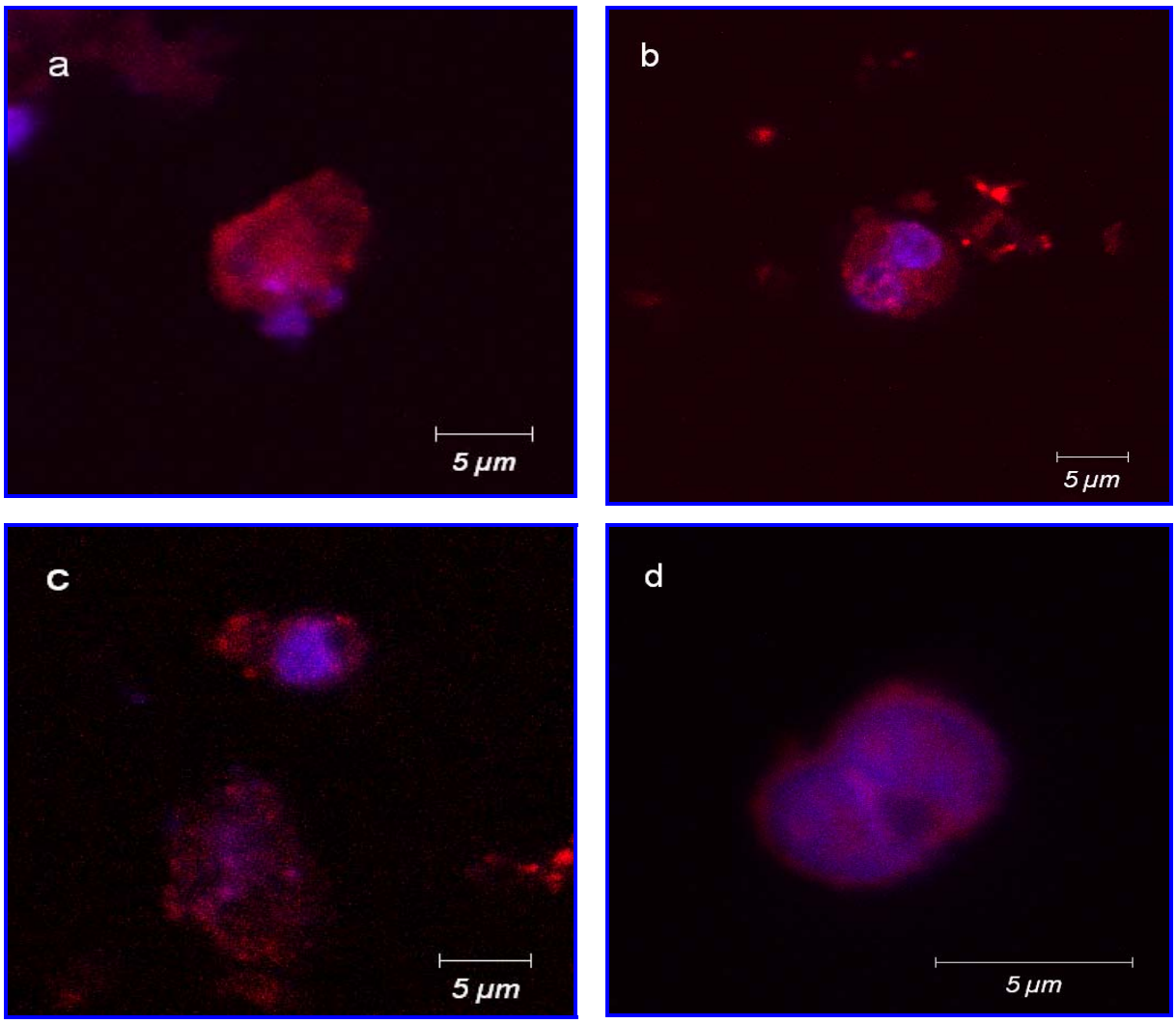

Figure 6.4 A: Muscle cells exposed to 0.05% Triton X-100 after two hours pre-treatment with CoQ10, stained with Mito Tracker Red and DAPI. **a** & **b**): Muscle cells pre-treated with 0.1mg/ml CoQ10. A definite blue signal was obtained in (**a**) with DAPI, the signal was in 3 distinct portions visible, indicating that the nucleus was not intact. The cell was probably in the process of undergoing apoptosis. The detectable morphological changes in the nucleus are chromatin condensation and, at a later stage, the fragmentation of the nucleus into several particles (Häcker, 2000). An intense red signal was produced by Mito Tracker Red, indicating active respiring mitochondria. In (**b**), two distinct blue signals can be observed, representing two intact nuclei, an intense red signal can be seen, with spreading of the red signal outside the direct vicinity of the nuclei, it is possible that membrane disruption occurred. **c** & **d**): Muscle cells pre-treated with 0.05mg/ml CoQ10. The blue signal in the top cell in **c** is intense and the shape indicate and intact nucleus, surrounded by respiring mitochondria. The blue signal in (**d**) is spread throughout the cell, with an invagination in the overall shape at the bottom part of the cell. This cell might be in the process of undergoing mitosis.

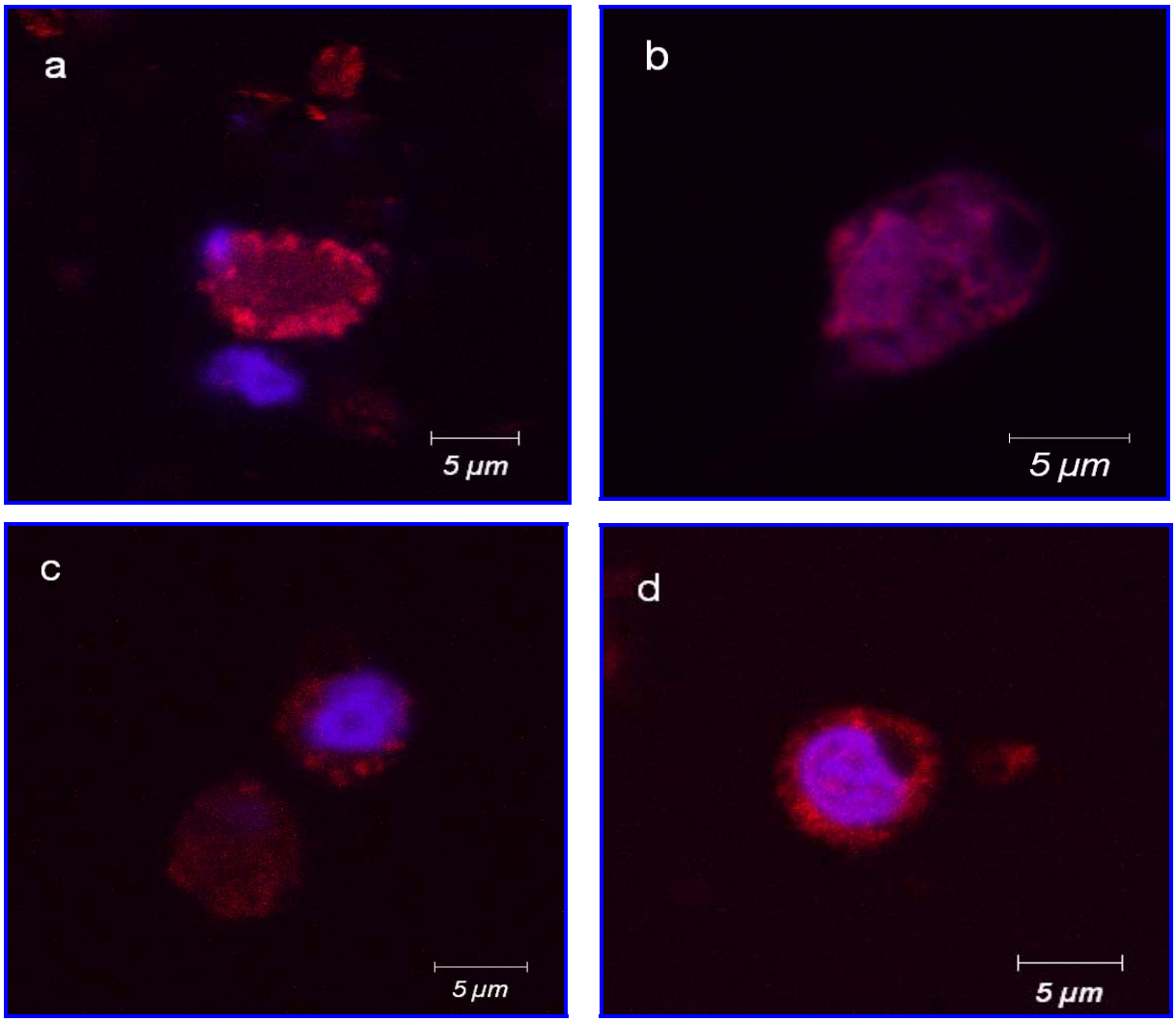

Figure 6.4 B: Muscle cells exposed to 0.005% Triton X-100 after two hours pre-treatment with CoQ10, stained with Mito Tracker Red and DAPI. **a** & **b**): Muscle cells pre-treated with 0.1mg/ml CoQ10. In (**a**) two distinct intense blue signals were obtained with DAPI, indicating intact nuclear morphology. Intense red fluorescence was also seen. In (**b**), the blue signal was spread in a non-condensed fashion throughout the cytoplasm merged with the red signal produced by Mito Tracker Red, indicating that the cell is probably in the process of undergoing mitosis. **c** & **d**): Muscle cells pre-treated with 0.05mg/ml CoQ10. In both (**c**) and (**d**), a very intense blue signal was obtained by DAPI staining indicating, intact nuclei. A red signal was obtained in both cells, indicating active respiring mitochondria. The more intense red signal in **d**, might be the result of a more negative membrane potential, as it compare well to the control group (Figure 6.1 **a**), the red signal in **c** might also be less intense due to photobleaching.

Wakelam, 1985, described skeletal muscle fibres as permanent multinucleated, non-mitotic cells. In 1983 Masuko *et al*., observed distinct changes in surface structure and form of chick myoblasts during the cell cycle. During the G1 and S phase, the cells were spindle-shaped with a relatively smooth surface, by late G2, cells have bulged in anticipation of rounding from mitosis (Masuko *et al*., 1983), and many microvilli, some blebs, and long slender filopodia appeared on cell surfaces. During M, the cells were generally spherical and their surface covered with numerous microvilli and some blebs. After cell division, microvilli and blebs disappear as the cell spread over the substrate (Masuko *et al*., 1983). The changes in surface structure observed by Masuko *et al*., 1983, seemed to them to be a "general phenomena related to mitosis". During embryonic development, several hundred myoblasts, precursors of skeletal muscle fibers, line up end to end, fusing with one another to form multinucleated cells known as myotubes. These newly formed myotubes manufacture cytoplasmic constituents as well as contractile elements, myofilaments, responsible for the contractile capability of the cell (Gartner *et al*., 2007). Myogenic differentiation involves extensive changes in cell morphology and subcellular architecture. Upon differentiation, myoblasts fuse to form multinucleated syncitia that eventually develop into terminally differentiated muscle cells, the myofibers (Pizon *et al*., 2005). When cells prepare to fuse, they have sparse skeletal structure, lightly cross-linked, and nearly empty, with a few major filamentous cables that terminate at the cell periphery (Fulton *et al*., 1981). Two crucial events occur during the commitment of the muscle cell precursor to myogenesis: (i) the cessation of proliferation of the precursor cell determined by the upregulated expression of myogenic regulatory factors (MRFs), Myf5 and MyoD, and the downregulation of Pax7, a transcription factor, and (ii) the terminal differentiation of the muscle cell precursor, triggered by myogenin and MRF4 (Kierzenbaum, 2007). In myoblasts preparing to fuse, both the surface lamina and the internal networks shows highly specific spatial rearrangement; in addition, the internal networks become more extractible. After fusion, both the internal networks and the surface lamina rapidly reorganize in a stable arrangement as the muscle cell begins to construct the extensive contractile apparatus (Fulton *et al*., 1981).

Satellite cells are a cell population distinct from the myoblasts. They attach to the surface of the myotubes before a basal lamina surrounds the satellite cell and myotube. Satellite cells are of considerable significance in muscle maintenance, repair, and regeneration in the adult. Satellite cells are mitotically quiescent in the adult, but can

resume self renewal and proliferation in response to stress or trauma. MyoD expression induces the proliferation of satellite cells. The descendants of the activated satellite cells, called myogenic precursor cells, undergo multiple rounds of cell division before they can fuse with existing or new myofibers. A population of stem cells in adult skeletal muscle, called side-population cells, has the capacity to differentiate into all major blood cell lineages as well as myogenic satellite cells. These cells are present in bone marrow and may give rise to myogenic cells that can participate in muscle regeneration (Kierzenbaum, 2007).

Yu *et al*., 1973, showed that Triton X-100 extraction of cells or membranes solubilizes the bilayer and most integral membrane proteins, leaving only the spectrin matrix and associated proteins in an insoluble and thus readily form (Yu *et al*., 1973). Apgar *et al*., 1985, found that extraction of intact cells (P815 tumour cells) with 1% Triton X-100 resulted in structures with a continuous layer of detergent-insoluble protein at the cell periphery. Confined within this peripheral layer was a nuclear remnant (also seen in Figure 5.4 b, thin white arrow in the present study), the cytoplasmic space was largely empty and clearly lacked filamentous cytoskeletal elements (as seen in Figure 5.3) (Apgar *et al*., 1985). Allen *et al*., 1964, incorporated Triton X-100 into reaction mixtures used for the visualization of esterases and acid phosphatases separated by electrophoresis in starch gels. The net effect was apparent enhancement of enzymatic activity with certain substrates and apparent inhibition of enzymatic activity with other substrates. It was shown by both quantitative and electrophoretic studies that Triton X-100 is an activator of certain esterases (Allen *et al*., 1964).

CoQ10 is a lipid-soluble component of virtually all cell membranes, and is located in the hydrophobic domain of the phospholipid bilayer of cellular membranes (Quinzii *et al*., 2007a; Sohal *et al*., 2007), it is also the only known lipid-soluble antioxidant that animal cells can synthesize *de novo*, and for which there exist enzymatic mechanisms which can regenerate it from its oxidized product formed in the course of its antioxidant function (Ernster *et al*., 1995). Free radicals are highly reactive molecules or chemical species containing unpaired electrons that cause oxidative stress, which can be defined as an imbalance between antioxidants in favor of the oxidants, potentially leading to damage (Sies, 1997). They are formed during normal physiological metabolism or caused by toxins in the environment. Oxidative stress can damage lipids, proteins,

enzymes, carbohydrates and DNA in cells and tissue, leading to membrane damage, fragmentation or random cross linking of molecules like DNA, enzymes and structural proteins and ultimately lead to cell death induced by DNA fragmentation and lipid peroxidation (Beckman *et al*., 1998). The physiological roles of CoQ10 in biological systems are most well characterized in the inner mitochondrial membrane, where three of its main functions are: (i) carrier of electrons from respiratory complexes I and II to complex III, (ii) generation of superoxide anion radical by autoxidation of ubisemiquinone and (iii) anti-oxidant quenching of free radicals (Sohal *et al*., 2007). Kagan *et al*., 1999, tested the use of CoQ10 as a generic anti-apoptotic compound and found that its ability to protect against apoptosis varies depending on both cell type and mode of cell death induction. It was established that the protective effect offered by CoQ10 was mediated by its effect on the mitochondrial function and viability (Kagan *et al*., 1999).

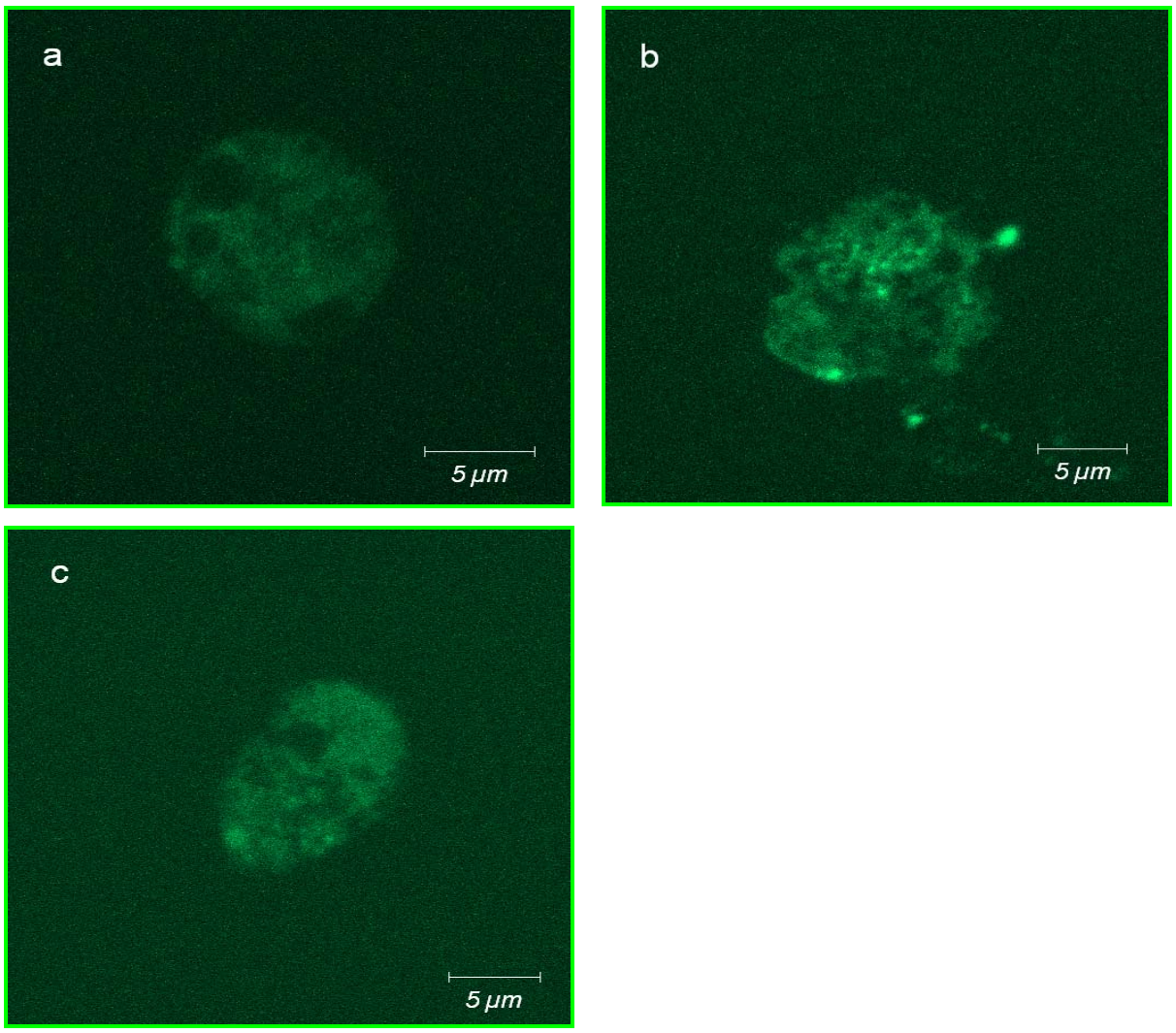

Figure 6.5: Muscle cells exposed to Triton X-100 stained with DCH_2FDA. **a**): 0.05% Triton X-100 produced a weak green fluorescence. It is possible that Triton X-100 induce cell death by a mechanism other than to produce ROS, or the weak signal may be due to photobleaching. **b**): 0.05% Triton X-100 produced a more intense green fluorescence, with the highest intensity localized to the boundary of the cell. **c**): 0.005% Triton X-100 produced a green signal throughout the whole cell, with background staining. In all the cells exposed to Triton X-100, the presence of ROS was detected with confocal microscopy.

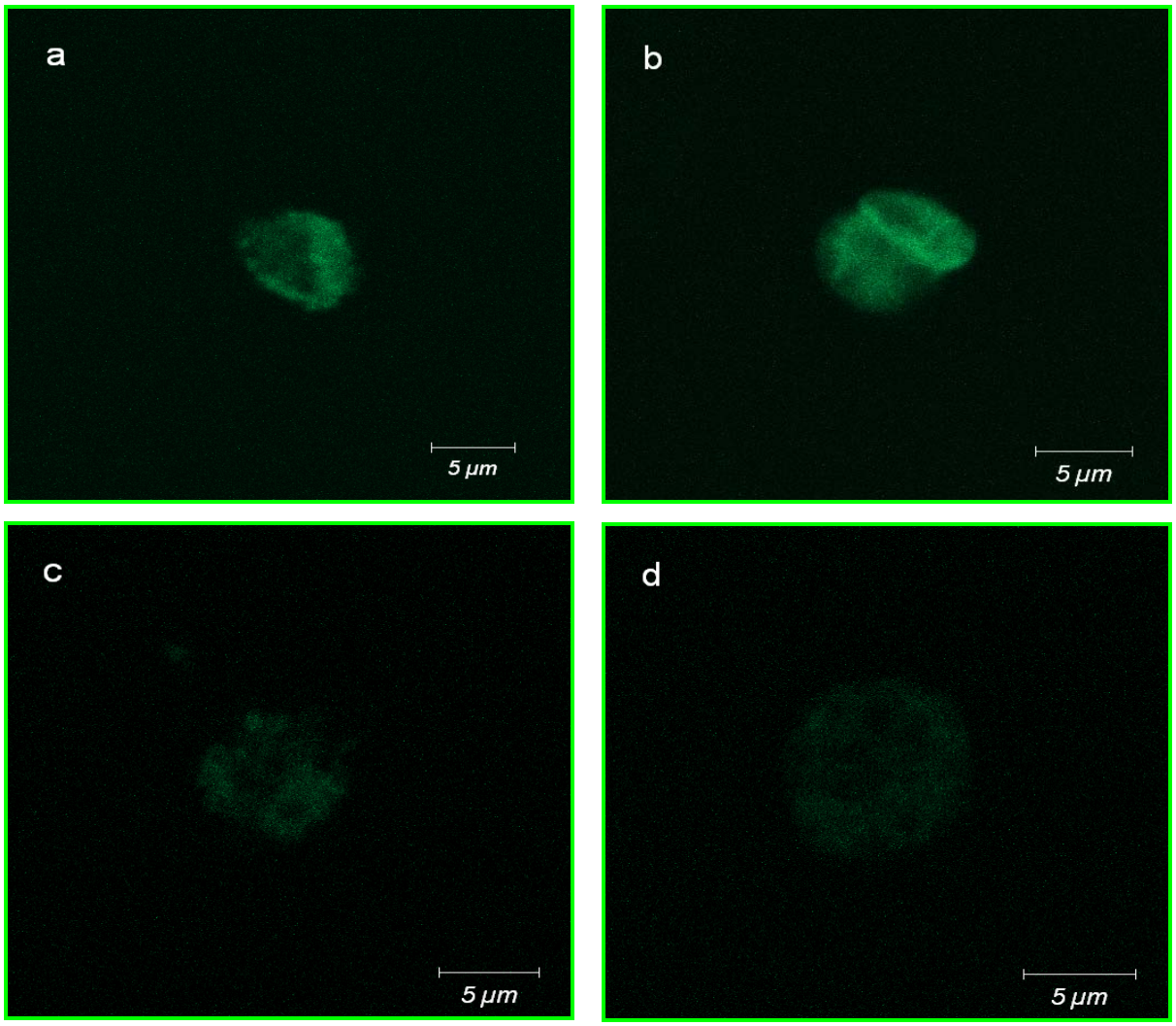

Figure 6.6 A: Muscle cells exposed to 0.05% Triton X-100, after two hours pre-treatment with CoQ10. **a** & **b**): Muscle cells pre-treated with 0.1mg/ml CoQ10. A mild green signal was obtained upon staining with DCH_2FDA in both cells, indicating the presence of ROS. **c** & **d**): Muscle cells pre-treated with 0.05mg/ml CoQ10. Almost no green signal was produced upon staining with DCH_2FDA, indicating the absence of ROS formation in cells exposed to 0.05% Triton X-100 after pre-treatment with 0.05mg/ml CoQ10.

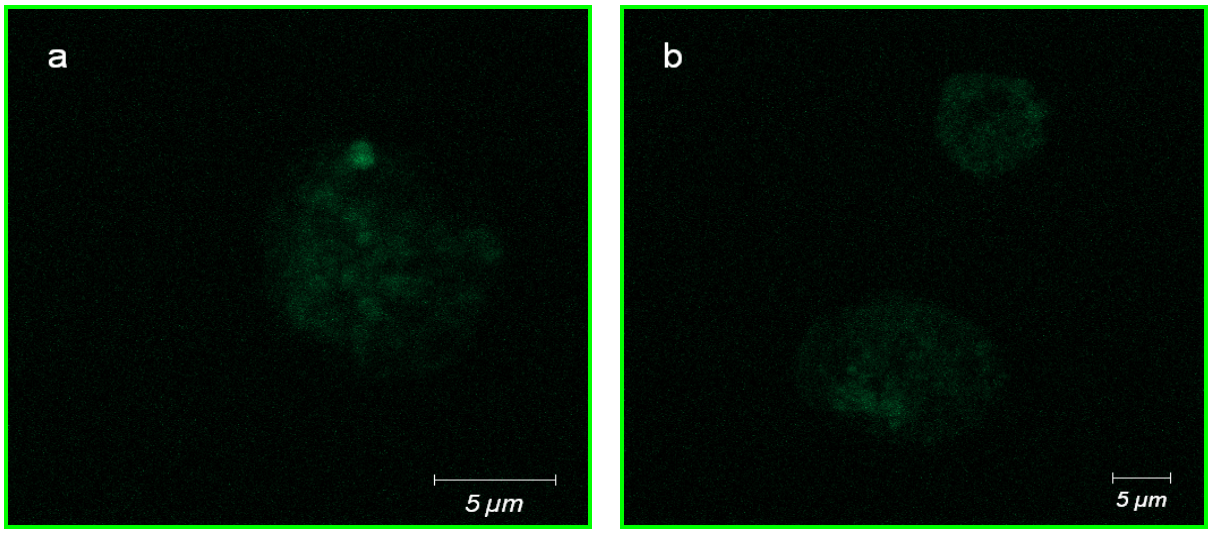

Figure 6.6 B: Muscle cells exposed to 0.005% Triton X-100, after two hours pre-treatment with CoQ10. Both (**a**) and (**b**) were pre-treated with 0.05mg/ml Triton X-100, almost no green fluorescence was detected upon staining with Dichlorodihydrofluorescein diacetate, indicating the absence of ROS and the absence in production thereof in the presence of 0.05mg/ml CoQ10 when cells are exposed to 0.005% Triton X-100.

6.4 Conclusion

A confocal microscope provides a significant imaging improvement over conventional microscopes. It creates sharper, more detailed 2D images, and allows collection of data in three dimensions. In biological applications it is especially useful for measuring dynamic processes (Semowegerere *et al*., 2005). The results obtained using confocal microscopy upon staining with Mito Tracker Red, DAPI and DCH_2FDA, confirmed the results obtained with SEM in Chapter 5 of this study. The counterstaining with Mito Tracker and DAPI offered great contrast and ease of interpreting the results. It was seen in Chapter 5, that solubilisation of muscle cells with Triton X-100 resulted in structures with a continuous layer of detergent-insoluble protein at the cell periphery, confined within this peripheral layer was a nuclear remnant, this was confirmed by DAPI staining of cells exposed to 0.5% - 0.005% Triton X-100 (Figure 6.2 A & B), nuclear material was present and produced a blue signal. CoQ10 cleary enhanced the process of cell proliferation in muscle cells, since myotube formation was only seen in this group. In Figure 6.3A, c & d, nuclei were very close together, characteristically of two mononucleated myoblasts fusing to form a multinucleated myotube. The process of fusion was seen with the SEM in Chapter 5, although nuclei could not be visualized using SEM, some cells had the surface and size characteristics of myotubes. Confocal microscopy confirmed the process of myotube formation in the CoQ10 group. In the presence of CoQ10, cells with dividing nuclei, characteristic of the process of mitosis were seen (Figure 6.3 B, e; and Figure 6.4 A, b & d), it is possible that CoQ10 promote mitotic formation of new cells in skeletal and cardiac muscle cells. Confocal microscopy also confirmed the possible protection CoQ10 offered to muscle cells exposed to Triton X-100. In Chapter 5, SEM images of a “membrane patch” in certain cells of which the membranes were injured by Triton X-100, after pre-treatment with CoQ10, suggested that CoQ10 offer some form of protection to the muscle cells. Confocal microscopy produced a blue signal indicating intact nuclei and active respiring mitochondria in muscle cells exposed to Triton X-100, after pre-treatment with CoQ10. Muscle cells in the Triton X-100 group, stained with DCH_2FDA produced a green signal, indicating the presence of ROS formation. In cells pre-treated with CoQ10, and exposed to Triton X-100 at concentrations 0.05% and 0.005%, little to no green fluorescence was obtained, indicating that CoQ10’s antioxidant function was able to scavenge the free radicals produced by Triton X-100 exposure. Muscle cells in the CoQ10 group, produced no

green fluorescence upon staining with DCH_2FDA, confirming that CoQ10 do not produce reactive oxygen species in cells but offer protection against it.

Chapter 7: Concluding Discussion

Coenzyme Q10 is a lipid-soluble coenzyme, synthesized in mammalian tissue to support energy production, and also act as an antioxidant, by scavenging free radicals present in the body. Because of the fact that CoQ10 synthesis becomes less efficient as people age, CoQ10 is thought to play a role in immune system modulation and disease. Certain medication and stress may deplete the body's endogenous CoQ10 store, by interrupting the biosynthetic pathway (Horowitz, 2003). Numerous disease conditions such as Parkinson's disease, AIDS, Alzheimer disease, autoimmune asthma, migraine, cancer, diabetes, mitochondrial disorders, muscle disorders, periodontal disease, male fertility and cardiac conditions, including hypertension, congestive heart failure, angina and cardiomyopathy has been shown to benefit from CoQ10 supplementation (Horowitz, 2003). Dr. John Ely at the University of Washington reported that CoQ10 and ascorbic acid (Vitamin C) are the two most important essential nutrients. They, along with other essential nutrients, have been rejected as unpatentable and unprofitable by certain "interests", according to expose's by Pauling and others (Pauling, 1987 and Ely, 1999). These were possibly the most lethal errors of modern medicine because no cell, organ, function, remedy, etc, can avoid failure unless essential nutrients, especially these two, are optimal. Supplementation of both is mandatory: for ascorbate, lifelong (since humans can't synthesize it); for CoQ10, it is increasingly necessary with age, stress, or disease (Ely, http://faculty.washington.edu/ely/turnover.html).

Results presented by Linnane *et al*., in 2002, indicate that CoQ10 functions as a major skeletal muscle gene regulator and as such, profoundly modulates cellular metabolism. Their data also suggested that CoQ10 treatment can act to influence the fibre type composition of muscle, toward the fibre type profile generally found in younger individuals (Linnane *et al*., 2002). Microarray gene expression analyses and differential gene display analyses demonstrated independently that the expression of a large number of genes is affected by CoQ10. Proteome analysis reflected the global gene response of CoQ10 supplementation on the protein expression profile of muscle tissue (Linnane *et al*., 2002).

Until recently, attention has been focused on requirements for CoQ10 in energy conversion in the mitochondrial compartment of cells or on the antioxidant properties of

CoQ10. New evidence shows that CoQ10 is present in other cell membranes. In the outer membrane it may contribute to the control of cell growth (Langsjoen, 1994). The membrane stabilizing property of CoQ10 has been postulated to involve the phospholipids-protein interaction that increases prostaglandin (especially prostacyclin) metabolism. It is thought that CoQ10 stabilizes myocardial calcium-dependent ion channels and prevents the depletion of metabolites essential for ATP synthesis (Greenberg *et al*., 1990). It is also thought that the isoprenoid side chain of CoQ10 may help to stabilize the lipid bilayer (Lenaz *et al*., 1999).

Triton X-100 is a well known membrane disrupter and is used extensively by cell biologists for that purpose (Macarulla *et al*., 1989). A concentration range of Triton X-100 between $5x10^{-5}$ to 0.5% has been selected in the present study to provide membrane disruption in various degrees of severity, ranging from complete cell lysis to slight membrane rupture. Triton X-100 offered the ideal membrane disrupter properties at the chosen concentration range to investigate whether CoQ10 might offer protection to cells in culture, more specifically to cell membranes exposed to disrupting agents. It was incidentally found that the chemical structure of Triton X-100 show correlation to that of nonylphenol, one of the most studied estrogen mimics that appear to interact with development in several organisms. Upon investigation, using the Recombinant Yeast Screen Assay (RCBA) for oestrogenic activity, it was found that Triton X-100 induced weak estrogenic activity. Due to the structural similarity to NPE the possibility of non receptor mediated estrogenic effects, triggered by alternative pathways in the cell that eventually elicit endocrine disruption, should be investigated. The variation in the dose-response curve shape were indistinct and obscure and were not interpretable, showing the inability to obtain repeatability with Triton X-100. The results confirmed high toxicity of Triton X-100. Further investigations should be done on the strange and indefinable properties elicited by Triton X-100.

Primary cell cultures of chick embryonic cardiac and skeletal muscle cells were successfully established using 13 day old chick embryos, as they provided significantly developed leg muscle and heart tissue. Most favourable results were obtained when the medium of the cells were not changed during the incubation period. To avoid fibroblast contamination, cells were pre-plated in flasks for 45 to 60 minutes. The advantage of using primary cultures include the ease of obtaining the tissue type that needs to be

studied, furthermore, primary cell cultures have the advantage in that they tend to retain the basic characteristics of the more complex *in vivo* system. The success of the culture establishment was confirmed by light microscopy used to investigate cell morphology. Well established populations of Crystal Violet stained cardiac and skeletal muscle cells, respectively, as well as myotube formation, a differentiation process, which arises from the fusion of mononucleated myoblasts, thought to be an irreversible process toward muscle formation (Hjiantoniou *et al*., 2007), were observed. The cell cultures provided a useful tool for studying the possible cytotoxic effects of Triton X-100 and CoQ10. Using the MTT, NR and CV assays in the form of a combined colorimetric assay, Triton X-100 showed to increase cell viability of ~ 9% in both cultures as measured by the MTT assay, to decrease lysosomal membrane integrity between 30 and 60% as measured by the NR assay, and appeared to have no significant effect on the cell number as evaluated by the CV assay. These results indicate that Triton X-100 might evoke its toxic response by mechanisms other than mitochondrial enzyme activity and cellular protein alterations. Coenzyme Q10 showed to slightly enhance mitochondrial enzyme activity, measured by the MTT assay, indicated by the average increase of ~10% in cell viability over the two cell cultures. The NR assay showed that CoQ10 disrupted an average of 47% of lysosomal membrane integrity, leading to lysosmal emptying of contents into the cytoplasm, and ultimately cell death. Coenzyme Q10 had no effect on cellular proteins as indicated by the CV assay. The results of NR assay evoked a suspicion about the reliability of the assay in the present application, since no known properties of CoQ10 indicate the ability of disrupting lysosomal membrane integrity to an extend where it will definitely induce cell death. Cytotoxicity was measured in cardiac and skeletal muscle cells pre-treated with CoQ10, two hours prior to Triton X-100 exposure at concentrations 0.05 and 0.005%, respectively, in both cell cultures by the NR assay. Cell viability was increased in both cell cultures and no effect was seen in cellular proteins, measured by the CV assay. These results indicate toxic insult to cardiac and skeletal muscle cells in culture by Triton X-100 and CoQ10, alone, and in combination.

Scanning electron microscopy is a useful method for studying the cell surface during muscle development in cell culture (Shimada, 1972). This very useful method was applied in the present study to observe the cellular alterations caused by the membrane disrupter properties of Triton X-100, at concentrations ranging form $5x10^{-5}$% to 0.5%. The results obtained reflect that of earlier studies describing the use of Triton X-100 to

extract the cytoskeletons of cells for morphological studies (Wallace *et al*., 1979 and Fulton *et al*., 1981). At the highest concentration (0.5%), we saw complete membrane lysis and, parallel to the findings of Vale et al., 1985, with PC12 cells, Triton X-100 solubilized membranes of cardiac and skeletal muscle cells and left behind a nucleus and an array of cytoskeletal filaments (Figure 5.2 b,) at a concentration of 0.5%. As the concentration of Triton X-100 decreased, the severity of membrane solubilization was decreased to where membrane tears, apoptotic blebs and membrane shrinkage was observed. At none of the concentrations of Triton X-100 tested in the study, after 24 hours of exposure, did cells in culture show any reparative actions. No remarkable differences between the cardiac and skeletal muscle cell alterations were observed. Triton X-100 is a useful tool for investigating cytoskeletal composition and properties, as indicated by the highest two concentrations (0.5 and 0.05%) used in the study, which enables the visualization of cytoskeletal components and variation in the cytoskeletal composition as the cell progress through the different phases of the cell cycle (as observed by Masuko *et al*., 1983).

No cellular or morphological damage to cardiac and skeletal muscle cells in culture were detected in the presence of the different concentrations of CoQ10 (0.2mg/ml – 0.02mg/ml) tested in the study. Cell membranes appeared smooth, intact, and most of the cells seemed to be in the process of fusion or postproliferative, which might indicate that CoQ10 might enhance the proliferation process in muscle cells. Fusion of myoblasts into myotubes were seen at 0.05 and 0.01mg/ml CoQ10 (Figure 5.17 & 5.18, and Figure 5.22 & 5.23), and not in any cultures exposed to Triton X-100 or in the control group, indicating that CoQ10 enhances the process of proliferation and syncytium formation in cardiac and skeletal muscle cells in culture. Membrane surfaces were remarkably smooth and intact, confirming the membrane stabilizing properties of CoQ10 discussed by Greenberg *et al*., 1990 and Dallner *et al*., 2000, with the presence of microvilli and small spherical protrusions, characterizing certain phases of the cell cycle. In all cells exposed to CoQ10, very distinct pores were visible (e.g. Figure 5.12; 0.2mg/ml), in some instances they appeared in larger quantities. These pores designated “ion channels” according to the literature, are clearly activated or their function is enhanced in the presence of CoQ10 to such an extend that they appear in larger numbers in an “open” state on the surface of the cell membranes. Ion channels were present at all the concentrations of CoQ10 being tested confirming the ability of

CoQ10 to maintain the integrity of myocardial calcium ion channels as described by Greenberg *et al*., 1990, Dallner *et al*., 2000, Shinde *et al*., 2005 and Terao *et al*., 2006.

In muscle cells pre-treated with the different concentrations of CoQ10 (0.02 – 0.2mg/ml) prior to exposure to 0.05% Triton X-100, membrane alteration were seen, correlating with that seen in the group of cells exposed to Triton X-100, alone. This indicates that the concentrations of CoQ10 tested, did not offer protection to muscle cells and their membranes exposed to the disrupting insult of 0.05% Triton X-100. In muscle cells exposed to 0.005% Triton X-100, a rare formation of a "membrane patch" was observed on the membrane surface of cells pre-treated with 0.05 and 0.1mg/ml CoQ10. Cell integrity of cells exposed to this concentration of Triton X-100 was retained, after pre-treatment with 0.05 – 0.1mg/ml CoQ10, indicating that CoQ10 is able to offer membrane protection to cardiac and skeletal muscle cells in culture, exposed to a concentration of 0.005% Triton X-100. Coenzyme Q10 also plays a role in the opening/activation of ion channels, and remarkably enhances the process of myotube formation in cardiac and skeletal muscle cells in culture.

The results obtained using confocal microscopy upon staining with Mito Tracker Red, DAPI and DCH_2FDA, confirmed the results on cellular morphology and structure obtained with SEM. DAPI staining of cells exposed to 0.5% - 0.005% Triton X-100, produced a blue signal showing that nuclear material was present, indicating the presence of the nuclear remnant seen with SEM upon solubilization of cells with Triton X-100. Coenzyme Q10 cleary showed to enhance the process of cell proliferation and differentiation in muscle cells, since myotube formation was only seen in the group of muscle cells treated with CoQ10. In the presence of CoQ10, cells with dividing nuclei, characteristic of the process of mitosis were seen (Figure 6.3 B, e; and Figure 6.4 A, b & d). It is possible that CoQ10 promotes mitotic formation of new cells in skeletal and cardiac muscle cells in culture. In Figure 6.3A, c & d, nuclei were very close together, characteristically of two mononucleated myoblasts fusing to form a multinucleated myotube. Confocal microscopy confirmed the process of myotube formation in the CoQ10 group. It also confirmed the possible protection CoQ10 offered to muscle cells exposed to Triton X-100. In Chapter 5, SEM images of a "membrane patch" in certain cells of which the membranes were injured by Triton X-100, after pre-treatment with CoQ10, suggested that CoQ10 offer some form of protection to the muscle cells.

Confocal microscopy produced a blue signal indicating intact nuclei, and a red signal indicating active respiring mitochondria, in muscle cells exposed to Triton X-100, after pre-treatment with CoQ10. Muscle cells in the Triton X-100 group, stained with DCH_2FDA produced a green signal, indicating the presence of ROS formation. In cells pre-treated with CoQ10, and exposed to Triton X-100 at concentrations 0.05% and 0.005%, little to no green fluorescence was obtained, indicating that CoQ10's antioxidant function was able to scavenge the free radicals produced by Triton X-100 exposure. Muscle cells in the CoQ10 group, produced no green fluorescence upon staining with DCH_2FDA, confirming that CoQ10 do not produce reactive oxygen species in cells but offer protection against it.

The study provides, in parallel with the literature, apparent evidence that CoQ10 offers protection to cardiac and skeletal muscle cells in culture after exposure to relatively low concentrations of the membrane disrupter, Triton X-100. Coenzyme Q10 also promotes the process of proliferation and differentiation in primary chick embryonic cultures of cardiac and skeletal muscle cells.

Chapter 8:References

Aberg F, Appelkvist EL, Dallner G, Ernster L. Distribution and redox state of ubiquinones in rat and human tissues. *Archives of Biochemistry and Biophysics*, 1992; **295**:230-234

Al-Hasso S. Coenzyme Q10: a review. Hosp Pharm, 2001; **36**(**1**):51-66

Allen SL, Allen JM, Light BM. Effects of Triton X-100 upon the activity of some electrophoretically separated acid phosphatases and esterases. *The Journal of Histochemistry and Cytochemistry*, 1964; **13**(**6**):434-440

Alleva R, Tomasetti M, Andera L, Gellert N, Borghi B, Weber C, Murphy MP, Neuzil J. Coenzyme Q blocks biochemical but not receptor-mediated apoptosis by increasing mitochondrial antioxidant protection. *FEBS Letters*, 2001; **503**:46-50

Aneck-Hahn NH, De Jager C, Bornman MS, Du Toit D. Oestrogenic activity using a recombinant yeast screen assay (RCBA) in South African laboratory water sources. *Water SA*, 2005; **31**(**2**):253-256

Apgar JR, Herrmann SH, Robinson JM, Mescher MF. Triton X-100 extraction of P815 tumor cells:Evidence for a plasma membrane structure. *The Journal of Cell Biology*, 1985; **100**(**5**):1369-1378

Arnold SF, Collins BM, Robinson MK, Guillette LJ, McLachlan JA. Differential interaction of natural and synthetic estrogens with extracellular binding proteins in a yeast estrogen screen. *Steroids*, 1996; **61**:642-646

Bader AV, Bader JP. Transformation of cells by rous sarcoma virus:cytoplasmic vacuolization. *Journal of Cellular Physiology*, 1976; **1**:33-46

Becher, P. Micelle formation in aqueous and nonaqueous solutions. ***In*** *Nonionic Surfactants. Surfactant Science Series*. Vol. **1.** M. J. Schick, editor. Marcel Dekker, New York, 1967; 478-515.

Becker PL. Quantitative fluorescence measurements. In *Fluorescence Imaging Spectroscopy and Microscopy*; Wang XF, Herman B, Eds.; John Wiley & Sons, Inc.:New York, 1996; 1–29

Beckman KB, Ames BN. The free radical theory of aging matures. *Physiological Reviews*, 1998; **78**:547-81

Bedner E, Li X, Gorczyca W, Melamed MR, Darzynkiewicz Z. Analysis of apoptosis by laser scanning cytometry. *Cytometry*, 1999; **35**:181-95

Begley TP, Kinsland C, Taylor S, Tandon M, Nicewonger R, Wu M, Chiu HJ, Kelleher N, Campobasso N, Zhang Y. Cofactor biosynthesis:a mechanistic perspective. *Current Chemical Reactions*, 1998; **195**:93-142

Bentinger M, Brismar K, Dallner G. The antioxidant role of coenzyme Q. *Mitochondrion*, 2007; **7S**:S41-S50

Ben-Ze'ev A, Duerr A, Solomon F, Penman S. The outer boundary of the cytoskeleton:a lamina derived from plasma membrane proteins. *Cell*, 1979; **17**:859-865

Beresford N, Routledge EJ, Harris CA, Sumpter JP. Issues arising when interpreting results from an *in vitro* assay for estrogenic activity. *Toxicology and Applied Pharmacology*, 2000 **162**:22-33

Bhagavan HN, Chopra RK. Potential role of ubiquinone (coenzyme Q10) in pediatric cardiomyopathy. *Clinical Nutrition*, 2005; **24**:331–338

Birnbaum LS. Developmental effects of dioxins. *Environmental Health Perspectives*. 1995. **103**(suppl**7**):89-94.

Bkaily G, Pothier P, D'Orléans-Juste, Simaan M, Jacques D, Jaalouk D, Belzile F, Hassan G, Boutin C, Haddad G, Neugebauer W. The use of confocal microscopy in the investigation of cell structure and function in the heart, vascular endothelium and smooth muscle cells. *Molecular and Cellular Biochemistry*, 1997; **172**:171-194

Bonetti PO, Lerman LO, Napoli C, Lerman A. Statin effects beyond lipid lowering-are they clinically relevant? *European Heart Journal*, 2003; **23**:225-248

Borman WH, Yorde DE. Analysis of chick somite myognesis by *in situ* confocal microscopy of Desmin expression. *The Journal of Histochemistry and Cytochemistry*, 1994; **42**(**2**):265-272

Boucher Y, Doolittle WF. The role of lateral gene transfer in the evolution of isoprenoid biosynthesis pathways. *Molecular Microbiology*, 2000; **37**:703-716

Bounous DI, Campagnoli RP, Brown J. Comparison of MTT Colorimetric assay and triatiated thymidine uptake for lymphocyte proliferation assays using chicken splenocytes. *Avian Diseases*, 1992; **36**:1022-1027

Bova MP, Tam D, McMahon G, Mattson MN. Troglitazone induces a rapid drop of mitochondrial membrane potential in liver HepG2 cells. *Toxicology Letters*, 2005; **155**:41-50

Boyde A, Maconnachie E. Volume changes during preparation of mouse embryonic tissue for scanning electron microscopy. *Scanning*, 1979; **2**:149-163

Brancato R, Schiavone N, Siano S, Lapucci A, Papucci L, Donnini M, Formigli L, Zecchi Orlandini S, Carella G, Carones F, Capaccioli S. Prevention of corneal keratocyte apoptosis after argon fluoride excimer laser irradiation with the free radical scavenger ubiquinone Q10. *European Journal of Ophthalmology*, 2000; **10**:32-38

Brancato R, Fiore T, Papucci L, Schiavone N, Formigli L, Zecchi Orlandini S, Gobbi PG, Carones F, Donnini M, Lapucci A, Capaccioli SJ. Concomitant effect of topical application of ubiquinone Q10 and vitamin E to prevent keratocyte apoptosis after rabbit corneal excimer laser photoablation. *Journal of Refractive Surgery*, 2002; **18**:135-9

Brand MD. The stoichiometry of proton pumping and ATP synthesis in mitochondria. *Biochemistry*, 1994; **16**:20-24

Breithofer A, Graumann K, Scicchitano MS. Karathanasis SK, Butt TR, Jungbauer A. Regulation of human estrogen receptor by phytoestrogens in yeast and human cells. *The Jounal for Steroid Biochemistry and Molecular Biology*, 1998; **67**:421429

Bretscher MS, Raff MC. Mammalian plasma membranes. *Nature*, 1975; **258**:43-49

Brown WV. Novel approaches to lipid lowering:what is on the horizon? *The American Journal of Cardiology*, 2001; **87**:23B-27B

Castro-Garza J, Barrios-García HB, Cruz-Vega DE, Said-Fernández S, Carranza-Rosales P, Molina-Torres CA, Vera-Cabrera L. Use of a colorimetric assay to measure differences in

cytotoxicity of Mycobacterium tuberculosis strains. *Journal of Medical Microbiology*, 2007; **56**:733-7

Chemical structures for Triton X-100, Nonylphenol, Nonylphenol Etoxylate: http://en.wikipedia.org

Chen H, Swedlow JR, Grote M, Sedat, JW, Agard DA. The collection, processing, and display of digital three-dimensional images of biological specimens. In *Handbook of Biological Confocal Microscopy*, 2nd Ed.; Pawley, J.B., Ed.; Plenum Press:New York, 1995; 197–210

Chevallier A, Kieny M, Mauger A. Limb-somite relationship:origin of the limb musculature. *Journal of Embryological and Experimental Morphology,* 1977; **41**:245-258.

Chini CCS, Grande JP, Chini EN, Dousa TP. Compartementalization of cAMP singaling in mesangial cells by phosphodiesterase isozymes PDE3 and PDE4 regulation of superoxidation and mitogenesis. *Journal of Biological Chemistry* 1997; **272**(**15**):9854-9859

Choi JH, Ryu YW, Seo JH. Biotechnological producton and applications of coenzyme Q10. *Applied Microbiology and Biotechnology*, 2005; **68**:9-15

Chopra RK, Goldman R, Sinatra ST, Bhagavan HN. Relative bioavailability of coenzyme Q10 formulations in human subjects. *International Journal for Vitamin and Nutrition Research*, 1998; **68**(**2**):109-113

Cimino M, Alamo L, Salazar L. Permeabilization of the mycobaterial envelope for protein cytolocalization studies by immunofluorescence microscopy. *BMC Microbiology*, 2006; **6**(**35**) doi:10.1186/1471-2180-6-35

Clarke CF. New advances in coenzyme Q biosynthesis. *Protoplasma*, 2000; **213**:134-147

Colborn T, Vom Saal FS, Soto A. Developmental effects of endocrine-disrupting chemicals in wildlife and humans. *Environmental Health Perspectives,* 1993; **101**(**5**):378-384

Coldham NG, Dave M, Sivapathasundaram S, McDonnell DP, Connor C, Sauer MJ. Evaluation of a recombinant yeast cell estrogen screening assay. *Environmental Health Perspectives*, 1997; **105**(**7**):734-742

Coleman ML, Sahai EA, Yeo M, Bosch M, Dewar A, Olson MF. Membrane blebbing during apoptosis results from caspase-mediated activation of ROCK I. *Nature Cell Biology*, 2001; **3**:339-345

Collins C, Kemper KJ. Coenzyme Q10 (CoQ10 or Ubiquinone). The *Longwood Herbal Task Force and The Center for Holistic Pediatric Education and Research*, 1999, http://www.mcp.edu/herbal/default.htm

Connoly JA. Role of the cytoskeleton in the formation, stabilization and removal of acetylcholine receptor clusters in cultured muscle cells. *The Journal of Cell Biology*, 1984; **99**(**1**):148-54.

Cook JA, Mitchell JB. Viability measurement in mammalian systems. *Analytical Biochemistry*, 1989; **179**:1-7

Crane FL, Hatefi Y, Lester RI, Widmer C. Isolation of a quinone from mitochondria. *Biochimica et Biophys Acta*, 1957; **25**:220-221

Crane FL, Morré DJ, Löw H, eds. Plasma membrane oxidoreductases in control of animal and plant growth. Plenum, New York, 1988

Crane FL, Morré DJ, Löw H, eds. Oxidoreduction at the plasma membrane:relation to growth and transport. *CRC*, Boca Raton, FL. Vol **1**. 1990

Crane FL. Focus on cellular biochemistry:New functions for coenzyme Q. *Protoplasma*, 2000; **213**:127-133

Crane FL. Biochemical functions of coenzyme Q10. *Journal of the American College of Nutrition*, 2001; **20**(**6**):591-598

Crane FL. Discovery of ubiquinone (coenzyme Q) and an overview of function. *Mitochondrion*, 2007; **7S**:S2-S7

Cunningham FX, Jr., Lafond TP, Gantt E. Evidence of a role for LytB in the nonmevalonate pathway of isoprenoid biosynthesis. *Journal of Bacteriology*, 2000; **182**:5841-5848

Dallner G, Sindelar PJ. Regulation of ubiquinone metabolism. *Free Radical Biology and Medicine*, 2000; **29**:285-294

Dayeh VR, Chow SL, Schirmer K, Lynn DH, Bols NC. Evaluating the toxicity of Triton X-100 to protozoan, fish, and mammalian cells using fluorescent dyes as indicators of cell viability. *Ecotoxicology and Evironmental Safety*, 2004; **57**:375-382

De Boever P, Demaré W, Vanderperren E, Cooreman K, Bossier P, Verstraete W. Optimization of a yeast estrogen screen and its applicability to study the release of estrogenic isoflavones from soygerm powder. *Environmental Health Perspectives*, 2001; **109**(**7**):691-697

Deamer DW, Crofts A. Action of Triton X-100 on chloroplast membranes. Mechanisms of structural and functional disruption. *The Journal of Cell Biology*, 1967; **33**(**2**):395-410

DeHahn T, Barr R, Morrè DJ. NADH oxidase activity present on both the external and internal surfaces of soybean plasma membranes. *Biochimica et Biophysica Acta*, 1997; **1328**:99-108

Denk W, Horstmann H. Serial block-face scanning electron microscopy to reconstruct three-dimensional tissue nanostructure. *PLoS Biology*, 2004; **2**(**11**):e329

Dennis E. Kinetic dependence of phospholipase A_2 activity on the detergent Triton X-100. *Journal of Lipid Research*, 1973; **14**:152-159

DiMauro S, Quinzii CM, Hirano M. Mutations in coenzyme Q10 biosynthetic genes. *The Journal of Clinical Investigation*, 2007; **117**(**3**):587-589

Do TQ, Hsu AY, Jonassen T, Lee PT, Clarke CF. A defect in coenzyme Q biosynthesis is responsible for the respiratory deficiency in *Saccharomyces cerevisiae* abc1 mutants. *The Journal of Biological Chemistry*, 2001; **276**:18161-18168

Dunahay TG, Staehelin LA, Scibert M, Ogilvie PD, Berg SP. Structural, biochemical, and biophysical characterization of four oxygen-evolving photosystem II preparations from spinach. *Biochimica et Biophysica Acta*, 1984; **764**:179-193

Dunn KW, Wang E, Murray JM, Paddock SW, Hazen EJ, DeVries J, Pawley JB, Piston DW, Spring KR, Parry-Hill MJ, Fellers TJ, Davidson MW. Laser Scanning Confocal Microscopy. *Molecular Expressions*™, 2006; **258**:43-49

Ehler E, Rother BM, Hämmrle SP, Komiyama M, Perriard J. Myofibrillogenesis in the developing chicken heart:assembly of Z-disk, M-line and the thick filaments. *Journal of Cell Sciences*, 1999; **112**:1529-1539

Eisenreich W, Bacher A, Arigoni D, Rohdich F. Biosynthesis of isoprenoids via the non-mevalonate pathway. *Cellular and Molecular Life Sciences*, 2004; **61**:1401-1426

Eisenreich W, Rohdich F, Bacher A. Deoxyxylulose phosphate pathway to terpenoids. *Trends in Plant Science*, 2001; **6**:78-84

Elinder F, Nilsson J, Århem P. On the opening of voltage-gated ion channels. *Physiology and Behavior*, 2007; **92**:1-7

Ely JTA: Ascorbic acid and some other modern analogs of the germ theory. *Journal of Orthomolecular Medicine*. 1999; **14**:143-156

Ely JTA. Urgent update on Ubquinone (Coenzyme Q10).
http://faculty.washington.edu/ely/turnover.html

Ernster L, Dallner G. Biochemical, physiological and medical aspects of ubiquinone function. *Biochemica et Biophysica Acta*, 1995; **1271**:195-204

Escolar M, et al., Research Center for Genetic Medicine, Children's Research Institute, Washington. *CNMC0301*:An open-label pilot study of Coenzyme Q10 in steroid-treated Duchenne muscular dystrophy. 2001; Amendment 2 (07/15/01):1-43

Fambrough DM, Devreotes PN. Newly synthesized acetylcholine receptors are located in the Golgi apparatus. *Journal of Cell Biology*, 1978; **76**:237-244

Fang S, Christensen J, Conklin JL, Murray JA, Clark G. Roles of Triton X-100 in NADPH-diaphorase histochemistry. *The Journal of Histochemistry and Cytochemistry* 1994; **42**(**11**):1519-1524

Fernández-Ayala DJM, López-Lluch G, García-Valdés M, Arroyo A, Navas P. Specificity of coenzyme Q10 for a balanced function of respiratory chain and endogenous ubiquinone biosynthesis in human cells. *Biochimica et Biophysica Acta*, 2005; **1706**:174-183

Folkers K. The potential of coenzyme Q10 (NSC-140865) in cancer treatment. *Cancer Chemotherapy Reports*, 1974; **4**:19-23

Folkers K, Vadhanavikit S, Mortensen SA. Biochemical rationale and myocardial tissue data on the effective therapy of cardiomyopathy with coenzyme Q10. *Proceedings of the National Academy of Sciences of the United States of America*, 1985; **82**:901-904

Folkers K. Relevance of the biosynthesis of coenzyme Q10 and of the four bases of DNA as a rationale for the molecular causes of cancer therapy. *Biochemical and Biophysical Research Communications*, 1996; **224**:358-361

Fonorow OR. CoQ10 and statins: the vitamin connection. From *The Townsend Letter, the Examiner of Alternative Medicine*, February/March 2006; http://www.townsendletter.com/FebMar006/coq100206.htm

Fontaine E, Bernardi P. Progress on the mitochondrial permeability transition pore:regulation by complex I and ubiquinone analogs. *Journal of Bioenergetics and Biomembranes*, 1999; **31**:335-345

Forsgren M, Attersand A, Lake S, Grunler J, Swiezewska E, Dallner G, Climent I. Isolation and functional expression of human COQ2, a gene encoding a polyprenyl transferase involved in the synthesis of CoQ. *The Biochemical Journal*, 2004; **382**:519–526

Frank D, Kuhn C, Katus HA, Frey N. The sarcomeric Z-disc:a nodal point in signalling and disease. *Journal of Molecular Medicine*, 2006; **84**:446-468

Fresheny RI. Culture of animal cells: a manual of basic technique, 3rd edition. New York:Wiley-Liss. 1994

Fuke C, Krikorian SA, Couris RR. Coenzyme Q10: A review of essential functions and clinical trials. *US Pharmacist.* A Johnson publication. 2002; 25:10 http://www.uspharmacist.com/oldformat.asp?url=newlook/files/comp/acfaa8.htm

Fulton AB, Prives J, Farmer SR, Penman S. Developmental reorganization of the skeletal framework and its surface lamina in fusing muscle cells. *The Journal of Cell Biology*, 1981; **91**:103-112

Gartner LP, Hiatt JL. Color textbook of Histology. 3rd edition (International edition). Saunders Elsevier. Philadelphia, 2007

Gazdik F, Gvozdjáková A, Nádvorníková R, Repická L, Jahnová E, Kucharská J, Piják MR, Gazdíková K. Decreased levels of coenzyme Q10 in patients with bronchial asthma. *Allergy*, 2002; **57**:811-814

Ge L, Zhang X, Guo R. Microstructure of Triton X-100/poly (ethylene glycol) complex investigated by fluorescence resonance energy transfer. *Polymer*, 2007; **48**:2681-2691

Gempel K, Topaloglu H, Talim B, Schneiderat P, Schoser BGH, Hans VH, Pálmafy B, Kale G, Tokatli A, Quinzii C, Hirano M, Naini A, DiMauro S, Prokisch H, Lochmüller H, Horvath R. The myopathic form of coenzyme Q10 deficiency is caused by mutations in the electron-transferring-flavoprotein dehydrogenase (ETFDH) gene. *Brain*, 2007; [ePub ahead of print PMID 17412732]

Gerlier D, Thomasset N. Use of MTT colorimetric assay to measure cell activation. *Journal of Immunological Method*s, 1986; **94**:57-63.

Geromel V, Darin N, Chrétien D, Bénit P, DeLonlay P, Rötig A, Munnich A, Rustin P. Coenzyme Q10 and idebenone in the therapy of respiratory chain diseases. *Molecular Genetics and Metabolism*, 2002; **77**:21-30

Gille L, Nohl H. The existence of a lysosomal redox chain and the role of ubiquinone. *Archives of Biochemistry and Biophysics*, 2000; **375**:347–354

Gillies RJ, Didier N, Denton M. Determination of cell number in monolayer cultures. *Analytical Biochemistry*, 1986; **159**:109–113

Giraudo CG, Eng WS, Melia TJ, Rothman JE. A clamping mechanism involved in SNARE-dependent exocytosis. *Science*, 2006; **313**:676–680

Goewert RR. Studies on the biosynthesis of ubiquinone. Saint Louis University, St. Louis, MO, 1980

Goldman R D, Berg G, Bushnell A, Chang CM, Dickerman L, Hopkins N, Miller ML, Pollack R, Wang E. Fibrillar systems in cell motility. *Ciba Foundation Symposium, 1973*; **14:**83-103

Goldstein JL, Brown MS. Regulation of the mevalonate pathway. *Nature*, 1990; **343**:425-430

Gómez-Díaz C, Barroso MP, Navas P. Plasma membrane coenzyme Q10 and growth control. *Protoplasma*, 2000; **214**:19-23

Green DR, Reed JC. Mitochondria and apoptosis. *Science*, 1998; **281**:1309-1312

Greenberg S, Frishman WH. Coe-enzyme Q10:a new drug for cardiovascular disease. *Journal of Clinical Pharmacology*, 1990; **30**:569-608

Grishko V, Solomon M, Breit JF, Killilea DW, Ledoux SP, Wilson GL, Gillespie MN. Hypoxia promotes oxidative base modifications in the pulmonary artery endothelial cell VEGF gene. *The Federation of American Societies for Experimental Biology Journal*, 2001; **15**:1267-1269

Grivennikova VG, Maklashina EO, Gavrikova EV, Vinogradov AD. Interaction of the mitochondrial NADH-ubiquinone reductase with rotenone as related to the enzyme active/inactive transition. *Biochimica et Biophysica Acta*, 1997; **1319**:223-232

Grünler J, Ericcson J, Dallner G. Branch-point reations in the biosynthesis of cholesterol, dolichol, ubiquinone and prenylated proteins. *Biochimica et Biophysica Acta*, 1994; **1212**:259-277

Häcker G. The morphology of apoptosis. *Cell and Tissue Research*, 2000; **301**:5-17

Hamburger V, Hamilton HL. A series of normal stages in the development of the chick embryo. *Journal of Morphology*, 1951; **88**(**1**):49-92

Hanke LD, technical staff of Materials Evaluation and Engineering, Inc. (MEE). *Handbook of analytical methods for materials*. Materials Evaluation and Engineering, Inc., Plymouth., 2006; www.mee-inc.com

Harmon D. Free radicals in aging. *Molecular and Cellular Biochemistry*, 1988; **84**:1 55-166

Harris M, Zacharewski T, Safe S. Effects of 2,3,7,8-tetrachlorodibenzo-pdioxin and related compounds on the occupied nuclear estrogen receptor in MCF-7 human breast cancer cells. *Cancer Research*, 1990; **50**:3579-3584

Harrison ML, Rathinavelu P, Arese P, Geahlin RL, Low PS. Role of band 3 tyrosine phosphorylation in the regulation of erythrocyte glycolysis. *The Journal of Biological Chemistry*, 1991; **266**:4106-4111

Hauβ T, Dante S, Haines TH, Dencher NA. Localization of coenzyme Q10 in the center of a deuterated lipid membrane by neutron diffraction. *Biochimica et Biophysica Acta*. 2005; **1710**:57-62

Hayashi YK. Membrane-repair machinery and muscular dystrophy. *The Lancet*, 2003; **362**:843-844

Herman BA, Fernandez SM. Changes in membrane dynamics associated with myogenic cell fusion. *Journal of Cellular Physiology*, 1978; **94**:253-264

Hibbs A. Confocal Microscopy for Biologists:An Intensive Introductory Course. BIOCON ed., 2000; 2-9.

Hipler U.C., Wollina U., Denning D., Hipler B. Fluorescence analysis of reactive oxygen species (ROS) generated by six isolates of *aspergillus fumigatus*. *BMG Labtechnologies* 2002; Application Note:**105**

Hjiantoniou E, Anayasa M, Nicolaou P, Bantounas I, Saito M, Iseki S, Uney JB, Phylactou LA. 2007. Twist induces reversal of myotube formation. *Differentiation* (OnlineEarly Articles). doi:10.1111/j.1432-0436.2007.00195.x

Horowitz S. Coenzyme Q10: one antioxidant, many promising applications. *Alternative and Complementary Therapies*, 2003; 9(3):111–116

http://www.vitacost.com/NSI-CoQ10-Q-Gel-Mega

Huang HL, Singer RH, Lazarides E. Actin-containing microprocesses in the fusion of cultured chick myoblasts. *Muscle and Nerve*, 1978; **1**:219-229

Hunte C, Palsdottir H, Trumpower BL. Protonmotive pathways and mechanisms in the cytochrome bc_1 complex. *FEBS Letters*, 2003; **545**:39-46

Huxley HE. Electron-microscope studies on the structure of natural and synthetic membranes. *Science,* 1963; **175**:720-731

Introduction to dose-response curves. GraphPad Software, 1999. www.curvefit.com

Invitrogen™. http://probes.invitrogen.com/lit/catalog/3/sections/1919.html

Ishikawa H, Bischoff R, Holtzer H. Formation of arrowhead complexes with heavy meromyosin in a variety of cell types. *Journal of Cell Biology,*1969*;* **43**:312-328.

Ishiyama M, Tominaga H, Shiga M, Sasamoto K, Ohkura Y, Ueno K, Watanabe M. Novel cell proliferation and cytotoxicity assays using a tetrazolium salt that produce formazan dye. *In Vitro Toxicology*, 1995; **8**:187-190

Ishiyama M, Tominaga H, Shiga M, Sasamoto K, Ohkura Y, Ueno K. A combined assay of cell viability and in vitro cytotoxicity with a high water-soluble tetrazolium sal, Neutral Red and Crystal Violet. *Biological and Pharmaceutical Bulletin*, 1996; **19**(**11**):1518-20

Ishizaki Y, Cheng L, Mudge AW, Raft MC. Programmed cell death by default in embryonic cells, fibroblasts and cancer cells. *Cellular and Molecular Biology*, 1995; **6**:1443-1458

Jayadev S, Liu B, Bielawska AE, Lee JY, Nazaire F, Pushkareva MY, Obeid and LM, Hannun YA. Role for ceramide in cell cycle arrest, *The Journal of Biological Chemistry,* 1995; **270**:2047–2052.

Jonassen T, Clarke CF. Genetic analysis of coenzyme Q biosynthesis. In:Kagan VE, Quinn PJ (Eds.), Coenzyme Q:Molecular mechanisms in health and diseases. Crc Press, Boca Raton FL, 2001

Kagan V, Serbinova E, Packer L. Antioxidant effects of ubiquinones in microsomes and mitochondria are mediated by tocopherol recycling. *Biochemical and Biophysical Research Communications*, 1990; **169**:851-857

Kagan VE, Nohl H, Quinn PJ. Coenzyme Q: its role in scavenging and generation of radicals in membranes, in: *Handbook of Antioxidants*, E. Cadenas and L. Packer, eds, Marcel Dekker, Inc., New York, 1996; 157–201

Kagan T, Davis C, Lin L, Zakeri Z. Coenzyme Q10 can in some circumstances block apoptosis and this effect is mediated through the mitochondria. *Annals of the New York Academy of Sciences*, 1999; **887**:31-47

Kalderon N, Gilula NB. Membrane events involved in myoblast fusion. *Journal of Cell Biology*, 1979; **81**:411-425

Kalin A, Norling B, Appelkvist EL, Dallner G. Ubiquinone synthesis in the microsomal fraction of rat liver. *Biochimica et Biophysica Acta*, 1987; **926**:70-78

Kanduc D, Mittelman A, Serpico F, et al., Cell death:Apoptosis versus necrosis (review). *International Journal of Oncology*, 2002; **21**:165-170

Karlsson J, Diamant B, Theorell H, Folkers K. Ubiquinone and alpha-tocopherol in plasma; means of translocation or depot. *Clinical Investigations,* 1993; **71**:S84-S91.

Kawamukai M. Biosynthesis, bioproduction and novel roles of ubiquinone. *Journal of Bioscience and Bioengineering*, 2002; **94**(**6**):511-517

Kierzenbaum AL. Histology and cell biology:an introduction to pathology. 2nd edition. Mosby Elsevier. Philadelphia, PA, 2007

Kim H, Lee TH, Park ES, Suh JM, Park SJ, Chung HK, Kwon OY, Kim YK, Ro HK, Shong M Role of peroxiredoxins in regulating intracellular hydrogen peroxide and hydrogen peroxide-induced apoptosis in thyroid cells. *Journal of Biololgical Chemistry,* 2000; **276**(**24**):18266-18270

Kirat KE, Morandat S. Cholesterol modulation of membrane resistance to Triton X-100 explored by atomic force microscopy. *Biochimica et Biophysica Acta*, 2007; 1768(9):2300-2309

Klein KO, Baron J, Colli MJ, McDonnell D, Cutler GB. Estrogen levels in childhood determined by an ultrasensitive recombinant cell bioassay. *The Journal of Clinical Investigation*, 1994; **94**:2475-2480

Klotz MD, Beckman BS, Hill SM, McLachlan JA, Walters MR, Arnold SF. Identification of environmental chemicals with estrogenic activity using a combination of *in vitro* assays. *Environmental Health Perspectives*, 1996; **104**(**10**):1084-1089

Konieczny SF, Lawrence JB, Coleman JR. Analysis of muscle protein expression in polyethylene glycol-induced chicken:rat myoblast heterokaryons. *The Journal of Cell Biology*, 1983; **97**:1348-55

Kőszegi T, Petrik J, Vladimir-Kneževíc S, Nagy S. Co-determination of ATP and proteins in Triton X-100 non-ionic detergent-opened monolayer cultured cells. *Luminescence*, 2007; 22(5):415-419

Kueng W, Silber E, Eppenberger U. Quantification of cells cultured on 96-well plates. *Analytical Biochemistry*, 1989; **185**:16-19

Kuzuyama T. Mevalonate and non-mevalonate pathways for the biosynthesis of isoprene units. *Bioscience, Biotechnology, and Biochemistry*, 2002; **66**:1619-1627

Lammerding J, Lee RT. Torn apart:membrane rupture in muscular dystrophies and associated cardiomyopathies. *The Journal of Clinical Investigation*, 2007; **117**(**7**):1749-1752

Lange BM, Rujan T, Martin W, Croteau R. Isoprenoid biosynthesis:the evolution of two ancient and distinct pathways across genomes. *Proceedings of the National Academy of Sciences of the United States of America*, 2000; **97**:13172-13177

Langsjoen PH. Introduction to Coenzyme Q10, 1994.
http://faculty.washington.edu/ely/coenzq10.html

Langsjoen PH, Langsjoen AM. Overview of the use of CoQ10 in cardiovascular disease. *Biofactors*, 1999; **9**:273-284

Laniado ME, Abel PD, Lalani E-N. Ion channels:new explanations for old diseases. Imperial School of Medicine, Hammersmith Hospital, London, 1997

Larm JA, Vaillant F, Linnane AW, Lawen A. Up-regulation of the plasma membrane oxidoreductase as a prerequisite for the viability of human namalwa ρ^0 cells. *The Journal of Biological Chemistry*, 1994; **269**:30097-30100

Le Ber I, Moreira MC, Rivaud-Pechoux S, et al. Cerebellar ataxia with oculomotor apraxia type 1: clinical and genetic studies. *Brain*, 2003; **126**:2761-2772

Le Ber I, Dubourg O, Benoist JF, Jardel C, Mochel F, Koenig M, Brice A, Lombès A, Dürr A. Muscle coenzyme Q10 deficiencies in ataxia with oculomotor apraxia 1. *Neurology*, 2007; **68**:295-297

Lemasters JJ, Chacon E, Zahrebelski G, Reece JM, Nieminen AL:Laser scanning confocal microscopy of living cells. In:B Herman and JJ Lemasters (eds). Optical *microscopy:Emerging Methods and Applications*. Academic Press, New York, 1993; 339–354

Lenaz G, Faro R, DeBernado S, Jarreta D, Costa A, Genova ML, Parenti Castelii G. Location and mobility of coenzyme Q in lipid bilayers and membranes. *Biofactors*, 1999; **9**:87-94

Linnane AW, Kopsidas G, Zhang C, Yarovaya N, Kovalenko S, Papakostopoulos P, Eastwood H, Graves S, Richardson M. Cellular redox activity of coenzyme Q10:Effect of CoQ10 supplementation on human skeletal muscle. *Free Radical Research*, 2002; **36**(**4**):445-453

Littarru GP, Ho L, Folkers K. Deficiency of coenzyme Q10 in human heart disease. Part I and II. *International Journal of Vitamins and Nutritional Research*, 1972; **42**(**2**):291-305

López LC, Schuelke M, Quinzii CM, Kanki T, Rodenburg RJT, Naini A, DiMauro S, Hirano M. Leigh syndrome with nephropathy and CoQ10 deficiency due to decaprenyl diphosphate synthase subuinit 2 (PDSS2) mutations. *The American Journal of Human Genetics*, 2006; **79**:1125-1129

López-Lluch G, Barroso MP, Martín SF, Fernández-Ayala DJM, Gómez-Díaz C, Villalba JM, Navas P. Role of plasma membrane coenzyme Q on the regulation of apoptosis. *BioFactors*, 1999; **9**:171-177

Lyons GE. Vertebrate heart development. *Current Opinion in Genetics and Development, 1996;* **6**:454-460

Macarulla JM, Alonso A, Gonzales-Manas JM, Goni FM, Gurtubay JI, Prado A, Urbaneja MA. 1989. Membrane solubilization by the non-ionic detergent triton X-100. A comparative study including model and cell membranes. *Revista Espanola de Fisiologia*. 45:suppl:1-8

Mader SS. Biology, 7th Edition, McGraw-Hill Education, New York, NY 10020, 2001

Marquardt H. *Toxicology*. London:Academic Press, 1999

Masuko S, Ishikawa Y. Changes in surface morphology of myogenic cells during the cell cycle, fusion and myotube formation. *Developmental Growth and Differentiation*, 1983; **25**(**1**):65-73

Matthiessen P, Sumpter JP. Effects of estrogenic substances in the aquatic environment. In:*Fish Ecotoxicology*. Switzerland:Birkhäuser Verlag, Basel, 1998; 319-335

McCain ER, McLaughlin JS. Developmental and physiological aspects of the chicken embryonic heart. Pages 85-100, *in* Tested studies for laboratory teaching, Volume **20** (S. J. Karcher, Editor). *Proceedings of the 20th Workshop/Conference of the Association for Biology Laboratory Education (ABLE)*, 1999; 399

McDonnell DP, Nawaz *Z,* Densmore C, Weigel NL, Pham TA, Clark JH, O'Malley BW. High level expression of biologically active estrogen receptor in *Sarcharomyces cereuisiae. The Journal of Steroid Biochemistry and Molecular Biology*, 1991a; **39**:291-297

McDonnell DP, Nawaz *Z,* O'Malley BW. In *situ* distinction between steroid receptor binding and transactivation at a target gene. *Molecular and Cellular Biology*, 1991b; **11**:43504355

McNeil PL, Steinhardt RA. Plasma membrane disruption:repair, prevention, adaptation. *Annual Review of Cell and Developmental Biology,* 2003; **19**:697–731

McNeil PL, Kirchhausen T. An emergency response team for membrane repair. *Nature Reviews. Molecular Cell Biology,* 2005; **6**:499–505

Meganathan R. Ubiquinone biosynthesis in microorganisms. *FEMS Microbiology Letters*, 2001; **203**:131-139

Mellors A, Tappel AL. The inhibition of mitochondrial peroxidation by ubiquinones and ubiquinol. *Journal of Biological Chemistry*, 1966; **241**:4353-4356

Mescher MF, Jose MJL, Balk SP. Actin containing matrix associated with the plasma membrane of murine tumor and lymphoid cells. *Nature*, 1981; **289**:139-144

Minsky M. Memoir on inventing the confocal microscope. *Scanning,* 1988; **10**:128–138.

Misner B. Ubiquinone biosynthesis:coenzyme Q-10 impacts health and aerobic metabolism. *Journal of Endurance*. December 2005; **12**:1-27

Mitchell P. Protonmotive redox mechanism of the cytochrome *b-cl* complex in the respiratory chain:protonmotive ubiquinone cycle. *FEBS Letters*, 1975a; **56**:1-6

Mitchell P. The protonmotive Q cycle:a general formulation. *FEBS Letters*, 1975b; **59**(**2**):137-139

Mitchell P. The classical mobile carrier function of lipophilic quinones in the osmochemistry of electron driven proton translocation. In:Lenaz G, Bernabei D, Rabbi A, Battino M (eds) Highlights in ubiquinone research. Taylor and Francis, London,1990; 77-82

Mollet J, Giurgea I, Schlemmer D, Dallner G, Chretien D, Delahodde A, Bacq D, de Lonlay P, Munnich A, Rötig A. Prenyldiphosphate synthase, subunit 1 (PDSS1) and OH- benzoate polyprenyltransferase (COQ2) mutations in ubiquinone deficiency and oxidative phosphorylation disorders. *The Journal of Clinical Investigation*, 2007; **117**(**3**):765-772

Mortensen SA, Perspectives on therapy of cardiovascular diseases with coenzyme Q10 (ubiquinone). *The Journal of Clinical Investigation,* 1993; **71**:116–123

Morton RA, Wilson GM, Lowe JS, Leat WMF. Ubiquinone. Chemical Industry, London, 1957:1649

Mossman T. Rapid colorimetric assay for cellular growth and survival:Application to proliferation and cytotoxicity assays. *Journal of Immunological Methods*, 1983; **65**:55-63

Munetaka I, Tominaga H, Shiga M, Kazumi S, Yosuke O, Keiyu U. A combined assay of cell viability and *in vitro* cytotoxicity with a highly water soluble tetrazolium salt, neutral red and crystal violet. *Biological and Pharmaceutical Bulletin*, 1996; **10**:1518-1520

Murphy DJ, Prinsley RT. Interaction of Triton X 100 with the pigment-protein complexes of photosynthetic membranes. *The Biochemical Journal*, 1985; **229**:31-37

Murray F. 100 Super supplements for longer life. Los Angeles:Keats Publishing. 2000

Mutter KL. Prescribing antioxidants. In:Rakel D, ed. *Integrative Medicine*. Philadelphia:Saunders, 2003

Naderi J, Somayajulu-Nitu M, Mukerji A, Sharda P, Sikorska M, Borowy-Borowski H, Antonsson B, Pandey S. Water-soluble formulation of coenzyme Q10 inhibits Bax-induced destabilization of mitochondria in mammalian cells. *Apoptosis*, 2006; **11**(**8**):1359-1369

Nambudiri AMD, Brockman D, Alam SS, Rudney H. Alternate routes for ubiquinone biosynthesis in rats. *Biochemical and Biophysical Research Communications*, 1977; **76**:282-288

Natural Resources Defense Council, 1998, http://www.nrdc.org/health/effects/qendoc.asp

Nohl H, Kozlov AV, Staniek K, Gille L. The multiple functions of coenzyme Q. *Bioorganic Chemistry*, 2001; **29**:1-13

O'Neill MC, Stockdale FE. A kinetic analysis of myogenesis *in vitro*. *The Journal of Cellular Biology*, 1972; **52**:52-65

Okamoto T, Kubota N, Takahata K, Takahashi T, Goshima K, Kishi T. Protective effect of coenzyme Q10 on cultured skeletal muscle cell injury induced by continuous electric field stimulation. *Biochemical and Biophysical Research Communications*, 1995; **216**(**3**):1006-1012

Okazaki K, Holtzer H. Myogenesis: fusion, myosin synthesis, and the mitotic cycle. *Proceedings of the National Academy of Sciences of the United States of America*, 1966; **56**:1484-1490

Papa S, Schulachev VP. Reactive oxygen species, mitochondria, apoptosis and aging. *Molecular and Cellular Biochemistry*, 1997; **174**:305-319

Papucci L, Schiavone N, Witort E, Donnini M, Lapucci A, Tempestini A, Formigli L, Zecchi-Orlandini S, Orlandini G, Carella G, Brancato R, Capaccioli S. Coenzyme Q10 prevents apoptosis by inhibiting mitochondrial depolarization independently of its free radical scavenging property. *Journal of Biological Chemistry*, 2003; **278**(**30**):28220-28228

Pariete JL, Kim BS, Atala A. *In vitro* biocompatibility evaluation of naturally derived and synthetic biomaterials using normal human bladder smooth muscle cells. *Journal of Urology*, 2002; **164**:1867-1871

Parish CR, Müllbatcher M. Automated colorimetric assay for T cell cytotoxicity. *Journal of Immunological Methods*, 1983; **58**:225-237

Pauling LJ: How to live longer and feel better. New York, Avon Books, 1987; 413

Pham TA, Hwung Y-P, McDonnell DP, O'Malley BW. Transactivation functions facilitate the disruption of chromatin structure by, estrogen receptor derivatives *in vivo. Journal of Biological Chemistry*, 1991; **266**:18179-18187

Picache ER, Hassanieh L, Broek D, Schönthal AH. Inhibition of tumour cell growth by Triton X-100 through specific effects on cell-cycle-regulatory components. *Journal of Biomedical Science*, 2004; **11**:95-103

Pizon V, Gerbal F, Cifuentes Diaz C, Karsenti E. Microtubule-dependent transport and organization of sarcomeric myosin during skeletal muscle differentiation. *The EMBO Journal*, 2005; **24**:3781-3792

Post G. The History And Usefulness Of Coenzyme Q10. *EzineArticles,* 2005 http://ezinearticles.com/?The-History-And-Usefulness-Of-Coenzyme-Q10&id=14231

Poulter CD, Rilling HC. Prenyl transferases and isomerases. In:Porter JW, Spurgeon SL, eds. *Biosynthesis of isoprenoid compounds*. New York:John Wiley, 198; 161-224

Prives J, Shinitzky M. Increased membrane fluidity precedes fusion of muscle cells. *Nature,* 1977; **268**:761-763

Prives J, Christian C, Penman S, Olden K. Neuronal regulation of muscle acetylcholine receptors:role of muscle cytoskeleton and receptor carbohydrate. In *Tissue Culture in Neurobiology*. Giacobini E, Vernadakis A, Shabar A, editors. Raven Press, New York, 1980; 35-52

Prives J, Fulton AB, Penman S, Daniels MP, Christian CN. Interaction of the cytoskeletal framework with actylcholine receptor on the surface of embryonic muscle cells in culture. *The Journal of Cell Biology*, 1982; **92**(**1**):231-236.

Pudney JA, Singer RH. Intracellular filament bundles in whole mounts of chick and human myoblasts extracted with Triton X-100. *Tissue & Cell*, 1980; **12**:595-612

Quinzii CM, DiMauro S, Hirano M. Human coenzyme Q10 deficiency. Neurochemical Research, 2007a; **32**:723-727

Quinzii CM, Hirano M, DiMauro S. CoQ10 deficiency diseases in adults. *Mitochondrion*, 2007b; **7S**:S122–S126

Qureshi N, Porter JW. Conversion of acetyl-coenzyme A to ispentyl pyrophosphate. *Biosynthesis of Isoprenoid Compounds*, 1981; **1**:47-94

Reed JC. Mechanism of apoptosis. *American Journal of Pathology*, 2000; **157**(**5**):1415-1430

Roche Molecular Biochemicals. Apoptosis and cell proliferation. Cell death – apoptosis and necrosis. 2nd. Rev.ed. *Roche*:1-63

Roche. http://www.roche-applied-science.com/pack-insert/1332481a.pdf

Routledge EJ, Sumpter JP. Estrogenic activity of surfactants and some of their degradation products assessed using a recombinant yeast screen. *Environmental Toxicology and Chemistry*, 1996; **15**(**3**):241-248.

Rundek T, Naini A, Sacco R, Coates K, DiMauro S. Atorvastatin decreases the coenzyme Q10 level in the blood of patients at risk for cardiovascular disease and stroke. *Archives of Neurololgy*, 2004; **61**:889-892

Shinde S, Patil N, Tendolkar A. Coenzyme Q10: A Review of Essential Functions. *The Internet Journal of Nutrition and Wellness.* 2005; **1**(**2**): http://www.ispub.com/ostia/index.php?xmlFilePath=journals/ijnw/archives.xml

Scivittaro V, Ganz MB, Weiss MF. Age induce oxidative stress and activate protein kinase C-II in neonatal mesanglial cells. *American Journal of Renal Physiology,* 2000; **278**:F676-F683

Semwogerere D, Weeks ER. Confocal Microscopy. *Encyclopedia of Biomaterials and* Biomedical Engineering, Taylor and Francis, London, 2005; 1-10

Sgouras D, Duncan R. Methods for evaluation of biocompatibility of soluble synthetic polymers which have potential for biomedical use: Use of tetrazolium-based colorimetric

assay (MTT) as a preliminary screen for evaluation of *in vitro* cyotoxicity. *Journal of Material Sciences. Materials in Medicine*, 1990; 1:61-68

Sheppard CJR, Shotton DM. Confocal fluorescence microscopy. In *Confocal Laser Scanning Microscopy*; Springer-Verlag New York Inc.:New York, 1997; 61–70

Shimada Y. Scanning electron microscopy of myogenesis in monolayer culture: a preliminary study. *Developmental Biology*, 1972; **29**:227-233

Sies H. Oxidative stress:oxidants and antioxidants. *Experimental Physiology*, 1997; **82**:291-295

Sigma Product Information Sheet, http://www.snowpure.com/docs/triton-x-100-sigma.pdf

Silverthorn DU. Human physiology: an integrated approach, 3rd Edition, Pearson Education, Inc. San Francisco, 2004

Singer SJG, Nicolson L. The fluid mosaic model of the structure of cell protein filaments from striated muscle. *Journal of Molecular Biology,* 1972; **7**:281-308

Singer RH, Pudney JA. Filament-directed intercellular contacts during differentiation of cultured chick myoblasts. *Tissue and Cell*, 1984; **16**:17-29

Slater TF, Sawyer B, Strauli U. Studies on succinate-tetrazolium reductase systems III Point of coupling of four different tetrazolium salts. *Biochimica et Biophysica Acta*, 1963; **77**:383-393

Sohal R, Forster MJ. Coenzyme Q, oxidative stress and aging. *Mitochondrion*, 2007; **7S**:S103-S111

Soto AM, Sonneschein C, Chung KL, Fernandez MF, Olea N, Serrano FO. The E-screen assay as a tool to identify estrogens - an update on estrogenic environmental pollutants. *Environmental Health Perspectives*, 1995; **103** (Suppl. **7**):113-122

Sperelakis N, Shigenobu K. Changes in membrane properties of chick embryonic hearts during development. *The Journal of General Physiology*, 1972; **60**:430-453

Stadtman ER, Levine RL. Protein oxidation. *Annals of the New York Academy of Sciences*, 2000; **899**:191-208

Stya M, Axelrod D. Mobility and detergent extractability of acetylcholine receptors on cultured rat myotubes:a correlation. *Journal of Cell Biology*, 1983; **97**:48-51

Sultan K, Haagsman H. Species-specific primary cell cultures:a research tool in veterinary science. *Veterinary Sciences Tomorrow*, 2001; **1**:1-7

Sun IL, Sun EE, Crane FL, Morré DJ, Lindgren A, Löw H. Requirement for coenzyme Q in plasma membrane electron transport. *Proceedings of the National Academy of Sciences of the United States of America*, 1992; **89**:11126-11130

Tank DW, Wu E-S, Webb WW. 1982. Enhanced molecular diffusibility in muscle blebs:release of lateral constraints. *Journal of Cell Biology*, 1982; **92**:207-212

Teclebrhan H, Olsson J, Swiezewska E, Dallner G. Biosynthesis of the side chain of ubiquinone:transprenyltransferase in rat liver microsomes. *Journal of Biological Chemistry*, 1993; **268**:23081-23086

Terao K, Nakata D, Fukumi H, Schmid G, Arima H, Hirayama F, Uekama K. Enhancement of oral bioavailability of coenzyme Q10 by complexation with γ-cyclodextrin in healthy adults. *Nutrition Research*, 2006; **26**:503-508

Timbrell JA. Principles of Biochemical Toxicology. Taylor & Francis, London, 2000

Tokuyasu KT, Maher PA. Immunocytochemical studies of cardiac myofibrillogenesis in early chick embryos. I. Presence of immunofluorescent titin spots in premyofibril stages. *Journal of Cellular Biology,* 1987; **105**:2781-2793

Tomono Y, Hasegawa J, Seki T, Motegi K, Morishita N. Pharmacokinetic study of deuterium labelled coenzyme Q10 in man. *International Journal of Clinical Pharmacology, Therapy, and Toxicology,* 1986; **24**:536-41

Toppari J, Larsen JC, Christiansen P, Giwercman A, Grandjean P, Guilette LJ (Jr.), Jégou B, Jensen TK, Jounnet P, Keiding N, Leffers H, McLachlan JA, Meyer O, Müller J, Rajpert-De Meyts E, Scheike T, Sharpe R, Sumpter J, Skakkebaek NE. Male reproductive health and

environmental xenoestrogens. *Environmental Health Perspectives,* 1996*;* **104**(Suppl. **4**):741-803

Tortora G, Grabowski J. *Principles of anatomy and physiology*, 10th ed., John Wiley and sons, Inc., 2003; chapter 10; 274-307

Tran U, Clarke FC. Endogenous synthesis of coenzyme Q in eukaryotes. *Mitochondrion*, 2007; **7S**:S62-S71

Trotter JA, Foerder BA, Keller JM. Intracellular fibres in cultured cells:analysis by scanning and transmission electron microscopy and by SDS-polyacrylamide gel electrophoresis. *Journal of Cell Science*, 1978; **31**:369-392

Trumpower BL, Houser RM, Olson RE. Studies on ubiquinone. Demonstration of total biosynthesis of ubiquinone-9 in rat liver mitochondria. *Journal of Biological Chemistry*, 1974; **249**:3041-3048

Trumpower BL. The protonmotive cycle. Energy transduction by coupling of proton translocation to electron transfer by the cytochrome bc1 complex. *The Journal of Biological Chemistry*, 1990; **265**(**20**):11409-11412

Turunen M, Appelkvist EL, Sindelar P, Dallner G. Blood concentration of coenzyme Q10 increases in rats when esterified forms are administered. *Journal of Nutrition,* 1999; **129**:2113-2118

Turunen M, Swiezewska E, Chojnacki T, Sindelar P, Dallner G. Regulatory aspects of coenzyme Q metabolism. *Free Radical Research*. 2002; **36**(**4**):437-443

Turunen M, Olsen J, Dallner G. Metabolism and function of coenzyme Q. *Biochimical et Biophysical Acta*, 2004; **1660**:171-199

Ushakova AV, Grivennikova VG, Ohnishi T, Vinogradov AD. Triton X-100 as a specific inhibitor of the mammalian NADH-ubiquinone oxidoreductase (Complex I). *Biochimica et Biophysica Acta*, 1999; **1409**:143-153

Vale RD, Ignatius MJ, Shooter EM. Association of nerve growth factor receptors with the Triton X-100 cytoskeleton of PC12 cells. *The Journal of Neurosciences*, 1985; **5**(**10**):2762-2770

Van Belzen R, Kotlyar AB, Moon N, Dunham WR, Albracht SP. The iron–sulfur clusters 2 and ubisemiquinone radicals of NADH:ubiquinone oxidoreductase are involved in energy coupling in submitochondrial particles. *Biochemistry*, 1997; **36**:886–893

Van den Heuvel L, Smeitink J. The oxidative phosphorylation (OXPHOS) system:Nuclear genes and human genetic diseases. *BioEssays,* 2001; **23**:518-525

Van der Merwe CF, Peacock J. Enhancing conductivity of biological material for SEM. *Microscopy Society of Southern Africa – Proceedings*, 1999; **29**

Vazquez-Duhalt R, Marquez-Rocha F, Ponce E, Licea AF, Viana MT. Nonylphenol, an integrated vision of a pollutant. *Applied Ecology and Environmental Research*, 2004; **4**(**1**):1-25

Venkat Ratnam D, Ankola DD, Bhardwaj V, Sahana DK, Ravi Kumar MNV. Role of antioxiants in prophylaxis and therapy:A pharmaceutical perspective. *Journal of Controlled Release*, 2006; **113**:189-207

Villalba JM, Navarro F, Córdoba F, Serrano A, Arroyo A, Crane FL, Navas P. Coenzyme Q reductase from liver plasma membrane:Purification and role in trans-plasma-membrane electron transport. *Proceedings of the National Academy of Sciences of the United States of America*, 1995; **92**:4887-91

Virmani A, Gaetani F, Binienda Z. Effects of metabolic modifiers such as carnitines, coenzyme Q10, and PUFAs against different forms of neurotoxic insults:metabolic inhibitors, MPTP, and metamphetamine. *Annals of the New York Academy of Sciences*, 2005; **1053**:183-191

Wakelam MJO. The fusion of myoblasts. *The Biochemical Journal*, 1985; **228**:1-12

Wallace IP, Fischman DA. High resolution scanning electron microscopy of isolated and *in situ* cytoskeletal elements. *The Journal of Cell Biology*, 1979; **83**(**1**):249-254

Walter L, Nogueira V, Leverve X, Heitz M, Bernardi P, Fontaine E. Three classes of ubiquinone analogs regulate the mitochondrial permeability transition pore through a common site. *The Journal of Biological Chemistry*, 2000; **275**(**38**):29521-29527

Weruaga E, Alonsoa JR, Porteros A, Crespo C, Arévalo R, Brinón JG, Velasco A, Aijón J. Nonspecific labeling of myelin with secondary antisera and high concentrations of Triton X-100. *Journal of Histochemistry and Cytochemistry,* 1998; **46**(**1**):109-11

Whistance GR, Field FE, Threlfall DR. Observations on the biosynthesis of ubiquinones by animals. *European Journal of Biochemistry*, 1971; **18**:46-52

Wilson VS, Bobseine K, Gray E(Jr). Development and characterization of a cell line that stably express an estrogen-responsive luciferase reporter for the detection of estrogen receptor agonist and antagonists. *Toxicological Sciences*, 2004; **81**:69-77

Yamada KM, Spooner BS, Wessels NK. Ultrastructure and function of growth cones and axons of cultured cells. *Journal of Cell Biology*, 1971; **49**:614-635

Yu, I., D. A. Fishman, and T. L. Steck. Selective solubilization of proteins and phospholipids from red blood cell membranes by nonionic detergents. *Journal of Supramolecular Structure,* 1973*;* **1**:233-248